

# Clinical pharmacological approaches to optimize anticancer drug dosing



Laura Molenaar-Kuijsten



# Clinical pharmacological approaches to optimize anticancer drug dosing

Laura Molenaar-Kuijsten

The research described in this thesis was performed at the Department of Pharmacy & Pharmacology, The Netherlands Cancer Institute - Antoni van Leeuwenhoek, Amsterdam, The Netherlands, in collaboration with other institutes.

Printing of this thesis was financially supported by Oncology Graduate School Amsterdam.

**ISBN**

978-94-6458-017-4

**Cover design and layout**

© evelienjagtman.com

**Print**

Ridderprint

© Laura Molenaar-Kuijsten, 2021

# Clinical pharmacological approaches to optimize anticancer drug dosing

**Klinisch farmacologische benaderingen voor het optimaliseren van de dosering van antikankergeneesmiddelen**

(met een samenvatting in het Nederlands)

## **Proefschrift**

ter verkrijging van de graad van doctor aan de Universiteit Utrecht  
op gezag van de rector magnificus, prof. dr. H.R.B.M. Kummeling,  
ingevolge het besluit van het college voor promoties  
in het openbaar te verdedigen op  
dinsdag 22 maart 2022 des middags te 12.15 uur

door

**Laura Molenaar-Kuijsten**

geboren op 31 januari 1991  
te Bunnik

**Promotoren:**

Prof. dr. A.D.R. Huitema

Prof. dr. J.H. Beijnen

**Copromotor:**

Dr. N. Steeghs

# TABLE OF CONTENTS

<b>Preface</b>		<b>9</b>
<hr/>		
<b>Chapter 1</b>	<b>Drug-drug interactions of oral anticancer drugs</b>	<b>15</b>
<hr/>		
<b>Chapter 1.1</b>	A review of CYP3A drug-drug interaction studies: practical guidelines for patients using targeted oral anticancer drugs <i>Frontiers in Pharmacology 2021; 12: 670862</i>	17
<b>Chapter 1.2</b>	Effects of the moderate CYP3A4 inhibitor erythromycin on the pharmacokinetics of palbociclib: a randomized crossover trial in patients with breast cancer <i>Clinical Pharmacology &amp; Therapeutics 2021 [Epub ahead of print]</i>	69
<hr/>		
<b>Chapter 2</b>	<b>Effect of body composition on pharmacokinetics</b>	<b>91</b>
<hr/>		
<b>Chapter 2.1</b>	Worse capecitabine treatment outcome in patients with a low skeletal muscle mass is not explained by altered pharmacokinetics <i>Cancer Medicine 2021; 10(14): 4781-4789</i>	93
<b>Chapter 2.2</b>	The association of cisplatin pharmacokinetics and skeletal muscle mass in head and neck cancer patients: the prospective PLATISMA study <i>Accepted for publication in European Journal of Cancer</i>	113
<b>Chapter 2.3</b>	Optimizing carboplatin dosing by an improved prediction of carboplatin clearance using a CT-enhanced estimate of renal function <i>Manuscript in preparation</i>	133
<hr/>		
<b>Chapter 3</b>	<b>Measurement of drug levels in alternative matrices</b>	<b>151</b>
<hr/>		
<b>Chapter 3.1</b>	Everolimus saliva concentrations as predictor of stomatitis: a feasibility study in cancer patients <i>Submitted for publication</i>	153
<b>Chapter 3.2</b>	Intra-tumoral pharmacokinetics of pazopanib in combination with radiotherapy in patients with non-metastatic soft-tissue sarcoma <i>Submitted for publication</i>	171

---

<b>Chapter 4</b>	<b>Conclusions and perspectives</b>	<b>197</b>
------------------	-------------------------------------	------------

---

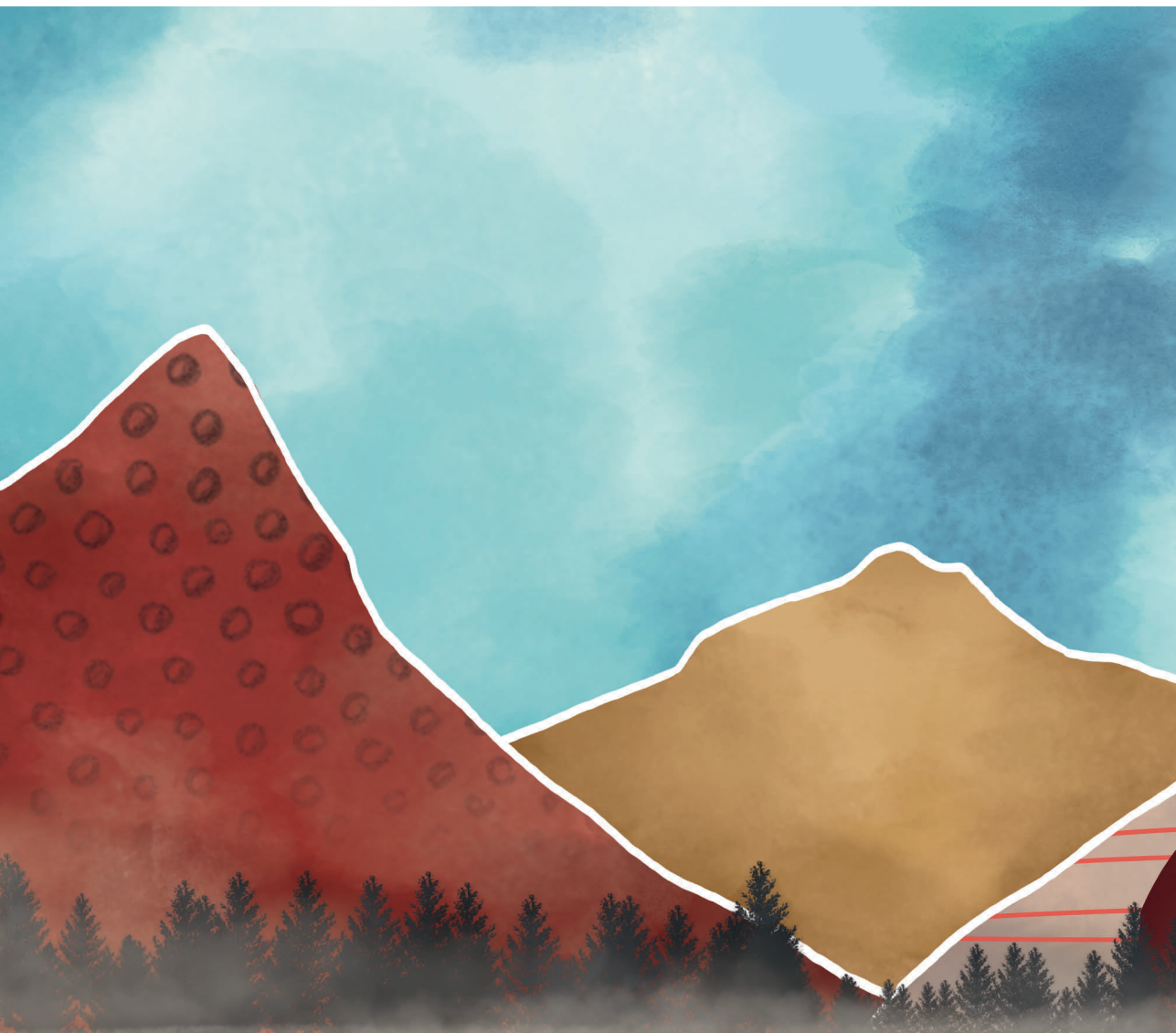
<b>Appendices</b>	<b>211</b>
-------------------	------------

---

Summary	213
Nederlandse samenvatting	219
Author affiliations	227
List of publications	235
Dankwoord	241
Curriculum vitae	247







# PREFACE







## PREFACE

Cancer is still a leading cause of death. More than 19 million people worldwide were diagnosed with cancer in 2020, with 10 million deaths (1). Fortunately, the treatment of cancer is rapidly evolving, with a shift from non-specific treatment to targeted therapy. The improved treatment of cancer has, amongst other improvements, led to an increased survival (2). In the change of cancer from a fatal to chronic disease, further individualization of therapy could play an important role.

The first step in individualization of therapy is to choose the right drug for the right patient. In order to treat patients as effectively and with as few side effects as possible, also dose optimization is of importance. Several aspects highly relevant for drug dosing in oncology are studied in this thesis.

Firstly, cancer patients are often treated with multiple drugs, and since most oral anticancer drugs are metabolized by cytochrome P450 enzyme 3A (CYP3A), the risk of drug-drug interactions is high. For these oral anticancer drugs, treatment efficacy and toxicity is often related to pharmacokinetic parameters, such as exposure (3). By means of a pharmacokinetic drug-drug interaction, exposure to a drug could be decreased, possibly resulting in treatment failure, or exposure could be increased, possibly resulting in adverse events. Therefore, co-medication should be considered carefully.

Secondly, body composition might be relevant for drug dosing. It has been shown for multiple anticancer drugs, that a low skeletal muscle mass negatively impacts toxicity and survival (4–6). The latter is probably inherent to suboptimal treatment because of intolerable side effects. To improve tolerability of chemotherapy, and thereby improve treatment, it is crucial to know the mechanism that causes body composition to have a negative effect on side effects, and subsequently survival. The reason could be an alteration of pharmacokinetics, because the volume of distribution of hydrophilic drugs is expected to be smaller in patients with a low skeletal muscle mass, which could for example lead to higher plasma levels of the drugs. If the effect on toxicity and survival can be explained by altered pharmacokinetics, it might be better to dose chemotherapy based on the skeletal muscle mass instead of the currently used body surface area.

Lastly, it is important to predict if the treatment will be effective and if toxicity will occur early after start of treatment. Thereby, exposure to ineffective treatments can be avoided, and toxicity can be prevented. Drug levels at the site of exposure could possibly be used to predict efficacy and toxicity, and thus used to improve treatment.

**Chapter 1** describes pharmacokinetic drug-drug interactions that occur through influencing the metabolism via CYP3A. In **Chapter 1.1** we summarize the results of drug-drug interaction studies performed for twelve oral anticancer drugs. Based on these results, we provide recommendations for clinical practice on how to deal with drug-drug interactions of oral anticancer drugs if only data from strong CYP3A inhibitors or inducers is available. **Chapter 1.2** describes the effect of the moderate CYP3A4 inhibitor erythromycin on the pharmacokinetics of palbociclib, which is used for the treatment of breast cancer.

**Chapter 2** focusses on the relationship between body composition and pharmacokinetics. **Chapter 2.1** describes the association between skeletal muscle mass and the pharmacokinetics of the chemotherapeutic drug capecitabine and its metabolites, including the active metabolite 5-fluorouracil. In **Chapter 2.2** we report the results of a prospective observational study in which the relationship between skeletal muscle mass and pharmacokinetics of cisplatin in head and neck squamous cell carcinoma patients was studied. In **Chapter 2.3** we evaluate the use of a CT-based estimate of renal function to predict carboplatin clearance. The administered dose of carboplatin is usually calculated with the Calvert formula, which includes target exposure and glomerular filtration rate (7). In the commonly used modified Calvert formula, the glomerular filtration rate is predicted by the creatinine clearance calculated by the Cockcroft-Gault formula (8). In this formula, the creatinine production rate is estimated using surrogate markers for muscle mass (9). The estimation of the creatinine production rate might be improved by a CT-based estimate of renal function, because actual skeletal muscle mass as shown on the CT-scan is incorporated in the formula.

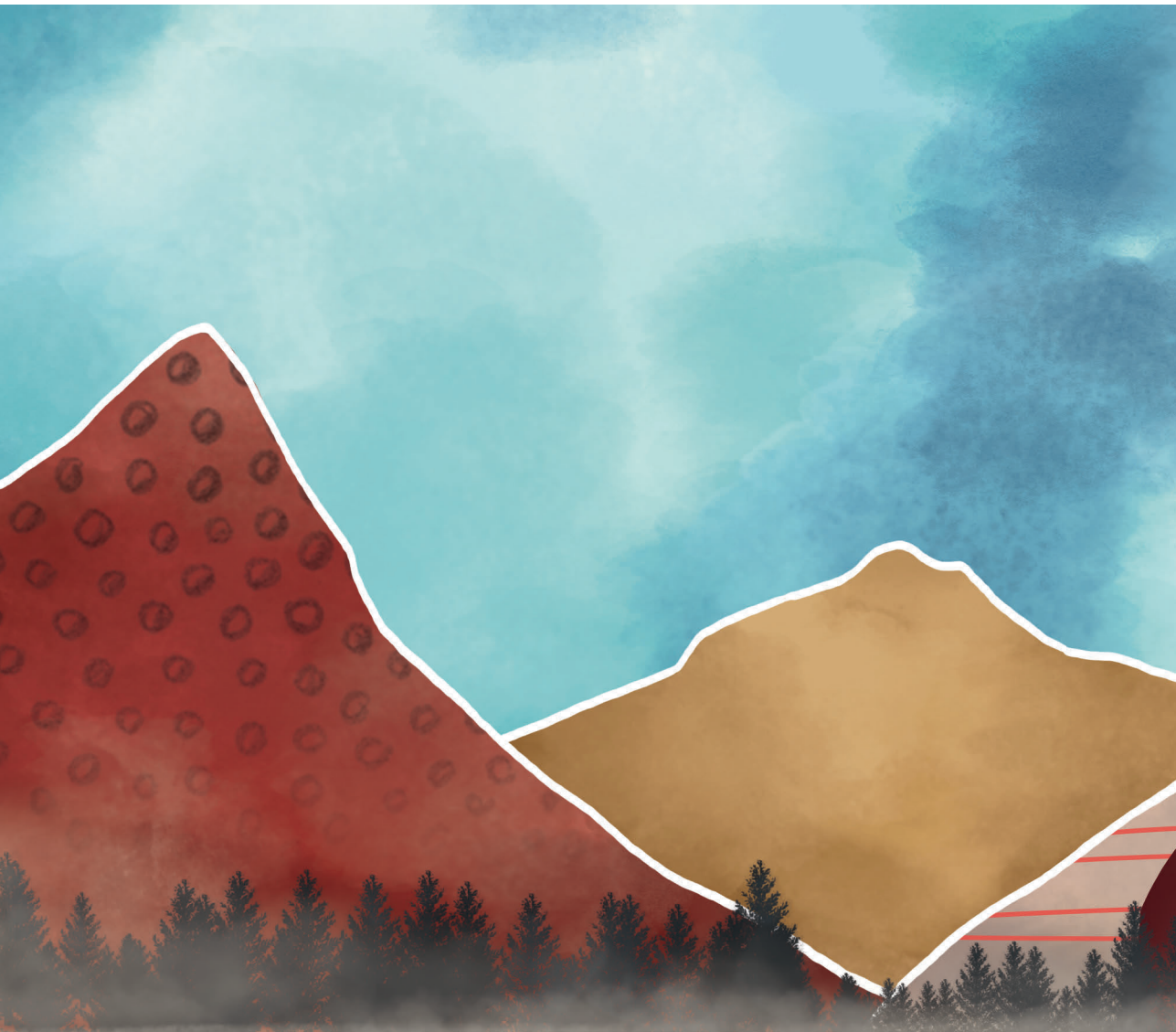
**Chapter 3** discusses the use of drug levels in alternative matrices as a predictor of efficacy or toxicity. **Chapter 3.1** gives an overview of the feasibility of everolimus saliva concentrations as an early predictor for the occurrence of stomatitis. **Chapter 3.2** describes a prospective clinical trial in which intra-tumoral drug levels of pazopanib were quantified in sarcoma patients and the correlation with efficacy was studied.

Overall, this thesis aims to optimize anticancer drug dosing based on co-medication, and body composition, and guided by drug levels at the site of exposure.



## REFERENCES

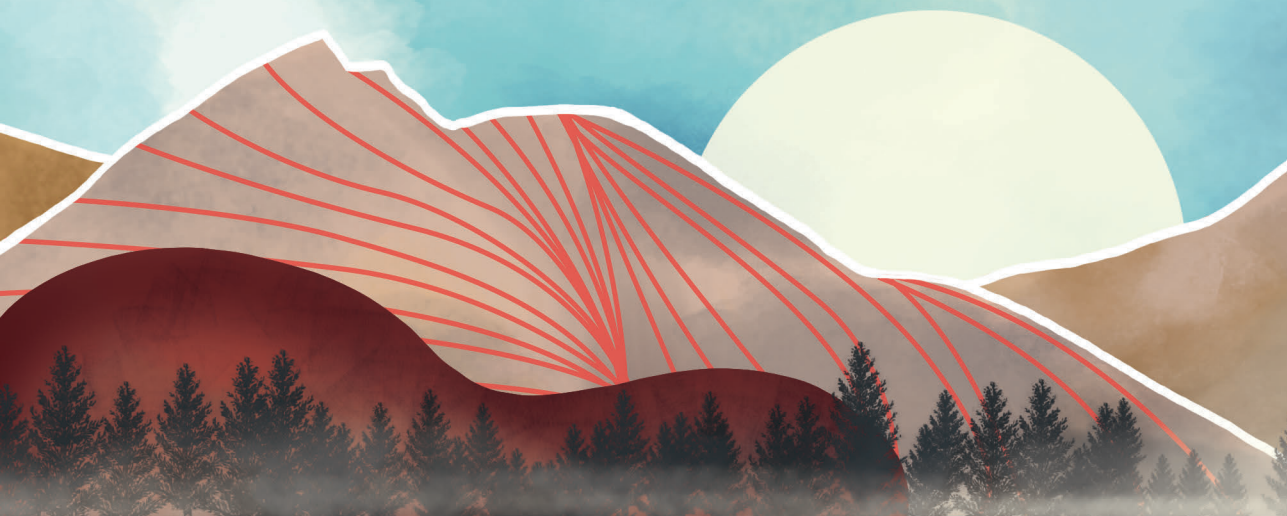
1. Ferlay J, Ervik M, Lam F, Colombet M, Mery L, Piñeros M. Global Cancer Observatory: Cancer Today [Internet]. Lyon: International Agency for Research on Cancer. 2020 [cited 2021 Aug 6]. Available from: <https://gco.iarc.fr/today/>
2. Arnold M, Rutherford MJ, Bardot A, Ferlay J, Andersson TML, Myklebust TÅ, et al. Progress in cancer survival, mortality, and incidence in seven high-income countries 1995–2014 (ICBP SURVMARK-2): a population-based study. *Lancet Oncol.* 2019;20(11):1493–505.
3. Verheijen RB, Yu H, Schellens JHM, Beijnen JH, Steeghs N, Huitema ADR. Practical Recommendations for Therapeutic Drug Monitoring of Kinase Inhibitors in Oncology. *Clin Pharmacol Ther.* 2017;102(5):765–76.
4. Wendrich AW, Swartz JE, Bril SI, Wegner I, de Graeff A, Smid EJ, et al. Low skeletal muscle mass is a predictive factor for chemotherapy dose-limiting toxicity in patients with locally advanced head and neck cancer. *Oral Oncol.* 2017;71:26–33.
5. Kurk S, Peeters P, Stellato R, Dorresteijn B, Jong P De, Jourdan M, et al. Skeletal muscle mass loss and dose-limiting toxicities in metastatic colorectal cancer patients. *J Cachexia Sarcopenia Muscle.* 2019;10(4):803–13.
6. Kurk SA, Peeters PHM, Dorresteijn B, de Jong PA, Jourdan M, Creemers GJM, et al. Loss of skeletal muscle index and survival in patients with metastatic colorectal cancer: Secondary analysis of the phase 3 CAIRO3 trial. *Cancer Med.* 2020;9(3):1033–43.
7. Calvert A, Newell D, Gumbrell L, O'Reilly S, Burnell M, Boxall F, et al. Carboplatin dosage: prospective evaluation of a simple formula based on renal function. *J Clin Oncol.* 1989;7(11):1748–56.
8. Nannan Panday VR, Van Warmerdam LJC, Huizing MT, Ten Bokkel Huinink WW, Vermorken JB, Giaccone G, et al. Carboplatin dosage formulae can generate inaccurate predictions of carboplatin exposure in carboplatin/paclitaxel combination regimens. *Clin Drug Investig.* 1998;15(4):327–35.
9. Cockcroft D, Gault M. Prediction of Creatinine Clearance from Serum Creatinine. *Nephron.* 1976;16:31–41.





# CHAPTER 1

Drug-drug interactions of  
oral anticancer drugs







# CHAPTER 1.1

## **A review of CYP3A drug-drug interaction studies:** practical guidelines for patients using targeted oral anticancer drugs

Laura Molenaar-Kuijsten, Dorieke E.M. van Balen, Jos H. Beijnen, Neeltje Steeghs, Alwin D.R. Huitema

Frontiers in Pharmacology 2021; 12: 670862

Author's contribution: LMK contributed to conception and design of the review, performed the data analysis, wrote the first draft of the manuscript and implemented the input and feedback of the co-authors.

## ABSTRACT

Many oral anticancer drugs are metabolized by CYP3A. Clinical drug-drug interaction (DDI) studies often only examine the effect of strong CYP3A inhibitors and inducers. The effect of moderate or weak inhibitors or inducers can be examined using physiologically based pharmacokinetic simulations, but data from these simulations are not always available early after approval of a drug. In this review we provide recommendations for clinical practice on how to deal with DDIs of oral anticancer drugs if only data from strong CYP3A inhibitors or inducers is available. These recommendations were based on reviewed data of oral anticancer drugs primarily metabolized by CYP3A and approved for the treatment of solid tumors from January 1st, 2013 to December 31st, 2015. In addition, three drugs that were registered before the new EMA guideline was issued (i.e., everolimus, imatinib and sunitinib), were reviewed. DDIs are often complex, but if no data is available from moderate CYP3A inhibitors/inducers, a change in exposure of 50% compared with strong inhibitors/inducers can be assumed. No *a priori* dose adaptations are indicated for weak inhibitors/inducers, because their interacting effect is small. In case pharmacologically active metabolites are involved, the metabolic pathway, the ratio of the parent to the metabolites, and the potency of the metabolites should be taken into account.

## INTRODUCTION

Oral targeted anticancer drugs are important drugs for the treatment of cancer. Most oral anticancer drugs are metabolized by CYP3A; therefore, patients are at risk for drug-drug interactions (DDI). Because many of these drugs show an exposure–efficacy and an exposure–toxicity relationship, a change in exposure to these drugs can be highly relevant (1,2). This change in exposure as a consequence of a DDI could result in adverse events if exposure is increased, or treatment failure if exposure is decreased (in case of prodrugs vice versa).

DDI studies are performed before registration of a drug, based on the metabolism of the drug and following the recommendations of the EMA and FDA (3–5). These studies use strong CYP3A inhibitors (e.g., itraconazole or ketoconazole) and inducers (e.g., rifampin) since the guidelines of the EMA and FDA advise a worst-case approach. Subsequently, the effects of moderate and weak inhibitors or inducers are extrapolated from these data using physiologically based pharmacokinetic (PBPK) simulations (4,5). In short, conducting a PBPK simulation consists of three steps: model development, model verification, and model application. First a physiologically based model is built for the substrate and interacting drug (for the latter also the SimCYP library can be used), including for example pharmacokinetic (PK) data. Secondly, the models are verified, e.g., by simulating a concentration–time profile and comparing it with the data from clinical studies. Subsequently, the two models are linked and drug–drug interactions can be simulated. Before the effects of moderate and weak inhibitors and inducers can be predicted, first the models should be verified using data from clinical DDI studies with strong inhibitors and inducers. The use of PBPK models is described in several guidelines of the FDA (5–7). There is, however, a critical problem with the above described DDI studies performed before drug approval. Despite the fact that moderate and weak inhibitors and inducers are far more frequently used than the strong CYP3A inhibitors and inducers, clinical data on moderate and weak inhibitors and inducers is often lacking. This problem is partly overcome by the, increasingly performed, PBPK simulations. But, data from these PBPK simulations are not always available early after approval of a drug. This is for example the case for drugs that are conditionally approved, as is the case for, for instance, larotrectinib and lorlatinib (8–11).

To determine which drugs might influence the metabolism of oral anticancer drugs, the Flockhart Table can be consulted (12). The Flockhart Table displays drugs that inhibit or induce specific CYP enzymes, for example CYP3A (12). The interacting drugs are placed in groups according to the inhibition or induction capacity, and are classified in



broad ranges. Weak inhibitors increase the AUC by  $\geq 1.25$ - $< 2$ -fold, moderate inhibitors by  $\geq 2$ - $< 5$ -fold, and strong inhibitors by  $\geq 5$ -fold (5,12). Weak inducers decrease the AUC by  $\geq 20$ - $< 50\%$ , moderate inducers by  $\geq 50$ - $< 80\%$ , and strong inducers by  $\geq 80\%$  (5).

The aim of this review was to provide recommendations for clinical practice on how to deal with DDIs of oral anticancer drugs if only data from strong CYP3A inhibitors or inducers is available. To achieve this goal, we compared results from DDI studies with strong inhibitors or inducers with results with moderate or weak inhibitors or inducers, to extrapolate results to clinical practice and formulate an advice on how to deal with DDIs for which data is lacking.

## METHODS

Oral anticancer drugs, used for the treatment of solid tumors, were selected based on their metabolism and year of approval. On January 1st, 2013, the EMA guideline on the investigation of DDIs came into effect (13). To allow several years of follow-up after approval, in which clinical DDI studies with these drugs might be conducted, an inclusion cut-off in December 2015 was chosen. Therefore, all drugs primarily metabolized by CYP3A and approved for the treatment of solid tumors from January 1st, 2013 to December 31st, 2015 were selected. In addition, we included three drugs that were registered before the new EMA guideline was issued (i.e., everolimus, imatinib and sunitinib), to illustrate how DDI studies were performed with the prior guideline. An overview of the drug selection is shown in **Figure 1**. Firstly, the US FDA Clinical Pharmacology and Biopharmaceutics Review and the Summary of Product Characteristics of these drugs were studied for data on DDI studies. Second, PubMed was searched using the search terms [drug name] AND [drug-drug interaction (study)] OR [drug name of most used potent inhibitor and inducer]. Furthermore, citation snowballing was used to find other articles of interest. The articles, including case reports, in which no AUCs were reported, or in which the dose of the victim drug was different between the control group and group with combination treatment, and *in vitro* studies were excluded. We searched the articles for the change in AUC (preferably the  $AUC_{0-\infty}$ ) of the victim drug in combination with the studied CYP3A inhibitor or inducer, compared with administration of the victim drug alone. We visualized this by making graphs using the ratios of adjusted means of the combination versus the victim drug alone, whereby the victim drug alone was rated as 100% exposure. The studied inhibitors and inducers were grouped according to their interaction potential, which was reported in the reviewed articles and checked with the Flockhart Table (12).



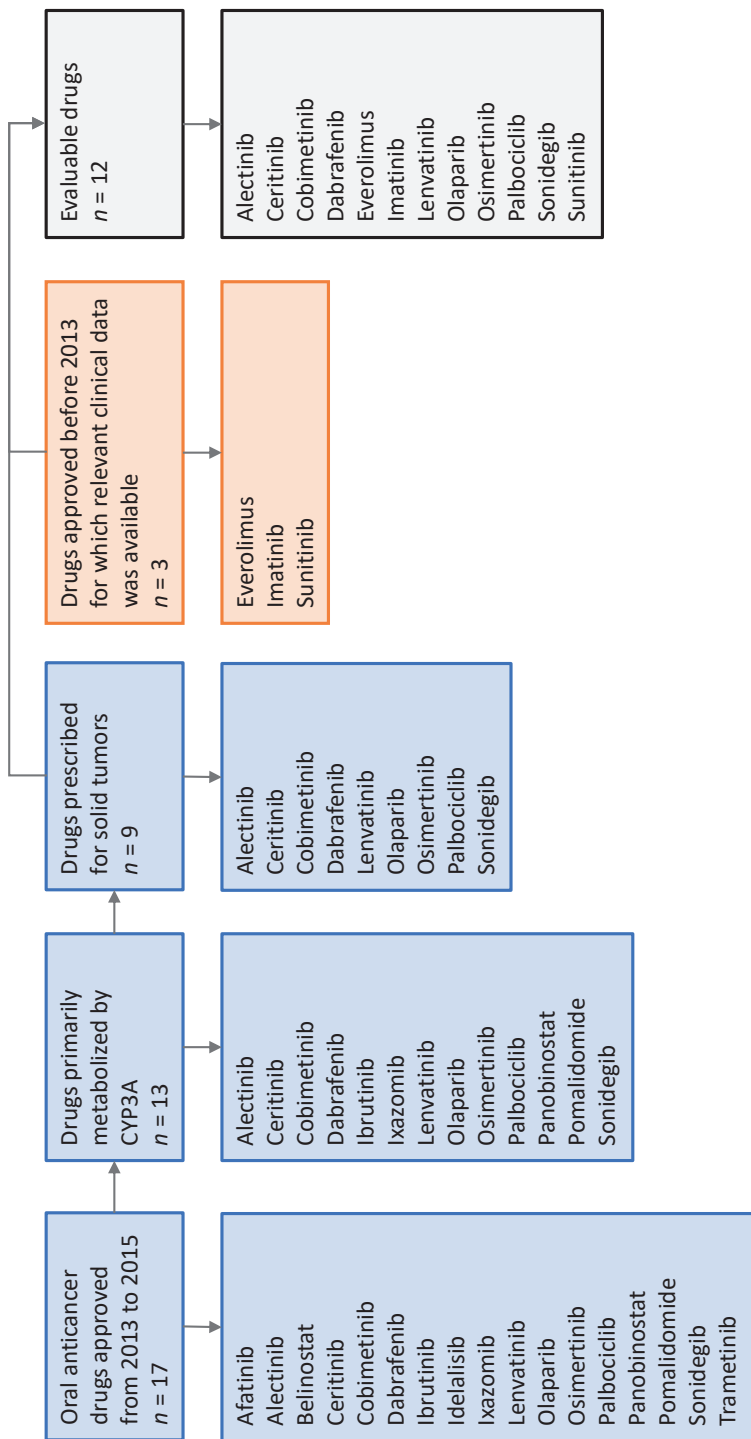


Figure 1. Schematic overview of drug selection.



## RESULTS

**Table 1** gives a summary of the DDI studies of the twelve selected oral anticancer drugs. In **Table 2**, a detailed overview of the results is shown. The results are described for the drugs without active metabolites first and for the drugs with active metabolites thereafter.

### Drugs without active metabolites

#### *Ceritinib*

When the strong CYP3A inhibitor ketoconazole was combined with a single-dose of ceritinib, the  $AUC_{0-\infty}$  of ceritinib increased by 190% ( $n=19$ )(16). In a PBPK study the effect of ketoconazole on steady-state exposure of ceritinib was simulated. Steady-state exposure increased by 51% (16). The difference between the effect of ketoconazole on single-dose and steady-state ceritinib concentrations can be explained by the auto-inhibition of CYP3A4 by ceritinib. Hereby, the fraction of ceritinib metabolized by CYP3A4 will be decreased at steady-state concentrations, thus the effect of a strong inhibitor will be smaller (16). The moderate inhibitor fluconazole increased the steady-state exposure of ceritinib by 37% in a PBPK simulation (16). The strong CYP3A inducer rifampin decreased the  $AUC_{0-\infty}$  of single-dose ceritinib by 70% ( $n=19$ ) and it was predicted to decrease the AUC on steady-state by 67%. In a simulation study, the moderate inducer efavirenz decreased the AUC of ceritinib by approximately half with 43% (16).

#### *Cobimetinib*

**Figure 2** shows the results of the DDI studies conducted with cobimetinib. It can be seen that CYP3A based DDIs have a large influence on the exposure to cobimetinib. The strong inhibitor itraconazole increased the  $AUC_{0-\infty}$  of cobimetinib by almost 600% ( $n=15$ )(17). The moderate CYP3A inhibitors erythromycin and diltiazem increased the AUC by around 300% in a PBPK simulation, which is half the effect of strong inhibitors, while weak inhibitors had no effect (17,18). The effect of rifampin on the exposure of cobimetinib was studied in a PBPK simulation study instead of a clinical trial, which is in contrast with most DDI studies performed with rifampin. In this simulation the AUC of cobimetinib decreased by 83% when combined with rifampin (17). Furthermore, the effect of the moderate CYP3A inducer efavirenz was studied in a PBPK simulation and a decrease in AUC of 72% was predicted (17,18). The weak inducer vemurafenib showed a decrease in  $AUC_{0-24h}$  of only 13% in a clinical trial ( $n=unknown$ )(17).

Table 1. Summary table of the results of DDI studies performed with the reviewed oral oncolytic drugs.

Drug	Effect CYP3A inhibitors <sup>a</sup>	
	Strong	Moderate
Alectinib <sup>b</sup>	36% ↑	
Ceritinib	118.5% ↑ (51-186)	37% ↑
Cobimetinib	572% ↑	280.5% ↑ (226-335)
Dabrafenib	71% ↑	
Hydroxy-dabrafenib	82% ↑	
Desmethyl-dabrafenib	68% ↑	
Carboxy-dabrafenib	16% ↓	
Everolimus	1430% ↑	220% ↑ (74-340)
Imatinib	18.5% ↑ (-3.1-40.1)	
N-desmethylinatinib	16.75% ↑ (-5-38.5)	
Lenvatinib	14.5% ↑	
Olaparib	161% ↑ (152-170)	115% ↑ (98-126)
Osimertinib	24.2% ↑	
Palbociclib	86.8% ↑	40% ↑ (38-42)
Sonidegib	122.8% ↑ (42-253)	98% ↑ (36-179)
Sunitinib <sup>c</sup>	51% ↑	11% ↑

<sup>a</sup> Reported as percentage of AUC change, if multiple DDI studies were performed the mean AUC change and range are reported.

<sup>b</sup> Sum of alectinib and M4.

<sup>c</sup> Sum of sunitinib and SU12662, except for the moderate inhibitor.

Effect CYP3A inducers <sup>a</sup>			
Weak	Strong	Moderate	Weak
	18.4% ↓		
	68.5% ↓ (67-70)	43% ↓	
3% ↑	83% ↓	72% ↓	13% ↓
	34% ↓		
	30% ↓		
	73% ↑		
	63% ↓		
	73.3% ↓ (72.5-74)		37.1% ↓ (30.2-44)
	10.8% ↓ (9.8-11.7)		4.1% ↑
	6.2% ↑ (-18.2-30.6)		
15% ↑ (1-2)	79% ↓ (71-87)	57.3% ↓ (53-60)	0% ↓
	78.5% ↓	42% ↓	0% ↓
0.4% ↑ (0.3-0.4)	85.2% ↓	35% ↓ (32-38)	
	76.6% ↓ (66-88)	49% ↓ (29-65)	
	46% ↓		



Table 2. Detailed overview of the results of DDI studies performed with the reviewed oral oncolytic drugs.

<b>Drug (year of market approval)</b>	<b>(Primary) meta-bolism</b>	<b>Target (1)</b>	<b>Inter-patient variability (%CV)</b>	<b>Dose-linearity</b>	<b>DDI study with (interaction potential)</b>
Alectinib (2015)	CYP3A	ALK	46%	Dose proportional exposure	Posaconazole (strong CYP3A inhibitor)  Rifampin (strong CYP3A inducer)
Ceritinib (2014)	CYP3A	ALK	74%	Nonlinear PK	Ketoconazole (strong CYP3A inhibitor)  Fluconazole (moderate CYP3A inhibitor)  Rifampin (strong CYP3A inducer)  Efavirenz (moderate CYP3A inducer)
Cobimetinib (2015)	CYP3A	MEK	61%	Dose proportional exposure	Itraconazole (strong CYP3A inhibitor)  Erythromycin (moderate CYP3A inhibitor)  Diltiazem (moderate CYP3A inhibitor)

Change in AUC	Recommendations Summary of Product Characteristics	Type of trial	References
AUC <sub>0-∞</sub> 75% ↑ (90% CI 57-95) M4 AUC <sub>0-∞</sub> 24.9% ↓ (90% CI 12.3-35.6) Sum alectinib and M4 AUC <sub>0-∞</sub> 36% ↑ (90% CI 24-49)	Be careful when combining alectinib with strong inhibitors of CYP3A	Clinical trial	(14,15)
AUC <sub>0-∞</sub> 73.2% ↓ (90% CI 69.9-76.2) M4 AUC <sub>0-∞</sub> 79% ↑ (90% CI 58-102) Sum alectinib and M4 AUC <sub>0-∞</sub> 18.4% ↓ (90% CI 9.9-26)	Be careful when combining alectinib with strong inducers of CYP3A	Clinical trial	(14,15)
<u>Single dose</u> AUC <sub>0-∞</sub> 186% ↑ (90% CI 146-233)	Avoid coadministration of strong CYP3A inhibitors or reduce the dose of ceritinib to 150 mg QD	Clinical trial	(16)
<u>Steady-state</u> AUC 51% ↑ (90% CI 43-59)		PBPK simulation	
AUC 37% ↑ (90% CI 31-42)		PBPK simulation	(16)
<u>Single dose</u> AUC <sub>0-∞</sub> 70% ↓ (90% CI 61-77)	Avoid coadministration of strong CYP3A inducers	Clinical trial	(16)
<u>Steady-state</u> AUC 67% ↓ (90% CI 64-70)		PBPK simulation	
AUC 43% ↓ (90% CI 38-48)		PBPK simulation	(16)
AUC <sub>0-∞</sub> 572% ↑ (90% CI 464-702)	Avoid coadministration of strong and moderate CYP3A inhibitors or reduce the dose of cobimetinib to 20 mg QD (short term use)	Clinical trial	(17)
AUC 335% ↑		PBPK simulation	(17,18)
AUC 226% ↑		PBPK simulation	(17,18)

Table 2. Continued.

<b>Drug (year of market approval)</b>	<b>(Primary) meta-bolism</b>	<b>Target (1)</b>	<b>Inter-patient variability (%CV)</b>	<b>Dose-linearity</b>	<b>DDI study with (interaction potential)</b>
					Fluvoxamine (weak CYP3A inhibitor) Rifampin (strong CYP3A inducer)  Efavirenz (moderate CYP3A inducer) Vemurafenib (weak CYP3A inducer)
Dabrafenib (2013)	CYP2C8/ CYP3A	BRAF	38%	Dose proportional exposure at single dose, but less than dose-proportional after repeat twice daily dosing (likely due to auto-induction)	Ketoconazole (strong CYP3A inhibitor)        Rifampin (strong CYP3A inducer)
Everolimus (2003)	CYP3A/ P-gp	mTOR	36%	Dose proportional exposure	Ketoconazole (strong CYP3A inhibitor)        Erythromycin (moderate CYP3A inhibitor) Verapamil (moderate CYP3A inhibitor)

Change in AUC	Recommendations Summary of Product Characteristics	Type of trial	References
AUC 3% ↑		PBPK simulation	(17,18)
AUC 83% ↓	Avoid coadministration of strong and moderate CYP3A inducers	PBPK simulation	(17,18)
AUC 72% ↓		PBPK simulation	(17,18)
AUC <sub>0-24h</sub> 13% ↓		Clinical trial	(17)
AUC <sub>0-12h</sub> 71% ↑ (90% CI 55-90) Hydroxy-dabrafenib AUC <sub>0-12h</sub> 82% ↑ (90% CI 61-105) Desmethyl-dabrafenib AUC <sub>0-12h</sub> 68% ↑ (90% CI 47-93) Carboxy-dabrafenib AUC <sub>0-12h</sub> 16% ↓ (90% CI 4-27)	Be careful when combining dabrafenib with strong inhibitors of CYP3A	Clinical trial	(19-21)
AUC 34% ↓ Desmethyl-dabrafenib AUC 30% ↓ Carboxy-dabrafenib AUC 73% ↑	Avoid coadministration of CYP3A inducers	Clinical trial	(19)
AUC <sub>0-∞</sub> 1430% ↑ (90% CI 1020-2150)	Avoid coadministration of strong CYP3A inhibitors. Avoid coadministration of moderate CYP3A inhibitors or reduce the dose of everolimus to 2.5 or 5 mg QD	Clinical trial	(22,23)
AUC <sub>0-∞</sub> 340% ↑ (90% CI 250-440)		Clinical trial	(22,24,25)
AUC <sub>0-∞</sub> 250% ↑ (90% CI 210-290)		Clinical trial	(22,24,26)

Table 2. Continued.

<b>Drug (year of market approval)</b>	<b>(Primary) meta-bolism</b>	<b>Target (1)</b>	<b>Inter-patient variability (%CV)</b>	<b>Dose-linearity</b>	<b>DDI study with (interaction potential)</b>
					Imatinib (moderate CYP3A inhibitor) Cyclosporine (moderate CYP3A inhibitor)  Rifampin (strong CYP3A inducer)
Imatinib (2001)	CYP3A	KIT, PDGFR, Bcr-Abl	40-60%	Dose proportional exposure	Ketoconazole (strong CYP3A inhibitor)  Ritonavir (strong CYP3A inhibitor)  Rifampin (strong CYP3A inducer)  Enzyme-inducing antiepileptic drugs (EIAEDs; e.g., carbamazepine, oxcarbazepine and phenytoin) (mixed potency; carbamazepine and phenytoin are potent inducers; oxcarbazepine is a weak inducer)



Change in AUC	Recommendations Summary of Product Characteristics	Type of trial	References
AUC 270% ↑		Clinical trial	(27)
<u>Neoral</u> <sup>®</sup> AUC <sub>0-∞</sub> 168% ↑ (90% CI 122-224)		Clinical trial	(28,29)
<u>Sandimmune</u> <sup>®</sup> AUC <sub>0-∞</sub> 74% ↑ (90% CI 49-104)			
AUC 63% ↓ (90% CI 54-70)	Avoid coadministration of strong CYP3A inducers or increase the dose of everolimus to 10 or 20 mg QD	Clinical trial	(22,24,30)
<u>Single dose</u> AUC <sub>0-∞</sub> 40.1% ↑ (90% CI 31-49.9)	Be careful when combining imatinib with inhibitors of CYP3A	Clinical trial	(27,31)
N-desmethylimatinib AUC <sub>0-∞</sub> 5% ↓ (90% CI -3-12.5)			
<u>Steady-state</u> AUC <sub>0-24h</sub> 3.1% ↓ (90% CI -12.5-16.5)		Clinical trial	(32)
N-desmethylimatinib AUC <sub>0-24h</sub> 38.5% ↑ (90% CI 15.9-65.6)			
AUC <sub>0-∞</sub> 74% ↓ (90% CI 71-76)	Avoid coadministration of strong CYP3A inducers	Clinical trial	(27,33)
N-desmethylimatinib AUC <sub>0-∞</sub> 11.7% ↓ (90% CI 3.3-19.4)			
AUC <sub>0-∞</sub> 72.5% ↓		Clinical trial	(34)
N-desmethylimatinib AUC <sub>0-∞</sub> 9.8% ↓			

Table 2. Continued.

<b>Drug (year of market approval)</b>	<b>(Primary) meta-bolism</b>	<b>Target (1)</b>	<b>Inter-patient variability (%CV)</b>	<b>Dose-linearity</b>	<b>DDI study with (interaction potential)</b>
					St John's Wort (weak CYP3A inducer)
Lenvatinib (2015)	CYP3A	VEGFR	36-78%	Dose proportional exposure	Itraconazole (strong CYP3A inhibitor)  Rifampin (strong CYP3A inducer)
Olaparib (2014)	CYP3A	PARP	38%	Dose-proportionality cannot be concluded based on available PK data	Itraconazole (strong CYP3A inhibitor)    Fluconazole (moderate CYP3A inhibitor)    Fluvoxamine (weak CYP3A inhibitor)

Change in AUC	Recommendations Summary of Product Characteristics	Type of trial	References
<u>Study 1</u> AUC <sub>0-∞</sub> 30.2% ↓ (90% CI 25-34.9) N-desmethylimatinib AUC <sub>0-72h</sub> 4.1% ↑ (90% CI -8.4-18.3)		Clinical trial	(35)
<u>Study 2</u> AUC <sub>0-∞</sub> 44% ↓ (90% CI 30-54)			(36)
AUC <sub>0-∞</sub> 14.5% ↑ (90% CI 8.5-20.9)	None	Clinical trial	(37,38)
<u>Single dose</u> AUC <sub>0-∞</sub> 30.6% ↑ (90% CI 22.7-39)		Clinical trial	(37,39)
<u>Multiple doses</u> AUC <sub>0-∞</sub> 18.2% ↓ (90% CI 8.7-26.7)			
<u>Study 1: tablet</u> AUC <sub>0-∞</sub> 170% ↑ (90% CI 144-197)	Reduce dose of olaparib to 150 mg BID when combined with strong CYP3A inhibitors and reduce dose to 200 mg BID when combined with moderate CYP3A inhibitors (tablets)	Clinical trial	(40,41)
<u>Study 2: capsule</u> AUC 152% ↑ (95% CI 139-167)		PBPK simulation	(42)
<u>Study 1: tablet</u> AUC 126% ↑ (95% CI 115-130)		PBPK simulation	(40)
<u>Study 2: tablet</u> AUC 121% ↑ (95% CI 114-128)		PBPK simulation	(42)
<u>Study 2: capsule</u> AUC 98% ↑ (95% CI 92-105)			
<u>Tablet</u> AUC 2% ↑ (95% CI 1-2)		PBPK simulation	(42)
<u>Capsule</u> AUC 1% ↑ (95% CI 1-2)			

Table 2. Continued.

<b>Drug (year of market approval)</b>	<b>(Primary) meta-bolism</b>	<b>Target (1)</b>	<b>Inter-patient variability (%CV)</b>	<b>Dose-linearity</b>	<b>DDI study with (interaction potential)</b>
					Rifampin (strong CYP3A inducer)
					Efavirenz (moderate CYP3A inducer)
					Dexamethasone (weak CYP3A inducer)
Osimertinib (2015)	CYP3A	EGFR	37%	Dose proportional exposure	Itraconazole (strong CYP3A inhibitor)
					Rifampin (strong CYP3A inducer)
					Efavirenz (moderate CYP3A inducer)
					Dexamethasone (weak CYP3A inducer)
Palbociclib (2015)	CYP3A	CDK4/6	29%	Dose proportional exposure	Itraconazole (strong CYP3A inhibitor)
					Diltiazem (moderate CYP3A inhibitor)
					Verapamil (moderate CYP3A inhibitor)
					Fluvoxamine (weak inhibitor)

Change in AUC	Recommendations Summary of Product Characteristics	Type of trial	References
<u>Study 1: tablet</u> AUC <sub>0-∞</sub> 87% ↓ (90% CI 84-89)	Avoid coadministration of strong and moderate CYP3A inducers	Clinical trial	(40,41)
<u>Study 2: capsule</u> AUC 71% ↓ (95% CI 69-73)		PBPK simulation	(42)
<u>Study 1: tablet</u> AUC 59% ↓ (95% CI 58-62)		PBPK simulation	(40)
<u>Study 2: tablet</u> AUC 60% ↓ (95% CI 57-62)		PBPK simulation	(42)
<u>Study 2: capsule</u> AUC 53% ↓ (95% CI 50-56)			
<u>Tablet</u> AUC 0 (95% CI -1-0)		PBPK simulation	(42)
<u>Capsule</u> AUC 0 (95% CI -1-0)			
AUC <sub>0-∞</sub> 24.2% ↑ (90% CI 14.6-34.5)	None	Clinical trial	(43,44)
AZ5104 AUC <sub>0-∞</sub> 8.3% ↑ (90% CI -5.6-24.2)			
AZ7550 AUC 51% ↓ (90% CI 45-56.3)			
AUC <sub>0-24h</sub> 78.5% ↓ (90% CI 76.2-80.5)	Avoid coadministration of strong and moderate CYP3A inducers	Clinical trial	(43,44)
AZ5104 AUC <sub>0-24h</sub> 81.2% ↓ (90% CI 78.8-83.4)			
AZ7550 AUC <sub>0-24h</sub> 29.8% ↑ (19.1-41.4)			
AUC 42% ↓ (95% CI 40-44)		PBPK simulation	(45)
AUC 0.001% ↓ (95% CI 0.001-0.001)		PBPK simulation	(45)
AUC <sub>0-∞</sub> 86.8% ↑ (90% CI 72.9-101.9)	Avoid coadministration of strong CYP3A inhibitors or reduce dose of palbociclib to 75 mg QD	Clinical trial	(46,47)
AUC <sub>0-216h</sub> 42% ↑		PBPK simulation	(48)
AUC <sub>0-216h</sub> 38% ↑		PBPK simulation	(48)
AUC <sub>0-216h</sub> 0.4% ↑		PBPK simulation	(48)

Table 2. Continued.

<b>Drug (year of market approval)</b>	<b>(Primary) meta-bolism</b>	<b>Target (1)</b>	<b>Inter-patient variability (%CV)</b>	<b>Dose-linearity</b>	<b>DDI study with (interaction potential)</b>
					Fluoxetine (weak CYP3A inhibitor) Rifampin (strong CYP3A inducer) Efavirenz (moderate CYP3A inducer) Modafinil (moderate CYP3A inducer)
Sonidegib (2015)	CYP3A	Smoothened	CL/F 67% V/F 213%	Dose proportional exposure with doses up to 400 mg, with higher dose less than proportional (due to dose-dependent absorption)	Ketoconazole (strong CYP3A inhibitor)

Change in AUC	Recommendations Summary of Product Characteristics	Type of trial	References
AUC <sub>0-216h</sub> 0.3% ↑		PBPK simulation	(48)
AUC <sub>0-∞</sub> 85.2% ↓ (90% CI 81.4-88.2)	Avoid coadministration of strong CYP3A inducers	Clinical trial	(46)
AUC <sub>0-168h</sub> 38% ↓		PBPK simulation	(48)
AUC <sub>0-∞</sub> 32% ↓		Clinical trial	(47)
<u>Study 1: healthy subjects</u> AUC <sub>0-240h</sub> 125% ↑ (90% CI 78-186)	Reduce dose of sonidegib to 200 mg every other day when combined with strong CYP3A inhibitors	Clinical trial	(49,50)
<u>Study 2: cancer patients, sonidegib 1 day, ketoconazole 14 days</u> AUC <sub>0-24h</sub> 42% ↑ (90% CI 39-45)		PBPK simulation	(49,51)
<u>Study 2: sonidegib 120 days, ketoconazole 120 days</u> AUC <sub>0-24h</sub> 253% ↑ (90% CI 231-276)			
<u>Study 2: sonidegib 133 days, ketoconazole 14 days</u> AUC <sub>0-24h</sub> 101% ↑ (90% CI 92-111)			
<u>Study 2: sonidegib QOD 133 days, ketoconazole 14 days</u> AUC <sub>0-24h</sub> 93% ↑ (90% CI 84-102)			

Table 2. Continued.

<b>Drug (year of market approval)</b>	<b>(Primary) meta-bolism</b>	<b>Target (1)</b>	<b>Inter-patient variability (%CV)</b>	<b>Dose-linearity</b>	<b>DDI study with (interaction potential)</b>
					Erythromycin (moderate CYP3A inhibitor)
					Rifampin (strong CYP3A inducer)
					Efavirenz (moderate CYP3A inducer)
Sunitinib (2006)	CYP3A	VEGFR	40%	Dose proportional exposure	Ketoconazole (strong CYP3A inhibitor)



Change in AUC	Recommendations Summary of Product Characteristics	Type of trial	References
<u>Sonidegib 1 day, erythromycin 14 days</u> AUC <sub>0-24h</sub> 36% ↑ (90% CI 33-39)		PBPK simulation	(49,51)
<u>Sonidegib 120 days, erythromycin 120 days</u> AUC <sub>0-24h</sub> 179% ↑ (90% CI 76-361)			
<u>Sonidegib 133 days, erythromycin 14 days</u> AUC <sub>0-24h</sub> 79% ↑ (90% CI 71-86)			
<u>Study 1: healthy subjects</u> AUC <sub>0-240h</sub> 72.4% ↓ (90% CI 65.1-78.1)	Avoid coadministration of strong CYP3A inducers, but if necessary, consider to increase the dose to 400-800 mg	Clinical trial	(49,50)
<u>Study 2: cancer patients, sonidegib 1 day, rifampin 14 days</u> AUC <sub>0-24h</sub> 66% ↓ (90% CI 63-68)		PBPK simulation	(49,51)
<u>Study 2: sonidegib 120 days, rifampin 120 days</u> AUC <sub>0-24h</sub> 88% ↓ (90% CI 87-89)			
<u>Study 2: sonidegib 133 days, rifampin 14 days</u> AUC <sub>0-24h</sub> 80% ↓ (90% CI 78-82)		PBPK simulation	(49,51)
<u>Sonidegib 1 day, efavirenz 14 days</u> AUC <sub>0-24h</sub> 29% ↓ (90% CI 26-31)		PBPK simulation	(49,51)
<u>Sonidegib 120 days, efavirenz 120 days</u> AUC <sub>0-24h</sub> 65% ↓ (90% CI 62-67)			
<u>Sonidegib 133 days, efavirenz 14 days</u> AUC <sub>0-24h</sub> 53% ↓ (90% CI 50-56)			
Sum sunitinib and SU12662 AUC <sub>0-∞</sub> 51% ↑	Reduce dose of sunitinib to 37.5 mg QD in GIST and MRCC patients and to 25 mg QD in pancreatic/NET patients when combined with strong CYP3A inhibitors	Clinical trial	(52)

Table 2. Continued.

Drug (year of market approval)	(Primary) meta-bolism	Target (1)	Inter-patient variability (%CV)	Dose-linearity	DDI study with (interaction potential)
--------------------------------	-----------------------	------------	---------------------------------	----------------	--

Grapefruit juice (moderate CYP3A inhibitor)  
 Rifampin (strong CYP3A inducer)

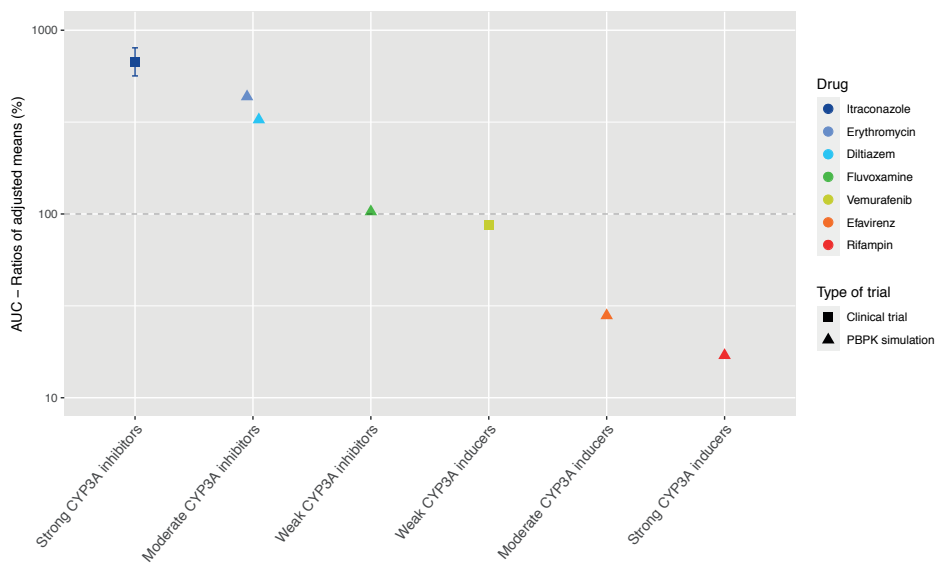


Figure 2. Overview of the results from DDI studies of cobimetinib combined with CYP3A inhibitors and inducers. The colored symbols represent the increase or decrease in AUC caused by the interacting drug, expressed as adjusted mean  $\pm$ 90% confidence interval (if available). The dashed line represents the baseline AUC.

Change in AUC	Recommendations Summary of Product Characteristics	Type of trial	References
AUC <sub>0-24h</sub> 11% ↑		Clinical trial	(53)
Sum sunitinib and SU12662 AUC <sub>0-∞</sub> 46% ↓	Increase the dose of sunitinib in steps of 12.5 mg with a maximum of 87.5 mg QD when combined with CYP3A inducers	Clinical trial	(52)

### Everolimus

The strong inhibitor ketoconazole increased the AUC<sub>0-∞</sub> of everolimus by 1,430% ( $n=12$ ) (22,23). Therefore, it is not recommended to coadminister strong CYP3A4 inhibitors with everolimus (22). The effect size of moderate inhibitors was around 25% compared with ketoconazole (increase in exposure of 340% for erythromycin ( $n=16$ ), 250% for verapamil ( $n=16$ ), 270% for imatinib ( $n$ =unknown), and 121% as average for two different cyclosporin formulations ( $n=12$ ))(24–26,28–30). Rifampin decreased the AUC of everolimus by 63% ( $n=12$ )(30). The effect of the moderate inhibitors was small compared with the strong inhibitor ketoconazole. An explanation for this finding is that ketoconazole also inhibits P-glycoprotein (P-gp), which influences the PK of everolimus in addition to CYP3A (54,55).

### Lenvatinib

Lenvatinib is for more than 80% metabolized by CYP3A to different metabolites *in vitro*. Furthermore, *in vitro* data suggests that lenvatinib is a substrate for P-gp. But *in vivo*, oxidation by aldehyde oxidase and glutathione conjugation play an important role in the metabolism of lenvatinib, next to the metabolism via CYP3A (37). Since the potency of lenvatinib is at least 20 times higher than of the metabolites, the metabolites were considered inactive (37,39). The strong CYP3A inhibitor ketoconazole increased the AUC<sub>0-∞</sub> of lenvatinib by 15% ( $n=18$ )(37,38). The strong CYP3A inducer rifampin decreased the AUC<sub>0-∞</sub> of lenvatinib by 18% when multiple doses were given ( $n=15$ )(37,39). In contrast, a single dose of rifampin increased the AUC<sub>0-∞</sub> of lenvatinib by 31%. Shumaker *et al.* explained this by a presystemic inhibition of P-gp, which is consistent with the study of Rietman *et al.* who described that rifampin can inhibit the efflux of drugs into the intestinal lumen (39,56).

The marginal effects of ketoconazole and rifampin on the lenvatinib AUC suggest that the role of CYP3A in the metabolism of lenvatinib is small. In addition, the effects of ketoconazole and rifampin on the AUC of lenvatinib could also be caused by inhibition and induction of P-gp, because both ketoconazole and rifampin have an effect on P-gp (37,54).

### *Olaparib*

Clinical DDI studies investigated the influence of itraconazole and rifampin on the AUC of olaparib administered as tablets (40,41). In PBPK simulations, the effect of inhibitors and inducers on the AUC of olaparib formulated as capsules was simulated. The effect on olaparib tablets and capsules were predicted to be similar (42).

The strong CYP3A inhibitor itraconazole increased the  $AUC_{0-\infty}$  of olaparib by 170% ( $n=59$ ) (40,41). The moderate inhibitor fluconazole increased the AUC of olaparib with an average of 115% in three PBPK simulations (40,42). Furthermore, the weak inhibitor fluvoxamine, was simulated to have no effect on the AUC of olaparib (42). Rifampin, a strong CYP3A inducer, decreased the olaparib  $AUC_{0-\infty}$  by 87% ( $n=22$ ) (40). The moderate inducer efavirenz decreased the AUC of olaparib by approximately 75%, compared with rifampin, with a decrease of 60% in a PBPK simulation (42). The weak inducer dexamethasone, was simulated to have no effect on the AUC of olaparib (42).

### *Palbociclib*

**Figure 3** shows the results of the DDI studies performed with palbociclib. The strong inhibitor itraconazole increased the palbociclib  $AUC_{0-\infty}$  by 87% ( $n=12$ ) (46,47). The moderate CYP3A inhibitors diltiazem and verapamil were simulated to increase the  $AUC_{0-216h}$  of palbociclib by half compared with itraconazole, with an increase of 40% (46,48). No effect of the weak inhibitors fluvoxamine and fluoxetine on the  $AUC_{0-216h}$  of palbociclib was predicted in a simulation study (48). Moderate CYP3A inducers decreased the palbociclib AUC by approximately half compared with strong CYP3A inducers. The strong inducer rifampin decreased the  $AUC_{0-\infty}$  of palbociclib by 85% ( $n=14$ ) (46). The moderate inducer efavirenz decreased the  $AUC_{0-168h}$  by 38% in a simulation study and modafinil decreased the  $AUC_{0-\infty}$  by 32% in a clinical trial ( $n=14$ ) (47,48).

### *Sonidegib*

In a clinical trial with healthy subjects, the strong CYP3A inhibitor ketoconazole increased the  $AUC_{0-240h}$  of sonidegib 800 mg by 125% (same was simulated for sonidegib 200 mg) (parallel study;  $n=16$  in control group and  $n=15$  in combination group) (49–51). Ketoconazole was simulated to increase the  $AUC_{0-24h}$  of sonidegib given as a single dose by 42% in cancer patients (49,51). The smaller effect of ketoconazole in cancer patients, can be explained by a decreased hepatic clearance with an elimination half-life of 28

days in cancer patients, and 10 days in healthy subjects (49). After long-term exposure to sonidegib, ketoconazole was simulated to increase the  $AUC_{0-24h}$  by 101-253%, dependent on the duration of combined use (49,51).

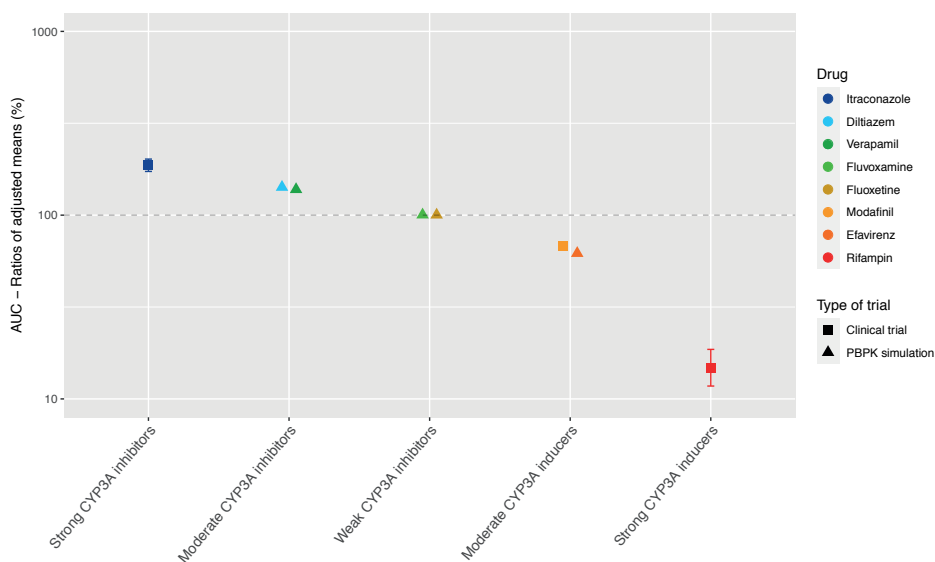


Figure 3. Overview of the results from DDI studies of palbociclib combined with CYP3A inhibitors and inducers. The colored symbols represent the increase or decrease in AUC caused by the interacting drug, expressed as adjusted mean  $\pm$ 90% confidence interval (if available). The dashed line represents the baseline AUC.

The moderate CYP3A inhibitor erythromycin increased the  $AUC_{0-24h}$  of sonidegib given as a single dose by 36% (49,51). The  $AUC_{0-24h}$  of sonidegib given long-term was increased by 79-179%, dependent on the duration of combined use with erythromycin (49,51). Compared with the simulations for ketoconazole, according to the same treatment schedule, the increases in sonidegib AUC were more than half.

In a clinical trial with healthy subjects, the strong CYP3A inducer rifampin decreased the  $AUC_{0-24oh}$  of sonidegib 800 mg by 72.4% (same was simulated for sonidegib 200 mg) (parallel study;  $n=16$  in control group and  $n=16$  in combination group)(49-51). Rifampin was simulated to decrease the  $AUC_{0-24h}$  of sonidegib given as a single dose by 66% in cancer patients (49,51). The smaller decrease in cancer patients can be explained by a decreased hepatic clearance. The  $AUC_{0-24h}$  of sonidegib was decreased by 80-88% when sonidegib given long-term and rifampin were combined, dependent on the duration of combined use (49,51).

The moderate CYP3A inducer efavirenz was simulated to decrease the  $AUC_{0-24h}$  of sonidegib given as a single dose by 29% (49,51). Efavirenz decreased the  $AUC_{0-24h}$  of sonidegib given long-term by 53-65%, dependent on the duration of combined use (49,51). Compared with the simulations of rifampin, according to the same treatment schedule, a decrease of approximately 70% was seen in sonidegib steady-state AUC.

To summarize, the interacting effect on sonidegib is influenced by the patient population and duration of therapy with sonidegib and the interacting agent.

### Drugs with active metabolites

#### *Alectinib*

Alectinib is mainly metabolized by CYP3A to the active metabolite M4. Alectinib and M4 show a similar potency and plasma protein binding *in vitro* (15,57). Therefore, the sum of alectinib and M4 concentration was reported as the pharmacologically active exposure in the DDI studies with posaconazole and rifampin (15).

**Figure 4** shows the results of the DDI studies performed with alectinib. The strong inhibitor posaconazole increased the exposure to the sum of alectinib and M4 by 36% ( $n=17$ )(14,15). The strong inducer rifampin decreased the sum of exposure by 18% ( $n=24$ )(14,15). Based on the small effects of posaconazole and rifampin, the effects of other CYP3A inhibitors and inducers on the exposure of alectinib and M4 were considered clinically irrelevant.

#### *Dabrafenib*

Dabrafenib is partially metabolized to active metabolites. It is firstly oxidized by CYP enzymes to hydroxy-dabrafenib, which is further oxidized to carboxy-dabrafenib. Carboxy-dabrafenib is converted to desmethyl-dabrafenib via a non-enzymatic process or excreted in urine or bile. Subsequently, desmethyl-dabrafenib is oxidized to other metabolites (58). Dabrafenib auto-induces its metabolism via CYP3A4 (21). Hydroxy-dabrafenib and desmethyl-dabrafenib show a similar potency and may contribute to the clinical activity of dabrafenib, on the other hand carboxy-dabrafenib does not relevantly contribute to the activity (20).

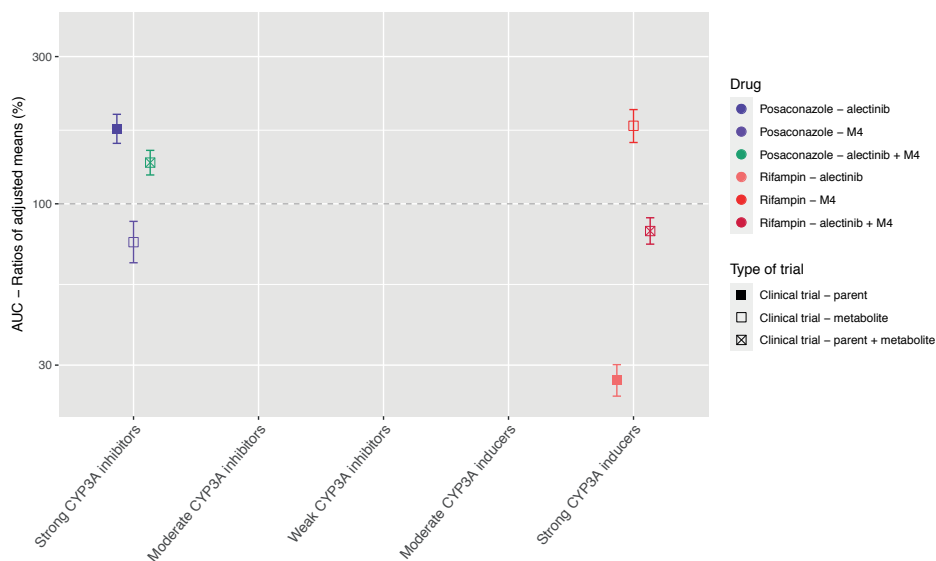


Figure 4. Overview of the results from DDI studies of alectinib combined with CYP3A inhibitors and inducers. The colored symbols represent the increase or decrease in AUC caused by the interacting drug, expressed as adjusted mean  $\pm$ 90% confidence interval (if available). The dashed line represents the baseline AUC.

The strong inhibitor ketoconazole increased the  $AUC_{0-12h}$  of dabrafenib and the metabolites hydroxy-dabrafenib and desmethyl-dabrafenib by 71, 82 and 68%, respectively, while the  $AUC_{0-12h}$  of carboxy-dabrafenib decreased by 16% ( $n=16$ )(19,20). In the DDI study with the strong inducer rifampin the opposite was seen, the AUCs of dabrafenib and desmethyl-dabrafenib decreased by 34 and 30%, respectively, and the AUC of the inactive carboxy-dabrafenib increased by 73% ( $n=23$ )(19). These results for both parent and metabolites when combined with a strong inhibitor versus a strong inducer were as expected because the conversion of dabrafenib, hydroxy-dabrafenib and desmethyl-dabrafenib is mediated by CYP enzymes and thus influenced by inhibitors and inducers of CYP3A. On the contrary, the non-enzymatic conversion of carboxy-dabrafenib is not affected by CYP3A inhibitors and inducers (58). The comparable or even higher increase in AUC for hydroxy-dabrafenib and desmethyl-dabrafenib compared to the parent, indicates higher involvement of CYP3A in elimination of the metabolites compared to their production (19,20).

### *Imatinib*

Imatinib is mainly metabolized by CYP3A. Other CYP enzymes play a minor role. Auto-inhibition of CYP3A by imatinib was shown *in vitro*, but no *in vivo* data is available (31). The main metabolite is N-desmethylimatinib also known as CGP 74588. N-desmethylimatinib is as potent as the parent compound *in vitro*. The exposure to N-desmethylimatinib is approximately 10% compared to the exposure to imatinib, therefore the effect of the metabolite is considered clinically irrelevant (59,60).

Ketoconazole in combination with a single dose of imatinib increased the imatinib  $AUC_{0-\infty}$  by 40% ( $n=14$ )(27,31). Ritonavir combined with imatinib, at imatinib steady-state, decreased the imatinib  $AUC_{0-24h}$  by 3% ( $n=11$ )(32). According to the Flockhart Table, ritonavir and ketoconazole share the same interaction potential (12). But ritonavir is also an inhibitor of CYP2D6 and inducer of CYP2C19 (12), which both play a minor role in the metabolism of imatinib (27,60). Especially the induction of CYP2C19 could be an explanation for the difference seen between the effects of ketoconazole and ritonavir. Furthermore, the difference could be caused by a shift to alternative elimination routes when imatinib is administered chronically, especially because auto-inhibition of CYP3A was shown *in vitro* (31). The two described hypotheses are supported by the *in vitro* experiment of Van Erp *et al.* which showed that ritonavir completely inhibited the metabolism of imatinib via CYP3A, but in human liver microsomes by only 50% (32). In DDI studies with CYP3A inducers large effects of the drugs rifampin and enzyme-inducing antiepileptic drugs (EIAEDs) such as carbamazepine, oxcarbazepine and phenytoin on imatinib AUC were seen. The strong inducer rifampin decreased the  $AUC_{0-\infty}$  of imatinib by 74% ( $n=14$ )(27,33). EIAEDs (mixed potency; carbamazepine and phenytoin are potent inducers, oxcarbazepine is a weak inducer (61)) decreased the  $AUC_{0-\infty}$  of imatinib by 72.5% ( $n=50$ ;  $n=27$  in EIAED group and  $n=23$  in non-EIAED group)(34). The effect of St John's Wort on imatinib exposure was smaller with an average decrease of 37% in 2 studies ( $n=12$  in study Frye *et al.*;  $n=10$  in study Smith *et al.*)(35,36). To summarize, DDI studies with mostly strong CYP3A inhibitors and inducers were performed. The effects of these drugs on imatinib were variable. This can be due to differences in study design, characteristics of the interacting drugs and also the inter-individual variability of 40-60% will have an effect (31).



### *Osimertinib*

Osimertinib is converted into different metabolites by predominantly CYP3A, among which the active metabolites AZ5104 and AZ7550. The exposure to the active metabolites is, however, less than 10% of the total drug exposure, therefore the effects of the metabolites are considered clinically irrelevant (43). Next to the metabolism by CYP3A, in *in vitro* studies CYP1A2, CYP2A6, CYP2C9, CYP2E1 also play a minor role in the metabolism of osimertinib (43,62). *In vitro* studies also showed that osimertinib is an inhibitor of CYP3A, but no *in vivo* data is available (63).

The strong inhibitor itraconazole increased the  $AUC_{0-\infty}$  of osimertinib by 24% ( $n=38$ )(43,44). On the other hand, the effect of rifampin on osimertinib exposure was large, rifampin decreased the  $AUC_{0-24h}$  by 78.5% ( $n=32$ )(43,44). The moderate inducer efavirenz was simulated to decrease the exposure by approximately 50% compared with rifampin, with a decrease in AUC of 42% (45). Dexamethasone, a weak CYP3A inducer, had no effect on the AUC of osimertinib in a PBPK simulation (45). The presence of a clinically relevant effect for the interaction of osimertinib with rifampin, while it was lacking for the interaction between osimertinib and itraconazole, could be explained by the fact that rifampin induces multiple enzymes and transporters, and that, next to CYP3A, other CYP enzymes play a role in the metabolism of osimertinib (43). For the drugs tivozanib and ixazomib, also a clinically relevant effect was shown for rifampin, while it was lacking for a CYP3A inhibitor (43,64,65).

### *Sunitinib*

Sunitinib is metabolized by CYP3A to the active metabolite SU12662, which is equally potent (52). SU12662 is metabolized further by CYP3A and transported by P-gp (66).

The strong inhibitor ketoconazole increased the sum of the  $AUC_{0-\infty}$  of sunitinib and SU12662 only by 51% ( $n=27$ )(52). Grapefruit juice, a moderate CYP3A inhibitor, increased the  $AUC_{0-24h}$  of sunitinib by 11%, which was considered negligible ( $n=8$ )(53). In this study only the AUC of sunitinib was measured and not the AUC of the metabolite SU12662. Grapefruit juice mainly inhibits intestinal CYP3A with little effect on hepatic CYP3A, while ketoconazole inhibits both (67). In addition, the small increase in AUC could be explained by the fact that in the study with ketoconazole (52), only a single dose of sunitinib was administered in contrast to the multiple dosing in the grapefruit juice study (53), which could lead to a shift to other metabolic pathways. The strong CYP3A inducer rifampin reduced the sum of the  $AUC_{0-\infty}$  of sunitinib and SU12662 by 46% ( $n=28$ )(52).

## DISCUSSION

Most currently used oral targeted anticancer drugs have a narrow therapeutic range. Furthermore, most of these drugs are substrates of CYP3A and are, therefore, prone to DDIs with inhibitors or inducers of CYP3A. It is of crucial importance for clinical practice to have guidelines on how to deal with these DDIs in cases where data is lacking, which might be the case early after drug approval. This study reviewed the literature for DDI studies performed with twelve oral anticancer drugs. Based on this data, we formulated recommendations for clinical practice on how to deal with DDIs of oral anticancer drugs when only data from strong inducers or inhibitors is available.

In our approach, we extrapolated results from dedicated DDI studies with strong inhibitors and inducers to clinical practice. Since the extrapolation of the effects of CYP3A inhibitors and inducers is more complex in the presence of active metabolites, separate recommendations are given for the drugs metabolized to inactive and with active metabolites. The recommendations are summarized in a flowchart (**Figure 5**). When interested in a victim drug without active metabolites, start in the left of the figure in the upper blue box. Follow the flowchart depending on the characteristics (inhibitor or inducer; interaction potential) of the drug you are interested in. The last box will show you our recommendation regarding the interaction. When interested in a victim drug with active metabolites, start in the right of the figure in the upper orange box. When the metabolite contributes less than 10% to total drug exposure or less than 50% to total drug effect, the presence of an active metabolite can be neglected. Therefore, the part of the flowchart for drugs without active metabolites can be followed. If the metabolite has a relevant contribution to total drug exposure and effect, the part of the flowchart for drugs without active metabolites can be followed, using the sum of parent and metabolite, or assessing the effect of parent and metabolite separately.

For the studied drugs without active metabolites, **Tables 1** and **2** show that the effect of moderate CYP3A inhibitors on the AUC is roughly approximate to 50% of the effect of the strong inhibitors. The same effect can be seen for moderate inducers in comparison with strong inducers. Furthermore, it can be noted that weak inhibitors and inducers had marginal effects on the exposure of the studied drugs. In **Figures 2** and **3**, these results are visualized for the drugs cobimetinib and palbociclib, which gives a good representation of the effects seen for all seven drugs without active metabolites (the **Supplementary Material** shows figures for the other drugs).

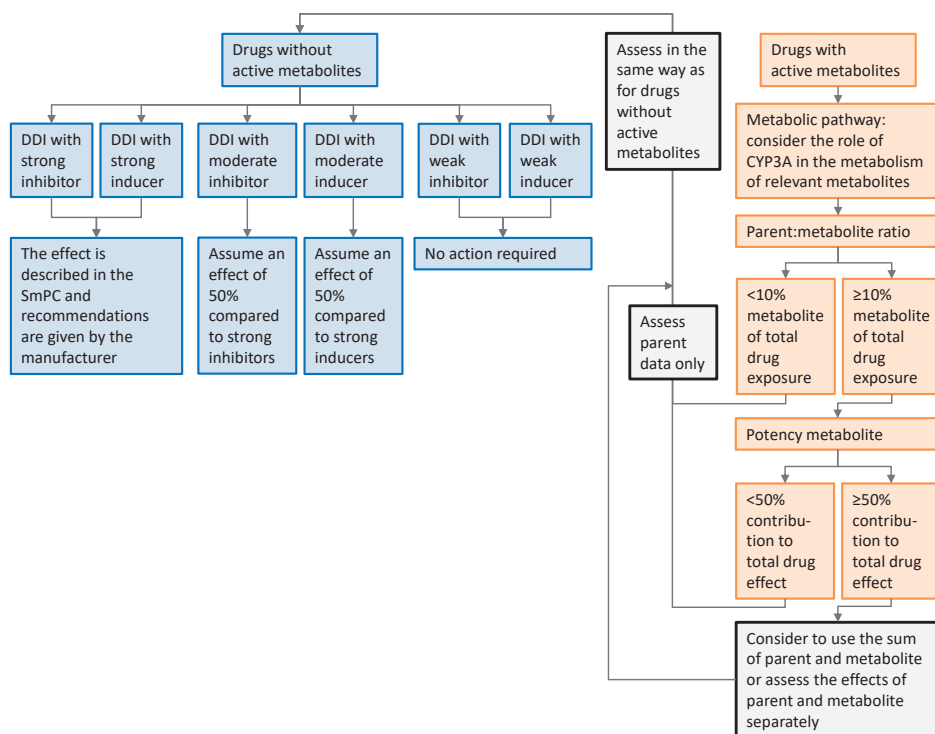


Figure 5. Flowchart of the recommendations on how to handle DDIs for oral anticancer drugs metabolized by CYP3A if only clinical data from strong CYP3A inhibitors or inducers is available. Caution should be taken while using the flowchart for drugs in which auto-induction or -inhibition plays a role and drug-drug interaction studies are not performed on steady-state, or for drugs with nonlinear dose-exposure relationships.

Regarding drug selection for this review we made the following decisions. Drugs which have been approved for solid tumors from January 1st, 2013 to December 31st, 2015, and three drugs (everolimus, imatinib, sunitinib) authorized before 2013 based on the availability of relevant clinical data were selected. This resulted in a selection of twelve drugs. This was decided since 1) no difference is to be expected in quality of PBPK simulations performed in early years (2013 to 2015) compared to later years, and 2) the results of all twelve analyzed drugs in this review roughly indicate the same direction on the extrapolation of the effects of DDI studies. For the twelve drugs selected in our analysis, only for sunitinib and palbociclib a clinical trial was performed with a moderate CYP3A inhibitor and inducer, respectively. Also for the seven drugs that were approved after 2015 and met the inclusion criteria regarding metabolism and indication (abemaciclib, brigatinib, entrectinib, larotrectinib, lorlatinib, neratinib, and ribociclib) no clinical DDI studies with moderate inhibitors/

inducers, but only PBPK simulations were performed (or no DDI studies at all). Furthermore, we decided to focus on oral anticancer drugs in our review. However, our recommendations are probably also applicable to other drugs metabolized by CYP3A.

It is important to take into account the following, regarding our recommendations. First, a large variability in the PK after multiple doses occurred in the studied drugs, with a range of 23-78%. Similarly, Verheijen *et al.* showed that there is a high inter-individual variability in the exposure to kinase inhibitors (1). This is also reflected by the large variability in the effect of CYP3A inhibitors and inducers for some drugs. Possibly, this variability in exposure could partly be explained by the highly variable CYP3A4 activity among patients, which is for 60 to 90% genetically determined (68,69). For example, the *CYP3A4*\*22 polymorphism has been described, resulting in a two-fold increase of the formation of a non-functional variant of CYP3A4 (70). If the CYP3A4 activity is decreased by a genetic polymorphism, the magnitude of the effect of a CYP3A inhibitor will theoretically be decreased. Furthermore, caution should be taken while using the flowchart for drugs in which auto-induction or -inhibition plays a role and drug-drug interaction studies are not performed on steady-state, or for drugs with nonlinear dose-exposure relationships. In these cases it might not be possible to extrapolate results from DDI studies with strong inhibitors and inducers, or dose recommendations based on these results. While interpreting the results of this review it is necessary to bear in mind this large variability in PK, and the exceptions in which our recommendations might not be applicable.

Next to the results of the drugs without active metabolites, **Tables 1** and **2** show that for drugs that have active metabolites the results are less straightforward. As a visual example **Figure 4** was made, which shows the effect of interacting drugs on the AUC of the parent drug alectinib and its active metabolite (similar figures are presented in the **Supplementary Material** for the other studied drugs). There are three factors to take into account while interpreting the results of DDI studies with drugs with active metabolites. Firstly, the metabolic pathway is important. For example, in case of dabrafenib not only the parent, but also two of the active metabolites are metabolized by CYP3A, whereas the third metabolite is converted non-enzymatically. This results in an effect of CYP3A inhibitors and inducers on both parent and some of the metabolites, but not all of them.

Secondly, the ratio between parent and metabolites should be taken into account. As a cut-off value a contribution of less than 10% of the metabolite to total drug exposure could be used. This is in line with the EMA recommendation to characterize metabolites structurally that contribute to more than 10% of the AUC of a drug in *in vitro* studies (13). An example of a drug with an active metabolite which contributes to less than 10% of total drug exposure is osimertinib. Thirdly, the potency of the metabolites plays an important role. A cut-off value of 50% contribution to the total drug effect can be used when considering the relevance of the contribution of an active metabolite. This cut-off value is supported by the EMA (13). Shown by the recommendation to conduct an *in vivo* DDI study not only for drugs where enzymes contribute to at least 25% of the overall elimination but also for drugs with pharmacologically active metabolites which contribute to 50% or more of the effect of the drug (and enzymes are involved in the formation or elimination of these metabolites)(13). For example, if a metabolite is as potent as the parent drug, the effect of an interacting drug on the sum of parent and metabolite might be reported as measure of total drug activity, as was done in the case of alectinib and sunitinib.

A practical example for the drug palbociclib is given. The assumption of an effect of 50% in comparison to that of strong inhibitors and inducers can be used to extrapolate the advice of the manufacturer. In case of palbociclib, the standard dose is 125 mg once daily (QD). The manufacturer recommends to reduce the dose of palbociclib to 75 mg QD if combination with a strong CYP3A inhibitor cannot be avoided. In combination with a moderate CYP3A inducer it could be considered to reduce the dose with 50% compared with the reduction in combination with strong inhibitors. This would result in a dose of 100 mg QD (46). A reason to reduce the dose of palbociclib is that a higher palbociclib exposure is associated with increased toxicity, specifically a larger decrease in absolute neutrophil count when compared with baseline. However, the limited data available on exposure-response and exposure-toxicity relationships could be a consideration to start with the standard starting dose and decrease the dose in case toxicity occurs (1,46,71).

After initiation of therapy with oral anticancer drugs in a reduced or increased dose, attainment of adequate drug exposure could be monitored by means of Therapeutic Drug Monitoring. Many of the oral anticancer drugs show an exposure-efficacy and an exposure-toxicity relationship, the strength of the evidence for these relationships is and recommendations for target plasma trough levels are discussed by Verheijen *et al.* (1).



## CONCLUSION

In conclusion, DDIs are often very complex and dependent on multiple factors. But, if only data from strong CYP3A inhibitors or inducers is available, in case of drugs without active metabolites, a change in exposure of 50% for moderate inhibitors/inducers compared with strong inhibitors/inducers can be assumed. We therefore recommend to start with a 50% dose reduction compared with the advised reduction in combination with strong inhibitors, and with a 50% dose increase compared to the advised increase in combination with strong inducers.

Since an effect of weak CYP3A inhibitors on the AUC of oral anticancer drugs is small in the twelve reviewed drugs, *a priori* dose adaptations are not indicated. Additionally, for only one of the drugs a DDI study was performed with a weak inducer, showing a small effect, therefore the effects of DDIs with weak inducers are considered irrelevant.

In the presence of active metabolites, the response on DDIs should be based on the metabolic pathway, the exposure to the metabolites compared with the parent drug and to the potency of the metabolites. Options are to ignore the presence of a metabolite (for example when a metabolite is not pharmacologically active or contributes minimal to the exposure of the drug) or to use the sum of the parent and metabolite (at least do this when parent and metabolite are equally potent).

## REFERENCES

1. Verheijen RB, Yu H, Schellens JHM, Beijnen JH, Steeghs N, Huitema ADR. Practical Recommendations for Therapeutic Drug Monitoring of Kinase Inhibitors in Oncology. *Clin Pharmacol Ther.* 2017;102(5):765–76.
2. Groenland SL, van Nuland M, Verheijen RB, Schellens JHM, Beijnen JH, Huitema ADR, et al. Therapeutic Drug Monitoring of Oral Anti-Hormonal Drugs in Oncology. *Clin Pharmacokinet.* 2019;58(3):299–308.
3. Food and Drug Administration. Center for Drug Evaluation and Research. Clinical Drug Interaction Studies - Study Design, Data Analysis, and Clinical Implications Guidance for Industry Draft Guidance [Internet]. 2009 [cited 2020 May 14]. Available from: <http://www.fda.gov/Drugs/GuidanceComplianceRegulatoryInformation/Guidances/default.htm>
4. European Medicines Agency Committee for Medicinal Products For Human Use (CHMP). Guideline on the investigation of drug interactions [Internet]. 2015 [cited 2020 May 14]. Available from: [https://www.ema.europa.eu/en/documents/scientific-guideline/guideline-investigation-drug-interactions-revision-1\\_en.pdf](https://www.ema.europa.eu/en/documents/scientific-guideline/guideline-investigation-drug-interactions-revision-1_en.pdf)
5. Food and Drug Administration. Center for Drug Evaluation and Research. Clinical Drug Interaction Studies — Cytochrome P450 Enzyme- and Transporter-Mediated Drug Interactions Guidance for Industry [Internet]. 2020 [cited 2020 Jun 11]. Available from: <https://www.fda.gov/media/134581/download>
6. Food and Drug Administration. Center for Drug Evaluation and Research. In Vitro Drug Interaction Studies — Cytochrome P450 Enzyme and Transporter Mediated Drug Interactions [Internet]. 2020 [cited 2021 Jul 9]. Available from: <https://www.fda.gov/media/134582/download>
7. Food and Drug Administration. Center for Drug Evaluation and Research. Physiologically Based Pharmacokinetic Analyses — Format and Content [Internet]. 2018 [cited 2021 Jul 8]. Available from: <https://www.fda.gov/media/101469/download>
8. Food and Drug Administration. Center for Drug Evaluation and Research Larotrectinib Multidiscipline Review [Internet]. 2018 [cited 2020 Dec 14]. Available from: [https://www.accessdata.fda.gov/drugsatfda\\_docs/nda/2018/210861Orig1s000\\_211710Orig1s000MultidisciplineR.pdf](https://www.accessdata.fda.gov/drugsatfda_docs/nda/2018/210861Orig1s000_211710Orig1s000MultidisciplineR.pdf)
9. Food and Drug Administration. Center for Drug Evaluation and Research Lorlatinib Multidiscipline Review [Internet]. 2017 [cited 2020 Dec 14]. Available from: [https://www.accessdata.fda.gov/drugsatfda\\_docs/nda/2018/210868Orig1s000MultidisciplineR.pdf](https://www.accessdata.fda.gov/drugsatfda_docs/nda/2018/210868Orig1s000MultidisciplineR.pdf)
10. Patel M, Chen J, McGrory S, O’Gorman M, Nepal S, Ginman K, et al. The Effect of Itraconazole on the Pharmacokinetics of Lorlatinib: Results of a Phase I, Open-Label, Crossover Study in Healthy Participants. *Invest New Drugs.* 2020;38:131–9.
11. Chen J, Xu H, Pawlak S, James LP, Peltz G, Lee K, et al. The Effect of Rifampin on the Pharmacokinetics and Safety of Lorlatinib: Results of a Phase One, Open-Label, Crossover Study in Healthy Participants. *Adv Ther.* 2020;37(2):745–58.
12. Flockhart DA. Drug Interactions: Cytochrome P450 Drug Interaction Table. [Internet]. Indiana University School of Medicine. 2007 [cited 2019 Sep 3]. Available from: <https://drug-interactions.medicine.iu.edu>
13. European Medicines Agency Committee for Medicinal Products For Human Use (CHMP). Guideline on the investigation of drug interactions [Internet]. 2015 [cited 2020 May 14]. Available from: [https://www.ema.europa.eu/en/documents/scientific-guideline/guideline-investigation-drug-interactions-revision-1\\_en.pdf](https://www.ema.europa.eu/en/documents/scientific-guideline/guideline-investigation-drug-interactions-revision-1_en.pdf)



14. Food and Drug Administration. Center for Drug Evaluation and Research Alectinib Clinical Pharmacology and Biopharmaceutics Review [Internet]. 2015 [cited 2019 Sep 20]. Available from: [https://www.accessdata.fda.gov/drugsatfda\\_docs/nda/2015/208434Orig1s000ClinPharmR.pdf](https://www.accessdata.fda.gov/drugsatfda_docs/nda/2015/208434Orig1s000ClinPharmR.pdf)
15. Morcos PN, Cleary Y, Guerini E, Dall G, Bogman K, De Petris L, et al. Clinical Drug–Drug Interactions Through Cytochrome P450 3A (CYP3A) for the Selective ALK Inhibitor Alectinib. *Clin Pharmacol Drug Dev.* 2017;6(3):280–91.
16. Food and Drug Administration. Center for Drug Evaluation and Research Ceritinib Clinical Pharmacology and Biopharmaceutics Review [Internet]. 2014 [cited 2019 Sep 20]. Available from: [https://www.accessdata.fda.gov/drugsatfda\\_docs/nda/2014/205755Orig1s000ClinPharmR.pdf](https://www.accessdata.fda.gov/drugsatfda_docs/nda/2014/205755Orig1s000ClinPharmR.pdf)
17. Food and Drug Administration. Center for Drug Evaluation and Research Cobimetinib Clinical Pharmacology and Biopharmaceutics Review [Internet]. 2014 [cited 2019 Sep 20]. Available from: [https://www.accessdata.fda.gov/drugsatfda\\_docs/nda/2015/206192Orig1s000ClinPharmR.pdf](https://www.accessdata.fda.gov/drugsatfda_docs/nda/2015/206192Orig1s000ClinPharmR.pdf)
18. Budha NR, Ji T, Musib L, Eppler S, Dresser M, Chen Y, et al. Evaluation of Cytochrome P450 3A4-Mediated Drug–Drug Interaction Potential for Cobimetinib Using Physiologically Based Pharmacokinetic Modeling and Simulation. *Clin Pharmacokinet.* 2016;55(11):1435–45.
19. European Medicines Agency Committee for Medicinal Products For Human Use (CHMP). Dabrafenib European Public Assessment Report [Internet]. 2018 [cited 2019 Sep 19]. Available from: [https://www.ema.europa.eu/en/documents/product-information/tafinlar-epar-product-information\\_en.pdf](https://www.ema.europa.eu/en/documents/product-information/tafinlar-epar-product-information_en.pdf)
20. Suttle AB, Grossmann KF, Ouellet D, Richards–Peterson LE, Aktan G, Gordon MS, et al. Assessment of the drug interaction potential and single- and repeat-dose pharmacokinetics of the BRAF inhibitor dabrafenib. *J Clin Pharmacol.* 2015;55(4):392–400.
21. Food and Drug Administration. Center for Drug Evaluation and Research Dabrafenib Clinical Pharmacology and Biopharmaceutics Review [Internet]. 2012 [cited 2021 Jul 20]. Available from: [https://www.accessdata.fda.gov/drugsatfda\\_docs/nda/2013/202806Orig1s000ClinPharmR.pdf](https://www.accessdata.fda.gov/drugsatfda_docs/nda/2013/202806Orig1s000ClinPharmR.pdf)
22. Food and Drug Administration. Center for Drug Evaluation and Research Everolimus Clinical Pharmacology and Biopharmaceutics Review [Internet]. 2008 [cited 2019 Sep 20]. Available from: [https://www.accessdata.fda.gov/drugsatfda\\_docs/nda/2009/022334s000\\_ClinPharmR.pdf](https://www.accessdata.fda.gov/drugsatfda_docs/nda/2009/022334s000_ClinPharmR.pdf)
23. Kovarik JM, Beyer D, Bizot MN, Jiang Q, Shenouda M, Schmouder RL. Blood concentrations of everolimus are markedly increased by ketoconazole. *J Clin Pharmacol.* 2005;45(5):514–8.
24. European Medicines Agency Committee for Medicinal Products For Human Use (CHMP). Everolimus European Public Assessment Report [Internet]. 2014. [cited 2019 Sep 19]. Available from: [https://www.ema.europa.eu/en/documents/product-information/afinitor-epar-product-information\\_en.pdf](https://www.ema.europa.eu/en/documents/product-information/afinitor-epar-product-information_en.pdf)
25. Kovarik JM, Beyer D, Bizot MN, Jiang Q, Shenouda M, Schmouder RL. Effect of multiple-dose erythromycin on everolimus pharmacokinetics. *Eur J Clin Pharmacol.* 2005;61(1):35–8.
26. Kovarik JM, Beyer D, Bizot MN, Jiang Q, Allison MJ, Schmouder RL. Pharmacokinetic interaction between verapamil and everolimus in healthy subjects. *Br J Clin Pharmacol.* 2005;60(4):434–7.
27. European Medicines Agency Committee for Medicinal Products For Human Use (CHMP). Imatinib European Public Assessment Report [Internet]. 2006 [cited 2019 Sep 19]. Available from: [https://www.ema.europa.eu/en/documents/product-information/glivec-epar-product-information\\_en.pdf](https://www.ema.europa.eu/en/documents/product-information/glivec-epar-product-information_en.pdf)



28. Kovarik JM, Beyer D, Schmouder RL. Everolimus Drug Interactions: Application of a Classification System for Clinical Decision Making. *Biopharm Drug Dispos.* 2006;27(October 2006):421-6.
29. Kovarik JM, Kalbag J, Figueiredo J, Rouilly M, O'Bannon L, Rordorf C. Differential Influence of Two Cyclosporine Formulations on Everolimus Pharmacokinetics: A Clinically Relevant Pharmacokinetic Interaction. *J Clin Pharmacol.* 2002;42:95-9.
30. Kovarik JM, Hartmann S, Figueiredo J, Rouilly M, Port A, Rordorf C. Effect of rifampin on apparent clearance of everolimus. *Ann Pharmacother.* 2002;36(6):981-5.
31. Food and Drug Administration. Center for Drug Evaluation and Research Imatinib Clinical Pharmacology and Biopharmaceutics Review [Internet]. 2001 [cited 2019 Sep 19]. Available from: [https://www.accessdata.fda.gov/drugsatfda\\_docs/nda/2001/21-335\\_Gleevec\\_biopharmr\\_P1.pdf](https://www.accessdata.fda.gov/drugsatfda_docs/nda/2001/21-335_Gleevec_biopharmr_P1.pdf)
32. Van Erp NP, Gelderblom H, Karlsson MO, Li J, Zhao M, Ouwerkerk J, et al. Influence of CYP3A4 inhibition on the steady-state pharmacokinetics of imatinib. *Clin Cancer Res.* 2007;13(24):7394-400.
33. Bolton AE, Peng B, Hubert M, Krebs-Brown A, Capdeville R, Keller U, et al. Effect of rifampicin on the pharmacokinetics of imatinib mesylate (Gleevec, ST1571) in healthy subjects. *Cancer Chemother Pharmacol.* 2004;53(2):102-6.
34. Wen PY, Yung WKA, Lamborn KR, Dahia PL, Wang Y, Peng B, et al. Phase I/II study of imatinib mesylate for recurrent malignant gliomas: North American Brain Tumor Consortium Study 99-08. *Clin Cancer Res.* 2006;12(16):4899-907.
35. Frye RF, Fitzgerald SM, Lagattuta TF, Hruska MW, Egorin MJ. Effect of St John's wort on imatinib mesylate pharmacokinetics. *Clin Pharmacol Ther.* 2004;76(4):323-9.
36. Smith PF, Bullock JM, Booker BM, Haas CE, Berenson CS, Jusko WJ. The influence of St. John's Wort on the pharmacokinetics and protein binding of imatinib mesylate. *Pharmacotherapy.* 2004;24(11):1508-14.
37. Food and Drug Administration. Center for Drug Evaluation and Research Lenvatinib Clinical Pharmacology and Biopharmaceutics Review [Internet]. 2015 [cited 2019 Sep 20]. Available from: [https://www.accessdata.fda.gov/drugsatfda\\_docs/nda/2015/206947Orig1s000ClinPharmR.pdf](https://www.accessdata.fda.gov/drugsatfda_docs/nda/2015/206947Orig1s000ClinPharmR.pdf)
38. Shumaker R, Aluri J, Fan J, Martinez G, Thompson GA, Ren M. Effects of ketoconazole on the pharmacokinetics of lenvatinib (E7080) in healthy participants. *Clin Pharmacol Drug Dev.* 2015;4(2):155-60.
39. Shumaker RC, Aluri J, Fan J, Martinez G, Thompson GA, Ren M. Effect of rifampicin on the pharmacokinetics of lenvatinib in healthy adults. *Clin Drug Investig.* 2014;34(9):651-9.
40. Food and Drug Administration. Center for Drug Evaluation and Research Olaparib Clinical Pharmacology and Biopharmaceutics Review [Internet]. 2014 [cited 2019 Sep 20]. Available from: [https://www.accessdata.fda.gov/drugsatfda\\_docs/nda/2014/206162Orig1s000ClinPharmR.pdf](https://www.accessdata.fda.gov/drugsatfda_docs/nda/2014/206162Orig1s000ClinPharmR.pdf)
41. Dirix L, Swaisland H, Verheul HMW, Rottey S, Leunen K, Jerusalem G, et al. Effect of Itraconazole and Rifampin on the Pharmacokinetics of Olaparib in Patients With Advanced Solid Tumors: Results of Two Phase I Open-label Studies. *Clin Ther.* 2016;38(10):2286-99.
42. Pilla Reddy V, Bui K, Scarfe G, Zhou D, Learoyd M. Physiologically Based Pharmacokinetic Modeling for Olaparib Dosing Recommendations: Bridging Formulations, Drug Interactions, and Patient Populations. *Clin Pharmacol Ther.* 2019;105(1):229-41.

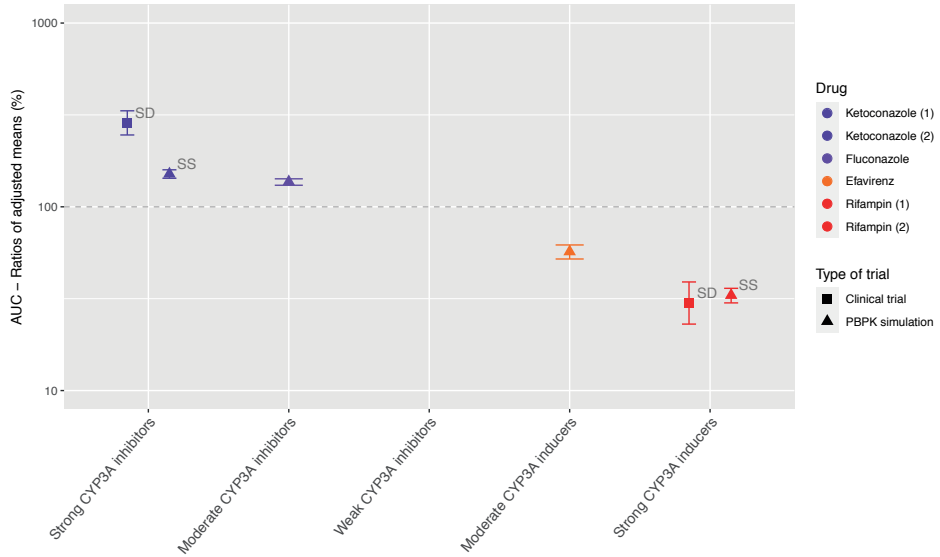
43. Vishwanathan K, Dickinson PA, So K, Thomas K, Chen YM, De Castro Carpeño J, et al. The effect of itraconazole and rifampicin on the pharmacokinetics of osimertinib. *Br J Clin Pharmacol*. 2018;84(6):1156-69.
44. European Medicines Agency Committee for Medicinal Products For Human Use (CHMP). Osimertinib European Public Assessment Report [Internet]. 2016 [cited 2019 Sep 20]. Available from: [https://www.ema.europa.eu/en/documents/product-information/tagrisso-epar-product-information\\_en.pdf](https://www.ema.europa.eu/en/documents/product-information/tagrisso-epar-product-information_en.pdf)
45. Reddy VP, Walker M, Sharma P, Ballard P, Vishwanathan K. Development, verification, and prediction of osimertinib drug-drug interactions using PBPK modeling approach to inform drug label. *CPT Pharmacometrics Syst Pharmacol*. 2018;7(5):321-30.
46. Food and Drug Administration. Center for Drug Evaluation and Research Palbociclib Clinical Pharmacology and Biopharmaceutics Review [Internet]. 2014 [cited 2019 Sep 20]. Available from: [https://www.accessdata.fda.gov/drugsatfda\\_docs/nda/2015/207103Orig1s000ClinPharmR.pdf](https://www.accessdata.fda.gov/drugsatfda_docs/nda/2015/207103Orig1s000ClinPharmR.pdf)
47. European Medicines Agency Committee for Medicinal Products For Human Use (CHMP). Palbociclib European Public Assessment Report [Internet]. 2016 [cited 2019 Sep 20]. Available from: [https://www.ema.europa.eu/en/documents/product-information/ibrance-epar-product-information\\_en.pdf](https://www.ema.europa.eu/en/documents/product-information/ibrance-epar-product-information_en.pdf)
48. Yu Y, Loi C-M, Hoffman J, Wang D. Physiologically Based Pharmacokinetic Modeling of Palbociclib. *J Clin Pharmacol*. 2017;57(2):173-84.
49. Food and Drug Administration. Center for Drug Evaluation and Research Sonidegib Clinical Pharmacology and Biopharmaceutics Review [Internet]. 2015 [cited 2020 May 25]. Available from: [https://www.accessdata.fda.gov/drugsatfda\\_docs/nda/2015/205266Orig1s000ClinPharmR.pdf](https://www.accessdata.fda.gov/drugsatfda_docs/nda/2015/205266Orig1s000ClinPharmR.pdf)
50. European Medicines Agency Committee for Medicinal Products For Human Use (CHMP). Sonidegib European Public Assessment Report [Internet]. 2015 [cited 2020 Jun 2]. Available from: [https://www.ema.europa.eu/en/documents/product-information/odomzo-epar-product-information\\_en.pdf](https://www.ema.europa.eu/en/documents/product-information/odomzo-epar-product-information_en.pdf)
51. Einolf HJ, Zhou J, Won C, Wang L, Rebello S. A physiologically-based pharmacokinetic modeling approach to predict drug-drug interactions of sonidegib (LDE225) with perpetrators of CYP3A in cancer patients. *Drug Metab Dispos*. 2017;45(4):361-74.
52. Food and Drug Administration. Center for Drug Evaluation and Research Sunitinib Clinical Pharmacology and Biopharmaceutics Review [Internet]. 2005 [cited 2019 Sep 20]. Available from: [https://www.accessdata.fda.gov/drugsatfda\\_docs/nda/2006/021938\\_S000\\_Sutent\\_BioPharmR.pdf](https://www.accessdata.fda.gov/drugsatfda_docs/nda/2006/021938_S000_Sutent_BioPharmR.pdf)
53. Van Erp NP, Baker SD, Zandvliet AS, Ploeger BA, Den Hollander M, Chen Z, et al. Marginal increase of sunitinib exposure by grapefruit juice. *Cancer Chemother Pharmacol*. 2011;67(3):695-703.
54. European Medicines Agency Committee for Medicinal Products For Human Use (CHMP). Ketoconazole HRA European Public Assessment Report [Internet]. 2014 [cited 2019 Sep 19]. Available from: [https://www.ema.europa.eu/en/documents/product-information/ketoconazole-hra-epar-product-information\\_en.pdf](https://www.ema.europa.eu/en/documents/product-information/ketoconazole-hra-epar-product-information_en.pdf)
55. Ravaud A, Urva SR, Grosch K, Cheung WK, Anak O, Sellami DB. Relationship between everolimus exposure and safety and efficacy: Meta-analysis of clinical trials in oncology. *Eur J Cancer*. 2014;50(3):486-95.

56. Reitman ML, Chu X, Cai X, Yabut J, Venkatasubramanian R, Zajic S, et al. Rifampin's acute inhibitory and chronic inductive drug interactions: Experimental and model-based approaches to drug-drug interaction trial design. *Clin Pharmacol Ther.* 2011;89(2):234–42.
57. Fowler S, Morcos PN, Cleary Y, Martin-Facklam M, Parrott N, Gertz M, et al. Progress in Prediction and Interpretation of Clinically Relevant Metabolic Drug-Drug Interactions: a Minireview Illustrating Recent Developments and Current Opportunities. *Curr Pharmacol Reports.* 2017;3(1):36–49.
58. Bershas DA, Ouellet D, Mamaril-Fishman DB, Nebot N, Carson SW, Blackman SC, et al. Metabolism and disposition of oral dabrafenib in cancer patients: Proposed participation of aryl nitrogen in carbon-carbon bond cleavage via decarboxylation following enzymatic oxidation. *Drug Metab Dispos.* 2013;41(12):2215–24.
59. Peng B, Lloyd P, Schran H. Clinical pharmacokinetics of imatinib. *Clin Pharmacokinet.* 2005;44(9):879–94.
60. Whirl-Carrillo M, McDonagh E, Hebert J, Gong L, Sangkuhl K, Thorn C, et al. Pharmacogenomics knowledge for personalized medicine. *Clin Pharmacol Ther [Internet].* 2012; Available from: <https://www.pharmgkb.org/pathway/PA164713427/overview>
61. Riva R, Albani F, Contin M, A B. Pharmacokinetic interactions between antiepileptic drugs. Clinical considerations. *Clin Pharmacokinet.* 1996;31(6):470–93.
62. Dickinson PA, Cantarini M V., Collier J, Frewer P, Martin S, Pickup K, et al. Metabolic disposition of osimertinib in rats, dogs, and humans: Insights into a drug designed to bind covalently to a cysteine residue of epidermal growth factor receptor. *Drug Metab Dispos.* 2016;44(8):1201–12.
63. Food and Drug Administration. Center for Drug Evaluation and Research Osimertinib Clinical Pharmacology and Biopharmaceutics Review [Internet]. 2015 [cited 2021 Jul 12]. Available from: [https://www.accessdata.fda.gov/drugsatfda\\_docs/nda/2015/208065Orig1s000ClinPharmR.pdf](https://www.accessdata.fda.gov/drugsatfda_docs/nda/2015/208065Orig1s000ClinPharmR.pdf)
64. Gupta N, Hanley MJ, Venkatakrishnan K, Bessudo A, Rasco DW, Sharma S, et al. Effects of Strong CYP3A Inhibition and Induction on the Pharmacokinetics of Ixazomib, an Oral Proteasome Inhibitor: Results of Drug-Drug Interaction Studies in Patients With Advanced Solid Tumors or Lymphoma and a Physiologically Based Pharmacokinetic Ana. *J Clin Pharmacol.* 2018;58(2):180–92.
65. Cotreau MM, Siebers NM, Miller J, Strahs AL, Slichenmyer W. Effects of ketoconazole or rifampin on the pharmacokinetics of tivozanib hydrochloride, a vascular endothelial growth factor receptor tyrosine kinase inhibitor. *Clin Pharmacol Drug Dev.* 2015;4(2):137–42.
66. Heath EI, Blumenschein GR, Cohen RB, Lorusso PM, Loconte NK, Kim ST, et al. Sunitinib in combination with paclitaxel plus carboplatin in patients with advanced solid tumors: Phase I study results. *Cancer Chemother Pharmacol.* 2011;68(3):703–12.
67. Saito M, Hirata-Koizumi M, Matsumoto M, Urano T, Hasegawa R. Undesirable effects of citrus juice on the pharmacokinetics of drugs: Focus on recent studies. *Drug Saf.* 2005;28(8):677–94.
68. Westlind-Johnsson A, Malmbo S, Johansson A, Otter C, Andersson TB, Johansson I, et al. Comparative analysis of CYP3A expression in human liver suggests only a minor role for CYP3A5 in drug metabolism. *Drug Metab Dispos.* 2003;31(6):755–61.
69. Özdemir V, Kalow W, Tang BK, Paterson AD, Walker SE, Endrenyi L, et al. Evaluation of the genetic component of variability in CYP3A4 activity: A repeated drug administration method. *Pharmacogenetics.* 2000;10(5):373–88.

70. Wang D, Guo Y, Wrighton SA, Cooke GE, Sadee W. Intronic polymorphism in CYP3A4 affects hepatic expression and response to statin drugs. *Pharmacogenomics J.* 2011;11(4):274–86.
71. Flaherty KT, Lorusso PM, Demichele A, Abramson VG, Courtney R, Randolph SS, et al. Phase I, Dose-Escalation Trial of the Oral Cyclin-Dependent Kinase 4/6 Inhibitor PD 0332991, Administered Using a 21-Day Schedule in Patients with Advanced Cancer. 2012;18(12):568–77.

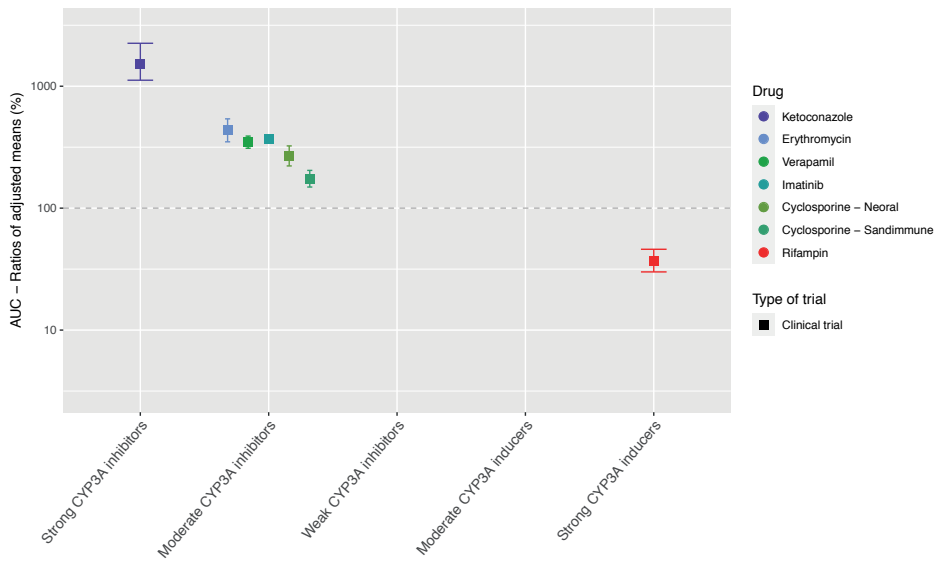
## SUPPLEMENTARY MATERIAL

### Figures for drugs without active metabolites

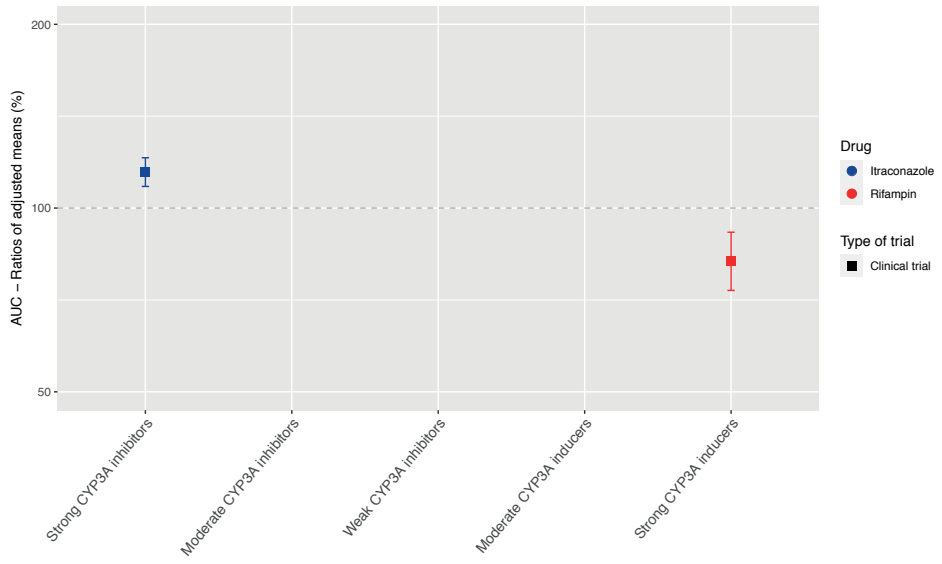


Supplementary Figure S1. Overview of the results from DDI studies of ceritinib combined with CYP3A inhibitors and inducers. The colored symbols represent the increase or decrease in AUC caused by the interacting drug, expressed as adjusted mean  $\pm$  90% confidence interval (if available). The dashed line represents the baseline AUC. SD, single dose; SS, steady-state.

1

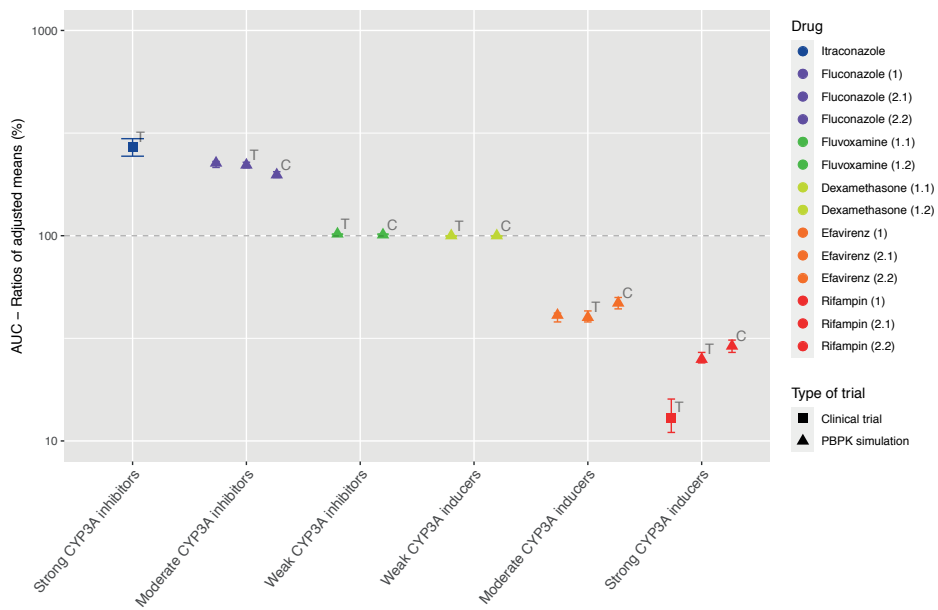


Supplementary Figure S2. Overview of the results from DDI studies of everolimus combined with CYP3A inhibitors and inducers. The colored symbols represent the increase or decrease in AUC caused by the interacting drug, expressed as adjusted mean  $\pm$ 90% confidence interval (if available). The dashed line represents the baseline AUC.



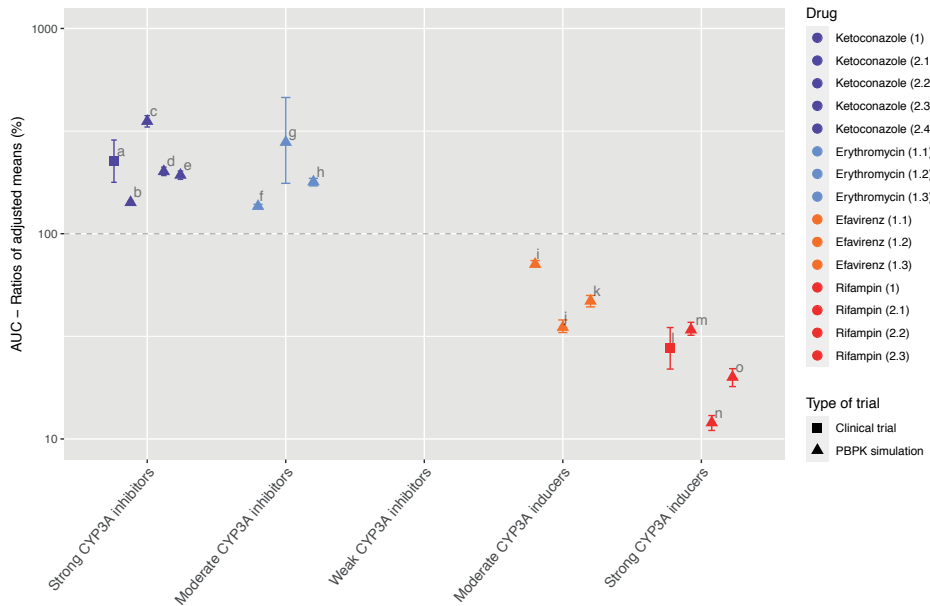
Supplementary Figure S3. Overview of the results from DDI studies of lenvatinib combined with CYP3A inhibitors and inducers. The colored symbols represent the increase or decrease in AUC caused by the interacting drug, expressed as adjusted mean  $\pm$ 90% confidence interval (if available). The dashed line represents the baseline AUC.





Supplementary Figure S4. Overview of the results from DDI studies of olaparib combined with CYP3A inhibitors and inducers. The colored symbols represent the increase or decrease in AUC caused by the interacting drug, expressed as adjusted mean  $\pm$ 90% confidence interval (if available). The dashed line represents the baseline AUC. T, DDI study with olaparib tablets; C, DDI study with olaparib capsules.

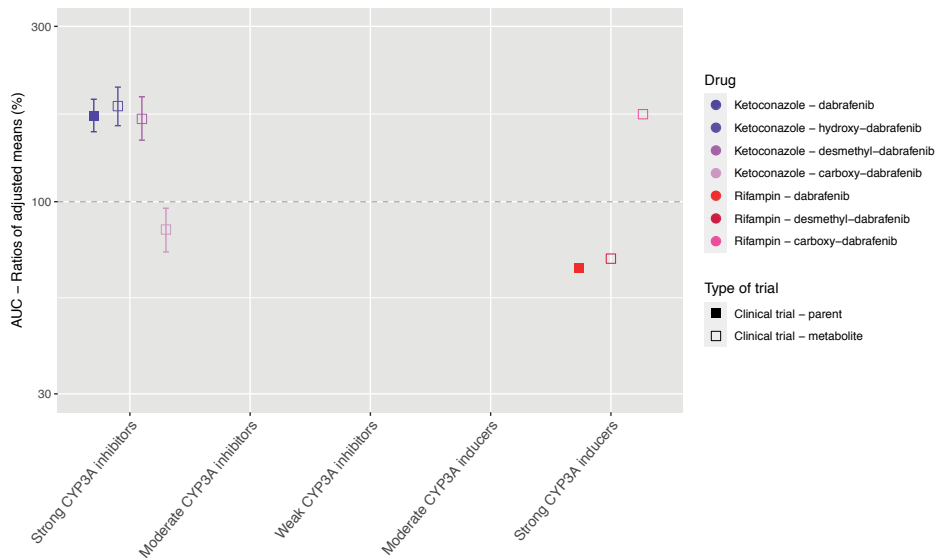




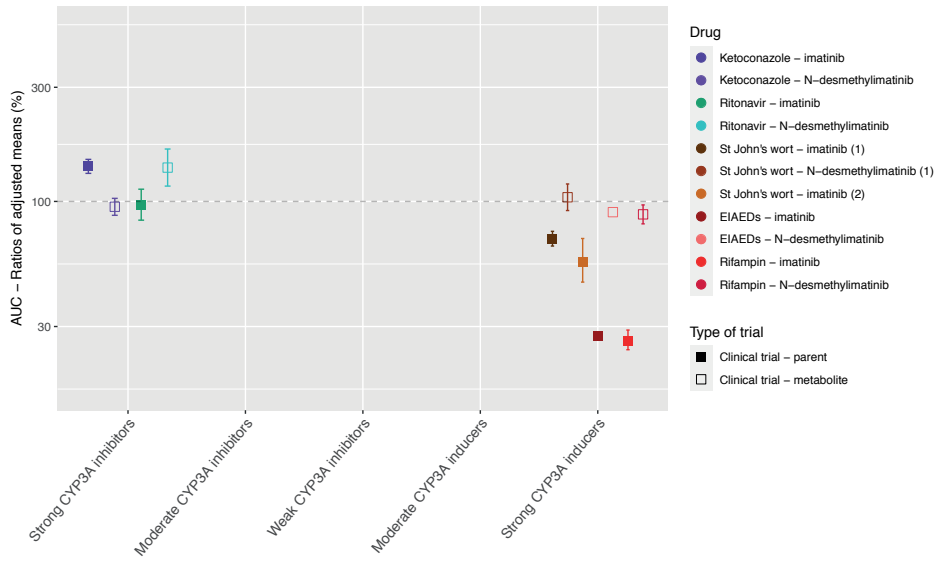
Supplementary Figure S5. Overview of the results from DDI studies of sonidegib combined with CYP3A inhibitors and inducers. The colored symbols represent the increase or decrease in AUC caused by the interacting drug, expressed as adjusted mean  $\pm$ 90% confidence interval (if available). The dashed line represents the baseline AUC.

- a: sonidegib 800 mg single dose + ketoconazole 14 days in healthy subjects
- b: sonidegib 200 mg single dose + ketoconazole 14 days in cancer patients
- c: sonidegib 200 mg 120 days + ketoconazole 120 days in cancer patients
- d: sonidegib 200 mg 133 days + ketoconazole 14 days in cancer patients
- e: sonidegib 200 mg every other day 133 days + ketoconazole 14 days in cancer patients
- f: sonidegib 200 mg single dose + erythromycin 14 days in cancer patients
- g: sonidegib 200 mg 120 days + erythromycin 120 days in cancer patients
- h: sonidegib 200 mg 133 days + erythromycin 14 days in cancer patients
- i: sonidegib 200 mg single dose + efavirenz 14 days in cancer patients
- j: sonidegib 200 mg 120 days + efavirenz 120 days in cancer patients
- k: sonidegib 200 mg 133 days + efavirenz 14 days in cancer patients
- l: sonidegib 800 mg single dose + rifampin 14 days in healthy subjects
- m: sonidegib 200 mg single dose + rifampin 14 days in cancer patients
- n: sonidegib 200 mg 120 days + rifampin 120 days in cancer patients
- o: sonidegib 200 mg 133 days + rifampin 14 days in cancer patients

### Figures for drugs with active metabolites

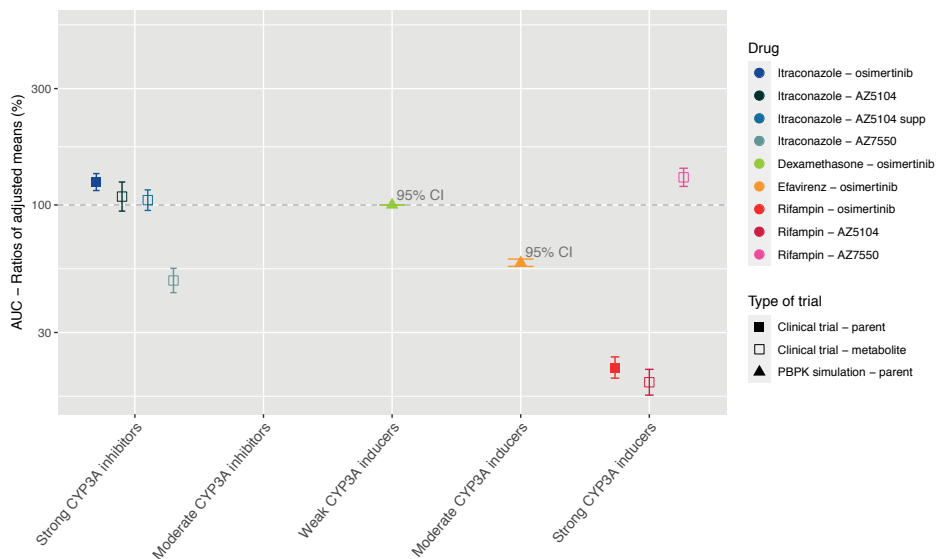


Supplementary Figure S6. Overview of the results from DDI studies of dabrafenib combined with CYP3A inhibitors and inducers. The colored symbols represent the increase or decrease in AUC caused by the interacting drug, expressed as adjusted mean  $\pm$ 90% confidence interval (if available). The dashed line represents the baseline AUC.

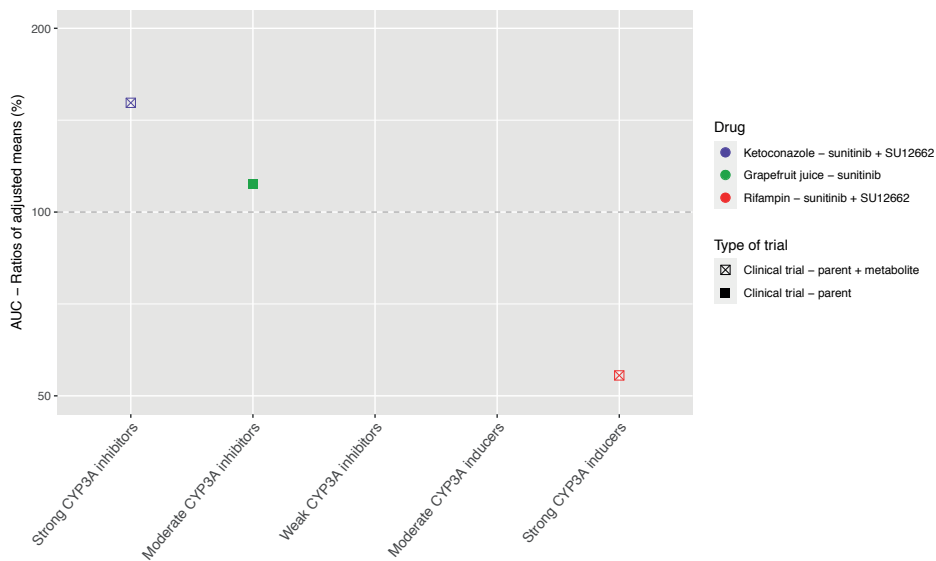


Supplementary Figure S7. Overview of the results from DDI studies of imatinib combined with CYP3A inhibitors and inducers. The colored symbols represent the increase or decrease in AUC caused by the interacting drug, expressed as adjusted mean  $\pm$ 90% confidence interval (if available). The dashed line represents the baseline AUC.





Supplementary Figure S8. Overview of the results from DDI studies of osimertinib combined with CYP3A inhibitors and inducers. The colored symbols represent the increase or decrease in AUC caused by the interacting drug, expressed as adjusted mean  $\pm$ 90% confidence interval (if available). The dashed line represents the baseline AUC. 95% CI, a 95% confidence interval is shown instead of a 90% confidence interval.



Supplementary Figure S9. Overview of the results from DDI studies of sunitinib combined with CYP3A inhibitors and inducers. The colored symbols represent the increase or decrease in AUC caused by the interacting drug, expressed as adjusted mean. The dashed line represents the baseline AUC.





# CHAPTER 1.2

## Effects of the moderate CYP3A4 inhibitor erythromycin on the pharmacokinetics of palbociclib: a randomized crossover trial in patients with breast cancer

Laura Molenaar-Kuijsten\*, C. Louwrens Braal\*, Stefanie L. Groenland\*, Niels de Vries, Hilde Rosing, Jos H. Beijnen, Stijn L.W. Koolen, Annelie J.E. Vulink, Marloes G.J. van Dongen, Ron H.J. Mathijssen, Alwin D.R. Huitema, Neeltje Steeghs

\* These authors contributed equally

On behalf of the Dutch Pharmacology Oncology Group

Clinical Pharmacology & Therapeutics 2021 [Epub ahead of print]

Authors contribution: SG contributed to the design of the study and the writing of the protocol. LMK, LB and SG approached patients for participation in the study, and were responsible for pharmacokinetic sampling and data management. SG performed an interim analysis of the data. LMK performed the final data analysis. LMK, LB and SG wrote the first draft of the manuscript and implemented the input and feedback of the co-authors.

## ABSTRACT

Palbociclib is an oral inhibitor of cyclin-dependent kinases 4 and 6 used in the treatment of locally advanced and metastatic breast cancer, and is extensively metabolized by cytochrome P450 enzyme 3A4 (CYP3A4). A pharmacokinetic/pharmacodynamic relationship between palbociclib exposure and neutropenia is well known. This study aimed to investigate the effects of the moderate CYP3A4 inhibitor erythromycin on the pharmacokinetics of palbociclib.

We performed a randomized crossover trial comparing the pharmacokinetics of palbociclib monotherapy 125 mg once daily (QD) with palbociclib 125 mg QD plus oral erythromycin 500 mg three times daily for seven days. Pharmacokinetic sampling was performed at steady-state for both dosing schedules.

Eleven evaluable patients have been enrolled. For palbociclib monotherapy, geometric mean area under the plasma concentration-time curve from 0 to 24 hours ( $AUC_{0-24h}$ ), maximum plasma concentration ( $C_{max}$ ), and minimum plasma concentration ( $C_{min}$ ) were  $1.46 \cdot 10^3$  ng $\cdot$ h/mL (coefficient of variation (CV) 45.0%), 80.5 ng/mL (CV 48.5%), and 48.4 ng/mL (CV 38.8%), respectively, compared with  $2.09 \cdot 10^3$  ng $\cdot$ h/mL (CV 49.3%,  $p=0.000977$ ), 115 ng/mL (CV 53.7%,  $p=0.00562$ ), and 70.7 ng/mL (CV 47.5%,  $p=0.000488$ ) when palbociclib was administered concomitantly with erythromycin. Geometric mean ratios (90% confidence intervals) of  $AUC_{0-24h}$ ,  $C_{max}$ , and  $C_{min}$  for palbociclib plus erythromycin versus palbociclib monotherapy were 1.43 (1.24-1.66), 1.43 (1.20-1.69), and 1.46 (1.30-1.63). Minor differences in adverse events were observed, and only one grade  $\geq 3$  toxicity was observed in this short period of time.

To conclude, concomitant intake of palbociclib with the moderate CYP3A4 inhibitor erythromycin resulted in an increase in palbociclib  $AUC_{0-24h}$  and  $C_{max}$  of both 43%. Therefore, a dose reduction of palbociclib to 75 mg QD is rational, when palbociclib and moderate CYP3A4 inhibitors are used concomitantly.



## STUDY HIGHLIGHTS

### **What is the current knowledge on the topic?**

Exposure to palbociclib is increased when combined with a strong cytochrome P450 enzyme 3A4 (CYP3A4) inhibitor. No clinical trial with moderate CYP3A4 inhibitors was performed so far, while these moderate inhibitors are more frequently used in clinical practice. A higher palbociclib exposure is related to an increased risk of toxicity.

### **What question did this study address?**

This study aimed to investigate the effects of the moderate CYP3A4 inhibitor erythromycin on the pharmacokinetics of palbociclib.

### **What does this study add to our knowledge?**

Palbociclib exposure was increased by more than 40% when administered concomitantly with erythromycin in this clinical trial.

### **How might this change clinical pharmacology or translational science?**

In case concomitant administration of palbociclib with a moderate CYP3A4 inhibitor is necessary, it is rational to reduce the palbociclib dose by 40%, i.e., to 75 mg once daily.



## INTRODUCTION

Palbociclib is an orally administered inhibitor of cyclin-dependent kinases 4 and 6, and is currently approved in combination with an aromatase inhibitor or fulvestrant for the treatment of hormone receptor positive, human epidermal growth factor receptor 2 (HER2)-negative, locally advanced or metastatic breast cancer (1–3). In the pivotal PALOMA2 (palbociclib (PD 0332991) combined with letrozole versus letrozole for first-line treatment of postmenopausal women with ER-positive, HER2-negative advanced breast cancer) study, patients receiving palbociclib plus letrozole as a first-line treatment had a significantly longer median progression-free survival compared with patients treated with letrozole alone (24.8 months versus 14.5 months, hazard ratio 0.58,  $p < 0.001$ ) (4). Similarly, the addition of palbociclib to fulvestrant was superior to fulvestrant alone in second or subsequent treatment lines in the PALOMA3 (palbociclib (PD 0332991) combined with fulvestrant versus fulvestrant in hormone receptor-positive, HER2-negative metastatic breast cancer after endocrine failure) study (median progression-free survival 9.2 versus 3.8 months, hazard ratio 0.42,  $p < 0.001$ ) (5). The approved dose of palbociclib is 125 mg once daily (QD) in a 3-weeks-on/1-week-off dosing schedule.

As palbociclib is extensively metabolized by cytochrome P450 enzyme 3A4 (CYP3A4), its exposure can be markedly affected by concomitant administration with CYP3A4 modulators (1,3). In a previous drug-drug interaction study in twelve healthy male volunteers, co-administration of itraconazole, a strong CYP3A4 inhibitor, in a dose of 200 mg for 5 days resulted in an increase in the area under the plasma concentration-time curve from zero to infinity ( $AUC_{0-\infty}$ ) and maximum plasma concentration ( $C_{max}$ ) of 87% and 34%, respectively, after a single dose of palbociclib on day 5 (1,3,6,7). Based on these data, it is recommended in the drug label of both U.S. Food and Drug Administration (FDA) and the European Medicines Agency (EMA) to avoid concomitant use of strong CYP3A4 inhibitors, or otherwise to reduce the palbociclib dose to 75 mg QD instead of the standard dose of 125 mg QD (1,3).

No clinical studies have been performed to study the effects of moderate CYP3A4 inhibitors on palbociclib pharmacokinetics. Simulations with a physiologically based pharmacokinetic (PBPK) model of palbociclib predicted that concomitant administration of palbociclib with moderate CYP3A4 inhibitors diltiazem and verapamil would lead to an increase in palbociclib AUC and  $C_{max}$  of 38% and 22% for verapamil, and 42% and 23% for diltiazem, respectively (7). It has been concluded that the risk of drug-drug interactions for palbociclib co-administered with moderate CYP3A4 inhibitors is modest and that dose adjustments are thus not needed. However, we argue that a 40% increase in exposure could be clinically relevant, as higher palbociclib exposure

is related to an increased risk of toxicity (i.e., neutropenia)(8,9). In the pivotal studies, 30 to 40% of patients needed a dose reduction due to toxicity (4,5,10). Especially in these patients, concomitant administration with moderate CYP3A4 inhibitors could lead to increased adverse events. Based on these simulations, dose reductions to 75 mg QD or 100 mg QD (60% or 80% of the standard dose) might be a strategy to reduce the risk of toxicities, while maintaining adequate exposure. The effect of drug-drug interactions via CYP3A4 has thus far only been evaluated in single dose studies in healthy male volunteers and PBPK simulations. Therefore, a drug-drug interaction study at steady-state concentration in real-life patients treated with palbociclib, would provide the most essential and clinically relevant information. Moreover, this could serve as a showcase for other oral targeted therapies metabolized by CYP3A4 and other moderate CYP3A4 inhibitors.

Based on the above, we conducted a randomized pharmacokinetic crossover trial to study the effects of the moderate CYP3A4 inhibitor erythromycin on the pharmacokinetics of palbociclib in female breast cancer patients.



## METHODS

### Study design

We performed a prospective, multi-center, randomized clinical trial with a crossover design, according to the guideline of the FDA for drug-drug interaction studies (11). **Figure 1** provides a schematic overview of the study design. Patients were randomized to start with either palbociclib 125 mg QD combined with erythromycin 500 mg three times daily (TID)(arm A) or palbociclib monotherapy 125 mg QD (arm B). Pharmacokinetic exposure was determined at both dosing schedules. Erythromycin was selected as a moderate CYP3A4 inhibitor, because this drug shows few side effects compared with other moderate CYP3A4 inhibitors. The selected dose was within the therapeutic range and the dose was in agreement with other DDI studies where erythromycin was used (12–15). Taking into account the duration-dependent inhibition of CYP3A4 by erythromycin and the mean elimination half-life of palbociclib of 29 hours, one week was considered to be sufficient to reach steady-state concentrations (1,15). As erythromycin is inhibiting CYP3A4 irreversibly, it can take up to one week until CYP3A4 function is returned to baseline function after discontinuation of erythromycin (16,17). Therefore, a washout period of one week followed by one week to reach new steady-state concentrations has been chosen. The crossover design of the study was chosen to evaluate potential effects of this washout on outcome. Erythromycin was administered for seven days on either day 1–7 or day 15–21, depending on randomization. Randomization was performed by block randomization in ALEA (FormsVision BV, Abcoude, The Netherlands). The block size was four, and blocks were only visible for a system administrator. Patients were instructed to take palbociclib at 8.00 AM, and erythromycin three times daily at 8.00 AM, 4.00 PM, and 12.00 AM, both palbociclib and erythromycin together with food (diet of own choice of the patient). Patients requiring a dose interruption or dose reduction or who discontinued treatment during the study were considered non-evaluable for the pharmacokinetic analyses and were replaced. At the end of the trial, palbociclib treatment was continued as part of standard care.

### Patient population

Patients with histological or cytological proof of cancer with an indication for treatment with palbociclib (i.e., advanced breast cancer) at the standard dose of 125 mg QD were eligible for inclusion. Further inclusion criteria were age  $\geq 18$  years, World Health Organization performance status of 0, 1, or 2, and adequate organ function per judgment of the treating physician.

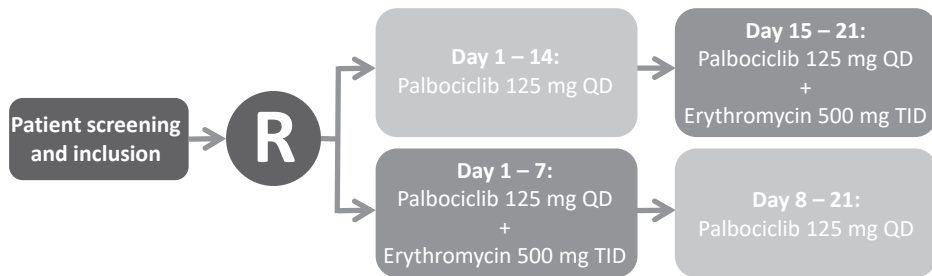


Figure 1. Schematic overview of clinical trial design. Pharmacokinetic sampling was performed at day 7 and day 21 of the study. R, randomization; QD, once daily; TID, three times daily.

Exclusion criteria were concomitant use of other medication that could influence the pharmacokinetics of palbociclib within 14 days or five half-lives of the drug (whichever was shorter) before start of the study, including (but not limited to) CYP3A4 inhibitors or inducers, or a QT duration corrected for heart rate (QTc) >450 milliseconds (or >480 milliseconds for patients with bundle branch block) because erythromycin may potentially prolong the QTc interval. Therefore, an electrocardiogram (ECG) was performed at screening.

### Pharmacokinetics

At day 7 and day 21 of the study, patients were admitted to the hospital and blood samples were collected for pharmacokinetic analyses. Time points were before dosing (directly before ingestion of palbociclib) and 1, 2, 3, 4, 5, 6, 7, 8, 9, 10, 11, 12, and 24 hours post dosing (just before ingestion of a new palbociclib dose). At each time point, a blood sample was collected in a 3-mL K<sub>2</sub> EDTA tube and centrifuged directly after collection (1,500 g, 5 min, 4°C). Plasma was stored at -20°C until analysis. Plasma palbociclib concentrations were quantified using a validated liquid chromatography-tandem mass spectrometry method (18). This method was validated according to the EMA and FDA guidelines on bioanalytical method validation over a linear range of 50–1000 ng/mL (19,20).

### Study endpoint

The primary objective of this trial was to study the effect of the moderate CYP3A4 inhibitor erythromycin on the pharmacokinetics of palbociclib, measured as  $AUC_{0-24h}$ ,  $C_{max}$ , and minimum plasma concentration ( $C_{min}$ ). As a secondary objective, the incidence and severity of adverse events (AEs) with and without erythromycin was compared, according to Common Terminology Criteria for Adverse Events (CTCAE), version 5.0 (21).

**Safety assessments**

Patients were instructed to use a diary to keep track of AEs. Recording of AEs, vital signs, and hematology and blood chemistry assessments were performed at day 7 and day 21 of the study. The incidence, severity and start and end dates of all AEs were recorded and graded according to the CTCAE version 5.0.

**Statistics**

For the sample size calculation, it was assumed that concomitant administration with erythromycin would result in a 40% increase in palbociclib exposure, based on previous simulations. By assuming an intra-individual standard deviation of the difference of 50% between the two dosing schedules, eleven evaluable patients had to be included to obtain 80% power (one-sided  $\alpha=0.05$ ) to detect an increase of  $\geq 40\%$  in exposure. Pharmacokinetic parameters were calculated using non-compartmental analysis.  $AUC_{0-24h}$  was calculated using the linear/log trapezoidal method.  $C_{max}$  was defined as the highest measured concentration.  $C_{min}$  was defined as the mean value of the pre-dose and 24 hours post dose concentration.  $AUC_{0-24h}$ ,  $C_{max}$  and  $C_{min}$  of palbociclib monotherapy and combined with erythromycin were compared using one-sided Wilcoxon signed rank tests because of the small sample size. The relative difference was calculated by dividing the value for the treatment with palbociclib plus erythromycin by the value for palbociclib monotherapy. Statistical analyses were performed using R version 3.6.3 (R Project, Vienna, Austria), and the geometric mean and confidence intervals were calculated using the Gmean function in the DescTools package (22).

**Ethics approval and consent to participate**

The study was approved by the Medical Ethics Committee of The Netherlands Cancer Institute, Amsterdam. Participating centers were The Netherlands Cancer Institute and the Erasmus Medical Center (MC) Cancer Institute. Local approval was obtained in each participating center. The study was conducted in compliance with Good Clinical Practice and the Declaration of Helsinki. All patients provided written informed consent prior to inclusion in the trial. This study was registered in the Netherlands Trial Register ([www.trialregister.nl](http://www.trialregister.nl), NL7549) and the EudraCT database (2018-004032-29). The full trial protocol can be accessed upon reasonable request by contacting the corresponding author.

## RESULTS

### Patient characteristics

Twelve female patients were enrolled in the study from April 2019 until May 2021. One patient withdrew informed consent before pharmacokinetic (PK) sampling at the second dosing schedule, and was excluded. Baseline characteristics of the evaluable patients are provided in **Table 1**. Median age was 59 years and the median time on palbociclib treatment before enrollment in the study was 10.1 months.

Table 1. Baseline characteristics (n=11).

Characteristic	n (%) or median [range]
Gender, female	11 (100%)
Age (years)	59 [36-79]
Tumor type	
Breast cancer	11 (100%)
Combination therapy	
Fulvestrant	9 (82%)
Anastrozole	1 (9%)
Letrozole	1 (9%)
WHO performance status	
0	8 (73%)
1	3 (27%)
Previous lines of systemic treatment in metastatic setting (number)	1 [0 - 6]
Previous systemic treatment	
Chemotherapy	11 (100%)
Anti-hormonal therapy	11 (100%)
Time on palbociclib at study inclusion (months)	10.1 [1.2-22.8]

WHO, World Health Organization.

### Pharmacokinetics

Palbociclib exposure was higher, for all but one patient, when administered concomitantly with erythromycin (**Figure 2, Figure 3, Table 2**) (no differences were observed between arms). For palbociclib monotherapy, geometric mean  $AUC_{0-24h}$ ,  $C_{max}$ , and  $C_{min}$  were  $1.46 \cdot 10^3$  ng·h/mL (coefficient of variation (CV) 45.0%), 80.5 ng/mL (CV 48.5%), and 48.4 ng/mL (CV 38.8%), respectively. When palbociclib was administered in combination with erythromycin, this resulted in an increase in  $AUC_{0-24h}$ ,  $C_{max}$ , and  $C_{min}$  to  $2.09 \cdot 10^3$  ng·h/mL (CV 49.3%,  $p=0.000977$ ), 115 ng/mL (CV 53.7%,  $p=0.00562$ ), and 70.7 ng/mL (CV 47.5%,

$p=0.000488$ ), respectively. Geometric mean ratios (90% confidence intervals) of  $AUC_{0-24h}$ ,  $C_{max}$ , and  $C_{min}$  for palbociclib plus erythromycin versus palbociclib monotherapy were 1.43 (1.24-1.66), 1.43 (1.20-1.69), and 1.46 (1.30-1.63), respectively. The elimination half-life of palbociclib was 29.8 hours (CV 42.0%) for palbociclib monotherapy, compared with 42.6 hours (CV 39.4%) for palbociclib plus erythromycin ( $p=0.00928$ ).

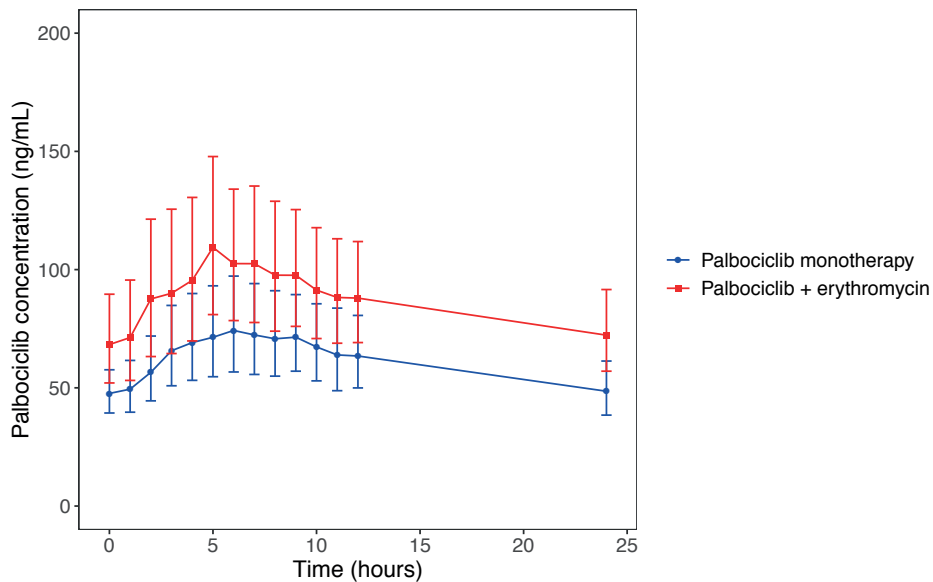


Figure 2. Palbociclib plasma concentration-time curves of palbociclib monotherapy or combined with the moderate CYP3A4 inhibitor erythromycin. Data are represented as geometric mean +90% confidence interval. CYP3A4, cytochrome P450 enzyme 3A4.

### Treatment-related adverse events

An overview of all treatment-related AEs is provided in **Table 3**. Nine patients experienced one or more treatment-related AEs. No patients discontinued treatment and none required a dose reduction. Only one grade 3 toxicity (neutropenia) occurred during the treatment with palbociclib plus erythromycin.



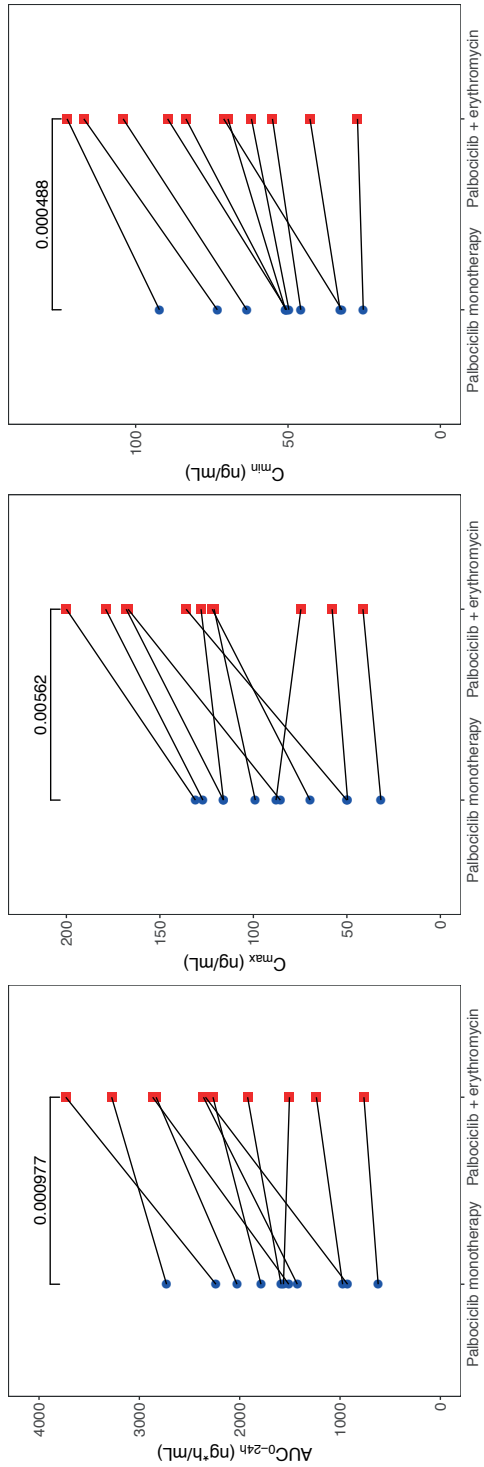


Figure 3. Plots of palbociclib  $AUC_{0-24h}$ ,  $C_{max}$  and  $C_{min}$  for palbociclib monotherapy and combined with the moderate CYP3A4 inhibitor erythromycin for each individual patient. Wilcoxon signed rank tests were performed to calculate  $p$ -values (printed above the brackets).  $AUC_{0-24h}$  was calculated using the linear/log trapezoidal method.  $C_{max}$  was defined as the highest measured concentration for each dosing schedule.  $C_{min}$  was defined as the median value of the pre-dose and 24 hours post dose sample.  $AUC_{0-24h}$ , area under the plasma concentration-time curve from 0 to 24 hours;  $C_{max}$ , maximum plasma concentration;  $C_{min}$ , minimum plasma concentration; CYP3A4, cytochrome P450 enzyme 3A4.

Table 2. Pharmacokinetic parameters of palbociclib with and without the moderate CYP3A4 inhibitor erythromycin.

PK parameter	Palbociclib monotherapy	Palbociclib + erythromycin	Geometric mean ratio [90% CI]	p-value <sup>a</sup>
AUC <sub>0-24h</sub> (ng·h/mL) <sup>b</sup>	1.46·10 <sup>3</sup> (45.0%)	2.09·10 <sup>3</sup> (49.3%)	1.43 [1.24-1.66]	0.000977
C <sub>max</sub> (ng/mL) <sup>c</sup>	80.5 (48.5%)	115 (53.7%)	1.43 [1.20-1.69]	0.00562
C <sub>min</sub> (ng/mL) <sup>d</sup>	48.4 (38.8%)	70.7 (47.5%)	1.46 [1.30-1.63]	0.000488
t <sub>1/2</sub> (h)	29.8 (42.0%)	42.6 (39.4%)	1.43 [1.14-1.79]	0.00928

Pharmacokinetic parameters are expressed as geometric mean (CV%). Administered doses were 125 mg QD for palbociclib and 500 mg TID for erythromycin.

<sup>a</sup> Wilcoxon signed rank tests were performed to calculate *p*-values

<sup>b</sup> AUC<sub>0-24h</sub> was calculated using the linear/log trapezoidal method

<sup>c</sup> C<sub>max</sub> was defined as the highest measured concentration for each dosing schedule

<sup>d</sup> C<sub>min</sub> was defined as the median value of the pre-dose and 24 hours post dose sample

PK, pharmacokinetic; CI, confidence interval; AUC<sub>0-24h</sub>, area under the plasma concentration-time curve from 0 to 24 hours; C<sub>max</sub>, maximum plasma concentration; C<sub>min</sub>, minimum plasma concentration; CV, coefficient of variation; QD, once daily; TID, three times daily; t<sub>1/2</sub>, elimination half-life; CYP3A4, cytochrome P450 enzyme 3A4.

Table 3. Treatment-related adverse events (AEs) according to CTCAE v5.0.

Adverse event	Palbociclib monotherapy		Palbociclib plus erythromycin	
	Any grade (n)	Grade $\geq 3$ (n)	Any grade (n)	Grade $\geq 3$ (n)
<b>All patients</b>				
Diarrhea	0	0	4	0
Nausea	0	0	2	0
Vomiting	0	0	1	0
Neutropenia	3	0	2	1
Total number of patients experiencing AEs	4	0	7	1
<b>Patients in arm A</b>				
Diarrhea	0	0	3	0
Nausea	0	0	1	0
Vomiting	0	0	0	0
Neutropenia	3	0	0	0
Total number of patients experiencing AEs	3	0	3 <sup>a</sup>	0
<b>Patients in arm B</b>				
Diarrhea	0	0	1	0
Nausea	0	0	1	0
Vomiting	0	0	1	0
Neutropenia	0	0	2	1
Total number of patients experiencing AEs	1	0	4 <sup>b</sup>	1

<sup>a</sup> One patient experiencing both diarrhea and nausea, therefore total number of patients is lower than number of adverse events.

<sup>b</sup> One patient experiencing both diarrhea and neutropenia, therefore total number of patients is lower than number of adverse events.

AE, adverse event; CTCAE, Common Terminology Criteria for Adverse Events; arm A, started with palbociclib combined with erythromycin; arm B, started with palbociclib monotherapy.

## DISCUSSION

Here, we reported the results of a prospective randomized crossover study assessing the effects of the moderate CYP3A4 inhibitor erythromycin on the pharmacokinetics of palbociclib. Concomitant administration resulted in a significantly higher palbociclib exposure, with increases in  $AUC_{0-24h}$ ,  $C_{max}$ , and  $C_{min}$  of 43%, 43%, and 46%, respectively, which is of clinical relevance. Minor differences in adverse events were observed, and only one grade 3 toxicity was observed, in this short period of time.

The observed effect size in the current study was in line with previous simulations for  $AUC_{0-24h}$ , but substantially larger for  $C_{max}$ , as earlier simulations with diltiazem and verapamil predicted an increase of  $\pm 40\%$  in  $AUC$  and  $\pm 23\%$  in  $C_{max}$  (7). Notably, the effect on  $C_{max}$  as found in our study is even higher than the effect on  $C_{max}$  of the strong CYP3A4 inhibitor itraconazole (i.e., 34%)(1,6). Although no full explanation could be found for this discrepancy in effect size, this may partly be explained by the applied sampling schedule in the drug-drug interaction study with itraconazole (i.e., 2, 4, 6, 8, 12 h post dose, instead of each hour up to 12 h post dose in the current study, which may have missed the true  $C_{max}$ )(1,6).

The fact that a similar increase in  $AUC_{0-24h}$ ,  $C_{max}$  and  $C_{min}$  was observed (**Table 2**), suggests that the effect of erythromycin is -for an important part- determined by an increased bioavailability (i.e., via inhibition of intestinal CYP3A4). Yet, the elimination half-life was also significantly longer for palbociclib plus erythromycin compared with palbociclib monotherapy, which means that a lower clearance (i.e., via inhibition of hepatic CYP3A4) plays a role as well. The prolonged half-life of palbociclib when it is combined with erythromycin, may imply that the washout period was shorter than five times the half-life. Still, the washout period was at least four times the half-life, which allowed for 94% of new steady-state. Most importantly, no difference in palbociclib PK when given as monotherapy was observed between treatment arms, and therefore, it could be concluded that the washout period was sufficient. Apart from being a moderate CYP3A4 inhibitor, erythromycin also inhibits P-glycoprotein (P-gp)(23). Theoretically, inhibition of P-gp could also explain the observed increase in bioavailability, as palbociclib is a substrate of P-gp (24,25). However, a previous study in mice demonstrated that P-gp mainly restricted the brain penetration of palbociclib, whereas its oral bioavailability was only marginally affected (25). Therefore, we expect the effect of P-gp inhibition on the palbociclib plasma concentrations in the current study to be minimal.

An important advantage of the drug-drug interaction study described here, is that it was performed in the target population of (female) breast cancer patients. In the pivotal drug-drug interaction study with the strong CYP3A4 inhibitor itraconazole, only male

healthy volunteers were included (7). The subsequently performed PBPK simulations to predict the effect of moderate CYP3A4 inhibitors were based on the results found in the male subjects. To exclude the possibility of a gender effect, e.g., on CYP3A4 enzyme activity, this study was conducted in female patients, which are the patients using palbociclib in clinical practice.

Because of pharmacogenetic differences, the exposure to palbociclib could be different between patients. For CYP3A4 the polymorphism *CYP3A4*\*22 has been described by Wang *et al.* (26). In liver samples with a *CYP3A4*\*22 polymorphism approximately 15% of total CYP3A4 was non-functional, compared to 6% in wildtype liver samples. Because, in case of this polymorphism, still the majority of CYP3A4 will be functional, the genotype will have little effect on the extent of drug inhibition. Therefore, a meaningful comparison could be made between palbociclib monotherapy and palbociclib plus erythromycin combination therapy, without the need of prior pharmacogenetic analyses.

Neutropenia is the most common adverse event during palbociclib treatment. Higher palbociclib exposure has been related to an increased risk of neutropenia in previous studies (8,9). It is, therefore, logical to assume that concomitant administration of palbociclib and moderate CYP3A4 inhibitors will result in a higher incidence of neutropenia, depending on dose and duration of concomitant administration of the inhibitor. The secondary outcome of the current study was to compare toxicities between the two dosing schedules (i.e., palbociclib monotherapy and palbociclib plus erythromycin). However, neutropenia is a cumulative toxicity that is most pronounced at the end of each palbociclib cycle. Therefore, comparisons of neutropenia between day 7 and day 21 of a cycle are not meaningful. Instead, comparisons could be made with previous palbociclib cycles, in which no moderate CYP3A4 inhibitors were used. However, only one grade 3 neutropenia was observed in our study, probably as a result of the short duration of erythromycin treatment of seven days. The patient who experienced a grade 3 neutropenia at the end of the studied period, had a grade 2 neutropenia at the end of her previous treatment cycles. Because of the short duration of concomitant use of a moderate CYP3A4 inhibitor, a meaningful comparison of toxicity could not be performed. However, as these patients had no indication to use a moderate CYP3A4 inhibitor, it was considered unethical to prescribe these drugs longer than necessary to reach steady-state concentrations. Since an exposure-toxicity relationship for palbociclib has already been described, the comparison between palbociclib monotherapy and palbociclib plus erythromycin based on PK was considered sufficient to give a dose recommendation for the interaction.

As palbociclib exposure increased by more than 40% when administered concomitantly with erythromycin, and palbociclib pharmacokinetics change in a dose-proportional manner (1,3), it is rational to reduce the palbociclib dose by 40%, i.e., to 75 mg QD, in case of concomitant administration with moderate CYP3A4 inhibitors, without fear for underdosing. For patients who already received prior dose reductions, e.g., due to toxicity, it could be considered to reduce the dose even further by switching to an every other day dosing schedule (as no smaller capsule size than 75 mg is currently available). Adjusting the dosing schedule to 5 days on/2 days off every 7 days with no weeks off therapy might also be possible, since it has been described that this alternative schedule leads to a better tolerability (27). For strong CYP3A4 inhibitors, a dose reduction to 75 mg QD was recommended as well, while  $AUC_{0-\infty}$  was increased by 87% in that case (1,3,6). However, first of all that combination should be avoided according to the drug label. Secondly, 75 mg capsules are the lowest dose currently available in the market.

Next to palbociclib, there are other cyclin-dependent kinases 4 and 6 (CDK4/6) inhibitors available for the treatment of breast cancer (2,28–31). However, these CDK4/6 inhibitors are also substrates of CYP3A4 (28,29). Combination with a strong CYP3A4 inhibitor increased the AUC of palbociclib by 1.9-fold, compared with an increase of 3.2-fold for ribociclib, and 1.7 to 2.5-fold for abemaciclib plus active metabolites (potency adjusted)(1,28–31). Complicating factors are the auto-inhibition of CYP3A4 by ribociclib, and the metabolism of abemaciclib to active metabolites (28–31). Since the effect of CYP3A4 inhibition on ribociclib is much larger than on palbociclib, the use of palbociclib is preferred if concomitant administration with a CYP3A4 inhibitor is necessary (1,29). The effect of CYP3A4 inhibition on abemaciclib exposure seems comparable to the effect on palbociclib, but the effect of a moderate inhibitor on palbociclib is now studied in a clinical trial. Therefore, we recommend to use palbociclib if concomitant administration with a CYP3A4 inhibitor is necessary.

## CONCLUSION

To conclude, concomitant intake of palbociclib and the moderate CYP3A4 inhibitor erythromycin results in an increase in  $AUC_{0-24h}$  and  $C_{max}$  of palbociclib of both 43%, which is clinically relevant. Therefore, in case of concomitant use of palbociclib and moderate CYP3A4 inhibitors, it is rational to reduce the palbociclib dose to 75 mg QD, without fear for underexposure. This is especially relevant for the 30 to 40% of patients who need a dose reduction of palbociclib during regular treatment due to toxicity (4,5,10). It should be considered to update the drug label of palbociclib to include these findings and recommendations, and add moderate CYP3A4 inhibitors to the list of potentially interacting drugs for CDK4/6 inhibitors.



## REFERENCES

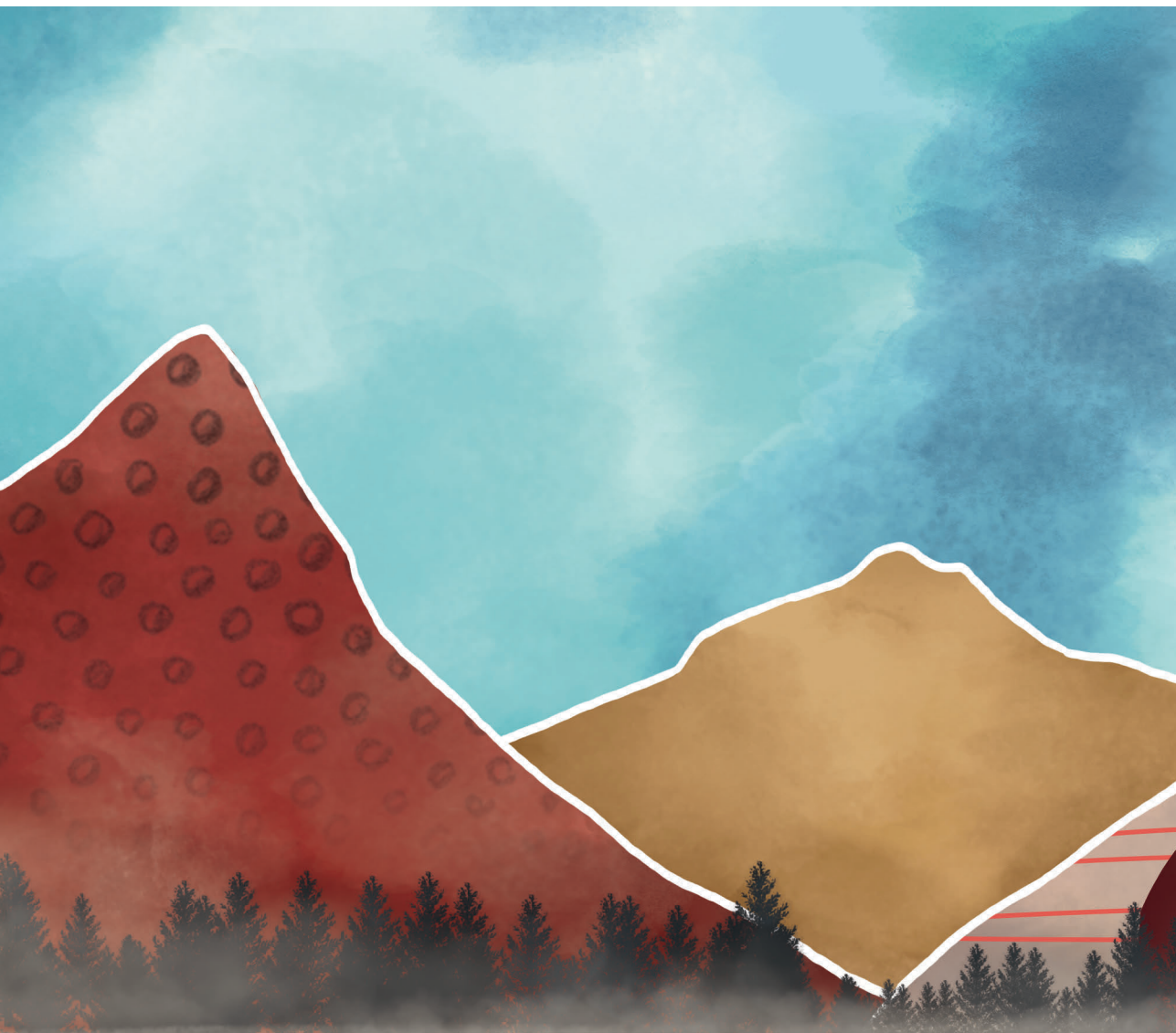
1. Food and Drug Administration. Center for Drug Evaluation and Research. Palbociclib Clinical Pharmacology and Biopharmaceutics Review [Internet]. 2014 [cited 2021 Jun 11]. Available from: [https://www.accessdata.fda.gov/drugsatfda\\_docs/nda/2015/207103Orig1s000ClinPharmR.pdf](https://www.accessdata.fda.gov/drugsatfda_docs/nda/2015/207103Orig1s000ClinPharmR.pdf)
2. Braal CL, Jongbloed EM, Wilting SM, Mathijssen RHJ, Koolen SLW, Jager A. Inhibiting CDK4/6 in Breast Cancer with Palbociclib, Ribociclib, and Abemaciclib: Similarities and Differences. *Drugs*. 2021;81(3):317–31.
3. European Medicines Agency Committee for Medicinal Products For Human Use (CHMP). Palbociclib European Public Assessment Report [Internet]. 2016 [cited 2019 Sep 20]. Available from: [https://www.ema.europa.eu/en/documents/product-information/ibrance-epar-product-information\\_en.pdf](https://www.ema.europa.eu/en/documents/product-information/ibrance-epar-product-information_en.pdf)
4. Finn RS, Martin M, Rugo HS, Jones S, Im S-A, Gelmon K, et al. Palbociclib and Letrozole in Advanced Breast Cancer. *N Engl J Med*. 2016;375(20):1925–36.
5. Turner NC, Ro J, André F, Loi S, Verma S, Iwata H, et al. Palbociclib in hormone-receptor-positive advanced breast cancer. *N Engl J Med*. 2015;373(3):209–19.
6. Hoffman JT, Loi C-M, O’Gorman M, Plotka A, Kosa M, Jakubowska A, et al. A phase I open-label, fixed-sequence, two-period crossover study of the effect of multiple doses of Itraconazole on Palbociclib (PD-0332991) pharmacokinetics in healthy volunteers. [abstract]. In: Proceedings of the 107th Annual Meeting of the American As. *Cancer Res*. 2016;76(14 Suppl):Abstract nr LB-196.
7. Yu Y, Loi C-MM, Hoffman J, Wang D. Physiologically Based Pharmacokinetic Modeling of Palbociclib. *J Clin Pharmacol*. 2017;57(2):173–84.
8. Flaherty KT, LoRusso PM, DeMichele A, Abramson VG, Courtney R, Randolph SS, et al. Phase I, dose-escalation trial of the oral cyclin-dependent kinase 4/6 inhibitor PD 0332991, administered using a 21-day schedule in patients with advanced cancer. *Clin Cancer Res*. 2012;18(2):568–76.
9. Schwartz GK, Lorusso PM, Dickson MA, Randolph SS, Shaik MN, Wilner KD, et al. Phase I study of PD 0332991, a cyclin-dependent kinase inhibitor, administered in 3-week cycles (Schedule 2/1). *Br J Cancer*. 2011;104(12):1862–8.
10. Finn RS, Crown JP, Lang I, Boer K, Bondarenko IM, Kulyk SO, et al. The cyclin-dependent kinase 4/6 inhibitor palbociclib in combination with letrozole versus letrozole alone as first-line treatment of oestrogen receptor-positive, HER2-negative, advanced breast cancer (PALOMA-1/TRIO-18): A randomised phase 2 study. *Lancet Oncol*. 2015;16(1):25–35.
11. Food and Drug Administration. Center for Drug Evaluation and Research. Clinical Drug Interaction Studies — Cytochrome P450 Enzyme- and Transporter-Mediated Drug Interactions Guidance for Industry [Internet]. 2020 [cited 2020 Jun 11]. Available from: <https://www.fda.gov/media/134581/download>
12. Lexicomp. Erythromycin (systemic): Drug information [Internet]. 2021 [cited 2021 Aug 30]. Available from: <https://www.uptodate.com/contents/erythromycin-systemic-drug-information>
13. Kovarik JM, Beyer D, Bizot MN, Jiang Q, Shenouda M, Schmouder RL. Effect of multiple-dose erythromycin on everolimus pharmacokinetics. *Eur J Clin Pharmacol*. 2005;61(1):35–8.



14. Budha NR, Ji T, Musib L, Eppler S, Dresser M, Chen Y, et al. Evaluation of Cytochrome P450 3A4-Mediated Drug-Drug Interaction Potential for Cobimetinib Using Physiologically Based Pharmacokinetic Modeling and Simulation. *Clin Pharmacokinet*. 2016;55(11):1435-45.
15. Okudaira T, Kotegawa T, Imai H, Tsutsumi K, Nakano S, Ohashi K. Effect of the treatment period with erythromycin on cytochrome P450 3A activity in humans. *J Clin Pharmacol*. 2007;47(7):871-6.
16. Yang J, Liao M, Shou M, Jamei M, Yeo KR, Tucker GT, et al. Cytochrome P450 Turnover: Regulation of Synthesis and Degradation, Methods for Determining Rates, and Implications for the Prediction of Drug Interactions. *Curr Drug Metab*. 2008;9:384-93.
17. Chan CYS, Roberts O, Rajoli RKR, Liptrott NJ, Siccardi M, Almond L, et al. Derivation of CYP3A4 and CYP2B6 degradation rate constants in primary human hepatocytes: A siRNA-silencing-based approach. *Drug Metab Pharmacokinet*. 2018;33(4):179-87.
18. Janssen JM, de Vries N, Venekamp N, Rosing H, Huitema ADR, Beijnen JH. Development and validation of a liquid chromatography-tandem mass spectrometry assay for nine oral anticancer drugs in human plasma. *J Pharm Biomed Anal*. 2019;174:561-6.
19. European Medicines Agency Committee for Medicinal Products For Human Use (CHMP). Guideline on bioanalytical method validation [Internet]. 2012 [cited 2020 Oct 16]. Available from: [https://www.ema.europa.eu/en/documents/scientific-guideline/guideline-bioanalytical-method-validation\\_en.pdf](https://www.ema.europa.eu/en/documents/scientific-guideline/guideline-bioanalytical-method-validation_en.pdf)
20. Food and Drug Administration. Center for Drug Evaluation and Research. Bioanalytical Method Validation - Guidance for Industry [Internet]. 2018 [cited 2020 Aug 26]. Available from: <https://www.fda.gov/regulatory-information/search-fda-guidance-documents/bioanalytical-method-validation-guidance-industry>
21. National Cancer Institute, National Institutes of Health Services, US Department of Health and Human. Common Terminology Criteria for Adverse Events (CTCAE) version 5.0 [Internet]. 2017 [cited 2021 Jul 5]. Available from: [https://ctep.cancer.gov/protocoldevelopment/electronic\\_applications/ctc.htm](https://ctep.cancer.gov/protocoldevelopment/electronic_applications/ctc.htm)
22. Signorell A, Aho K, Alfons A, Anderegg N, Aragon T, Arachchige C, et al. Package "DescTools" version 0.99.42 [Internet]. 2021 [cited 2021 Jul 5]. Available from: <https://cran.r-project.org/web/packages/DescTools/DescTools.pdf>
23. Eberl S, Renner B, Neubert A, Reisig M, Bachmakov I, König J, et al. Role of P-glycoprotein inhibition for drug interactions: Evidence from in vitro and pharmacoepidemiological studies. *Clin Pharmacokinet*. 2007;46(12):1039-49.
24. Raub TJ, Wishart GN, Kulanthaivel P, Staton BA, Ajamie RT, Sawada GA, et al. Brain exposure of two selective dual CDK4 and CDK6 inhibitors and the antitumor activity of CDK4 and CDK6 inhibition in combination with temozolomide in an intracranial glioblastoma xenograft. *Drug Metab Dispos*. 2015;43(9):1360-71.
25. De Gooijer MC, Zhang P, Thota N, Mayayo-Peralta I, Buil LCM, Beijnen JH, et al. P-glycoprotein and breast cancer resistance protein restrict the brain penetration of the CDK4/6 inhibitor palbociclib. *Invest New Drugs*. 2015;33(5):1012-9.
26. Wang D, Guo Y, Wrighton SA, Cooke GE, Sadee W. Intronic polymorphism in CYP3A4 affects hepatic expression and response to statin drugs. *Pharmacogenomics J*. 2011;11(4):274-86.
27. Krishnamurthy J, Luo J, Ademuyiwa F, Suresh R, Rigden C, Reardon T, et al. A phase II trial assessing the safety of an alternative dosing schedule of palbociclib (palbo) in hormone receptor positive (HR+), HER2 negative (HER2-) metastatic breast cancer (MBC): Alt Dose Palbo. In: Proceedings of the 2019 San Antonio Breast Cancer Symposium Cancer Res [Internet]. 2020. p. Abstract nr P1-19-13. Available from: [https://cancerres.aacrjournals.org/content/80/4\\_Supplement/P1-19-13](https://cancerres.aacrjournals.org/content/80/4_Supplement/P1-19-13)

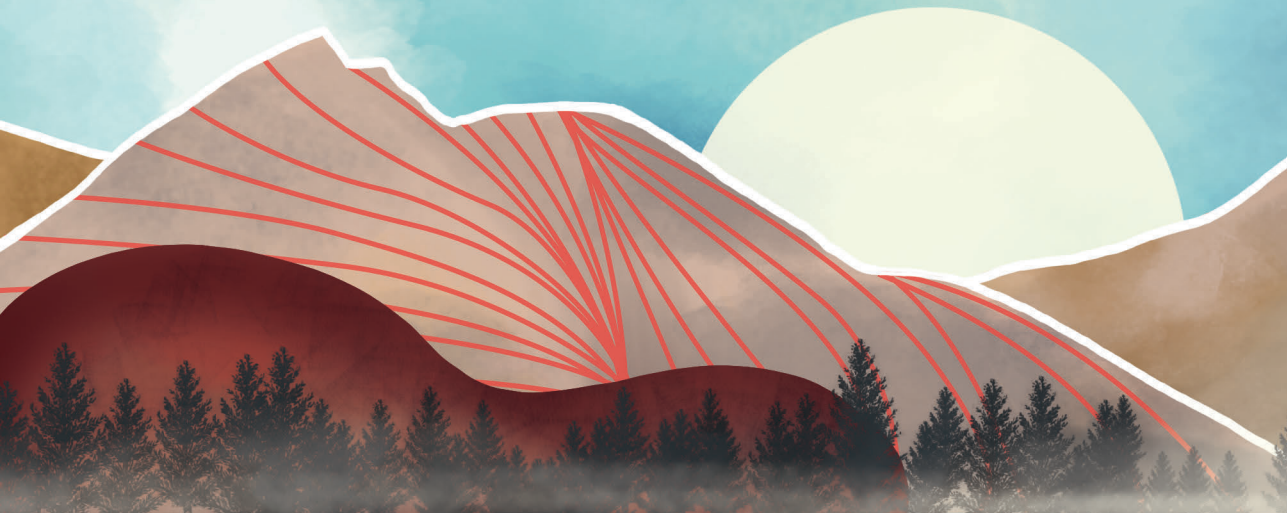
28. Food and Drug Administration. Center for Drug Evaluation and Research. Abemaciclib Multi-Discipline Review [Internet]. 2017 [cited 2021 Jun 11]. Available from: [https://www.accessdata.fda.gov/drugsatfda\\_docs/nda/2017/208716Orig1s000MultidisciplineR.pdf](https://www.accessdata.fda.gov/drugsatfda_docs/nda/2017/208716Orig1s000MultidisciplineR.pdf)
29. Food and Drug Administration. Center for Drug Evaluation and Research. Ribociclib Multi-Discipline Review [Internet]. 2017 [cited 2021 Jun 11]. Available from: [https://www.accessdata.fda.gov/drugsatfda\\_docs/nda/2017/209092Orig1s000MultidisciplineR.pdf](https://www.accessdata.fda.gov/drugsatfda_docs/nda/2017/209092Orig1s000MultidisciplineR.pdf)
30. European Medicines Agency Committee for Medicinal Products For Human Use (CHMP). Abemaciclib European Public Assessment Report [Internet]. 2018 [cited 2021 Jun 10]. Available from: [https://www.ema.europa.eu/en/documents/product-information/verzenios-epar-product-information\\_en.pdf](https://www.ema.europa.eu/en/documents/product-information/verzenios-epar-product-information_en.pdf)
31. European Medicines Agency Committee for Medicinal Products For Human Use (CHMP). Everolimus European Public Assessment Report [Internet]. 2014. [cited 2019 Sep 19]. Available from: [https://www.ema.europa.eu/en/documents/product-information/afinitor-epar-product-information\\_en.pdf](https://www.ema.europa.eu/en/documents/product-information/afinitor-epar-product-information_en.pdf)





# CHAPTER 2

Effect of body composition  
on pharmacokinetics







# CHAPTER 2.1

## Worse capecitabine treatment outcome in patients with a low skeletal muscle mass is not explained by altered pharmacokinetics

Laura Molenaar-Kuijsten, Bart A.W. Jacobs, Sophie A. Kurk, Anne M. May, Thomas P.C. Dorlo, Jos H. Beijnen, Neeltje Steeghs, Alwin D.R. Huitema

Cancer Medicine 2021; 10(14): 4781-4789

Author's contribution: LMK contributed to conception and design of the study, performed the data analysis, wrote the first draft of the manuscript and implemented the input and feedback of the co-authors.

# ABSTRACT

## Background

A low skeletal muscle mass (SMM) has been associated with increased toxicity and shorter survival in cancer patients treated with capecitabine, an oral prodrug of 5-fluorouracil (5-FU). Capecitabine and its metabolites are highly water soluble and, therefore, more likely to distribute to lean tissues. The pharmacokinetics (PK) in patients with a low SMM could be changed, for example, by reaching higher maximum plasma concentrations. In this study, we aimed to examine whether the association between a low SMM and increased toxicity and shorter survival could be explained by altered PK of capecitabine and its metabolites.

## Methods

Previously, a population PK model of capecitabine and metabolites in patients with solid tumors was developed. In our analysis, we included patients from this previous analysis for which evaluable abdominal computed tomography (CT)-scans were available. SMM was measured on CT-scans, by single slice evaluation at the third lumbar vertebra, using the Slice-o-Matic software. The previously developed population PK model was extended with SMM as a covariate, to assess the association between SMM and capecitabine and metabolite PK.

## Results

PK and SMM data were available from 151 cancer patients with solid tumors. From the included patients, 55% had a low SMM. No relevant relationships were found between SMM and the PK parameters of capecitabine and, the active and toxic metabolite, 5-FU. SMM only correlated with the PK of the, most hydrophilic, but inactive and non-toxic, metabolite  $\alpha$ -fluoro- $\beta$ -alanine (FBAL). Patients with a low SMM had a smaller apparent volume of distribution and lower apparent clearance of FBAL.

## Conclusion

No alterations in PK of capecitabine and the active and toxic metabolite 5-FU were observed in patients with a low SMM. Therefore, the previously identified increased toxicity and shorter survival in patients with a low SMM, could not be explained by changes in pharmacokinetic characteristics of capecitabine and metabolites.



## INTRODUCTION

The anticancer drug capecitabine is used for the treatment of colorectal, breast and gastric cancer (1). Capecitabine is metabolized through conversion to 5'-deoxy-5-fluorocytidine (dFCR), and 5'-deoxy-5-fluorouridine (dFUR), respectively, before it forms the pharmacologically active metabolite 5-fluorouracil (5-FU)(2). 5-FU is further activated by forming nucleotides intracellularly, and finally converted to the inactive metabolite  $\alpha$ -fluoro- $\beta$ -alanine (FBAL), which is renally excreted (1–3).

A major problem for capecitabine treatment is that more than 40% of the patients experience severe toxicity, when combined with other chemotherapy this number is even higher (4–6). The most common capecitabine-induced severe toxicities include diarrhea, vomiting, and hand-foot syndrome (4). Recently, Kurk *et al.* found that colorectal patients who experience skeletal muscle mass (SMM) loss during treatment with different combinations of palliative systemic treatment regimens, including capecitabine, were at increased risk of developing severe toxicity (relative risk 1.29), and a shorter survival was observed (hazard ratio 1.19 or 1.54 dependent on treatment phase)(5,7). In these studies, Kurk *et al.* hypothesized that altered drug pharmacokinetics (PK) may contribute to the observed increased toxicity and reduced survival (5,7).

Several population pharmacokinetic studies have been performed to study the PK of capecitabine and metabolites. Results of these studies demonstrated that there is no clinically relevant correlation between several body size measures such as body surface area (BSA) or body weight and PK of capecitabine and metabolites (8–10).

Since capecitabine and its metabolites are highly watersoluble, these compounds will distribute mainly to non-lipid tissues such as muscle tissue (11). A low SMM, which is common in cancer patients, may, therefore, result in a smaller volume of distribution and potentially lead to higher maximum plasma levels (which was for example described for the beta blocker bisoprolol)(2,12). Higher maximum plasma levels could be the cause of increased toxicity; a shorter survival could be caused by dose adjustments, dose delay, or early discontinuation of treatment due to toxicity.

We hypothesized that the increased risk of severe capecitabine-induced toxicity and shorter survival in patients with a low SMM may be the result of an altered distribution of capecitabine and metabolites. Additionally, patients with a low SMM may be less fit, potentially resulting in a reduced cardiac output, which might be associated with reduced clearance of the drug and metabolites (13).



Measurement of SMM on computed tomography (CT)-scans, magnetic resonance imaging (MRI), or dual-energy X-ray absorptiometry (DXA) analysis is thought to be the most accurate way of estimating SMM (14). Since CT-scans are available for most cancer patients in routine care, CT-scans are usually used to assess SMM in a population of cancer patients.

The primary aim of the current study was to examine the association between SMM and capecitabine and metabolite PK in a heterogeneous patient population, which might explain the previously found increased toxicity and shorter survival in colorectal cancer patients with a low SMM.

## METHODS

### Study population

Our research group previously published a population PK model of capecitabine and metabolites in patients with solid tumors who were treated with capecitabine-based chemotherapy with or without radiotherapy (15). For these patients, first, availability of a CT-scan in the 5 months before sample collection for PK analysis was checked (if more than one scan was available, the last scan before sample collection was chosen; PK analysis was also performed only with the patients with a difference in time between CT-scan and PK sampling of less than 2 months). Second, the evaluability of CT-scans was verified by screening for deviations on the CT-scans, which would make measurement of SMM impossible (e.g., radiation artifacts). Third, the availability of height and weight was checked. All patients for which evaluable CT-scans, height, and weight were available were included in the analysis. The study was conducted in accordance with Good Clinical Practice and the Declaration of Helsinki and was approved by the local Medical Ethics Committee. All patients provided written informed consent prior to enrollment in the study.

### Measurement skeletal muscle mass

The SMM was measured by using the Slice-o-Matic software (version 5.0; Tomovision). First, a slice at the third lumbar level (L3) was selected on the CT-scan, because the skeletal muscle area at a single slice at the L3 level highly correlates with total body SMM ( $r^2=0.86$ )(14). The first slice where both transverse processes and the spinous process were visible was chosen. The skeletal muscle area on the L3 slice was demarcated using thresholds of -29 to 150 Hounsfield Units (HU). Slice selection and demarcation were performed by a single trained analyst. SMM was calculated from the skeletal muscle area at L3 with the following equations (Equations 1 and 2)(16,17):

$$\text{Skeletal muscle volume (L)} = 0.166 \text{ L/cm}^2 \times \text{skeletal muscle area in cm}^2 + 2.142 \text{ L} \quad (1)$$

$$\text{SMM (kg)} = \text{skeletal muscle volume in L} \times 1.06 \text{ g/cm}^3 \quad (2)$$

To determine whether patients had a low SMM, the following threshold values were used. For males an SMM <26.8 kg if BMI <25 kg/m<sup>2</sup>, and an SMM <32.5 kg if BMI ≥25 kg/m<sup>2</sup>; for females an SMM <22.6 kg for any BMI. These threshold values were based on the skeletal muscle index (skeletal muscle area divided by the squared height of the patient) threshold values published by Martin *et al.* (18).



Furthermore, fat-free mass (FFM) was calculated to compare with the measured SMM. The equations of Janmahasatian *et al.* (Equations 3 and 4) were used to calculate FFM (19–22).

$$FFM \text{ (in males)} = \frac{9.27 \times 10^3 \times \text{weight}}{6.68 \times 10^3 + 216 \times BMI} \quad (3)$$

$$FFM \text{ (in females)} = \frac{9.27 \times 10^3 \times \text{weight}}{8.78 \times 10^3 + 244 \times BMI} \quad (4)$$

In these equations weight is the total body weight in kg of a patient and BMI is the body mass index (weight/height<sup>2</sup>; weight in kg and height in m).

The correlations between SMM, and weight and FFM were tested using the Pearson correlation coefficient.

### Population pharmacokinetic modeling

A population PK model of capecitabine and its four metabolites was previously developed by our research group (15). The developed model was based on data from seven clinical studies, in which pharmacokinetic samples were taken on day 1 or day 22 and 43 of treatment with capecitabine. Rich sampling schedules were used with samples taken between 0 and 8 hours after intake of capecitabine. The structural, covariate (which included *DPYD*\*2A and gastric surgery status), and random effects model from the published model were maintained, but parameter estimates were re-estimated. Various body composition descriptors were evaluated as covariates in this existing model: weight, SMM and FFM. Age and gender were initially removed from the covariate model, because theoretically the effects of age and gender can be caused by a lower SMM in older people and women. After evaluation of the candidate covariates weight, SMM and FFM, the effects of age and gender on metabolite PK were assessed again.

Weight, SMM and FFM were separately evaluated as covariates on apparent clearance (CL/F), apparent volume of distribution of the central compartment ( $V_c/F$ ), intercompartmental clearance (Q), and volume of distribution of the peripheral compartment ( $V_p$ ) or the elimination rate constant (k) of capecitabine, dFCR, dFUR, 5-FU, and FBAL.

The effects of body composition descriptors weight, SMM, and FFM on CL/F,  $V_c/F$ , Q, and  $V_p$  were estimated pairwise as follows (Equations 5 and 6)(23–26):

$$CL = CL_{baseline} \times \left( \frac{\text{body composition}}{\text{median body composition}} \right)^{0.75} \quad (5)$$

$$V = V_{baseline} \times \left( \frac{\text{body composition}}{\text{median body composition}} \right)^1 \quad (6)$$

In which CL and V are the body composition adjusted clearance and volume of distribution, respectively.  $CL_{baseline}$  and  $V_{baseline}$  are the baseline estimates for clearance and volume of distribution, respectively.

In case of dFUR and 5-FU, only k's were previously identifiable. For these metabolites, the effects of body composition descriptors weight, SMM, and FFM were estimated as follows (Equation 7):

$$k = k_{baseline} \times \left( \frac{\text{body composition}}{\text{median body composition}} \right)^{-0.25} \quad (7)$$

In which k is the body composition adjusted elimination rate constant, and  $k_{baseline}$  is the baseline estimate for the elimination rate constant.

Based on the theory of allometric scaling, fixed coefficients were used, when testing weight, SMM and FFM as covariates (23). In addition, the coefficients were also estimated, to further investigate the relationship between SMM and PK of capecitabine and metabolites.

### Model evaluation

For model evaluation, the likelihood ratio test was used and the model fit was assessed (indicated by successful minimization, parameter precision [obtained using the \$COVARIANCE option of NONMEM®], and a drop in inter-individual variability). Formal statistical testing of the effect of SMM on PK could not be performed, since the models using fixed allometric relationships were nonhierarchical compared to the models lacking these associations. Therefore, an arbitrary drop of 15 points in minus twice the log-likelihood value was considered relevant. For models in which the exponents of the allometric relationships were estimated, formal statistical testing could be performed using the likelihood ratio test with the degrees of freedom equal to the number of included relationships. To account for multiple testing, a *p*-value of 0.005 was used (27).



## RESULTS

A schematic overview of the patient selection is shown in **Figure 1**. For nine patients, the CT-scans were not evaluable, due to anatomical abnormalities, radiation artifacts or unavailability of scan data of the L3 slice. One patient was not evaluable because height and weight data were missing. Ultimately, full data was available for 151 patients. In **Table 1**, the patient characteristics are shown. From the included patients, 55% had a low SMM. The time between CT-scan and pharmacokinetic sampling had a median of less than a month, and was shorter than 2 months in 93% of patients, with exceptions to a maximum of 154 days.

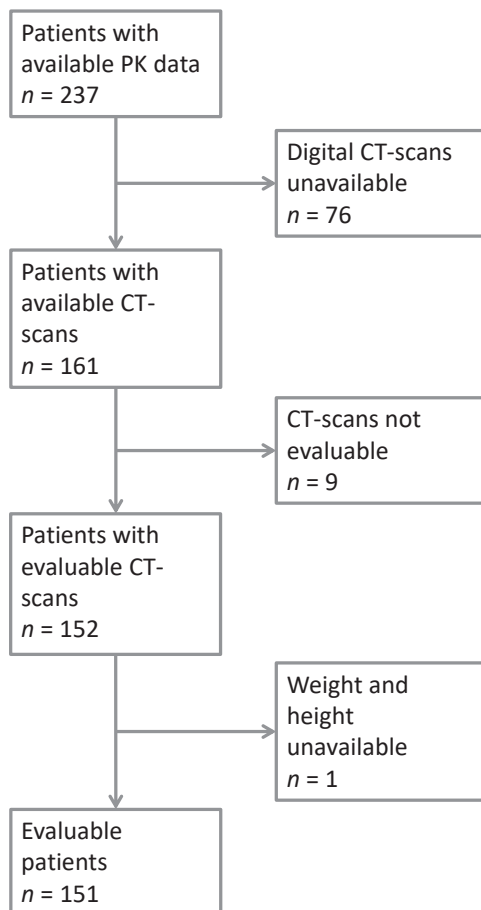


Figure 1. Schematic overview of patient selection, starting with the patients included in the population PK model published by Jacobs *et al.* PK, pharmacokinetic; CT-scan, computed tomography-scan.

Table 1. Patient characteristics (n=151).

Characteristic	n (%) or median [range]
Capecitabine dose (mg)	1,650 [300-2,600]
Gender	
Male	93 (62%)
Female	58 (38%)
Age (years)	58 [31-77]
DPYD*2A	
Wildtype	139 (92%)
Heterozygous mutant	12 (8%)
Gastric surgery	
No gastrectomy	103 (68%)
Total gastrectomy	15 (10%)
Partial gastrectomy	24 (16%)
Esophagogastrectomy	9 (6%)
Height (cm)	174 [152-201]
Weight (kg)	73 [39-99]
BSA (m <sup>2</sup> )	1.9 [1.3-2.3]
BMI (kg/m <sup>2</sup> )	24 [16-35]
Skeletal muscle mass (kg) <sup>a</sup>	27 [15-38]
Fat-free mass (kg) <sup>b</sup>	55 [29-73]
Low skeletal muscle mass <sup>c</sup>	
Yes	84 (56%)
No	67 (44%)
Time between CT-scan and PK sampling (days)	26 [0-154]

<sup>a</sup> Skeletal muscle mass as measured on computed tomography-scans.

<sup>b</sup> Fat-free mass as calculated by the formulas of Janmahasatian *et al.* (20).

<sup>c</sup> A low skeletal muscle mass was for males defined as a SMM <26.8 kg if BMI <25 kg/m<sup>2</sup> and as SMM <32.5 kg if BMI ≥25 kg/m<sup>2</sup> (calculated with a median height of 180 cm), and for females as a SMM <22.6 kg for any BMI (calculated with a median height of 168 cm)(18).

DPYD, dihydropyrimidine dehydrogenase.

SMM, weight and FFM were significantly but poorly correlated (Pearson correlation coefficients  $r=0.5$ , **Figures 2** and **3**). Therefore, weight, SMM and FFM were tested in separate PK models.

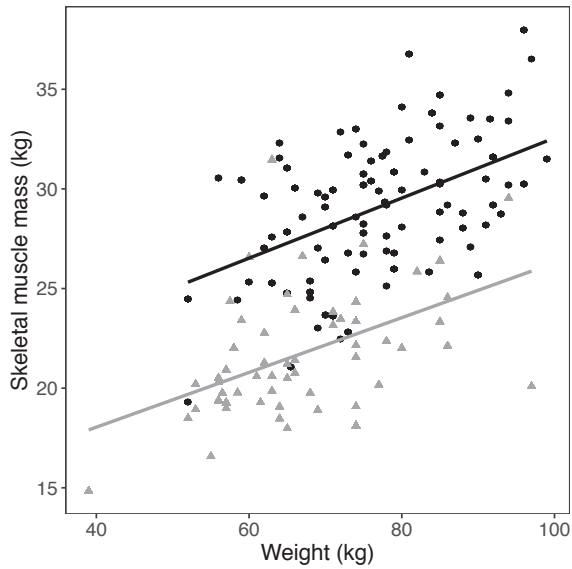


Figure 2. Correlation between weight and skeletal muscle mass, separated by gender. Males are displayed by black circles and females by grey triangles. Correlation coefficient males:  $R=0.49$ ,  $p<0.005$ ; females:  $R=0.47$ ,  $p<0.005$ .

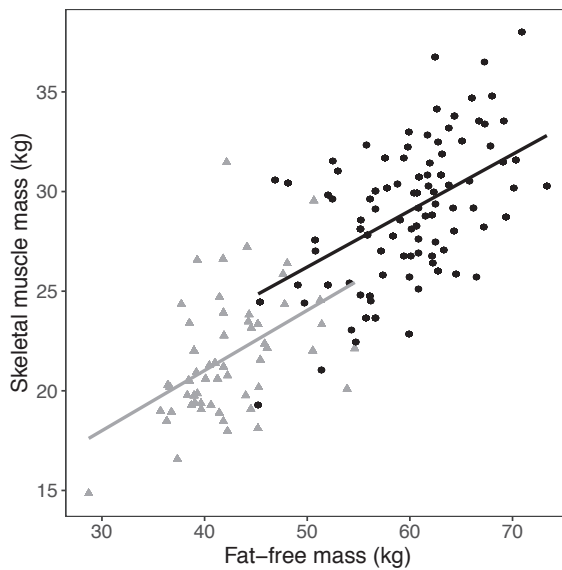


Figure 3. Correlation between calculated fat-free mass and skeletal muscle mass, separated by gender. Males are displayed by black circles and females by grey triangles. Correlation coefficient males:  $R=0.53$ ,  $p<0.005$ ; females:  $R=0.45$ ,  $p<0.005$ .



First, the PK model was extended with one of the three parameters for body composition (weight, SMM or FFM) as a covariate on the PK parameters ( $CL/F$ ,  $V_c/F$ ,  $Q$ ,  $V_p$ ,  $k$ ) of capecitabine and its four metabolites all at once, with fixed coefficients. In all cases, a small increase in minus twice log-likelihood value was found, demonstrating the lack of an overall effect of body size measures on the PK.

Second, weight, SMM, and FFM were separately added as potential covariates for the PK of capecitabine, dFCR, dFUR and 5-FU. Also here, no relevant relationships were found between PK parameters and the different measures for body size (no relationships reaching the 15 points minus twice log-likelihood value decrease threshold).

Finally, weight, SMM and FFM were introduced as potential covariates on  $CL/F$ ,  $V_c/F$ ,  $Q$  and  $V_p$  of FBAL. Addition of weight as potential covariate increased the minus twice log-likelihood value by 5 points. Addition of SMM and FFM resulted in a drop in minus twice the log-likelihood value of 28 points for SMM and 24 points for FFM, suggesting a relevant relationship with the pharmacokinetic parameters.

In **Table 2**, the results for inclusion of weight, SMM and FFM, with fixed coefficients, in the PK model are summarized. **Figure 4** shows the relationships between SMM and the individual PK parameters of capecitabine, 5-FU and FBAL, before SMM was added as a covariate on the corresponding compound. In case a relationship between SMM and the pharmacokinetic parameters exists, the figure should show a correlation.

Table 2. Effect of body composition, age and gender on the pharmacokinetic model using the likelihood ratio test.

Model	$\Delta$ minus twice log-likelihood value relative to baseline model
Covariate effect on $CL/F$ , $V_c/F$ , $Q$ , and $V_p$ of capecitabine, dFCR and FBAL, and on $k$ of dFUR and 5-FU	
Weight	+7
SMM	+12
FFM	+4
Covariate effect on $CL/F$ , $V_c/F$ , $Q$ , and $V_p$ of capecitabine	
Weight	-8
SMM	-1
FFM	-1

Table 2. Continued.

Model	$\Delta$ minus twice log-likelihood value relative to baseline model
Covariate effect on CL/F, $V_c$ /F, Q, and $V_p$ of dFCR	
Weight	-8
SMM	+13
FFM	+3
Covariate effect on k of dFUR	
Weight	+8
SMM	+6
FFM	+8
Covariate effect on k of 5-FU	
Weight	+6
SMM	+5
FFM	+8
Covariate effect on CL/F, $V_c$ /F, Q, and $V_p$ of FBAL	
Weight	+5
SMM	-28
FFM	-24
Covariate effect on CL/F of FBAL	
Age and gender	-51
Covariate effect of SMM on CL/F, $V_c$ /F, Q, and $V_p$ of FBAL, combined with covariate effect of	
Age and gender on CL/F of FBAL	-50
Age on CL/F of FBAL	-50
Gender on CL/F of FBAL	-27

Coefficients were fixed based on the theory of allometric scaling. To calculate the difference in the minus twice log-likelihood value, the baseline model was used as a comparator. No *p*-values are shown because the tested models were nonhierarchical and therefore no formal statistical testing could be performed. A positive difference in minus twice log-likelihood value indicates a worse model fit, and a negative difference indicates a better model fit.

CL/F, apparent clearance;  $V_c$ /F, apparent volume of distribution for the central compartment; Q, intercompartmental clearance;  $V_p$ , volume of distribution of the peripheral compartment; k, elimination rate constant; SMM, skeletal muscle mass; FFM, fat-free mass; dFCR, 5'-deoxy-5-fluorocytidine; dFUR, 5'-deoxy-5-fluorouridine; 5-FU, 5-fluorouracil; FBAL,  $\alpha$ -fluoro- $\beta$ -alanine.

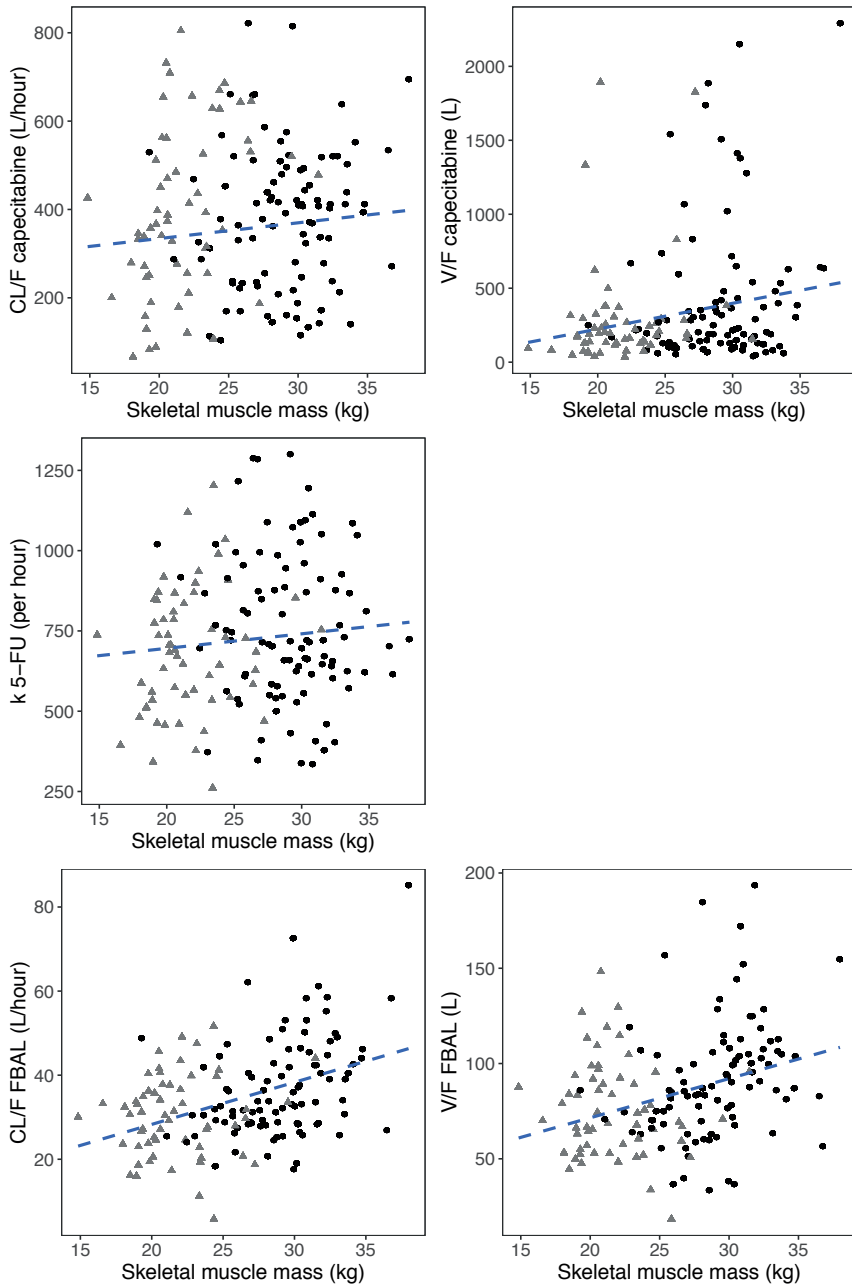


Figure 4. Relationships between skeletal muscle mass and the individual pharmacokinetic parameters of capecitabine, 5-FU and FBAL. Males are displayed by black circles and females by grey triangles including a linear regression line (dashed line). CL/F, apparent clearance; V/F, apparent volume of distribution central compartment; k, elimination rate constant; 5-FU, 5-fluorouracil; FBAL,  $\alpha$ -fluoro- $\beta$ -alanine.

Next, the exponents of the allometric relationships were estimated for SMM. In comparison to the results with a fixed coefficient, the minus twice log-likelihood value was between 5 and 21 points lower if the coefficient was estimated. The drop in minus twice log-likelihood value of 21 points was observed for dFCR, but compared to the baseline model without SMM as a covariate, it was only a drop of 7 points and therefore not considered clinically relevant. The estimated coefficient for capecitabine was 0.271 for CL/F and Q, and 1.5 for  $V_c/F$  and  $V_p$ . A coefficient of 0.0815 was estimated for the k of 5-FU. And the estimated coefficient for FBAL was 0.782 for CL/F and Q, and 0.559 for  $V_c/F$  and  $V_p$ . Except for the coefficient on V of capecitabine, the estimated coefficients were small (in allometric scaling 0.75 is used for CL and 1 for V). To determine if the difference in the coefficient on V of capecitabine was significant, SMM was added as covariate on V of capecitabine only, instead of adding it on V and CL of capecitabine simultaneously. This resulted in a significant different coefficient of 1.25 ( $p < 0.005$ , drop in minus twice log-likelihood value of 9 points), but with a large relative standard error (RSE) and 95% confidence interval of 42% and 0.43-2.07, respectively. To conclude, estimation of the coefficients did not result in a different interpretation of the outcomes.

In the previously published model age and gender were added as covariates on the CL of FBAL, which were initially removed in our analysis (15). After the introduction of SMM as a covariate on CL/F,  $V_c/F$ , Q, and  $V_p$  of FBAL, the addition of gender did not result in a significant improvement of the model anymore. This final model (with SMM as a covariate on CL/F,  $V_c/F$ , Q, and  $V_p$  of FBAL, and age as a covariate on CL/F of FBAL) was also tested without the patients with a difference in time between CT-scan and PK sampling of more than 2 months, which did not lead to a difference in the predicted parameter estimates.

## DISCUSSION

In patients treated with capecitabine, often given in combination with other toxic chemotherapy or targeted therapy, a low SMM has been associated with more treatment-related toxicity and a shorter survival (5,28–30). The primary aim of our study was to investigate whether this association could be explained by altered pharmacokinetics, such as higher maximum plasma concentrations of capecitabine and/or its metabolites due to a low SMM.

The results of our study showed no effects of SMM on the PK of capecitabine and its active metabolite 5-FU. However, SMM was associated with PK of the most hydrophilic metabolite FBAL. Previously, Gieschke *et al.* found that there is no relationship between the area under the concentration-time curve (AUC; indicator of exposure to the drug) of FBAL and treatment-related grade 3–4 adverse events, including treatment-related grade 3–4 diarrhea, grade 3 hand–foot syndrome, and grade 3–4 hyperbilirubinemia (9). Only a correlation between the AUC of FBAL and diarrhea was found, but this was probably due to FBAL being a marker for the amount of 5-FU formed (9). Also, there was no relation between the AUC of FBAL and time to progression and survival (9). Therefore, the identified effects of SMM on PK of FBAL are considered clinically irrelevant. Our results, thus, do not support the hypothesis that patients with a low SMM would show relatively low values for CL and/or V of capecitabine and metabolites, which thereby would provide an explanation for the increased toxicity and decreased survival in patients with a low SMM (9,31).

Previously, Gusella *et al.* studied the relationship between body composition and PK of intravenously administered 5-FU, in 43 patients with colorectal cancer (32). Significant but poor correlations between total body water and CL ( $r^2=0.15$ ), total body water and V ( $r^2=0.16$ ), FFM and CL ( $r^2=0.17$ ), and FFM and V ( $r^2=0.17$ ) were found. But also poor correlations were found between BSA and CL ( $r^2=0.12$ ), body weight and CL ( $r^2=0.21$ ), and between body weight and V ( $r^2=0.18$ ). We could not reproduce these findings in this much larger study for capecitabine, in which we included 151 patients. A major difference between our study and the study of Gusella *et al.* was the administration of the prodrug capecitabine instead of intravenous administration of 5-FU. It might be expected that variability in PK is much larger after oral administration of capecitabine than after intravenous administration of 5-FU, because of variability in absorption time and bioavailability of capecitabine. Indeed, inter-individual variability in PK parameters of capecitabine and metabolites was high. Therefore, it might be possible that a relative small effect of SMM on the PK of capecitabine, 5-FU and metabolites remains undetected in the overall large variability in PK. If so, the absence of significant relationships in our large study strongly suggests that these potential effects are only of minor clinical relevance.

An advantage over the study of Gusella *et al.* is that in our study body composition was measured on CT-scans. There are different ways of determining body composition, based on different physical and biological principles. In the study of Gusella *et al.*, bioelectrical impedance analysis (BIA) was used to determine fat-free mass, in which the rate of a low-voltage electrical current travelling through the body is measured (32). This technique is simple and safe, but not very accurate because it is dependent on hydration of the body (total body water is measured and FFM is calculated based on the assumption that 73% of the FFM consists of water)(33). Imaging methods are considered the most accurate to measure body composition and can therefore be seen as "gold standards" (14,19,33). Since CT-scans are available for most cancer patients in routine care, patients are not exposed to additional radiation for measurement of body composition using these scans. The most accurate results are obtained by using CT-scans just before the start of treatment with capecitabine (34). Due to the retrospective nature of our study, the range in time between CT-scans and PK sampling was up to 5 months, but with a median of less than 1 month, and it was shorter than 2 months in 93% of patients. The final model (with SMM as covariate on CL and V of FBAL, and age as covariate on CL of FBAL) was also tested without the ten patients with a range in time between CT-scans and PK sampling of more than 2 months, which did not lead to a difference in parameter estimates predicted by the model.

It could be seen as a limitation of our study that allometric scaling was applied when testing SMM as a covariate. Based on the theory of allometric scaling, which is a generally accepted theory for scaling of PK parameters between different body sizes, a fixed coefficient of 0.75 was used, when weight, SMM and FFM were tested as potential covariates on CL and Q (Equation 5). The basis of allometric scaling is a slope of 0.75 when body weight is plotted against basal metabolic rate, which most likely also applies to SMM (23–26). To further investigate the relationship between SMM and PK of capecitabine and metabolites, the exponents in the relationships were also estimated. Overall, these exponents were small and with large confidence intervals, indicating that indeed no relationship between SMM and PK could be found.

## CONCLUSION

To conclude, results of the analyses demonstrated that PK of capecitabine and its metabolite 5-FU are not associated with SMM. Therefore, alterations in capecitabine and metabolite PK do not provide an explanation for increased toxicity and decreased survival in patients with a low SMM.

## REFERENCES

1. European Medicines Agency Committee for Medicinal Products For Human Use (CHMP). Capecitabine European Public Assessment Report [Internet]. [cited 2019 Nov 15]. Available from: [https://www.ema.europa.eu/en/documents/product-information/xeloda-epar-product-information\\_en.pdf](https://www.ema.europa.eu/en/documents/product-information/xeloda-epar-product-information_en.pdf)
2. Reigner B, Blesch K, Weidekamm E. Clinical pharmacokinetics of capecitabine. *Clin Pharmacokinet*. 2001;40(2):85–104.
3. Derissen EJB, Jacobs BAW, Huitema ADR, Rosing H, Schellens JHM, Beijnen JH. Exploring the intracellular pharmacokinetics of the 5-fluorouracil nucleotides during capecitabine treatment. *Br J Clin Pharmacol*. 2016;81(5):949–57.
4. Hoff BPM, Ansari R, Batist G, Cox J, Kocha W, Kuperminc M, et al. Comparison of Oral Capecitabine Versus Intravenous Fluorouracil Plus Leucovorin as First-Line Treatment in 605 Patients With Metastatic Colorectal Cancer: Results of a Randomized Phase III Study. *J Clin Oncol*. 2001;19(8):2282–92.
5. Kurk S, Peeters P, Stellato R, Dorresteijn B, Jong P De, Jourdan M, et al. Skeletal muscle mass loss and dose-limiting toxicities in metastatic colorectal cancer patients. *J Cachexia Sarcopenia Muscle*. 2019;10(4):803–13.
6. Simkens LHJ, Van Tinteren H, May A, Ten Tije AJ, Creemers GJM, Loosveld OJL, et al. Maintenance treatment with capecitabine and bevacizumab in metastatic colorectal cancer (CAIRO3): A phase 3 randomised controlled trial of the Dutch Colorectal Cancer Group. *Lancet*. 2015;385(9980):1843–52.
7. Kurk SA, Peeters PHM, Dorresteijn B, de Jong PA, Jourdan M, Creemers GJM, et al. Loss of skeletal muscle index and survival in patients with metastatic colorectal cancer: Secondary analysis of the phase 3 CAIRO3 trial. *Cancer Med*. 2020;9(3):1033–43.
8. Cassidy J, Cameron D, Steward W, Byrne O, Jodrell D, Roos B, et al. Bioequivalence of two tablet formulations of capecitabine and exploration of age, gender, body surface area, and creatinine clearance as factors influencing systemic exposure in cancer patients. *Cancer Chemother Pharmacol*. 1999;44:453–60.
9. Gieschke R, Burger H, Reigner B, Blesch KS, Steimer J. Population pharmacokinetics and concentration – effect relationships of capecitabine metabolites in colorectal cancer patients. *Br J Clin Pharmacol*. 2003;55:252–63.
10. Urien S, Reza K. Pharmacokinetic Modelling of 5-FU Production from Capecitabine — A Population Study in 40 Adult Patients with Metastatic Cancer. *J Pharmacokinet Pharmacodyn*. 2005;32:817–33.
11. DrugBank.ca. Capecitabine [Internet]. [cited 2020 Jan 9]. Available from: <https://www.drugbank.ca/drugs/DB01101>
12. Cvan Trobec K, Grabnar I, Kerec Kos M, Vovk T, Trontelj J, Anker SD, et al. Bisoprolol pharmacokinetics and body composition in patients with chronic heart failure: a longitudinal study. *Eur J Clin Pharmacol*. 2016;72(7):813–22.
13. Toutain PL, Bousquet-Mélou A. Plasma clearance. *J Vet Pharmacol Ther*. 2004;27(6):415–25.
14. Mourtzakis M, Prado CMM, Lieffers JR, Reiman T, McCargar LJ, Baracos VE. A practical and precise approach to quantification of body composition in cancer patients using computed tomography images acquired during routine care. *Appl Physiol Nutr Metab*. 2008;33(5):997–1006.

15. Jacobs BAW, Deenen MJ, Joerger M, Rosing H, de Vries N, Meulendijks D, et al. Pharmacokinetics of capecitabine and four metabolites in a heterogeneous population of cancer patients: a comprehensive analysis. *CPT pharmacometrics Syst Pharmacol*. 2019;8:940–50.
16. Shen W, Punyanitya M, Wang Z, Gallagher D, St M, Albu J, et al. Total body skeletal muscle and adipose tissue volumes: estimation from a single abdominal cross-sectional image. *J Appl Physiol*. 2004;97:2333–8.
17. Ward SR, Lieber RL. Density and hydration of fresh and fixed human skeletal muscle. *J Biomech*. 2005;38:2317–20.
18. Martin L, Birdsell L, MacDonald N, Reiman T, Clandinin MT, McCargar LJ, et al. Cancer Cachexia in the Age of Obesity: Skeletal Muscle Depletion Is a Powerful Prognostic Factor, Independent of Body Mass Index. *J Clin Oncol*. 2013;31(12):1539–47.
19. Sinha J, Duffull SB, Al-Sallami HS. A Review of the Methods and Associated Mathematical Models Used in the Measurement of Fat-Free Mass. *Clin Pharmacokinet*. 2018;57(7):781–95.
20. Janmahasatian S, Duffull SB, Ash S, Ward LC, Byrne NM, Green B. Quantification of Lean Bodyweight. *Clin Pharmacokinet*. 2005;44(10):1051–65.
21. Halsne T, Muller, Spiten A, Sherwani AG, Tore L, Mikalsen G. The Effect of New Formulas for Lean Body Mass on Lean-Body-Mass-Normalized SUV in Oncologic 18F-FDG PET/CT. *J Nucl Med Technol*. 2018;46(3):253–9.
22. Boellaard R, Delgado-bolton R, Oyen WJG, Giammarile F, Tatsch K, Eschner W, et al. FDG PET/CT: EANM procedure guidelines for tumour imaging: version 2.0. *Eur J Nucl Med Mol Imaging*. 2015;42:328–54.
23. West GB, Brown JH, Enquist BJ. A General Model for the Origin of Allometric Scaling Laws in Biology. *Science*. 1997;276(5309):122–6.
24. Anderson BJA, Olford NHGH. Review Mechanistic Basis of Using Body Size and Maturation to Predict Clearance in Humans. *Drug Metab Pharmacokinet*. 2009;24(1):25–36.
25. Odore E, Lokiec F, Cvitkovic E, Bekradda M, Herait P, Bourdel F, et al. Phase I Population Pharmacokinetic Assessment of the Oral Bromodomain Inhibitor OTX015 in Patients with Haematologic Malignancies. *Clin Pharmacokinet*. 2016;55:397–405.
26. Rhodin MM, Anderson BJ, Peters AM, Coulthard MG, Wilkins B, Cole M, et al. Human renal function maturation: a quantitative description using weight and postmenstrual age. *Pediatr Nephrol*. 2009;24:67–76.
27. Boeckmann AJ, Sheiner LB, Beal SL. NONMEM Users Guide - Part V [Internet]. Ellicott City, Maryland, USA: ICON Development Solutions; 2011 [cited 2020 Aug 11]. Available from: <https://nonmem.iconplc.com/nonmem720/guides/>
28. Prado CMM, Baracos VE, McCargar LJ, Reiman T, Mourtzakis M, Tonkin K, et al. Sarcopenia as a Determinant of Chemotherapy Toxicity and Time to Tumor Progression in Metastatic Breast Cancer Patients Receiving Capecitabine Treatment. *Clin Cancer Res*. 2009;15(8):2920–7.
29. Prado CMM, Baracos VE, McCargar LJ, Mourtzakis M, Mulder KE, Reiman T, et al. Body composition as an independent determinant of 5-fluorouracil-based chemotherapy toxicity. *Clin Cancer Res*. 2007;13(11):3264–8.
30. Williams GR, Deal AM, Shachar SS, Walko CM, Patel JN, O'Neil B, et al. The impact of skeletal muscle on the pharmacokinetics and toxicity of 5-fluorouracil in colorectal cancer. *Cancer Chemother Pharmacol*. 2017;81(2):1–5.
31. Gieschke R, Reigner B, Blesch KS, Steimer J. Population Pharmacokinetic Analysis of the Major Metabolites of Capecitabine. *J Pharmacokinet Pharmacodyn*. 2002;29(1).



32. Gusella M, Toso S, Ferrazzi E, Ferrari M, Padrini R. Relationships between body composition parameters and fluorouracil pharmacokinetics. *Br J Clin Pharmacol*. 2002;54(2):131–9.
33. Lee S, Gallagher D. Assessment methods in human body composition. *Curr Opin Clin Nutr Metab Care*. 2008;11(5):566–72.
34. Kurk SA, Peeters PHM, Dorresteijn B, Jong PA De, Jourdan M, Kuijf HJ, et al. Impact of different palliative systemic treatments on skeletal muscle mass in metastatic colorectal cancer patients. *J Cachexia Sarcopenia Muscle*. 2018;9(5):909–19.







# CHAPTER 22

## The association of cisplatin pharmacokinetics and skeletal muscle mass in head and neck cancer patients: the prospective PLATISMA study

Laura Molenaar-Kuijsten\*, Najiba Chargi\*, Laura F.J. Huiskamp, Lot A. Devriese, Remco de Bree, Alwin D.R. Huitema

\* These authors contributed equally

Accepted for publication in European Journal of Cancer

Authors contribution: NC was responsible for pharmacokinetic sampling and analysis of CT-scans. NC and LMK contributed to data management. NC analyzed the cisplatin related toxicities. LMK performed the data analysis by population pharmacokinetic modeling. NC and LMK wrote the first draft of the manuscript and implemented the input and feedback of the co-authors.

# ABSTRACT

## Background

Locally advanced head and neck squamous cell carcinoma (HNSCC) is commonly treated with cisplatin-based chemoradiotherapy (CRT). Cisplatin is associated with severe toxicity, which negatively affects survival. In recent years, a relationship between low skeletal muscle mass (SMM) and increased toxicity has been described. This increased toxicity may be related to altered cisplatin distribution and binding in the fat-free body mass of which SMM is the largest contributor. This study aims to investigate the association between cisplatin pharmacokinetics and SMM in HNSCC patients.

## Methods

We performed a prospective observational study in HNSCC patients treated with CRT. Patients received standard-of-care chemotherapy with three cycles of cisplatin at a dose of 100 mg/m<sup>2</sup> per cycle. Quantitative data on SMM, measured on computed tomography-scans and cisplatin pharmacokinetics (total and ultrafilterable plasma concentrations) were collected, as well as data on toxicity.

## Results

45 evaluable patients were included in the study. A large proportion of the study population had a low SMM (46.7%). The majority of patients (57.8%) experienced cisplatin dose-limiting toxicities. Pharmacokinetic analysis showed a significant relationship between cisplatin pharmacokinetics and SMM, weight, fat-free mass and body surface area ( $p < 0.005$ ). In a simulation, patients with a low SMM (<25.8 kg) were predicted to reach higher bound cisplatin concentrations.

## Conclusion

We found an association between cisplatin pharmacokinetics and SMM, however, this relationship was also seen between cisplatin pharmacokinetics and other body composition descriptors.

## INTRODUCTION

Head and neck squamous cell carcinomas (HNSCCs) are among the most frequent tumors worldwide (1). Two-thirds of HNSCC patients present with advanced disease which is commonly treated with cisplatin-based chemoradiotherapy (CRT)(2).

Acute toxicity of cisplatin, such as nephrotoxicity and ototoxicity, results in dose reductions, treatment delay or treatment cessation (chemotherapy dose-limiting toxicity, CDLT) in at least 30% of treated patients (3–5). It has been described that patients who receive a lower cumulative dose of cisplatin have a worse oncological outcome (5). It is, therefore, assumed that CDLTs negatively affect survival because patients receive suboptimal treatment. In recent years, a relationship between radiologically assessed low skeletal muscle mass (SMM) and CDLT has been described for HNSCC (6–8). A retrospective study in HNSCC patients undergoing CRT showed that patients with low SMM had a 3-fold higher risk of experiencing CDLT (44.3% versus 13.7%), which resulted in a significantly shorter overall survival than for patients who were able to complete CRT (7).

An explanation for the relationship between low SMM and toxicity might be that hydrophilic drugs, including cisplatin, mainly distribute into the fat-free body mass of which SMM is the largest contributor (9). Cisplatin is a highly reactive drug and upon administration the drug will bind to tumor DNA causing its anticancer effect, but also to tissue causing side effects (e.g., in the nephrons causing nephrotoxicity), and lastly to tissue without any pharmacodynamic effect (e.g., muscle tissue)(10). We hypothesized that this latter compartment is highly related to SMM. In patients with a low SMM less tissue is available to which cisplatin can bind relatively harmless, but more reactive cisplatin is available to bind to tissue related to toxicity. This might lead to increased CDLTs negatively affecting outcome.

The primary aim of this prospective observational study was to investigate the relationship between SMM and pharmacokinetic (PK) parameters of cisplatin in HNSCC patients. We hypothesized that an altered distribution of cisplatin, which is reflected by differences in cisplatin plasma concentrations, could explain why patients with low SMM are more prone to experience cisplatin toxicity. As a secondary objective, the relationship between SMM and toxicity was studied.



## METHODS

### Ethical considerations

The Medical Research Ethics Committee (METC) of the University Medical Center Utrecht has reviewed the study in accordance with the Dutch Medical Research Involving Human Subjects Act (WMO) and other applicable Dutch and European regulations and has approved this study in June 2018 (METC 18-225/D). The study was conducted in compliance with Good Clinical Practice and the Declaration of Helsinki. All patients provided written informed consent prior to inclusion in the study.

### Study population, study design and sample size

This study was designed as a monocenter prospective observational cohort study in HNSCC patients receiving three-weekly high-dose (100 mg/m<sup>2</sup>) primary or adjuvant CRT. To estimate the sample size a clinical trial simulation ( $n=200$ ) was performed based on a previously published PK model on ultrafilterable cisplatin (14). An allometric relationship between SMM and cisplatin clearance was assumed. Patient characteristics (SMM and body surface area (BSA)) were simulated in accordance with clinical practice. It was estimated that data from 45 patients was sufficient to find a significant relationship between cisplatin clearance and SMM with a power of >80%. As PK models with SMM and BSA are nonhierarchical, the difference between the two models cannot be statistically tested. However, in approximately 70% of the trials, this relationship showed better goodness-of-fit than a BSA-based relationship. Finally, the allometric exponent could be estimated with acceptable precision (approximately 28% relative standard error) with a sample size of 45 patients.

### Skeletal muscle mass measurement

Segmentation of SMM was manually performed using the Slice-o-Matic software (Tomovision, Canada). Skeletal muscle area (SMA) was measured on pre-treatment computed tomography (CT)-imaging at the level of the third lumbar vertebra (L3) by a validated method (15). If no pre-treatment imaging was available at the level of L3, SMA was measured at the level of the third cervical vertebra (C3) and then converted to SMA at the level of L3 by use of an earlier defined formula (15). To correct for height, SMA was divided by squared height to yield the skeletal muscle mass index (SMI). Low SMM was defined as a lumbar SMI (LSMI)  $\leq 43.2$  cm<sup>2</sup>/m<sup>2</sup> (16). The LSMI was used for analysis of demographic and anthropometric measurements. For PK analysis, the absolute volume of the muscle compartment was used, because cisplatin will distribute to this absolute volume after administration to a patient, by converting SMA to SMM with use of the following equations (17,18):

$$\text{Skeletal muscle volume (L)} = 0.166 \text{ L/cm}^2 \times \text{skeletal muscle area in cm}^2 + 2.142 \text{ L} \quad (1)$$

$$\text{SMM (kg)} = \text{skeletal muscle volume in L} \times 1.06 \text{ g/cm}^3 \quad (2)$$

For simulation purposes, the threshold value of low LSMI was converted to a threshold value for SMM in kilograms. Using the median height in our patient population, the threshold for low SMM was defined to be  $\leq 25.8$  kg. SMM was compared with the calculated fat-free mass (FFM), which is another way to estimate body composition. For calculation of FFM the equations of Janmahasatian *et al.* were used (19):

$$\text{FFM (in males)} = \frac{9.27 \times 10^3 \times \text{weight}}{6.68 \times 10^3 + 216 \times \text{BMI}} \quad (3)$$

$$\text{FFM (in females)} = \frac{9.27 \times 10^3 \times \text{weight}}{8.78 \times 10^3 + 244 \times \text{BMI}} \quad (4)$$

In these equations BMI is the body mass index (weight/height<sup>2</sup>; weight in kg and height in m).

### Cisplatin bioanalysis

Plasma and ultrafilterable (using a filter of 30 kDa) samples were collected from patients at different time points (pre-dose, end of infusion and 1 hour, 3 hours, 7 hours and 20 hours after end of infusion) during the first cycle of cisplatin. Both total and ultrafilterable plasma concentrations of platinum were measured by inductively coupled plasma-mass spectrometry (ICP-MS) by a previously described method (20). For simplification, the terms free and bound cisplatin are used throughout to denote ultrafilterable and non-ultrafilterable platinum species, respectively.

### Cisplatin related toxicity

Toxicity was scored according to the Common Terminology Criteria for Adverse Events (CTCAE) guidelines, version 4.03 (21). CDLT was defined as any toxicity resulting in cisplatin dose reduction of  $\geq 50\%$ , a treatment delay of  $\geq 4$  days, or cessation of cisplatin after the first or second cycle of therapy.

### Pharmacokinetic analysis

For description of cisplatin PK a two-compartment model for free cisplatin, followed by one compartment for protein-bound cisplatin was used, as previously described by Urien *et al.* (14). Clearance of free cisplatin was considered negligible compared to binding to proteins and, therefore, not included in the model. More detailed information about the PK model can be found in the **Supplementary Material**.

The body composition descriptors weight, SMM, FFM, and BSA were separately evaluated as covariates on clearance of free cisplatin ( $CL_{free}$ ), volume of distribution of free cisplatin ( $V_{free}$ ), intercompartmental clearance (Q), and volume of distribution of the peripheral compartment ( $V_p$ ) of free cisplatin, clearance of bound cisplatin ( $CL_{bound}$ ) and volume of distribution of bound cisplatin ( $V_{bound}$ ). The body composition descriptors were evaluated using Equation 5:

$$\theta_i = \theta_{pop} \times \left( \frac{\text{body composition}}{\text{median body composition}} \right)^k \quad (5)$$

Where  $\theta_i$  represents the parameter estimate for individual  $i$ ,  $\theta_{pop}$  represents the typical parameter estimate for the population, and  $k$  represents the exponent.

Based on the theory of allometric scaling the exponent was fixed to 0.75 for evaluation of clearance, and to 1 for volume of distribution (22). For both clearance and volume of distribution the exponent was also estimated.

The glomerular filtration rate (GFR; calculated using the creatinine-based Cockcroft-Gault formula, or the Chronic Kidney Disease Epidemiology Collaboration (CKD-EPI) cystatin C equation and capped on a maximum value of 130 mL/min), and albumin were examined as additional relevant covariates, as described in the **Supplementary Material**.

In case the addition of the GFR and/or albumin resulted in a better fit of the baseline model (based on the objective function value (OFV), a drop in inter-individual variability (IIV) and a difference in effect size between the 25% and 75% quartile), body composition was also evaluated in combination with these covariates.

Lastly, the final model was used to simulate the effects of different SMMs on the population predicted cisplatin concentrations. In this simulation the effects of different SMMs around the threshold of 25.8 kg for low SMM were predicted. For the chosen SMMs, the corresponding BSAs were extracted from the data to calculate the given dose for the virtual patients.

### Statistical analysis

Formal statistical testing for the PK model was performed using the likelihood ratio test (by means of the OFV which is minus twice the log-likelihood) for the models without fixed coefficients, a  $p$ -value of 0.005 was used to take into account multiple testing (23) and the degrees of freedom were equal to the number of included relationships. For the models with fixed coefficients, the drop in OFV was used as a guidance. Other statistical



analyses were performed using R (version 3.6.3). Correlation analysis was performed by use of Pearson's correlation analysis for variables with a normal distribution and Spearman's correlation analysis was used for non-normally distributed variables. Chi-square statistics were used for analyzing differences between the frequencies of each categorical variable with the presence or absence of low SMM and DLT.



## RESULTS

### Patients characteristics

In total, 50 patients were included between July 2018 and September 2020. Five patients eventually did not participate in the study, 3 due to withdrawal of informed consent and 2 did not undergo CRT. **Table 1** shows the characteristics of the 45 evaluable patients, 21 patients (46.7%) had low SMI. Median LSMI was 44.06 cm<sup>2</sup>/m<sup>2</sup> (interquartile range (IQR) 37.7-50.9). Patients without low SMM were more likely to be overweight (58.3% versus 19%;  $p < 0.01$ ) and obese (25.0% versus 4.8%;  $p < 0.01$ ) compared to patients with low SMM.

The majority of patients were treated in a primary setting ( $n=40$ , 88.9%) and had a tumor, node, metastasis (TNM) stage IV tumor according to the 8<sup>th</sup> edition TNM cancer staging criteria ( $n=25$ , 55.5%). One patient received a weekly low-dose cisplatin schedule (40 mg/m<sup>2</sup> weekly) due to comorbidity.

### Cisplatin dose-limiting toxicity

Of the 45 included patients, 26 patients (57.8%) did not complete 3 cycles of cisplatin. All were due to CDLT and consisted of: creatinine increase grade 2 ( $n=11$ ) and grade 3 ( $n=2$ ), nausea grade 3 ( $n=3$ ), hearing impairment grade 2 ( $n=6$ ), neutropenia grade 3 ( $n=1$ ), heart failure grade 3 and increased creatinine grade 3 ( $n=1$ ), creatinine increase grade 2, hypomagnesaemia grade 3 and hyponatremia grade 3 ( $n=1$ ), hearing impaired grade 2 and neutropenia grade 4 ( $n=1$ ). In our dataset no correlation was found between CDLTs and SMM (unpaired T-test,  $p=0.39$ ), as illustrated in **Figure 1**.

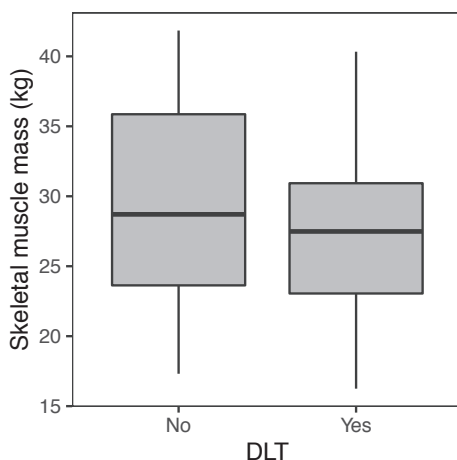


Figure 1. Correlation between dose-limiting toxicities (DLTs) of cisplatin and skeletal muscle mass (unpaired T-test;  $p=0.39$ ).

### Pharmacokinetic results

SMM and weight were significantly correlated with a Pearson correlation coefficient of 0.6, as shown in **Figure 2**. Based on goodness-of-fit plots the data were well described by the used PK model. For 5 patients no SMA at the L3 slice was available, therefore SMA at the C3 slice was used.

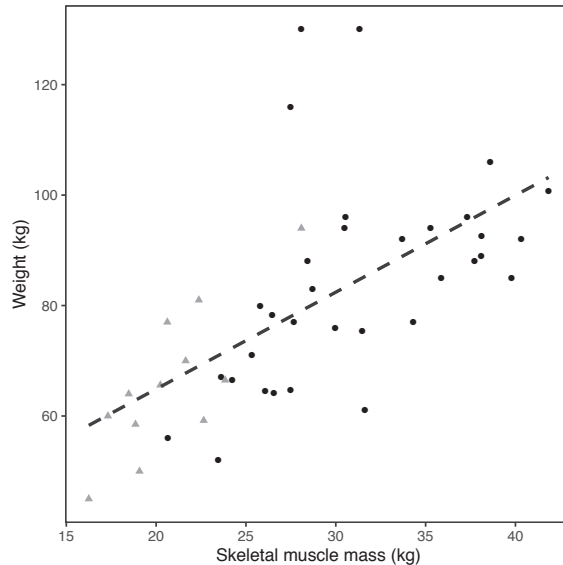


Figure 2. Correlation between weight and skeletal muscle mass. Males are displayed by black circles and females by grey triangles.  $R=0.63$ ,  $p<0.005$ .

Firstly, albumin and GFR were tested as covariates on the baseline model. No effect of albumin on the PK model was found. Addition of the GFR as a covariate on  $CL_{bound}$  resulted in a drop in OFV of 28 and 33 points, for the GFR calculated based on creatinine and cystatin C, respectively (nonhierarchical models). Also, a drop in IIV and a relevant difference in effect size were encountered. Therefore, GFR was also evaluated in combination with SMM.

Secondly, the PK model was extended with SMM, weight, and FFM as covariates. Using estimated exponents, compared to fixed exponents based on the theory of allometric scaling, led to a substantially better description of the data, as indicated by the OFV. The exponent was unidentifiable for  $V_{free}$  and Q. Addition of GFR, next to SMM, had no effect on the PK model (additional drop in OFV -5 and -4, for creatinine and cystatin C, respectively), which could be explained by a relationship between weight and GFR (weight is even used to calculate creatinine clearance in the Cockcroft-Gault formula).

Table 1. Demographic and anthropometric measurements according to SMM status and DLT status.

Parameter	Total	Without low SMM <sup>a</sup>	With low SMM
	<i>n</i> =45	<i>n</i> =24 (53.3%)	<i>n</i> =21 (46.7%)
	<i>n</i> (%) or mean (SD)	<i>n</i> (%) or mean (SD)	<i>n</i> (%) or mean (SD)
Gender			
Male	32 (71.1%)	23 (95.8%)	9 (42.9%)
Female	13 (28.9%)	1 (4.2%)	12 (57.1%)
Age (diagnosis)	59.1 (6)	58 (5.2)	60.3 (6.6)
Weight (kg)	79.9 (18.8)	90.4 (17.4)	67.9 (12.16)
Height (m)	1.8 (0.1)	1.8 (0.1)	1.8 (0.1)
BMI (kg/m <sup>2</sup> )			
<18.5	4 (8.9%)	0 (0%)	4 (19.0%)
18.5-24.9	16 (35.6%)	4 (16.7%)	12 (57.1%)
25-29.9	18 (40.0%)	14 (58.3%)	4 (19.0%)
≥30	7 (15.6%)	6 (25.0%)	1 (4.8%)
LSMI (cm <sup>2</sup> /m <sup>2</sup> ; median, IQR)	44.1 (37.7-50.9)	50.6 (5.2)	36.9 (4.1)

<sup>a</sup> Low SMM is defined as an LSMI ≤43.2 cm<sup>2</sup>/m<sup>2</sup>.

<sup>b</sup> DLT is defined as any toxicity resulting in cisplatin dose reduction of ≥50%, a treatment delay of ≥4 days, or cessation of cisplatin after the first or second cycle of therapy.

Therefore, SMM, weight, and FFM were added as potential covariates on  $CL_{free}$ ,  $CL_{bound}$ , and  $V_{bound}$  of cisplatin while estimating the exponents. The OFV was significantly decreased by addition of SMM (drop in OFV -64,  $p < 0.005$ ), weight (drop in OFV -77,  $p < 0.005$ ), and FFM (drop in OFV -70,  $p < 0.005$ ). Since cisplatin is dosed based on BSA, BSA was also tested as covariate in the final model, which resulted in a significant drop in OFV (drop in OFV -86,  $p < 0.005$ ). The parameter estimates and estimated exponents for the model with SMM are shown in **Supplementary Table S1**.

Thirdly, a simulation was performed. Plots of the population predicted cisplatin concentrations versus time derived from this simulation are shown in **Figure 3**, which shows that patients with a lower SMM are predicted to reach higher concentrations of bound cisplatin.

<i>p</i> -value	Without DLT <sup>b</sup>	With DLT	<i>p</i> -value
	<i>n</i> =19 (42.2%) <i>n</i> (%) or mean (SD)	<i>n</i> =26 (57.8%) <i>n</i> (%) or mean (SD)	
<b>&lt;0.01</b>	13 (68.4%)	19 (73.1%)	0.8
	6 (31.6%)	7 (26.9%)	
0.2	57.8 (4.6)	59.9 (6.7)	0.3
<b>&lt;0.01</b>	79.7 (18.9)	80.0 (19.2)	0.3
<b>&lt;0.01</b>	1.8 (0.1)	1.8 (0.1)	0.8
<b>&lt;0.01</b>	2 (10.5%)	2 (7.7%)	0.2
	4 (21.1%)	12 (46.2%)	
	11 (61.1%)	7 (26.9%)	
	2 (10.5%)	5 (19.2%)	
<b>&lt;0.01</b>	45.0 (8.6)	43.7 (8.3)	0.6

SMM, skeletal muscle mass; BMI, body mass index; LSMI, lumbar skeletal muscle mass index; DLT, dose-limiting toxicity.

Lastly, the correlation between CDLTs and the maximum plasma concentration ( $C_{\max}$ ) of bound cisplatin was examined. The subject receiving a weekly low-dose cisplatin schedule was excluded in this analysis, because this subject received a lower dose of cisplatin compared to the other patients. No correlation between CDLTs and the  $C_{\max}$  of bound cisplatin was found (Wilcoxon rank sum test;  $p=0.85$ ), which is illustrated by the boxplots in **Figure 4**.

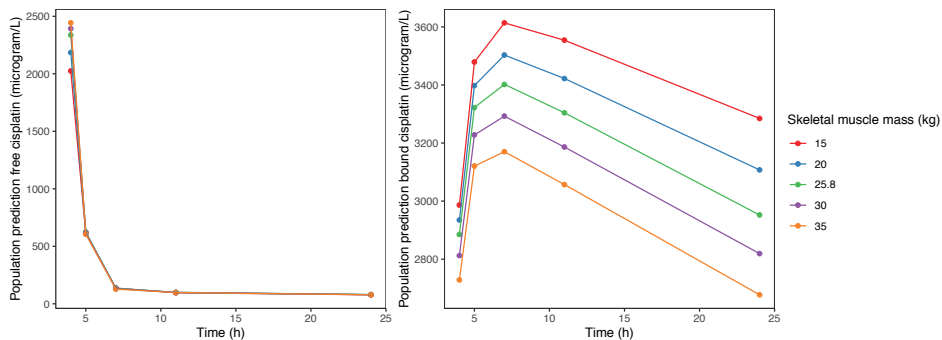


Figure 3. Population predicted cisplatin concentrations versus time. The left panel shows predicted free cisplatin concentrations, and the right panel shows predicted bound cisplatin concentrations. Simulations were performed using the model in which skeletal muscle mass was added as covariate on clearance of free cisplatin, and on clearance and volume of distribution of bound cisplatin. Skeletal muscle mass was simulated around the threshold of 25.8 kg for a low skeletal muscle mass, with corresponding body surface area and thus dose given.

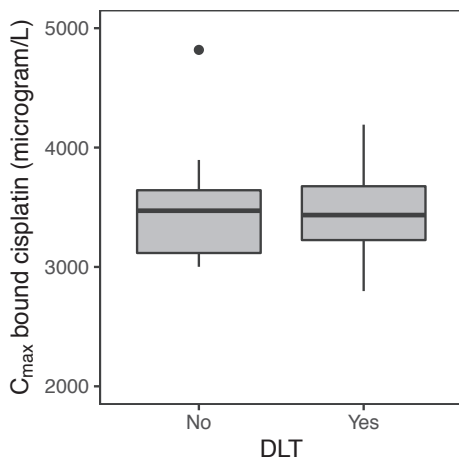


Figure 4. Correlation between dose-limiting toxicities (DLTs) of cisplatin and the maximum plasma concentration ( $C_{max}$ ) of bound cisplatin (Wilcoxon rank sum test;  $p=0.85$ ).

## DISCUSSION

In this prospective observational study, we investigated the relationship between cisplatin PK and SMM. We hypothesized that such relationship could explain the higher risk of toxicity in patients with a low SMM. As expected, we found an association between cisplatin PK, especially bound cisplatin, and SMM. A pharmacokinetic simulation showed that patients with low SMM reached higher concentrations of bound cisplatin, which could be a theoretical explanation for the higher toxicity in this patient group. The higher concentration of bound cisplatin could be seen as a reflection of the smaller volume of distribution. Because of this smaller volume, less tissue is available where, the hydrophilic and highly reactive, cisplatin can distribute to and bind with, without inducing toxicity.

We expected that patients experiencing CDLTs would have higher maximum concentrations of bound cisplatin in plasma, however we did not find a correlation between these two parameters. Furthermore, no relationship was found between DLTs and a low LSMI, which was seen in previous studies (7,24). These findings are most likely explained by the relatively low number of included patients. A relationship between SMM and toxicity has already been described. Wendrich *et al.* showed that HNSCC patients with a low SMM undergoing CRT had a 3-fold higher risk of experiencing CDLTs. Therefore, we did not power our study to find a relationship between SMM and toxicity, but we aimed to find a relationship between PK of cisplatin and SMM. A relationship between PK of cisplatin and SMM was found, and we provided a hypothesis how this could explain the toxicity of cisplatin.

Although we found a relationship between cisplatin PK and SMM, there was also a significant relationship between cisplatin PK and the other body composition descriptors. Based on the findings in this study, both SMM and the other body composition descriptors are weakly predictive for cisplatin pharmacokinetics. With the used population pharmacokinetic method, the influence of each body composition descriptor could only be statistically compared to the baseline model and not compared to each other, because in that matter the models were nonhierarchical. Therefore, we were not able to draw a conclusion about which body composition descriptor predicts cisplatin PK best. However, the differences in model fit were only minor, highly suggestive that all body size descriptors were similarly predictive. We did find SMM to be correlated with weight, which might explain why cisplatin pharmacokinetics is also related to weight and FFM. In contrast to BSA and weight, only SMM provided an explanation for the toxicity of cisplatin.



A limitation of the study is that no data was available on the concentration of bound cisplatin in tissue. Therefore, the hypothesis that higher concentrations of bound cisplatin reflected the distribution and tissue binding of cisplatin, and thus could explain toxicity, could not be tested. A study in which cisplatin PK was studied in mice in whole blood, serum, kidney, liver, testis, brain and tumor tissue, suggested that platinum serum concentrations can be used to predict the concentrations in tumor and tissue (25). This underlines our hypothesis. Measurement of platinum-DNA adducts in human tissue of patients treated with cisplatin is also possible (26). However, this was only studied in a small number of patients ( $n=3$ ). To further investigate the relationship between a low SMM and PK of cisplatin, platinum-DNA adducts could be measured in human tissue and the correlation with SMM could be studied. However, platinum-DNA adduct measurement is only feasible in surrogate tissue such as peripheral blood mononuclear cells (PBMCs).

## **CONCLUSION**

HNSCC patients with low SMM reach higher bound cisplatin concentrations, although no correlation was seen between cisplatin DLT and low SMM. Further studies which examine the level of bound cisplatin in tissue could further clarify the relationship between low SMM and cisplatin DLTs in HNSCC patients.



## REFERENCES

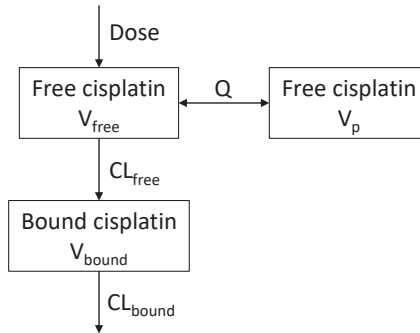
1. Bray F, Ferlay J, Soerjomataram I, Siegel RL, Torre LA, Jemal A. Global cancer statistics 2018: GLOBOCAN estimates of incidence and mortality worldwide for 36 cancers in 185 countries. *CA Cancer J Clin.* 2018;68(6):394-424.
2. Machiels JP, Leemans CR, Golusinski W, Grau C, Licitra L, Gregoire V. Squamous cell carcinoma of the oral cavity, larynx, oropharynx and hypopharynx: EHNS-ESMO-ESTRO Clinical Practice Guidelines for diagnosis, treatment and follow-up. *Ann Oncol.* 2020 Nov;31(11):1462-1475.
3. Beijer YJ, Koopman M, Terhaard CHJ, Braunius W/W, Van Es RJJ, De Graeff A. Outcome and toxicity of radiotherapy combined with chemotherapy or cetuximab for head and neck cancer: Our experience in one hundred and twenty-five patients. *Clin Otolaryngol.* 2013;38(1):69-74.
4. Al-Mamgani A, de Ridder M, Navran A, Klop WM, de Boer JP, Tesselar ME. The impact of cumulative dose of cisplatin on outcome of patients with head and neck squamous cell carcinoma. *Eur Arch Oto-Rhino-Laryngology.* 2017;274(10):3757-3765.
5. Mehanna H, Robinson M, Hartley A, et al. Radiotherapy plus cisplatin or cetuximab in low-risk human papillomavirus-positive oropharyngeal cancer (De-ESCALaTE HPV): an open-label randomised controlled phase 3 trial. *Lancet.* 2019;393(10166):51-60.
6. Rier HN, Jager A, Sleijfer S, Maier AB, Levin M. The Prevalence and Prognostic Value of Low Muscle Mass in Cancer Patients: A Review of the Literature. *Oncologist.* 2016;21(11):1396-1409.
7. Wendrich AW, Swartz JE, Bril SI, et al. Low skeletal muscle mass is a predictive factor for chemotherapy dose-limiting toxicity in patients with locally advanced head and neck cancer. *Oral Oncol.* 2017;71:26-33.
8. Sjöblom B, Benth JS, Grønberg BH, et al. Drug Dose Per Kilogram Lean Body Mass Predicts Hematologic Toxicity From Carboplatin-Doublet Chemotherapy in Advanced Non-Small-Cell Lung Cancer. *Clin Lung Cancer.* 2017;18(2):e129-e136.
9. Prado CM, Lieffers JR, McCargar LJ, et al. Prevalence and clinical implications of sarcopenic obesity in patients with solid tumours of the respiratory and gastrointestinal tracts: a population-based study. *Lancet Oncol.* 2008;9(7):629-635.
10. Karasawa T, Steyger PS. An integrated view of cisplatin-induced nephrotoxicity and ototoxicity. *Toxicol Lett.* 2015;237(3):219-227.
11. Felici A, Verweij J, Sparreboom A. Dosing strategies for anticancer drugs: The good, the bad and body-surface area. *Eur J Cancer.* 2002;38(13):1677-1684.
12. Mathijssen RHJ, de Jong FA, Loos WJ, van der Bol JM, Verweij J, Sparreboom A. Flat-Fixed Dosing Versus Body Surface Area-Based Dosing of Anticancer Drugs in Adults: Does It Make a Difference? *Oncologist.* 2007;12(8):913-923.
13. De Jongh FE, Verweij J, Loos WJ, et al. Body-surface area-based dosing does not increase accuracy of predicting cisplatin exposure. *J Clin Oncol.* 2001;19(17):3733-9.
14. Urien S, Lokiec F. Population pharmacokinetics of total and unbound plasma cisplatin in adult patients. *Br J Clin Pharmacol.* 2004;57(6):756-763.
15. Swartz JE, Pothen AJ, Wegner I, et al. Feasibility of using head and neck CT imaging to assess skeletal muscle mass in head and neck cancer patients. *Oral Oncol.* 2016;62:28-33.
16. Wendrich AW, Swartz JE, Bril SI, et al. Low skeletal muscle mass is a predictive factor for chemotherapy dose-limiting toxicity in patients with locally advanced head and neck cancer. *Oral Oncol.* 2017;71:26-33.



17. Shen W, Punyanitya M, Wang Z, et al. Total body skeletal muscle and adipose tissue volumes: estimation from a single abdominal cross-sectional image. *J Appl Physiol*. 2004;97:2333-2338.
18. Ward SR, Lieber RL. Density and hydration of fresh and fixed human skeletal muscle. *J Biomech*. 2005;38:2317-2320.
19. Janmahasatian S, Duffull SB, Ash S, Ward LC, Byrne NM, Green B. Quantification of Lean Bodyweight. *Clin Pharmacokinet*. 2005;44(10):1051-1065.
20. Brouwers EEM, Tibben MM, Rosing H, et al. Sensitive inductively coupled plasma mass spectrometry assay for the determination of platinum originating from cisplatin, carboplatin, and oxaliplatin in human plasma ultrafiltrate. *J Mass Spectrom*. 2006;41(9):1186-1194.
21. National Cancer Institute, National Institutes of Health Services, US Department of Health and Human. Common Terminology Criteria for Adverse Events (CTCAE) version 4.03 [Internet]. 2009 [cited 2021 Jan 7]. Available from: <http://www.meddrasso.com>
22. West GB, Brown JH, Enquist BJ. A General Model for the Origin of Allometric Scaling Laws in Biology. *Science*. 1997;276(5309):122-126.
23. Boeckmann AJ, Sheiner LB, Beal SL. NONMEM Users Guide - Part V. [Internet]. Ellicott City, Maryland, USA: ICON Development Solutions. Available from: <https://nonmem.iconplc.com>
24. Huiskamp LFJ, Chargin N, Devriese LA, May AM, Huitema ADR, de Bree R. The Predictive Value of Low Skeletal Muscle Mass Assessed on Cross-Sectional Imaging for Anti-Cancer Drug Toxicity: A Systematic Review and Meta-Analysis. *J Clin Med*. 2020;9(11):3780.
25. Johnsson A, Olsson C, Nygren O, Nilsson M, Seiving B, Cavallin-Stahl E. Pharmacokinetics and tissue distribution of cisplatin in nude mice: platinum levels and cisplatin-DNA adducts. *Cancer Chemother Pharmacol*. 1995;37(1-2):23-31.
26. Brouwers EEM, Tibben MM, Pluim D, Rosing H, Boot H, Cats A, et al. Inductively coupled plasma mass spectrometric analysis of the total amount of platinum in DNA extracts from peripheral blood mononuclear cells and tissue from patients treated with cisplatin. *Anal Bioanal Chem*. 2008;391(2):577-85.
27. Cockcroft D, Gault M. Prediction of Creatinine Clearance from Serum Creatinine. *Nephron*. 1976;16:31-41.
28. Keizer RJ, Karlsson MO, Hooker A. Modeling and simulation workbench for NONMEM: Tutorial on Pirana, PsN, and Xpose. *CPT Pharmacometrics Syst Pharmacol*. 2013;2(6):1-9. doi:10.1038/psp.2013.24
29. R Core Team. R: A Language and Environment for Statistical Computing. [Internet]. Vienna, Austria; 2020. Available from: <https://www.r-project.org>

## SUPPLEMENTARY MATERIAL

A schematic overview of the pharmacokinetic model of free and bound cisplatin is shown in the following figure:



Supplementary Figure S1. Details of the pharmacokinetic model of cisplatin.  $V_{\text{free}}$ , volume of distribution of free cisplatin;  $CL_{\text{free}}$ , clearance of free cisplatin;  $V_{\text{p}}$ , volume of distribution of the peripheral volume of free cisplatin;  $Q$ , intercompartmental clearance;  $V_{\text{bound}}$ , volume of distribution of protein-bound cisplatin;  $CL_{\text{bound}}$ , clearance of protein-bound cisplatin.

The interindividual variability (IIV) was described with an exponential model according to Equation S1:

$$\theta_i = \theta_{\text{pop}} \times \exp(\eta_i) \quad (\text{S1})$$

Where  $\theta_i$  represents the parameter estimate for individual  $i$ ,  $\theta_{\text{pop}}$  represents the typical parameter estimate for the population, and  $\eta_i$  represents the IIV for individual  $i$ .

The residual unexplained variability was described by a proportional model for free cisplatin and protein-bound cisplatin separately, according to Equation S2:

$$C_{\text{obs},ij} = C_{\text{pred},ij} \times (1 + \varepsilon_{\text{prop}}) \quad (\text{S2})$$

Where  $C_{\text{obs},ij}$  represents the observed concentration for individual  $i$  and observation  $j$ ,  $C_{\text{pred},ij}$  represents the predicted concentration for individual  $i$  and observation  $j$ , and  $\varepsilon_{\text{prop}}$  represents the proportional error which was assumed to be normally distributed with a mean of zero and a variance of  $\sigma^2$ .

In order to further investigate the effects of SMM on PK of cisplatin, glomerular filtration rate (GFR), and albumin were examined as additional relevant covariates. These potential covariates were first tested as covariates on the baseline model. GFR was evaluated on clearance of protein-bound cisplatin as follows:

$$CL_{bound} = \left( CL_{non-renal} + CL_{renal} \times \frac{GFR}{6} \right) \times \left( \frac{weight}{70} \right)^{0.75} \quad (S3)$$

Where  $CL_{bound}$  represents the total clearance of protein-bound cisplatin,  $CL_{non-renal}$  represents the non-renal clearance,  $CL_{renal}$  represents the renal clearance, and GFR represents the glomerular filtration rate as calculated by the Cockcroft-Gault formula or the Chronic Kidney Disease Epidemiology Collaboration (CKD-EPI) cystatin C formula, which is divided by 6 L/hour as 'normal' glomerular filtration rate, the clearance is standardized for a 70 kg person (27).

In case body composition was evaluated in combination with GFR the part in Equation S3 which standardizes for a 70 kg person, was replaced by the body composition description part of Equation 5.

Albumin was evaluated on CL of free cisplatin and V of protein-bound cisplatin, according to Equation S4:

$$\theta_i = \theta_{pop} \times (1 + \theta_{albumin} \times (albumin - median\ albumin)) \quad (S4)$$

Where  $\theta_i$  represents the parameter estimate for individual  $i$ ,  $\theta_{pop}$  represents the typical parameter estimate for the population with a median albumin, and  $\theta_{albumin}$  represents the fractional increase per unit albumin.

### Model evaluation

The fit of the baseline model was evaluated using goodness-of-fit (GOF) plots. Addition of the covariates GFR, albumin and body composition descriptors was evaluated by GOF plots, a drop in the objective function value (OFV; minus twice the log-likelihood), successful minimization, parameter precision (\$COVARIANCE option of NONMEM) and a drop in inter-individual variability (IIV).

## Software

Nonlinear mixed-effects modeling was performed using NONMEM (version 7.3, ICON Development Solutions, Ellicott City, USA) and Perl-speaks-NONMEM (PsN, version 4.7.0)(23). In order to obtain parameter estimates the first-order conditional estimation with interaction (FOCE-I) method was used. Model management was performed using Pirana (version 2.9.9)(28). R (version 3.6.3) was used for data management and graphical diagnostics (29).

Supplementary Table S1. Parameter estimates of cisplatin in the pharmacokinetic model with skeletal muscle mass imputed as covariate on  $CL_{free}$ ,  $CL_{bound}$  and  $V_{bound}$

Parameter	Estimate (RSE %)
$CL_{free}$ (L/h)	12.2 (4.2)
Effect of SMM	0.313 (23.8)
$V_{free}$ (L)	14.4 (5.7)
Q (L/h)	8.99 (9.1)
$V_p$ (L)	307 (11.3)
$CL_{bound}$ (L/h)	0.644 (4.6)
Effect of SMM	0.842 (17.1)
$V_{bound}$ (L)	32 (4.8)
Effect of SMM	0.67 (14)
<b>Inter-individual variability</b>	<b>%CV (RSE %)</b>
$CL_{free}$ (L/h)	12.7 (18.8)
$V_{free}$ (L)	27.3 (18)
$CL_{bound}$ (L/h)	15.9 (30.6)
$V_{bound}$ (L)	16.5 (9.9)
<b>Proportional residual unexplained variability</b>	<b>%CV (RSE %)</b>
Free cisplatin	17.1 (9.4)
Bound cisplatin	6.1 (10.8)

$CL_{free}$ , clearance of free cisplatin;  $V_{free}$ , volume of distribution of free cisplatin; Q, intercompartmental clearance;  $V_p$ , volume of distribution of the peripheral compartment of free cisplatin;  $CL_{bound}$ , clearance of bound cisplatin;  $V_{bound}$ , volume of distribution of bound cisplatin; RSE, relative standard error; %CV, percentage coefficient of variation.





# CHAPTER 2.3

## Optimizing carboplatin dosing by an improved prediction of carboplatin clearance using a CT-enhanced estimate of renal function

Laura Molenaar-Kuijsten, Tobias T. Pieters, Wouter B. Veldhuis, Pim Moeskops, Erik-Jan Rijkhorst, Thomas P.C. Dorlo, Jos H. Beijnen, Neeltje Steeghs, Maarten B. Rookmaker, Alwin D.R. Huitema

Manuscript in preparation

Author's contribution: LMK contributed to conception and design of the study, performed the data analysis, wrote the first draft of the manuscript and implemented the input and feedback of the co-authors.

# ABSTRACT

## Background

Carboplatin is generally dosed based on a modified Calvert formula, in which the Cockcroft-Gault based creatinine clearance (CRCL) is used as proxy for the glomerular filtration rate (GFR). The Cockcroft-Gault formula overpredicts CRCL in patients with an aberrant body composition. The CT-enhanced estimate of RenAl FunctiOn (CRAFT) was developed to compensate for this effect of an aberrant body composition. We aimed to evaluate whether carboplatin clearance is better predicted by CRCL based on the CRAFT formula compared to the Cockcroft-Gault formula.

## Methods

Data of four previously conducted trials was used. Creatinine production rate was calculated by the CRAFT formula, and divided by serum creatinine to derive CRCL. The difference between CRCL based on the CRAFT and Cockcroft-Gault formula was assessed by population pharmacokinetic modeling.

## Results

In total, 108 patients were included in the analysis. Addition of the CRAFT based CRCL as covariate on carboplatin clearance improved the model fit as indicated by a drop in objective function value (OFV) of 26 points. In contrast, addition of the Cockcroft-Gault based CRCL led to a worse model fit with an increase in OFV of 8 points.

## Conclusion

Carboplatin clearance is better predicted by CRCL based on the CRAFT versus Cockcroft-Gault formula. In subjects with a low serum creatinine, the calculated carboplatin dose using the Cockcroft-Gault formula exceeds the dose using the CRAFT formula, which might explain the need for dose capping when using the Cockcroft-Gault formula. Therefore, the CRAFT formula might be an alternative for dose capping while still dosing accurately.



## WHAT IS ALREADY KNOWN ABOUT THIS SUBJECT

- The carboplatin dose is overpredicted by the modified Calvert formula using the Cockcroft-Gault formula in patients with low serum creatinine or obesity
- Capping of the carboplatin dose to compensate overprediction prevents toxicity but results in inaccurate dosing
- Use of CT-enhanced estimates of RenAl FuncTion (CRAFT) improves prediction of creatinine clearance



## WHAT THIS STUDY ADDS

- Carboplatin clearance was best predicted by creatinine clearance based on the CRAFT formula
- The higher calculated carboplatin dose, in subjects with low serum creatinine, based on the Cockcroft-Gault formula might explain the need for dose capping
- CRAFT based dosing of carboplatin is a more accurate possible alternative for dose capping

## INTRODUCTION

Carboplatin is a chemotherapeutic drug used for the treatment of different types of tumors, amongst which ovarian, lung, and head and neck cancer (1). Its anti-tumor effect is caused by formation of platinum-DNA adducts, which result in cell cycle arrest and apoptosis (2). Because of the small therapeutic window of chemotherapeutic drugs, proper dosing is a challenge.

Carboplatin is eliminated by glomerular filtration, followed by tubular reabsorption (3,4). The correlation between the carboplatin clearance and glomerular filtration rate (GFR) was described to be linear ( $r=0.85$ ,  $p<0.05$ )(3). Therefore, the administered dose of carboplatin is commonly calculated based on the GFR and desired exposure using the Calvert formula (3):

$$\text{Carboplatin dose (mg)} = \text{target AUC} \times (\text{GFR} + 25) \quad (1)$$

In which AUC is the area under the plasma concentration-time curve (in  $\text{mg} \cdot \text{min} / \text{mL}$ ) as measure of exposure.

The GFR (in  $\text{mL} / \text{min}$ ) in the Calvert formula was based on chromium 51-ethylenediaminetetraacetic acid ( $^{51}\text{Cr}$ -EDTA) clearance, but in clinical practice a modified Calvert formula with creatinine clearance (CRCL) calculated by the Cockcroft-Gault formula is mostly used (3,5–7).

In the Cockcroft-Gault formula, the CRCL is determined by the ratio of the creatinine production rate and the creatinine serum concentration (6). The creatinine production rate is estimated using age, gender, weight, and race as surrogate markers of muscle mass. After standardization of serum creatinine assays, lower serum creatinine values were measured in patients with normal renal function as compared to the older methods, leading to overprediction of CRCL and higher calculated carboplatin doses based on the Calvert formula (8). Therefore, in 2010, the National Cancer Institute's Cancer Therapy Evaluation Program (NCI/CTEP) advised to use  $125 \text{ mL} / \text{min}$  as a maximum value for GFR, and to apply dose capping using this maximum GFR and the target AUC. As a consequence of this approach, the dose is only corrected in patients with a high CRCL which can be due to low serum creatinine values or a low skeletal muscle mass relative to the body weight. Overprediction of the CRCL by the Cockcroft-Gault formula was found for obese patients, which could be caused by misestimation of the creatinine production rate because body weight does not reflect muscle mass accurately in these patients (5,9).

Overprediction of carboplatin clearance, and subsequently, administration of higher carboplatin doses could lead to increased toxicity. In patients treated with uncapped versus capped carboplatin doses, the mean difference in pre- and post-platelet count was larger (10). In contrast, dose capping could also lead to a worse treatment outcome. It has been shown that for some patients the actual GFR is above 125 mL/min and in that case dose capping could lead to underdosing of carboplatin (10).

Application of alternative body size descriptors to predict the creatinine production rate might improve the prediction of CRCL and thus carboplatin dosing accuracy (11). Recently, Pieters *et al.* described an algorithm based on a fully automated deep learning-based method for body composition analysis of abdominal CT-scans to improve the estimation of the creatinine production rate in both patients and healthy people, called the CT-enhanced estimate of RenAl FuncTion (CRAFT) formula (Pieters T *et al.*, submitted). Since for almost all cancer patients a CT-scan is made before treatment, the use of the CRAFT formula could easily be implemented in clinical practice. The aim of our study was to evaluate if carboplatin clearance is better predicted by the CRCL based on the CRAFT formula compared to the CRCL based on the Cockcroft-Gault formula.



## METHODS

### Study population

Data of four previously conducted clinical trials including carboplatin treated patients was used for the current analysis (12–15). An overview of these studies is given in **Table 1**. The patients for whom carboplatin PK samples, and CT-scans were available and who had provided written informed consent were included in the analysis. All previous studies were conducted in accordance with Good Clinical Practice and the Declaration of Helsinki and were approved by the local Medical Ethics Committee.

Table 1. Overview of previous conducted trials included in the current analysis.

Study description	Number of patients	Sampling schedule (h after start infusion)	References
Phase I study of fixed dose rate gemcitabine infusion plus carboplatin as second-line treatment in patients with advanced ovarian cancers	23	0.5, 5	(12)
Phase I study of gemcitabine and carboplatin plus sorafenib in patients with advanced solid tumors	46	0.5, 4, 24	(14)
Phase II study of the WEE-1 inhibitor MK-1775 plus carboplatin in patients with p53 mutated epithelial ovarian cancer	24	0.5, 1.5, 5.5, 24	(13)
Phase I study of two cycles carboplatin-olaparib followed by olaparib monotherapy versus capecitabine as first line treatment in BRCA1- or BRCA2- mutated HER2-negative advanced breast cancer	25	0.25, 0.5, 1, 2, 4, 6, 8, 10, 24, 48	(15)

### Renal function

The creatinine production rate was calculated by the CRAFT 1 formula (in the rest of the manuscript referred to as CRAFT formula), as described by Pieters *et al.* (Pieters T *et al.*, submitted):

$$\begin{aligned}
& \text{Creatinine production rate (nanomol/min)} = -12.62 \\
& -0.031 \times 25^{\text{th}} \text{ percentile subcutaneous fat (HU)} \\
& -0.023 \times \text{mean visceral fat (HU)} \\
& +0.048 \times \text{mean psoas muscles} > -15 \text{ HU (HU)} \\
& +0.15 \times \text{area psoas muscle} > -15 \text{ HU (cm}^2\text{)} \\
& +0.017 \times \text{area abdominal wall muscle} > -15 \text{ HU (cm}^2\text{)} \\
& +0.035 \times 90^{\text{th}} \text{ percentile long spine muscles} > -15 \text{ (HU)} \\
& +0.079 \times \text{area long spine muscles} > -15 \text{ HU (cm}^2\text{)} \\
& +0.044 \times \text{height (cm)} \\
& -0.057 \times \text{age (years)} \\
& +0.033 \times \text{weight (kg)}
\end{aligned} \tag{2}$$

The radiomics parameters used in this formula were obtained by deep learning body composition analysis of abdominal CT-scans using Quantib Body Composition (version 0.2.0), as described by Moeskops *et al.* (also available online: <https://research.quantib.com>)(16). This approach was used because the automatic processing is compatible with future clinical application – where manual segmentation is not. The last CT-scan before PK sampling was selected for this analysis, and this CT-scan was considered evaluable if the scan included the third lumbar vertebra (L3 slice), which is commonly used in body composition analysis. The creatinine production rate was divided by the serum creatinine concentration to derive CRCL. The CRCL based on the CRAFT formula was compared to the CRCL calculated by the Cockcroft-Gault formula (6). The correlation between these CRCLs was tested with the Pearson's correlation coefficient using R (version 3.6.3).

### Population pharmacokinetic modeling

For PK analysis the model previously published by Ekhardt *et al.* was used (17). This model is a two-compartment model of ultrafilterable carboplatin, based on data of 178 patients with different types of cancer receiving conventional or high-dose carboplatin-based chemotherapy. The structural model was adjusted for the current analysis, by replacing the distribution rate constants  $k_{12}$  and  $k_{21}$  by an intercompartmental clearance (Q) and peripheral volume of distribution ( $V_p$ ). In addition, the between occasion variability (BOV) was not included in the current analysis because in our patient population only PK samples of one occasion were available. The rest of the structural and random effects model was maintained, but parameter estimates were re-estimated. Since during model building the inter-individual variability (IIV) on Q approached zero, it was eventually fixed to zero.

CRCL based on both the CRAFT formula and the Cockcroft-Gault formula was evaluated as covariate to predict total clearance (CL) of ultrafilterable carboplatin, as follows:

$$CL = CL_{\text{non-renal}} + CRCL \tag{3}$$

Furthermore, it was tested whether the non-renal clearance could best be estimated or fixed according to the modified Calvert formula (3). Therefore, the non-renal clearance in the equation was replaced by 25 mL/min and compared with an estimated non-renal clearance.

### Model evaluation

Model fit after addition of the covariates was evaluated by a drop in minus twice the log-likelihood value (objective function value (OFV)), successful minimization, parameter precision (sampling importance resampling procedure of NONMEM (version 7.3)(18)), and a drop in IIV. Formal statistical testing could not be performed, because the models to be compared were nonhierarchical. A drop in OFV of 3.84 points was used as a guidance indicating a better model fit.

Furthermore, the measured  $AUC_{0-\infty}$  in the baseline model was compared to the target AUC calculated with both the Cockcroft-Gault and CRAFT formula. The  $AUC_{0-\infty}$  was calculated using the following formula:

$$AUC_{0-\infty} = \frac{dose}{CL} \quad (4)$$

In which  $AUC_{0-\infty}$  is the individual area under the plasma concentration-time curve (in  $mg \cdot min/mL$ ) as measure of exposure, dose is the carboplatin dose (in mg), and CL is the individual carboplatin clearance (in mL/min) obtained through maximum *a posteriori* probability (MAP) Bayesian estimation using the \$POSTHOC option of NONMEM (version 7.3).

### Difference in carboplatin dose in a large heterogeneous population

Because the patient characteristics in the studied patient population were relatively homogeneous, the patient dataset of Pieters *et al.* (used for the development of the CRAFT formula) was used to study the difference in calculated carboplatin dose using the Cockcroft-Gault versus the CRAFT formula in a more heterogeneous population including a wider range in serum creatinine levels and more subjects with a low skeletal muscle mass and obesity (Pieters T *et al.*, submitted). All subjects in this dataset from whom radiomics data and serum creatinine were available, were included in our analysis. The congruence in carboplatin doses based on the Cockcroft-Gault and CRAFT formulas was evaluated using a Bland-Altman plot. A target AUC of 5  $mg \cdot min/mL$  was used to calculate the carboplatin dose. It should be noted that these subjects were not actually treated with carboplatin.

## RESULTS

Out of 118 patients included in previous studies, 108 patients were evaluable for analysis. An overview of the patient selection is shown in **Figure 1**. Patients were treated with a median dose of 392 mg carboplatin, based on a target exposure of 2 to 5 mg\*min/mL. The patient population was relatively homogeneous, with not much variation in serum creatinine levels, renal function, and skeletal muscle mass (SMM). For example, most of the patients had an adequate renal function based on the Cockcroft-Gault formula, with only two patients having a CRCL of less than 50 mL/min. Additionally, a minority of patients had a low SMM (26%). Among the included patients, there were only females with a BMI above 30 kg/m<sup>2</sup>, and all of these females with obesity had a normal SMM. Patient characteristics are summarized in **Table 2**.

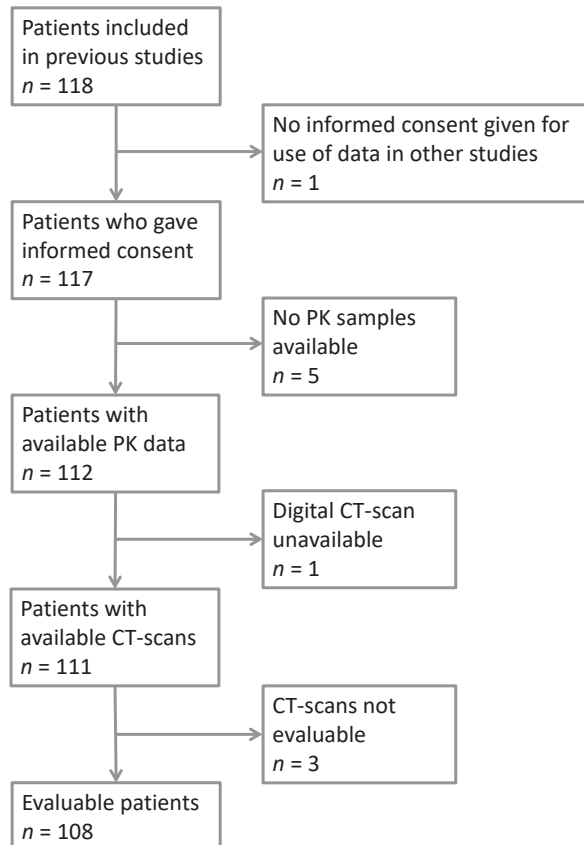


Figure 1. Schematic overview of patient selection. PK, pharmacokinetic; CT-scan, computed tomography-scan.

Table 2. Patient characteristics ( $n=108$ ).

Characteristic	<i>n</i> (%) or median [range]
Carboplatin dose (mg)	391.5 [154-1,315]
Gender	
Male	21 (19%)
Female	87 (81%)
Age (years)	58 [25-74]
Height (cm)	170 [155-187]
Weight (kg)	72 [49-129]
BMI (kg/m <sup>2</sup> )	25 [18-42]
Low skeletal muscle mass <sup>a</sup>	
Yes	28 (26%)
No	80 (74%)
Time between CT-scan and PK sampling (days)	6 [1-38]
Serum creatinine (μmol/L)	69 [47-121]
Creatinine clearance based on CRAFT formula (mL/min)	94 [48-179]
Creatinine clearance based on Cockcroft-Gault formula (mL/min)	92 [49-239]

<sup>a</sup> A low skeletal muscle mass was for males defined as a SMM <26.8 kg if BMI <25 kg/m<sup>2</sup> and as SMM <32.5 kg if BMI ≥25 kg/m<sup>2</sup> (calculated with a median height of 180 cm), and for females as a SMM <22.6 kg for any BMI (calculated with a median height of 168 cm)(19).

PK, pharmacokinetic; CRAFT, CT-enhanced estimate of RenAl FunctIon; BMI, body mass index.

The CRCLs based on the CRAFT formula and Cockcroft-Gault formula were highly correlated as shown in **Figure 2** ( $R=0.89$ ,  $p<0.05$ ). No particular trend in deviations from this correlation was observed for patients with low SMM and normal SMM.

Firstly, both the CRCL based on the CRAFT and Cockcroft-Gault formula were tested as covariates in the PK model. Addition of the CRAFT based CRCL improved the model fit as indicated by a drop in OFV of 26 points relative to the baseline model. However, a small increase in the inter-individual variability of the carboplatin clearance was observed. In contrast, addition of the Cockcroft-Gault based CRCL led to a worse model fit, with an increase in OFV of 8 points relative to the baseline model.

Secondly, addition of a fixed non-renal clearance of 25 mL/min, led to a drop of 18 points and an increase of 16 points in OFV for the CRAFT and Cockcroft-Gault based covariate models, respectively, relative to the baseline model. The most important parameter estimates of the different models are shown in **Table 3**.



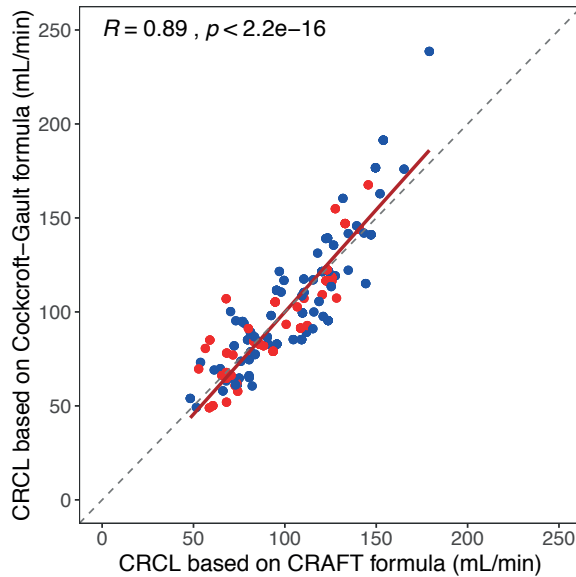


Figure 2. Correlation between the creatinine clearance based on the CRAFT formula and the creatinine clearance based on the Cockcroft-Gault formula (Pearson's correlation coefficient). The red dots represent patients with a low skeletal muscle mass, and the blue dots represent patients who do not have a low skeletal muscle mass. CRCL, creatinine clearance; CRAFT, CT-enhanced estimate of RenAl FunctIon.

Thirdly, the measured  $AUC_{0-\infty}$  was compared to the target AUC. The mean of the measured  $AUC_{0-\infty}$  was 17% higher than the target AUC when the Cockcroft-Gault formula was used to predict carboplatin clearance, and 16% higher when the CRAFT formula was used. The difference between measured and target AUC was between -20% and +20% for 56% of the patients when the Cockcroft-Gault formula was used, and for 60% of the patients when the CRAFT formula was used. An overview of the distribution of the differences is shown in **Figure 3**, with marginal differences between the two formulas.

Lastly, in the dataset of Pieters *et al.* for 409 subjects radiomics data and serum creatinine values were available. In this population, 114 out of 409 subjects had a low SMM, and 56 subjects (both male and female) had a BMI above  $30 \text{ kg/m}^2$  with 9 of them also having a low SMM. The median serum creatinine concentration was  $88 \text{ }\mu\text{mol/L}$  (range  $28\text{-}996 \text{ }\mu\text{mol/L}$ ). Hundred subjects had an impaired renal function (defined as a  $\text{CRCL} < 50 \text{ mL/min}$  according to the Cockcroft-Gault formula). A Bland-Altman plot of the difference in calculated carboplatin dose between the Cockcroft-Gault and CRAFT formula is shown in **Figure 4**, which shows that use of the Cockcroft-Gault formula would lead to higher calculated carboplatin doses especially in subjects with low serum creatinine levels.

Table 3. Parameter estimates of the different models.

Parameter	Baseline model	
	Estimate	SIR <sup>b</sup> 95% CI
Difference in OFV	N/A	N/A
CL <sup>c</sup> (L/h, RSE%)	6.37 (3.1)	5.97-6.77
IIV CL (%CV, RSE%)	29.8 (8.3)	25.3-34.8

<sup>a</sup> The non-renal clearance was fixed to 25 mL/min according to the Calvert formula.

<sup>b</sup> Five iterations; number of samples 1,000, 1,000, 1,000, 2,000, 2,000; number of resamples 200, 400, 500, 1,000, 1,000.

<sup>c</sup> Note that for the baseline model the parameter estimate includes the renal plus the non-renal clearance, for the models with creatinine clearance imputed the parameter estimates include only the non-renal clearance, unless the non-renal clearance was fixed because then there is no estimate at all.

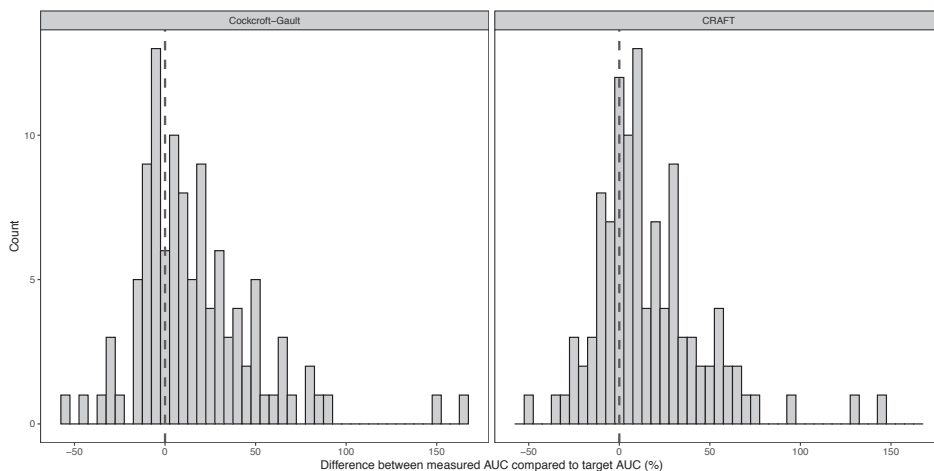


Figure 3. Distribution of the difference between the estimated AUC according to the baseline model, compared to the target AUC as calculated with the Cockcroft-Gault formula in the left panel, and the CRAFT formula in the right panel. The vertical line indicates no difference between estimated and target AUC. AUC, area under the plasma concentration-time curve; CRAFT, CT-enhanced estimate of RenAl Function.

Model with creatinine CL based on CRAFT – estimated/fixed non-renal CL <sup>a</sup>		Model with creatinine CL based on Cockcroft-Gault – estimated/fixed non-renal CL <sup>a</sup>	
Estimate	SIR <sup>b</sup> 95% CI	Estimate	SIR <sup>b</sup> 95% CI
-26/-18	N/A	+8/+16	N/A
1.12 (17.8)/N/A	0.97-1.81	1.38 (19.1)/N/A	0.77-1.53
31.1 (14.3)/26.7 (9)	30.1-44.2/24.5-32.5	36.9 (16.7)/ 28.6 (8.7)	25.2-37.9/22.7-30.9

CL, clearance; CRAFT, CT-enhanced estimate of RenAl FunctIon; SIR, sampling importance resampling; CI, confidence interval; OFV, objective function value which is equal to minus twice the log-likelihood; RSE, relative standard error; IIV, inter-individual variability; %CV, percentage coefficient of variation.

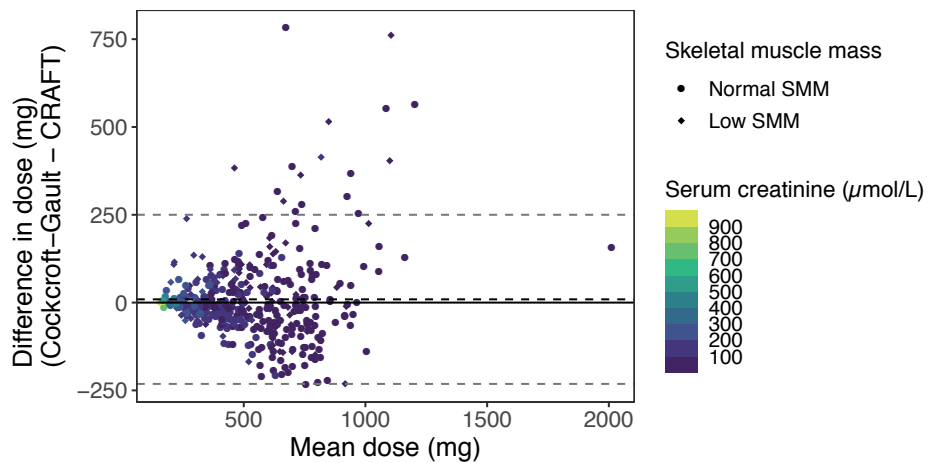


Figure 4. Bland-Altman plot with on the x-axis the mean carboplatin dose as calculated with the Cockcroft-Gault and CRAFT formula, and on the y-axis the difference between the carboplatin dose as calculated with the Cockcroft-Gault formula and the CRAFT formula (with a target AUC of 5 mg\*min/mL). The solid line indicates no difference between the two formulas. The black dashed line represents the mean difference in dose and the grey dashed lines represent the mean  $\pm 1.96$  \* standard deviation. AUC, area under the plasma concentration-time curve; CRAFT, CT-enhanced estimate of RenAl Function.



## DISCUSSION

Carboplatin is regularly dosed based on the Calvert formula, in which the GFR is used (3). This formula has been developed with the  $^{51}\text{Cr}$ -EDTA clearance as measure of the GFR, but in clinical practice the CRCL calculated by the Cockcroft-Gault formula is mostly used in a modified Calvert formula. However, it has been described that the CRCL calculated by the Cockcroft-Gault formula is overestimated in patients with abnormally low creatinine values and in obese patients (5,8,9). Therefore, dose capping is applied for carboplatin, usually based on a maximum GFR of 125 mL/min (8). We evaluated if carboplatin clearance is better predicted by CRCL based on the CRAFT formula compared to CRCL based on the Cockcroft-Gault formula, to prevent unnecessary under- and overdosing of patients. Indeed, addition of CRCL based on the CRAFT formula improved the model fit.

Serum creatinine based estimates of CRCL divide creatinine production rate by serum creatinine under the assumption of steady-state conditions. In our analysis, only the creatinine production rate was estimated differently by using either the CRAFT formula or the commonly used Cockcroft-Gault formula. Therefore, the improved prediction of the carboplatin clearance using the CRAFT formula was due to a better prediction of the creatinine production rate, which especially has an impact in patients with a low serum creatinine (e.g., because of a low muscle volume). The improved prediction of creatinine production rate was also found in the previously conducted study of Pieters *et al.* (Pieters T *et al.*, submitted). Addition of CRCL based on the Cockcroft-Gault formula worsened the model fit, which was in line with a previously published study showing no correlation between this CRCL and the clearance of carboplatin in a population with a normal renal function (17).

The relatively small differences in interindividual variability of carboplatin clearance when implementing CRCL as a covariate, and the small differences between estimated  $\text{AUC}_{0-\infty}$  and target AUC could be explained by the relatively homogeneous patient population. All patients were recruited from Phase I clinical trials in which strict in- and exclusion criteria were applied. Therefore, this group of patients might not be representative for clinical practice. Thus, before drawing any conclusions, the effect of using the CRAFT formula to dose carboplatin was studied in a more heterogeneous population. In the more heterogeneous patient dataset of Pieters *et al.* a wider range in serum creatinine levels was observed and more subjects with a low skeletal muscle mass and also male subjects with obesity were included. When the carboplatin dosing formula with the two different CRCLs was applied on this dataset, major differences in calculated carboplatin dose were observed. This indicates that in clinical practice, where a wide range of serum creatinine values and large differences in body composition will be observed, especially in cancer patients where loss of weight and skeletal muscle mass often occurs due to extensive treatment (20), use of the CRAFT

formula might have a bigger impact. Therefore, the eligibility of using the CRAFT formula to dose carboplatin without applying dose capping should be prospectively studied in real-life patients with a low serum creatinine, whom are treated with carboplatin.

In **Figure 4** it can be seen that the major differences in carboplatin dose mainly occur in subjects with a low serum creatinine ( $\leq 100$   $\mu\text{mol/L}$ ). It can be expected that the incidence of major differences in calculated carboplatin dose between the two formulas in subjects with a serum creatinine  $\leq 50$   $\mu\text{mol/L}$  is even higher, in the dataset only 21 subjects had a serum creatinine below this value with 9 of them having a difference in dose of more than 250 mg. The difference in calculated carboplatin dose, especially in subjects with a low serum creatinine, can be explained by a better prediction of the creatinine production having more impact on the estimated CRCL in this group. In patients actually treated with carboplatin, the dose would have been capped on 750 mg. For almost all subjects with a difference in dose exceeding the mean  $\pm 1.96$  \* standard deviation, the mean dose exceeds the 750 mg. Therefore, the CRAFT formula might possibly be used as an alternative for dose capping in patients with a low serum creatinine because it better predicts the creatinine production rate, whereby, overdosing could be prevented while still dosing accurately.

A disadvantage of the modified Calvert formula is the use of CRCL as proxy for GFR. The difference between CRCL and GFR is that creatinine is not only secreted by glomerular filtration, but also by tubular secretion (21). Therefore, the CRCL is higher than the GFR. Because carboplatin is eliminated by glomerular filtration, followed by tubular reabsorption, and not tubularly secreted, this leads to overprediction of the carboplatin clearance using the CRCL based on both the CRAFT and Cockcroft-Gault formula (3,4). It might be possible to correct for the mean overestimation of GFR by the CRCL, which is 10-20% (22). Despite overprediction of the GFR and thus carboplatin clearance by using both the CRAFT and Cockcroft-Gault formula, a better estimation of the creatinine production rate by the CRAFT formula was supposed to better approximate the real GFR as used in the Calvert formula.

## CONCLUSION

To conclude, carboplatin clearance is better predicted by CRCL based on the CRAFT formula than the Cockcroft-Gault formula, when compared using a model-based approach. Especially in subjects with a low serum creatinine, the calculated carboplatin dose using the Cockcroft-Gault formula exceeds the dose using the CRAFT formula. This might explain the need for dose capping when using the Cockcroft-Gault formula. Therefore, the CRAFT formula could possibly be used as an alternative for dose capping, in which overdosing could be prevented while still dosing accurately.

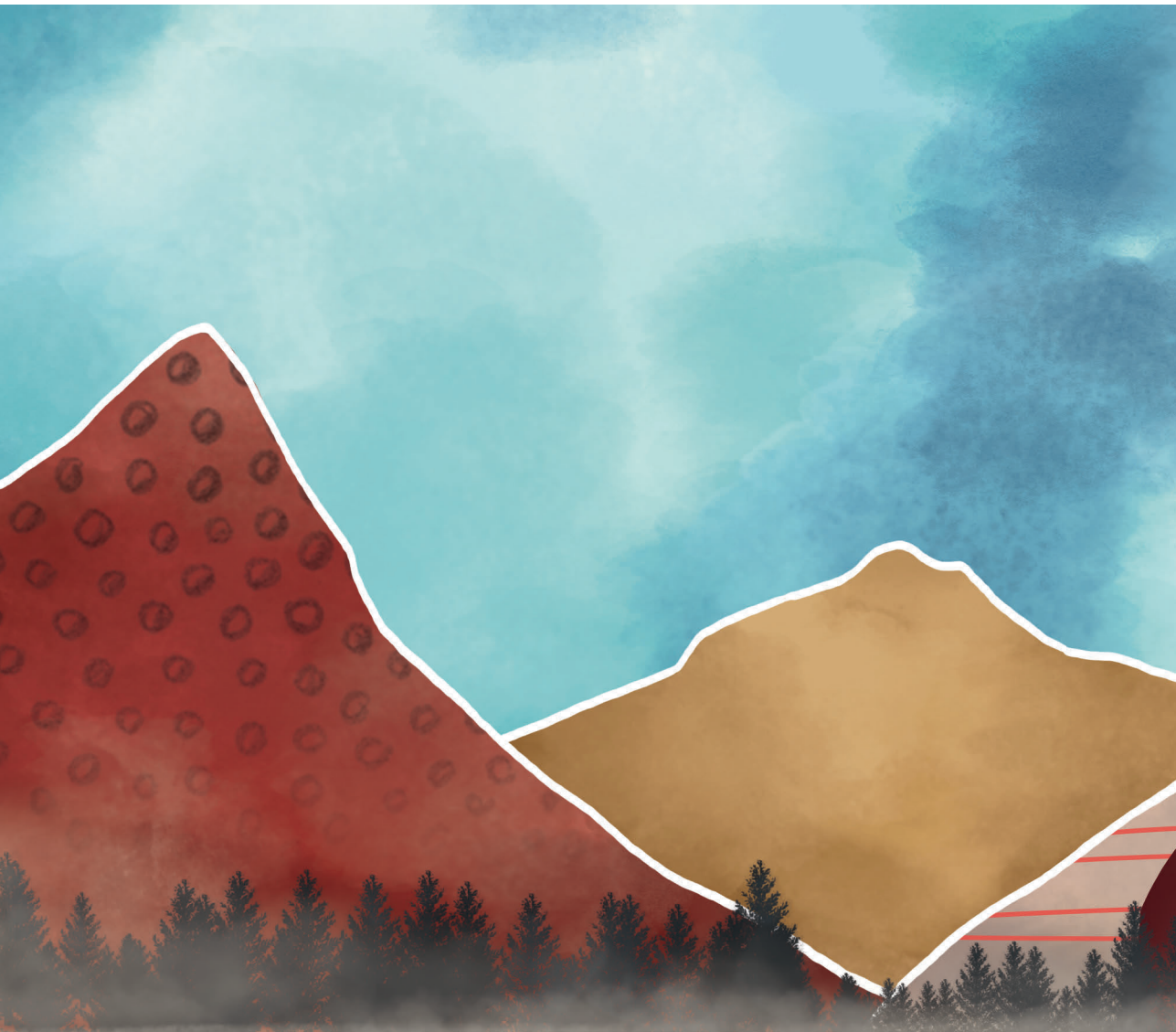


## REFERENCES

1. Dasari S, Bernard Tchounwou P. Cisplatin in cancer therapy: Molecular mechanisms of action. *Eur J Pharmacol.* 2014;740:364–78.
2. Marsh S, McLeod H, Dolan E, Shukla SJ, Rabik CA, Gong L, et al. Platinum Pathway [Internet]. Pharmacogenetics and genomics. 2009 [cited 2021 Feb 23]. Available from: <https://www.pharmgkb.org/pathway/PA150642262>
3. Calvert A, Newell D, Gumbrell L, O'Reilly S, Burnell M, Boxall F, et al. Carboplatin dosage: prospective evaluation of a simple formula based on renal function. *J Clin Oncol.* 1989;7(11):1748–56.
4. Sørensen B, Strömgen A, Jakobsen P, Nielsen J, Andersen L, Jakobsen A. Renal handling of carboplatin. *Cancer Chemother Pharmacol.* 1992;30(4):317–20.
5. Ekhardt C, Rodenhuis S, Schellens JHM, Beijnen JH, Huitema ADR. Carboplatin dosing in overweight and obese patients with normal renal function, does weight matter? *Cancer Chemother Pharmacol.* 2009;64(1):115–22.
6. Cockcroft D, Gault M. Prediction of Creatinine Clearance from Serum Creatinine. *Nephron.* 1976;16:31–41.
7. Nannan Panday VR, Van Warmerdam LJC, Huizing MT, Ten Bokkel Huinink WW, Vermorken JB, Giaccone G, et al. Carboplatin dosage formulae can generate inaccurate predictions of carboplatin exposure in carboplatin/paclitaxel combination regimens. *Clin Drug Investig.* 1998;15(4):327–35.
8. Ivy SP, Zwiebel J, Mooney M. FOLLOW-UP for INFORMATION LETTER REGARDING AUC-BASED DOSING OF CARBOPLATIN [Internet]. National Cancer Institute. 2010 [cited 2021 Sep 8]. Available from: [https://ctep.cancer.gov/content/docs/Carboplatin\\_Information\\_Letter.pdf](https://ctep.cancer.gov/content/docs/Carboplatin_Information_Letter.pdf)
9. O'Cearbhaill R, Sabbatini PS. New Guidelines for Carboplatin Dosing [Internet]. 2012 [cited 2021 Sep 8]. Available from: <https://www.mskcc.org/clinical-updates/new-guidelines-carboplatin-dosing>
10. Morrow A, Garland C, Yang F, De Luna M, Herrington JD. Analysis of carboplatin dosing in patients with a glomerular filtration rate greater than 125 mL/min: To cap or not to cap? A retrospective analysis and review. *J Oncol Pharm Pract.* 2019;25(7):1651–7.
11. Kaag D. Carboplatin dose calculation in lung cancer patients with low serum creatinine concentrations using CKD-EPI and Cockcroft-Gault with different weight descriptors. *Lung Cancer [Internet].* 2013;79(1):54–8. Available from: <http://dx.doi.org/10.1016/j.lungcan.2012.10.009>
12. Leijen S, Veltkamp SA, Huitema ADR, Van Werkhoven E, Beijnen JH, Schellens JHM. Phase I dose-escalation study and population pharmacokinetic analysis of fixed dose rate gemcitabine plus carboplatin as second-line therapy in patients with ovarian cancer. *Gynecol Oncol.* 2013;130(3):511–7.
13. Leijen S, Van Geel RMJM, Sonke GS, De Jong D, Rosenberg EH, Marchetti S, et al. Phase II study of WEE1 inhibitor AZD1775 plus carboplatin in patients with tp53-mutated ovarian cancer refractory or resistant to first-line therapy within 3 months. *J Clin Oncol.* 2016;34(36):4354–61.
14. Van der Noll R. Safety, pharmacokinetics and preliminary anti-tumor activity of novel (combinations of) targeted anti-cancer drugs [Internet]. The Netherlands Cancer Institute; 2014. Available from: <https://www.worldcat.org/title/safety-pharmacokinetics-and-preliminary-anti-tumor-activity-of-novel-combinations-of-targeted-anti-cancer-drugs/oclc/8968865972>

15. Schouten PC, Dackus GMHE, Marchetti S, van Tinteren H, Sonke GS, Schellens JHM, et al. A phase I followed by a randomized phase II trial of two cycles carboplatin-olaparib followed by olaparib monotherapy versus capecitabine in BRCA1- or BRCA2-mutated HER2-negative advanced breast cancer as first line treatment (REVIVAL): Study protocol for. *Trials*. 2016;17(1):1–9.
16. Moeskops P, De Vos B, Veldhuis W, De Jong P, Išgum I, Leiner T. Automatic quantification of body composition at L3 vertebra level with convolutional neural networks. In: *European Congress of Radiology*. 2020.
17. Ekhart C, De Jonge ME, Huitema ADR, Schellens JHM, Rodenhuis S, Beijnen JH. Flat dosing of carboplatin is justified in adult patients with normal renal function. *Clin Cancer Res*. 2006;12(21):6502–8.
18. Dosne AG, Bergstrand M, Karlsson MO. An automated sampling importance resampling procedure for estimating parameter uncertainty. *J Pharmacokinet Pharmacodyn*. 2017;44(6):509–20.
19. Martin L, Birdsell L, MacDonald N, Reiman T, Clandinin MT, McCargar LJ, et al. Cancer Cachexia in the Age of Obesity: Skeletal Muscle Depletion Is a Powerful Prognostic Factor, Independent of Body Mass Index. *J Clin Oncol*. 2013;31(12):1539–47.
20. Kurk SA, Peeters PHM, Dorresteijn B, de Jong PA, Jourdan M, Creemers GJM, et al. Loss of skeletal muscle index and survival in patients with metastatic colorectal cancer: Secondary analysis of the phase 3 CAIRO3 trial. *Cancer Med*. 2020;9(3):1033–43.
21. Nankivell BJ. Creatinine clearance and the assessment of renal function. *Aust Prescr*. 2001;24(1):15–7.
22. Shahbaz H, Gupta M. Creatinine Clearance [Internet]. *StatPearls*. 2021 [cited 2021 Sep 14]. Available from: <https://www.ncbi.nlm.nih.gov/books/NBK544228/>

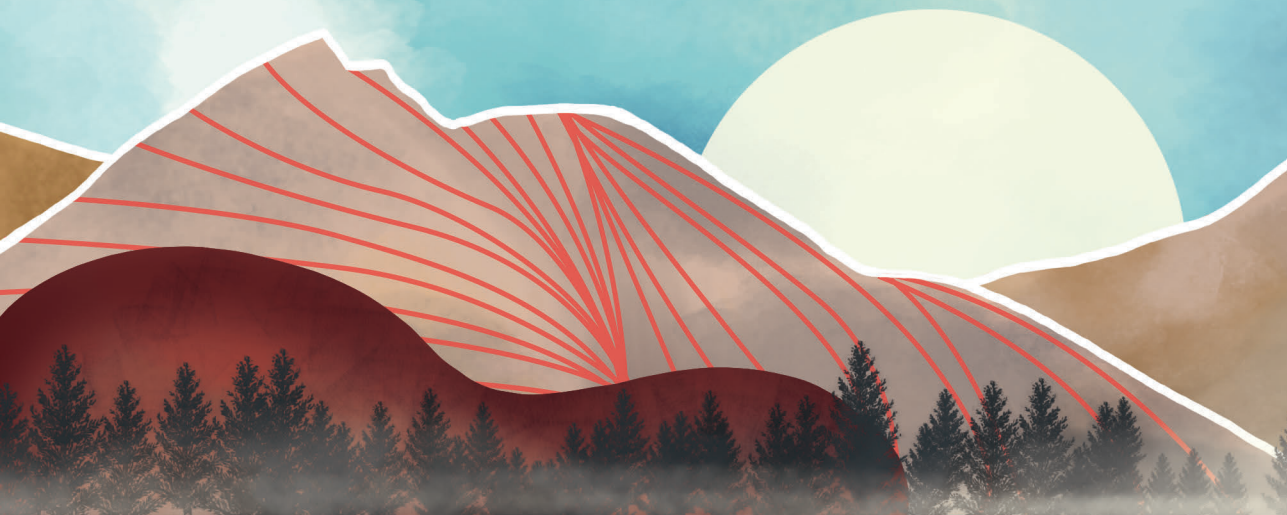






# CHAPTER 3

Measurement of drug levels  
in alternative matrices







# CHAPTER 3.1

## Everolimus saliva concentrations as predictor of stomatitis: a feasibility study in cancer patients

Laura Molenaar-Kuijsten, Remy B. Verheijen, Bart A.W. Jacobs, Bas Thijssen, Hilde Rosing, Thomas P.C. Dorlo, Jos H. Beijnen, Neeltje Steeghs, Alwin D.R. Huitema

Submitted for publication

Author's contribution: LMK contributed to the laboratory analysis, performed the data analysis by population pharmacokinetic modeling, wrote the first draft of the manuscript and implemented the input and feedback of the co-authors.

# ABSTRACT

## Background

More than half of cancer patients treated with everolimus experience stomatitis, which has serious negative impact on quality of life. Concentrations of everolimus in saliva might be predictive for the incidence and severity of stomatitis as these might reflect the concentration at the site of action. We aimed to examine whether it is feasible to quantify everolimus saliva concentrations and subsequently use these as a predictor of stomatitis.

## Methods

Saliva and whole blood samples were taken from cancer patients treated with everolimus 10 mg once daily and 5 mg twice daily. Everolimus was measured in saliva by liquid chromatography–tandem mass spectrometry (LC-MS/MS). A published population pharmacokinetic model was extended with everolimus saliva concentrations, to assess any association between everolimus in whole blood and saliva. Subsequently, the association between the occurrence of stomatitis and everolimus in saliva was studied.

## Results

Eleven patients were included in the study; saliva samples were available for 10 patients including three patients with low grade stomatitis. Everolimus concentrations in saliva were more than 100-fold lower than in whole blood, with an accumulation ratio of 0.00801 (relative standard error 32.5%). Inter-individual variability and residual unexplained variability were high with values of 67.7 and 84.0%, respectively. A trend was found between the occurrence of stomatitis and the individual predicted saliva concentrations of everolimus 1 hour post dose.

## Conclusion

Quantification of everolimus concentrations in saliva was feasible. A trend was found between saliva concentrations and the occurrence of stomatitis. Therefore, everolimus concentrations in saliva might be used as an early predictor of stomatitis without the need for invasive sampling. Subsequently, in patients with high everolimus saliva concentrations precautions can be taken to decrease the incidence and severity of stomatitis.

## INTRODUCTION

Everolimus inhibits the mammalian target of rapamycin (mTOR) and is used for the treatment of breast cancer, neuroendocrine tumors and renal cell carcinoma. The approved dose is 10 mg once daily (QD). In case of toxicity the dose can be reduced (1).

The most common adverse event of everolimus is stomatitis, often occurring in the first 8 weeks of treatment (1). Any grade of stomatitis occurs in 57% of cancer patients, while 6% of these patients experiences a grade 3-4 stomatitis (2). Stomatitis is problematic because it negatively impacts the quality of life of patients and is frequently dose-limiting. Therefore, it would be desirable to prevent this side effect from occurring.

In multiple studies, a correlation between toxicity and pharmacokinetic parameters of everolimus has been demonstrated. First of all, the maximum whole blood concentration ( $C_{max}$ ) of everolimus has been related to toxicity (3,4). Secondly, Ravaud *et al.* showed that the risk of stomatitis was increased with a relative risk of 1.49 (95% confidence interval 1.05-2.10) with a doubling of the everolimus trough concentrations ( $C_{min}$ ; the geometric mean everolimus  $C_{min}$  was 15.7 ng/mL in this study)(2). Lastly, De Wit *et al.* found a correlation between a higher exposure to everolimus in whole blood and stomatitis ( $p=0.047$ )(5).

Approximately 85% of the total amount of everolimus accumulates within erythrocytes whereas the unbound fraction of everolimus is thought to be responsible for the pharmacodynamic effects (6,7). We hypothesized that local exposure of the oral mucosa to everolimus is the cause of stomatitis, and therefore, that everolimus concentrations in saliva might be predictive for the incidence and severity of stomatitis.

Measuring everolimus concentrations in saliva might be attractive. Firstly, saliva sampling is non-invasive and can be done at home, without the need for an attending nurse (or other healthcare worker). This creates the opportunity to measure saliva concentrations early after start of treatment, without extra visits to the clinic. Secondly, for the relationship with stomatitis, it might better reflect the concentration at the site of toxicity. Taken together, everolimus concentrations in saliva might be used as an early predictor of stomatitis. Additionally, if saliva concentrations are correlated to whole blood concentrations, saliva might be used to assess systemic exposure.

The aim of this study was to examine whether it is feasible to measure everolimus saliva concentrations and to use them as a predictor for stomatitis. In order to determine the feasibility, the following items were investigated: 1) the feasibility of obtaining saliva samples in cancer patients; 2) the applicability of a previously developed bioanalytical method for everolimus in whole blood for saliva samples; 3) the correlation between whole blood and saliva concentrations; 4) the variability in saliva concentrations; and 5) the association between the incidence of stomatitis and everolimus concentrations in saliva.

## METHODS

### Study population

We previously performed a crossover study in which everolimus 10 mg QD was compared with 5 mg twice daily (BID), to investigate the possibility of reducing the  $C_{max}$ , in order to improve tolerability, while maintaining exposure to everolimus (3). In the current analysis, everolimus whole blood concentrations at steady-state from this study were used. Saliva samples were also collected from the participating patients as part of this study. The study was conducted in accordance with Good Clinical Practice and the Declaration of Helsinki and was approved by the local Medical Ethics Committee. All patients provided written informed consent prior to enrollment in the study. The trial was registered in the EudraCT database (2014-004833-25) and the Netherlands Trial Registry (NTR4908).

### Toxicity

Stomatitis was graded according to the Common Terminology Criteria for Adverse Events (CTCAE)(version 4.02)(8).

### Saliva sampling

Saliva samples were taken on steady-state, once per treatment schedule. For the 5 mg BID schedule, the sample was collected just before intake at the end of the 24-hour pharmacokinetic whole blood sampling period, and for the 10 mg QD schedule in principal 2 hours post dose (with the exceptions that for the first patients the sample was collected 4 or 5 hours post dose, and for one patient the sample was collected just before intake at the end of the 24-hour pharmacokinetic whole blood sampling period). The Greiner Bio-One Saliva Collection System (Greiner Bio-One B.V., Alphen aan den Rijn, The Netherlands) was used for saliva sampling (9). The subjects had to rinse their mouth for 2 minutes with Saliva Extraction Solution, which consisted of a citrate buffer (pH 4.2), and the yellow food dye tartrazine as an internal standard (9,10). After 2 minutes the saliva was collected, and the sample was stored at -20°C until analysis.

### Measurement everolimus in saliva

The collected saliva samples were diluted by use of the Saliva Extraction Solution. Therefore, the volume percentage of saliva was measured by ultraviolet-visible spectroscopy, using The Greiner Bio-One Saliva Quantification Kit (Greiner Bio-One B.V., Alphen aan den Rijn, The Netherlands)(11). Using the volume percentage of saliva, the everolimus concentrations measured in the diluted samples were converted to saliva concentrations.

The sample preparation and bioanalytical method were based on a validated method used for the measurement of everolimus in whole blood, as described by Verheijen *et al.* (3). The bioanalytical method was adjusted to increase the sensitivity by selecting a more sensitive tandem mass spectrometry (MS/MS) system for quantification [Qtrap 5500 (Sciex, Framingham, USA)] and switching from high performance liquid chromatography (HPLC) to ultra-performance liquid chromatography (UPLC). Furthermore, a higher volume of 10  $\mu\text{L}$  was injected in the liquid chromatography–tandem mass spectrometry (LC-MS/MS) system from the processed saliva sample.

### Pharmacokinetic (PK) analysis

Because of the limited number of samples and the heterogeneous sampling of saliva on different time points for each individual, nonlinear mixed-effects modeling was used to describe the population PK of everolimus measured in whole blood and saliva.

Since the sample size was small, we used the previously published model by De Wit *et al.* to describe the whole blood data, which was a 2-compartment model with first-order absorption and elimination (5). The structural and random effects model from the published base model were maintained, and parameter estimates were fixed to the published values. The model fit was evaluated based on goodness-of-fit plots.

Addition of the saliva data was tested in two ways. First, saliva concentrations were assumed to be in equilibrium with concentrations in the central compartment and an accumulation ratio was estimated using Equation 1 (12).

$$C_{saliva} = \text{accumulation ratio} \times C_{whole\ blood} \quad (1)$$

Where  $C_{saliva}$  is the measured everolimus concentration in saliva, and  $C_{whole\ blood}$  is the measured everolimus concentration in whole blood.

Secondly, it was tested whether saliva concentrations show a different dynamic relationship (e.g., everolimus enters the saliva compartment with a delay) compared to concentrations in the central compartment. For this, saliva concentrations were modelled as an effect compartment according to Equation 2 (13).

$$\frac{dC_{saliva}}{dt} = k_{e0} \times (C_{whole\ blood} - C_{saliva}) \quad (2)$$

Where  $\frac{dC_{saliva}}{dt}$  is the difference in measured everolimus concentrations in saliva over time,  $C_{whole\ blood}$  is the measured everolimus concentration in whole blood,  $C_{saliva}$  is the measured everolimus concentration in saliva, and  $k_{e0}$  is the equilibration rate constant.



Interindividual variability (IIV) was described with an exponential model according to Equation 3.

$$\theta_i = \theta_{pop} \times \exp(\eta_i) \quad (3)$$

Where  $\theta_i$  is the parameter estimate for individual  $i$ ,  $\theta_{pop}$  is the typical parameter estimate for the population, and  $\eta_i$  is the IIV for individual  $i$  which was assumed to be normally distributed with a mean of zero and a variance of  $\omega^2$ .

For both models, the residual unexplained variability was described by an exponential model according to Equation 4.

$$C_{obs,ij} = C_{pred,ij} \times (1 + \varepsilon_{prop}) \quad (4)$$

Where  $C_{obs,ij}$  is the observed concentration for individual  $i$  and observation  $j$ ,  $C_{pred,ij}$  is the predicted concentration for individual  $i$  and observation  $j$ , and  $\varepsilon_{prop}$  is the proportional error which was assumed to be normally distributed with a mean of zero and a variance of  $\sigma^2$ .

To determine if the occurrence of stomatitis correlates with the presence of everolimus in saliva, the correlation between stomatitis and both the Bayesian estimate of the accumulation ratio (assuming an exposure mediated effect), and the individual predicted saliva concentration 1 hour post dose ( $C_{max}$  of everolimus in whole blood (1); assuming a maximum concentration mediated effect) were studied. The individual predicted saliva concentration 1 hour post dose was obtained by prediction of the everolimus  $C_{max}$  based on the individual Bayesian estimates. For statistical comparison the non-parametric Wilcoxon test was used. Additionally, the correlation between stomatitis and  $C_{max}$  of everolimus in whole blood was also studied.

### Model evaluation

Model evaluation was based on the assessment of goodness-of-fit plots, successful minimization, parameter precision and a decrease in IIV. Parameter precision was obtained using the covariance step implemented in NONMEM.

### Software

NONMEM (version 7.5, ICON Development Solutions, Ellicott City, USA) and Perl-speaks-NONMEM (PsN, version 4.7.0) were used for nonlinear mixed-effects modeling (14). Parameter estimates were obtained with the first-order conditional estimation with interaction (FOCE-I) method. Pirana (version 2.9.9) was used for model management (15) R (version 3.6.3) was used for data management and graphical diagnostics (16).

## RESULTS

In total, 11 patients were included in the study. Patients were diagnosed with breast cancer, renal cell cancer or neuroendocrine tumors. One patient withdrew informed consent after pharmacokinetic sampling in the first treatment schedule. For the other 10 patients whole blood samples were available for both treatment schedules (5 mg BID and 10 mg QD). Saliva samples were available for 10 patients, but for 3 patients only for one of the treatment schedules. Three patients reported treatment emergent stomatitis, all grade 1 stomatitis, during the 4 weeks of treatment in the study. Patient characteristics are shown in **Table 1**.

Table 1. Patient baseline characteristics (n=11).

Characteristic	n (%) or mean [range]
Sex	
Male	6 (55%)
Female	5 (45%)
Age (years)	56 [43-77]
Height (cm)	171 [160-192]
Weight (kg)	76 [52-92]
WHO performance status	
0	7 (64%)
1	4 (36%)
Tumor type	
Breast	4 (36%)
Renal	4 (36%)
Neuroendocrine	3 (27%)
Occurrence of stomatitis (grade 1)	3 (27%)

Except the first patient, all patients could collect saliva samples at the nominal time points according to the study protocol. Everolimus concentrations were quantifiable in all saliva samples. The analytical range was 0.01-10 ng/mL (weighted linear regression ( $1/x^2$ ), coefficients all >0.99). Inter- and intra-run precision were  $\leq 9.5\%$ , and overall and intra-run bias were within  $\pm 12.8\%$ . Carry-over of the second blank after injection of an upper limit of quantification (ULOQ) sample was  $\leq 11.7\%$  of the lower limit of quantification (LLOQ; 0.01 ng/mL). No endogenous interferences were detected. The bias and coefficient of variation were within  $\pm 6.8\%$  and  $\leq 2.7\%$  after three freeze/thaw cycles (saliva sample;  $-70^\circ\text{C}/\text{ambient}$  with at least 12 hours between the freeze/thaw cycles), within

$\pm 8.0\%$  and  $\leq 5.7\%$  after one freeze/thaw cycle (saliva sample; ambient after at least two weeks of storage at  $-70^{\circ}\text{C}$ ), within  $\pm 13.2\%$  and  $\leq 5.7\%$  for the re-injection reproducibility (saliva sample;  $4^{\circ}\text{C}$  for at least 48 hours), and within  $\pm 12.3$  and  $\leq 5.3\%$  in the final extract ( $2-8^{\circ}\text{C}$  for at least 48 hours). In **Figure 1** everolimus concentration-time curves are shown for whole blood and saliva. The everolimus concentrations in saliva were approximately 100-fold lower than in whole blood.

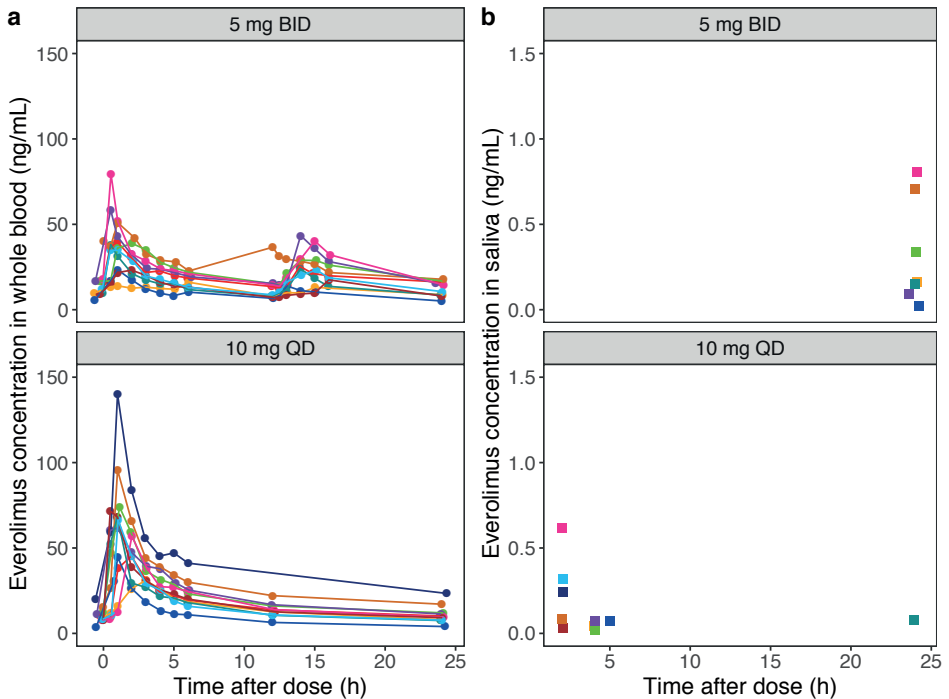


Figure 1. Everolimus concentrations in whole blood and saliva versus time after dose. In panel a whole blood concentrations are shown and in panel b saliva concentrations. For both panel a and b, the upper panel shows the measured everolimus concentrations for the 5 mg BID schedule, and the lower panel for the 10 mg QD schedule. Every color in the graph represents one patient. BID, twice daily; QD, once daily.

The whole blood data was described adequately by the model as assessed by the goodness-of-fit plots (left panels in **Supplementary Figure 1**). In **Table 2** the parameter estimates for the saliva part of the PK model are shown. The effect compartment model was unidentifiable and, therefore, the model with an accumulation ratio to describe saliva concentrations, was determined to be the final model (goodness-of-fit plots are shown in **Supplementary Figure 1**). A whole blood-saliva accumulation ratio of 0.00801 was estimated, with a relative standard error (RSE) of 32.5%.

Table 2. Parameter estimates for the saliva part of the population pharmacokinetic model of everolimus.

Parameter	Estimate	RSE (%)
Accumulation ratio	0.00801	32.5
Inter-individual variability (CV%)	67.7	35.2
Residual unexplained variability, proportional error saliva (CV%)	84.0	18.7

RSE, relative standard error; CV, coefficient of variation.

Large IIV for the accumulation ratio and very high residual variability was found. The high variability is also illustrated by the plot of everolimus concentrations in saliva versus everolimus concentrations in whole blood, both sampled at the same time point, as shown in **Figure 2**.

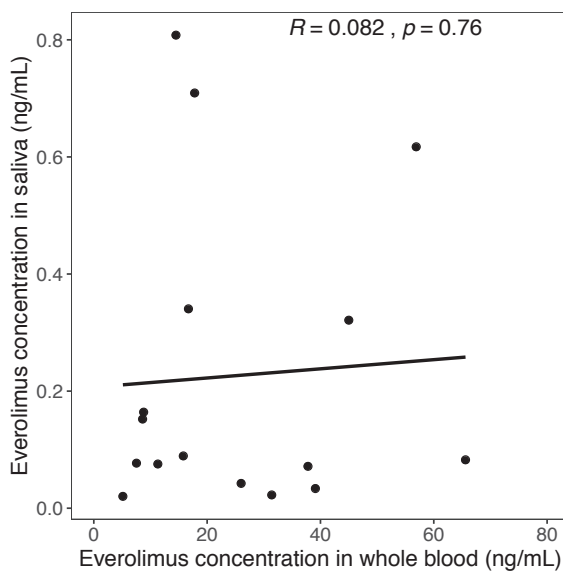


Figure 2. Everolimus concentrations in whole blood versus everolimus concentrations in saliva. The displayed everolimus concentrations in whole blood were taken on the same time points as the everolimus saliva samples.

Lastly, the correlation between the occurrence of stomatitis and the presence of everolimus in saliva was studied. A non-significant trend was found towards a higher Bayesian estimate of the accumulation ratio ( $p=0.28$ ; **Figure 3a**), and higher individual predicted saliva concentration 1 hour post dose ( $p=0.14$ ; **Figure 3b**) for the patients with stomatitis (all grade 1). The observed  $C_{max}$  of everolimus in whole blood was significantly higher in patients experiencing stomatitis ( $p=0.04$ ; **Figure 3c**).

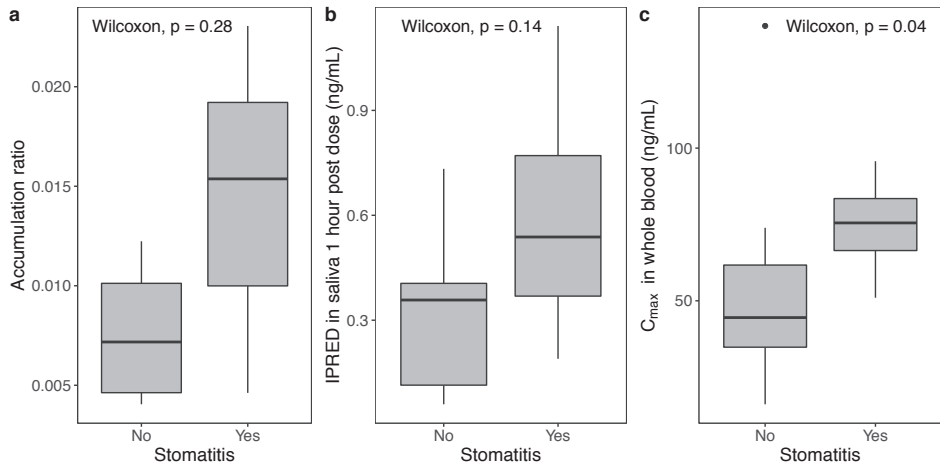


Figure 3. Correlation between the occurrence of stomatitis and pharmacokinetics of everolimus. In panel a the correlation with the individual everolimus whole blood-saliva accumulation ratio estimate, in panel b the correlation with the individual predicted everolimus concentration in saliva 1 hour post dose, and in panel c the correlation with the  $C_{max}$  of everolimus in whole blood is shown.  $C_{max}$ : maximum concentration; IPRED, individual predicted concentration.

## DISCUSSION

Stomatitis is a common adverse event of everolimus, which has serious negative impact on quality of life. We hypothesized that everolimus concentrations in saliva might be predictive for the incidence and severity of stomatitis. The aim of our study was to examine whether it is feasible to use everolimus saliva concentrations as a predictor of stomatitis.

In order to examine this feasibility, five items were considered. To summarize, firstly, it was feasible to collect saliva samples, even in patients with mild stomatitis. Secondly, to the best of our knowledge we were the first to show that, everolimus concentrations could be quantified in saliva samples. Thirdly, the PK of everolimus in saliva was highly variable. Fourthly, saliva concentrations were poorly correlated with whole blood concentrations. Lastly, a trend towards a higher Bayesian estimate of the accumulation ratio and higher individual predicted saliva concentration of everolimus 1 hour post dose for the patients with stomatitis was found. The  $C_{\max}$  of everolimus in whole blood was a better predictor for stomatitis, however, since whole blood sampling requires an extra hospital visit for outpatients, saliva sampling might be used as an alternative early predictor of stomatitis.

A poor relationship between everolimus concentrations in saliva and whole blood was found. The high variability of everolimus PK in saliva was considered the most important reason for this finding. In the current study a high variability in the accumulation ratio was found, with an IIV of 67.7%, and a high variability in the predictions of the saliva concentrations, with a residual variability of 84.0% (both coefficients of variation). A poor correlation between saliva and blood concentrations was also described in a previous study by Nudelman *et al.* ( $R^2=0.045$ ), who measured concentrations of sirolimus, an mTOR inhibitor like everolimus, in saliva following mouthwash application (17). This was explained by the variability of drug clearance from saliva in general, which is influenced by several factors, for example salivary gland function, water and electrolyte balance, protein binding, and pH (18,19).

Approximately 85% of the total amount of everolimus accumulates within erythrocytes, with a concentration dependent blood to plasma ratio (7). Saliva concentrations mostly represent the unbound drug concentration in the blood (19). Assuming 85% accumulation of everolimus in erythrocytes, the free fraction of everolimus in whole blood was still 15-fold higher than in saliva, in the studied patients.

The pH in saliva is between 5.8 and 8.4 (19). Since everolimus has pKa values between -2.7 and 9.96, and unionized lipophilic drugs are passively excreted from saliva, the clearance of everolimus from saliva is considered to be pH dependent (19–21). The concentration dependent accumulation of everolimus in erythrocytes, and the pH dependent clearance from saliva could be an explanation for the high variability of everolimus PK in saliva. Because the saliva samples were diluted by use of the Saliva Extraction Solution, measurement of the pH in the samples was not possible. To summarize, as a consequence of the high variability of everolimus PK in saliva and poor correlation between everolimus concentrations in saliva and whole blood, saliva sampling as a proxy for everolimus whole blood sampling is not feasible.

As described in the studies of Ravaud *et al.* and De Wit *et al.* patients who had a higher trough level of, or a higher exposure to, everolimus as measured in whole blood, had a higher risk of developing stomatitis (2,5). In our study, we also showed a statistically significant correlation between the  $C_{max}$  of everolimus in whole blood and the occurrence of stomatitis. Because of the small sample size and limited number of patients who developed stomatitis, we may not have been able to show a significant correlation between the occurrence of stomatitis and everolimus in saliva. Nevertheless, we showed a trend towards a higher Bayesian estimate of the accumulation ratio, and higher individual predicted saliva concentration of everolimus 1 hour post dose and stomatitis. This indicates that everolimus concentrations in saliva might be used as an early predictor of stomatitis, which can be done by home sampling of saliva early after start of treatment. As a precaution, patients with high everolimus concentrations in saliva could be treated with an alcohol-free corticosteroid oral solution to decrease the incidence and severity of stomatitis (1). Future, larger studies are needed to confirm the correlation between everolimus saliva concentrations and stomatitis, and to establish a cut-off value which is associated with a higher risk of stomatitis.

## CONCLUSION

To conclude, this is the first study to show the feasibility of obtaining saliva samples and quantifying everolimus concentrations in these samples. Saliva concentrations were poorly correlated with whole blood concentrations with an accumulation ratio of 0.00801 (IIV 67.7%). Since the individual predicted saliva concentration of everolimus 1 hour post dose for patients with stomatitis tended to be higher, it might be possible to use everolimus saliva concentrations as an early predictor for the occurrence of stomatitis and take precautions in these patients. To investigate this possibility, the correlation between everolimus saliva concentrations and stomatitis should be studied in a larger patient group.

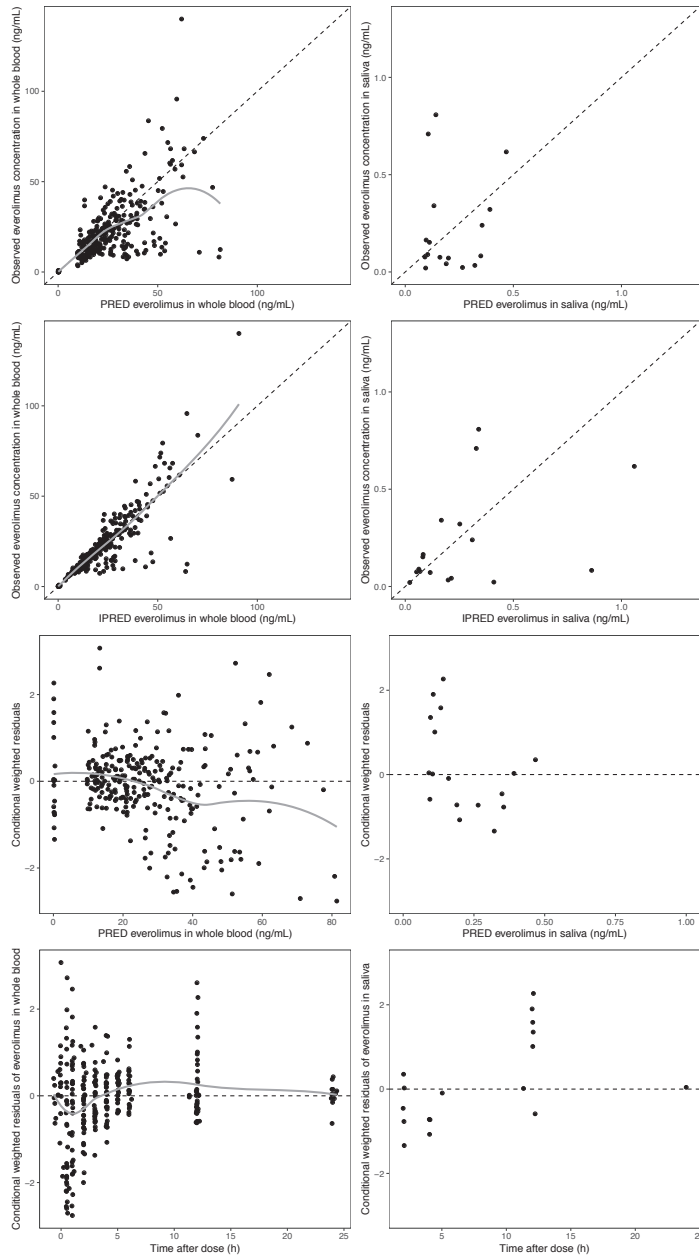


## REFERENCES

1. European Medicines Agency Committee for Medicinal Products For Human Use (CHMP). Everolimus European Public Assessment Report [Internet]. 2014. [cited 2019 Sep 19]. Available from: [https://www.ema.europa.eu/en/documents/product-information/afinitor-epar-product-information\\_en.pdf](https://www.ema.europa.eu/en/documents/product-information/afinitor-epar-product-information_en.pdf)
2. Ravaud A, Urva SR, Grosch K, Cheung WK, Anak O, Sellami DB. Relationship between everolimus exposure and safety and efficacy: Meta-analysis of clinical trials in oncology. *Eur J Cancer*. 2014;50(3):486–95.
3. Verheijen RB, Atrafi F, Schellens JHM, Beijnen JH, Huitema ADR, Mathijssen RHJ, et al. Pharmacokinetic Optimization of Everolimus Dosing in Oncology: A Randomized Crossover Trial. *Clin Pharmacokinet*. 2018;57(5):637–44.
4. Diederich A, Liechti K, Kuehl PCW. Pharmaceutical compositions comprising 40-O-(2-hydroxy) ethyl-rapamycin. [Internet]. 2013 [cited 2020 Apr 22]. Available from: <https://patents.google.com/patent/WO2013050419A1/en>
5. de Wit D, Schneider TC, Moes DJAR, Roozen CFM, den Hartigh J, Gelderblom H, et al. Everolimus pharmacokinetics and its exposure–toxicity relationship in patients with thyroid cancer. *Cancer Chemother Pharmacol*. 2016;78(1):63–71.
6. van Erp NP, van Herpen CM, de Wit D, Willemsen A, Burger DM, Huitema ADR, et al. A Semi-Physiological Population Model to Quantify the Effect of Hematocrit on Everolimus Pharmacokinetics and Pharmacodynamics in Cancer Patients. *Clin Pharmacokinet*. 2016;55(11):1447–56.
7. Food and Drug Administration. Center for Drug Evaluation and Research Everolimus Clinical Pharmacology and Biopharmaceutics Review [Internet]. 2008 [cited 2019 Sep 20]. Available from: [https://www.accessdata.fda.gov/drugsatfda\\_docs/nda/2009/022334s000\\_ClinPharmR.pdf](https://www.accessdata.fda.gov/drugsatfda_docs/nda/2009/022334s000_ClinPharmR.pdf)
8. National Cancer Institute. National Institutes of Health Services. US Department of Health and Human. Common Terminology Criteria for Adverse Events (CTCAE) version 4.02 [Internet]. 2009 [cited 2021 Jul 30]. Available from: [https://ctep.cancer.gov/protocoldevelopment/electronic\\_applications/ctc.htm](https://ctep.cancer.gov/protocoldevelopment/electronic_applications/ctc.htm)
9. Greiner Bio-One GmbH. Greiner Bio-One Saliva Collection System [Internet]. 2019 [cited 2020 May 4]. Available from: [https://www.gbo.com/fileadmin/user\\_upload/Downloads/IFU\\_Instructions\\_for\\_Use/IFU\\_Instructions\\_for\\_Use\\_Preanalytics/English/g80243\\_IFU\\_SCS\\_EN\\_rev04.pdf](https://www.gbo.com/fileadmin/user_upload/Downloads/IFU_Instructions_for_Use/IFU_Instructions_for_Use_Preanalytics/English/g80243_IFU_SCS_EN_rev04.pdf)
10. Greiner Bio-One GmbH. Greiner Bio-One Saliva Extraction Solution pH 4.2 [Internet]. 2021 [cited 2021 Jul 29]. Available from: <https://shop.gbo.com/en/row/products/preanalytics/saliva-collection-system/gbo-saliva-collection-system/gbo-saliva-collection-system-professionals/881112.html>
11. Greiner Bio-One GmbH. Greiner Bio-One Saliva Quantification Kit [Internet]. 2019 [cited 2020 May 4]. Available from: [https://www.gbo.com/fileadmin/user\\_upload/Downloads/IFU\\_Instructions\\_for\\_Use/IFU\\_Instructions\\_for\\_Use\\_Preanalytics/English/g80217\\_IFU\\_SCS\\_EN\\_rev04.pdf](https://www.gbo.com/fileadmin/user_upload/Downloads/IFU_Instructions_for_Use/IFU_Instructions_for_Use_Preanalytics/English/g80217_IFU_SCS_EN_rev04.pdf)
12. Ter Heine R, Mulder JW, Van Gorp ECM, Wagenaar JFP, Beijnen JH, Huitema ADR. Intracellular and plasma steady-state pharmacokinetics of raltegravir, darunavir, etravirine and ritonavir in heavily pre-treated HIV-infected patients. *Br J Clin Pharmacol*. 2010;69(5):475–83.

13. Upton RN, Mould DR. Basic concepts in population modeling, simulation, and model-based drug development: Part 3-introduction to pharmacodynamic modeling methods. *CPT Pharmacometrics Syst Pharmacol*. 2014;3(1):1–16.
14. Boeckmann AJ, Sheiner LB, Beal SL. NONMEM Users Guide - Part V [Internet]. Ellicott City, Maryland, USA: ICON Development Solutions; 2011 [cited 2020 Aug 11]. Available from: <https://nonmem.iconplc.com/nonmem720/guides/>
15. Keizer RJ, Karlsson MO, Hooker A. Modeling and simulation workbench for NONMEM: Tutorial on Pirana, PsN, and Xpose. *CPT Pharmacometrics Syst Pharmacol*. 2013;2(6):1–9.
16. R Core Team. R: A Language and Environment for Statistical Computing [Internet]. Vienna, Austria; 2020 [cited 2020 Aug 25]. Available from: <https://www.r-project.org>
17. Nudelman Z, Friedman M, Barasch D, Nemirovski A, Findler M, Pikovsky A, et al. Levels of sirolimus in saliva and blood following mouthwash application. *Oral Dis*. 2014;20(8):768–72.
18. de Almeida Pdel V, Grégio A, Machado M, de Lima A, Azevedo L. Saliva composition and functions: a comprehensive review. *J Contemp Dent Pr*. 2008;9(3):72–80.
19. Aravindha Babu N, Masthan KMK, Gopalakrishnan T, Elumalai M. Drug excretion in saliva - A review. *Int J Pharm Sci Rev Res*. 2014;26(1):76–7.
20. Wishart D, Feunang Y, Guo A, Lo E, Marcu A, Grant J, et al. DrugBank 5.0: Everolimus [Internet]. 2021 [cited 2021 Aug 10]. Available from: <https://go.drugbank.com/drugs/DB01590>
21. Food and Drug Administration. Center for Drug Evaluation and Research Everolimus Clinical Pharmacology and Biopharmaceutics Review [Internet]. 2012 [cited 2021 Aug 10]. Available from: [https://www.accessdata.fda.gov/drugsatfda\\_docs/nda/2012/203985Orig1s000ClinPharmR.pdf](https://www.accessdata.fda.gov/drugsatfda_docs/nda/2012/203985Orig1s000ClinPharmR.pdf)

## SUPPLEMENTARY MATERIAL



Supplementary Figure 1. Goodness-of-fit plots for model predicted everolimus concentrations in whole blood (left) and saliva (right). The grey lines are loess curves. PRED, population predicted concentration; IPRED, individual predicted concentration.





# CHAPTER 3.2

## Intra-tumoral pharmacokinetics of pazopanib in combination with radiotherapy in patients with non-metastatic soft-tissue sarcoma

Laura Molenaar-Kuijsten\*, Milan van Meekeren\*, Remy B. Verheijen, Judith V.M.G Bovée, Marta Fiocco, Bas Thijssen, Hilde Rosing, Alwin D.R. Huitema, Aisha B. Miah, Hans Gelderblom, Rick L.M. Haas, Neeltje Steeghs

\* These authors contributed equally

Submitted for publication

Authors contribution: MvM and LMK contributed to the data analysis, wrote the first draft of the manuscript and implemented the input and feedback of the co-authors.

## ABSTRACT

There is a lack of understanding whether plasma levels of anticancer drugs (such as pazopanib) correlate with intra-tumoral levels and whether the plasma compartment is the best surrogate for pharmacokinetic and pharmacodynamic evaluation. Therefore, we aimed to quantify pazopanib concentrations in tumor tissue, to assess the correlation between tumor concentrations and plasma concentrations, and between tumor concentrations and efficacy. In this clinical trial, non-metastatic soft-tissue sarcoma patients were treated with neo-adjuvant concurrent radiotherapy and pazopanib. Plasma samples and tumor biopsies were collected and pazopanib concentrations were measured using liquid chromatography-tandem mass spectrometry. Twenty-four evaluable patients were included. The median pazopanib tumor concentration was 19.2  $\mu\text{g/g}$  (range 0.149-200  $\mu\text{g/g}$ ). A modest correlation was found between tumor concentrations and plasma levels of pazopanib ( $\rho=0.41$ ,  $p=0.049$ ). No correlation was found between tumor concentrations and percentage of viable tumor cells ( $p>0.05$ ), however a trend towards less viable tumor cells in patients with high pazopanib concentrations in tumor tissue was observed in a categorical analysis. Possible explanations for the lack of correlation might be heterogeneity of the tumors, and timing of the biopsy procedure.

## SIMPLE SUMMARY

Pazopanib plasma levels have been associated with treatment efficacy. Since pazopanib targets receptors present on cells in the vicinity of the tumor and on tumor cells itself, measurement of pazopanib concentrations in tumor tissue might be an even better prognostic biomarker than plasma levels. The aim of our study was to quantify pazopanib concentrations in tumor tissue, correlate this with plasma concentrations, and assess whether this is a better biomarker for efficacy. A modest correlation was found between pazopanib tumor concentrations and plasma concentrations. Additionally, no correlation was found between pazopanib tumor concentrations and efficacy. We provide recommendations for future studies in which pazopanib concentrations are measured.

## INTRODUCTION

Pazopanib is a tyrosine kinase inhibitor (TKI), which targets the vascular endothelial growth factor receptor (VEGFR)-1, -2 and -3, platelet-derived growth factor (PDGFR)- $\alpha$ , and - $\beta$ , fibroblast growth factor receptor (FGFR)-1, -3 and -4, and stem cell factor receptor (c-KIT)(1,2). By targeting these receptors pazopanib inhibits tumor proliferation and angiogenesis (3). It is approved for the first-line treatment of advanced or metastatic renal cell carcinoma (RCC) and as second-line therapy of metastatic soft-tissue sarcoma (STS)(1). Haas *et al.* showed that the neoadjuvant use of pazopanib 800 mg once daily in combination with 50 Gy preoperative radiotherapy (RT) seems tolerable and shows promising results in terms of efficacy also in patients with non-metastatic, intermediate or high-grade STS of the extremities, in the phase I PASART-1 study (NCT01985295)(4). The combined treatment regimen was subsequently assessed in the phase II PASART-2 trial (NCT02575066)(5). The main efficacy endpoint of this single arm trial was the rate of pathological complete response (pCR), defined as  $\leq 5\%$  viable tumor cells in the resection specimen at central pathology review. The combination treatment led to a relatively low rate of major wound complications (24%). Out of 25 patients, 17 patients experienced grade 3 or higher acute toxicities, but as the vast majority of those were asymptomatic, transient ALT/AST elevations or hypertension, the regimen was deemed tolerable. A promising pCR rate of 20% (5/25 patients) was observed. This manuscript reports the results of the pharmacokinetic substudy of the PASART-2 trial.

Pazopanib targets receptors on tumor cells and on cells in the tumor micro-environment (TME). Therefore, at least theoretically, in order for pazopanib to be effective, adequate plasma levels must be achieved, so sufficient pazopanib molecules could potentially arrive in the vicinity of the tumor. Indeed, pazopanib efficacy has been related to plasma trough levels ( $C_{\min}$ ) in advanced or metastatic RCC, with a significant decrease in tumor size and longer progression free survival (PFS) for patients with a  $C_{\min}$  of  $\geq 20.5$  mg/L (6–8). In metastatic STS patients with a pazopanib  $C_{\min} > 20$  mg/L, a trend was found towards a decrease in tumor size and better PFS (8,9).

However, multiple factors, such as tumor vascularization, hypoxia and the presence of drug efflux transporters, could influence drug penetration from plasma to tumor tissue (10). Therefore, drug concentrations in tumor tissue could potentially serve as an even stronger prognostic biomarker, as pazopanib ultimately exerts its effects in the tumor tissue and tumor micro-environment, not in the plasma. Previously published research showed that the drug concentrations of multiple TKIs, for example gefitinib and erlotinib, could be measured in human tumor tissue (11–13). However, these



concentrations have not been correlated to efficacy parameters. For pazopanib, a method to measure drug concentrations and distribution in mouse tumor models has been described, which was used to study suboptimal pharmacokinetics as an explanation for drug resistance (14).

In this pharmacokinetic substudy of the PASART-2 trial, plasma samples and tumor biopsies were taken from patients with non-metastatic STS of the extremities, trunk, chest wall or head and neck region treated with neoadjuvant pazopanib in combination with preoperative RT. The aim of this study was to quantify pazopanib concentrations in tumor tissue and to determine the correlation between tumor and plasma concentrations, and between tumor concentrations and efficacy.

3

## METHODS

### Study design

This pharmacokinetic study was embedded in an international, multicenter phase II trial (NCT02575066)(5). Written informed consent was obtained, the study protocol was approved by the local ethics commissions and the study was conducted in accordance with the declaration of Helsinki.

### Study population

Patients were eligible if they were  $\geq 18$  years, had a WHO performance status of  $\leq 1$  and a histologically confirmed non-metastatic soft-tissue sarcoma localized in the extremities, trunk, chest wall or the head and neck region, for which standard therapy is surgery and radiotherapy. This means the tumor had to be deep seated and/or  $>5$  cm and/or grade II/III according to the Fédération Nationale des Centres de Lutte Contre Le Cancer (FNCLCC) definition and/or close resection margins had to be anticipated. Patients were excluded if they had prior malignancies (except if they were disease-free for at least 5 years) or recurrent sarcomas, and if they received chemotherapy or radiation therapy within 2 weeks prior to first dose of study medication or biological therapy within 28 days or five half-lives. Furthermore, female patients who were pregnant or breast-feeding were excluded, and all patients were required to employ effective methods of birth control.

### Study treatment

The planned radiotherapy dose was 50 Gy, in once daily 2 Gy fractions for 5 days a week, from day 1 to day 33. Pazopanib once daily 800 mg was commenced one week prior to the start of radiotherapy on day -7 and continued until radiotherapy completion. Surgery was performed 4-8 weeks post pazopanib and radiotherapy treatment.

### Pharmacokinetics

Blood samples were collected in  $K_2$  EDTA tubes at day 1 and day 22. The samples were centrifuged at 2200 g for 10 min. Plasma was stored at  $-20^\circ\text{C}$  until analysis.

Tumor samples were collected at day 22 of the study. These samples were snap frozen immediately after the biopsy procedure by immersing them in liquid nitrogen for 30 seconds. The samples were stored at  $-80^\circ\text{C}$  until further processing. Before processing, the tumor samples were weighted and 300  $\mu\text{L}$  control human  $K_2$  EDTA plasma was added. Subsequently, the samples were homogenized with a Polytron® PT 1200B homogenizer (Kinematica AG) for at least 3 min per sample. Lastly, samples were centrifuged at 3000 g for 1 min to get rid of the foam that arose during homogenization. The homogenized samples were stored at  $-80^\circ\text{C}$  until analysis.

Concentrations of pazopanib in plasma were measured using a validated liquid chromatography-tandem mass spectrometry (LC-MS/MS) method (32). The method for measurement of pazopanib in tumor homogenates was based on a validated LC-MS/MS method in plasma, however the sample preparation was adjusted to concentrate the samples (33). A 100  $\mu\text{L}$  aliquot of the homogenate was transferred to an Eppendorf tube and 200  $\mu\text{L}$  of methanol containing 0.1  $\mu\text{g}/\text{mL}$  internal standard ( $^{13}\text{C}^2\text{H}_3$ -pazopanib) was added before the sample was vortex mixed. Subsequently, the sample was centrifuged at 23,100  $g$  for 5 min and 100  $\mu\text{L}$  of the clear supernatant was transferred to a clean reaction tube and mixed with 100  $\mu\text{L}$  of 10 mmol/L ammonium hydroxide in water before injection. Pazopanib could be measured in tumor homogenates in a range of 0.01 to 10  $\mu\text{g}/\text{mL}$ .

An experiment was conducted to determine if all pazopanib was released from the tumor sample, because for some samples a small pellet of tumor tissue resided in the Eppendorf tube after homogenization and centrifugation. First, the concentration of pazopanib was measured in the tumor homogenate. Next, the residue was taken, and 200  $\mu\text{L}$  control human  $\text{K}_2$  EDTA plasma was added. The sample was homogenized and centrifuged again, following the same method as described earlier. The concentration in the plasma supernatant was measured. After that, the procedure was repeated, and the concentration in the plasma supernatant was measured.

The pazopanib plasma concentrations were corrected for the time after dose at which the sample was obtained by calculating pazopanib trough levels. The following formula was used (34):

$$C_{\min} = C_{\text{measured}} \times 0.5^{\frac{(\text{dosing interval} - \text{TAD})}{t_{1/2}}} \quad (1)$$

Where  $C_{\min}$  is the calculated pazopanib trough level,  $C_{\text{measured}}$  is the measured pazopanib concentration, TAD is the time after dose, and  $t_{1/2}$  is the elimination half-life which is 31 hours for pazopanib (1).

The pazopanib tumor concentrations were corrected for the dilution in human plasma, and the weight of the tumor sample, resulting in a concentration pazopanib in mg/g tumor tissue. In **Figure 1**, an overview of study procedures is given.

**Efficacy endpoint**

For this pharmacokinetic study, the percentage of viable tumor cells estimated on representative slides of each individual surgical specimen under the light microscope, as reported by an experienced soft tissue tumor pathologist (JVMGB), was used as efficacy parameter. Additionally, the percentage of viable tumor cells in the tumor biopsy on day 22 was scored in the same way, and compared with the results from the surgical specimen.

**Statistics**

Statistical analyses were performed using R version 3.6.3 (R Project, Vienna, Austria). Descriptive statistics were used to summarize treatment outcomes and pazopanib plasma and tumor levels. The Wilcoxon signed rank test was employed to test for differences between pazopanib plasma levels on day 1 and day 22. To study the associations between pazopanib plasma levels and pazopanib tumor levels, and percentage of viable tumor cells in tumor tissue on day 22 and in the resection specimen Spearman's rank correlation was used. The association between pazopanib tumor levels and percentage viable tumor cells, and pazopanib plasma trough levels and percentage viable tumor cells, were studied both numerical assuming a linear association, and categorical assuming a threshold for efficacy. For the numerical analysis of the association between drug concentration and efficacy, the Spearman's rank correlation was used. For the categorical analysis, pazopanib tumor levels were divided in quartiles and the association was tested with the Kruskal-Wallis test. Secondly, pazopanib tumor levels were divided in two equal groups, and the association was tested with the Wilcoxon signed rank test. The pazopanib plasma trough levels were divided in groups with a low and adequate exposure, according to the threshold value of 20 mg/L (6), and the association was tested with the Wilcoxon signed rank test.  $p \leq 0.05$  was considered statistically significant.

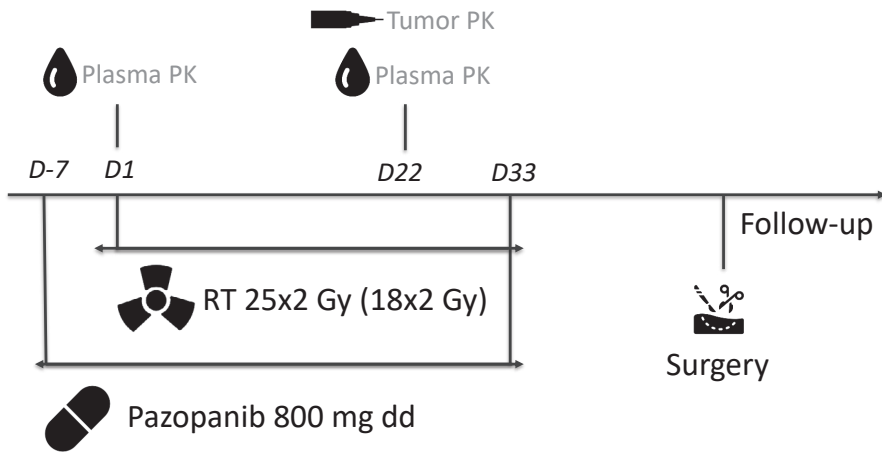


Figure 1. Overview of study procedures for the PASART-2 pharmacokinetic study.

## RESULTS

### Patient characteristics

Between March 2016 and December 2018, 25 patients with non-metastatic soft-tissue sarcoma were included in the study. The first 21 patients received 50 Gy radiotherapy. After an interim analysis the protocol was amended, and 4 additional patients were added to the study, whom were treated with a lower dose of 36 Gy radiotherapy, in once daily 2 Gy fractions for 5 days a week, from day 1 to day 24. For one patient we were not able to adequately homogenize the tumor tissue. Therefore, this patient was excluded from the analysis. Patient characteristics of the 24 remaining evaluable patients are shown in **Table 1**. Histological subtyping was done by the World Health Organization (WHO) 2013 classification (15).

### Pharmacokinetics

In order to determine if pazopanib was released from the tumor sample a recovery experiment was conducted. Almost all pazopanib was released from the tumor sample in this experiment. In the plasma supernatant, after the first extra homogenization step of the residue, only 5% of pazopanib was measured compared to the tumor homogenate. After the second homogenization step, less than 2% of pazopanib was measured compared to the tumor homogenate (value under lower limit of quantification (LLOQ)).

Pazopanib plasma concentrations were measured on day 1 and day 22 of the study, with exception of two patients where plasma concentrations were measured on day 1 or day 22 only. The median pazopanib trough concentration in plasma was 37.1 mg/L (range 4.47-78.1 mg/L) on day 1, and 33.5 mg/L (range 8.38-120.7 mg/L) on day 22. There was no statistically significant difference in plasma trough levels between day 1 and day 22 ( $p=0.64$ ), as shown in **Supplementary Figure S1**. For further data analysis, plasma trough levels on day 22 were used as also tumor concentrations were measured on day 22. For a single patient for whom no plasma trough level was available on day 22, the plasma trough level on day 1 was used.

The median pazopanib tumor concentration measured in tumor homogenates taken on day 22 was 19.2  $\mu\text{g/g}$  (range 0.149-200  $\mu\text{g/g}$ ). Two patients had high pazopanib tumor concentrations compared to the other patients (200 and 121  $\mu\text{g/g}$ ). One of these patients also had a high pazopanib plasma concentration (plasma concentrations were 91 and 36 mg/L respectively for the two patients). Both patients did not experience grade 3 or 4 toxicity. In addition, one patient was found to have a very low pazopanib tumor concentration (0.149  $\mu\text{g/g}$ ). This patient had an adequate

pazopanib plasma concentration (32 mg/L) and experienced grade 3 or 4 toxicity, including hypertension. Overall, a modest correlation was found between tumor concentrations and plasma trough levels of pazopanib ( $\rho=0.41$ ), which was borderline significant ( $p=0.049$ ), see **Figure 2**.

Table 1. Patient characteristics ( $n=24$ ).

Characteristic	<i>n</i> (%) or median [range]
Gender	
Male	14 (58%)
Female	10 (42%)
Age (years)	57 [24-79]
Tumor Histology	
Undifferentiated pleomorphic sarcoma	9 (38%)
Myxofibrosarcoma	8 (33%)
Spindle cell sarcoma (not otherwise specified)	2 (8%)
Myxoid liposarcoma	1 (4%)
Synovial sarcoma	1 (4%)
Spindle cell rhabdomyosarcoma	1 (4%)
Clear cell sarcoma	1 (4%)
Malignant peripheral nerve sheath tumor	1 (4%)
Pazopanib trough levels in plasma on day 22 (mg/L)	34.8 [8.38-120.7]
Pazopanib concentrations in tumor tissue ( $\mu\text{g/g}$ )	
Total	19.2 [0.149-200]
Undifferentiated pleomorphic sarcoma	27.4 [0.149-121]
Myxofibrosarcoma	18.9 [5.31-200]
Spindle cell sarcoma (not otherwise specified)	36.4 [9.08-63.7]
Myxoid liposarcoma	16.3 [N/A]
Synovial sarcoma	27.3 [N/A]
Spindle cell rhabdomyosarcoma	18.2 [N/A]
Clear cell sarcoma	16.0 [N/A]
Malignant peripheral nerve sheath tumor	11.0 [N/A]

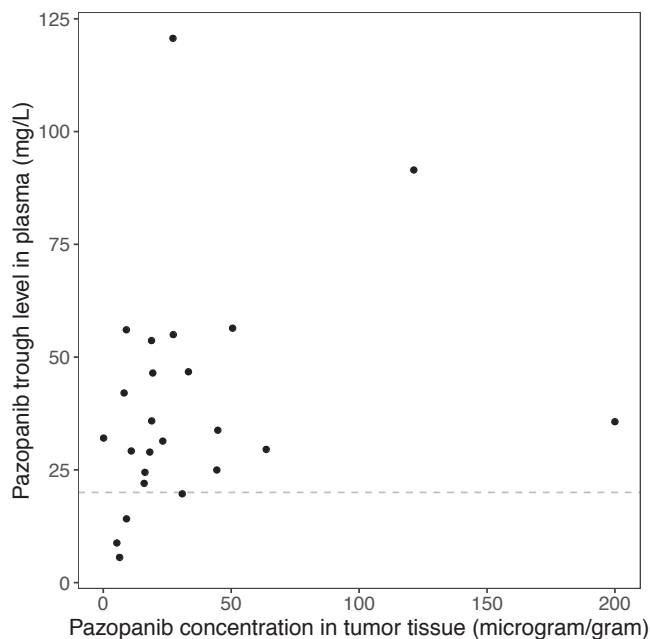


Figure 2. Pazopanib concentrations in tumor tissue versus pazopanib trough levels in plasma ( $\rho=0.41$ ,  $p=0.049$ ). The dashed line represents a pazopanib trough level of 20 mg/L, which is advised as the target for adequate drug exposure.

For 18 patients, the percentage of viable tumor cells could be evaluated on the biopsy from day 22. No statistically significant correlation was found between the percentage of viable tumor cells in the tumor biopsy on day 22 and in the resection specimen ( $\rho=0.21$ ;  $p=0.37$ ), see **Supplementary Figure S2**. For further data analysis, percentage of viable tumor cells in the resection specimen was used, in order to study tumor concentrations as a biomarker for efficacy of the total treatment.

No statistically significant correlation was found between tumor concentrations and efficacy measured by percentage of viable tumor cells in the resection specimen when numerically studied ( $\rho=-0.10$ ;  $p=0.63$ ), as depicted in **Figure 3**. When categorical analyzed, no statistically significant difference was found either ( $p=0.49$  when divided in two groups;  $p=0.67$  when divided in quartiles). However, visual inspection indicates a trend towards less viable tumor cells in patients with high pazopanib concentrations in tumor tissue, as shown in the boxplots in **Figure 4** (median 40.0% viable tumor cells for low tumor concentrations, and 22.5% for high tumor concentrations) and **Supplementary Figure S3**.



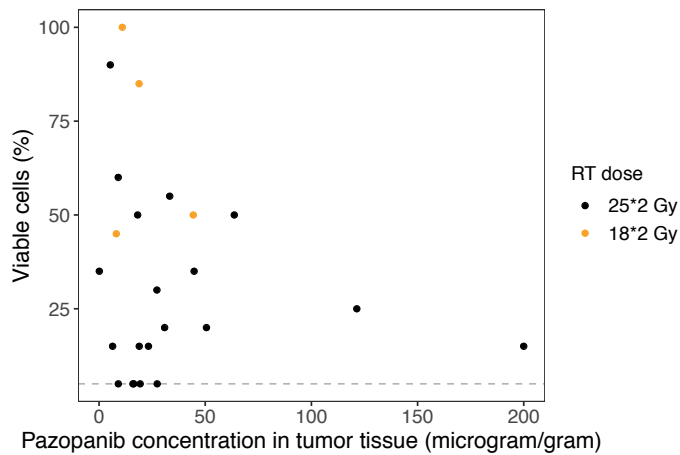


Figure 3. Pazopanib concentrations in tumor tissue versus percentage viable tumor cells in resection specimen ( $\rho=-0.10$ ,  $p=0.63$ ). The dashed line represents the cut-off value for a good response, which is  $\leq 5\%$  viable tumor cells. Patients which are shown as black dots were treated with a radiotherapy dose of 50 Gy, patients which are shown as orange dots were treated with a radiotherapy dose of 36 Gy.

Furthermore, no clear pattern was observed of the effect of radiotherapy dose and tumor type, as shown in **Figure 3** and **Supplementary Figure S4**, respectively.

No statistically significant correlation was found between pazopanib plasma trough levels and percentage viable tumor cells in resection specimen either ( $\rho=0.11$ ,  $p=0.62$ ), as shown in **Supplementary Figure S5** and **S6** (with radiotherapy and tumor type included in the plot, respectively). Since only four patients had a low exposure ( $< 20$  mg/L) no further categorical analysis has been performed.

3

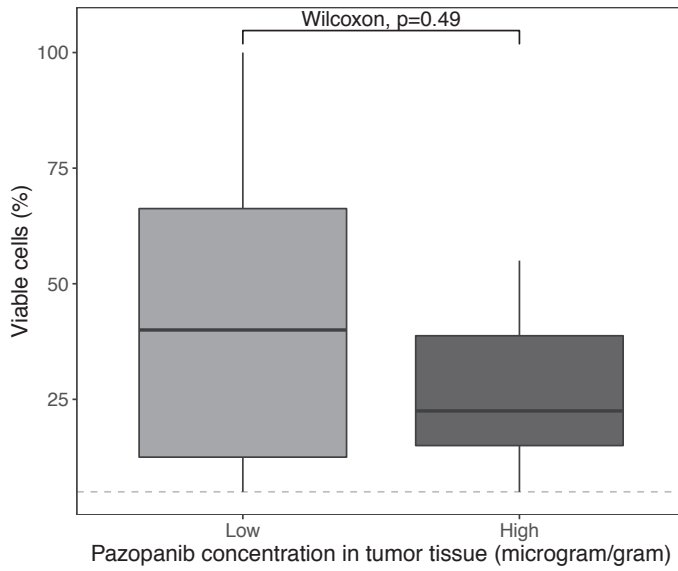


Figure 4. Pazopanib concentrations in tumor tissue, equally divided in two groups, versus percentage viable tumor cells in resection specimen. The dashed line represents the cut-off value for a good response, which is  $\leq 5\%$  viable tumor cells.

## DISCUSSION

In medical oncology, for several drugs it has been shown that drug levels in plasma can be measured to guide patient dosing for efficacy and to assess toxicity (16). Studies assessing intra-tumoral drug levels are extremely rare, and to the best of our knowledge for TKIs only erlotinib and gefitinib have been measured in human tumor tissue (11,12). Our study is the first to show that pazopanib levels can be quantified both in plasma and in human sarcoma tumor tissue. It is also the first to assess the correlation of intra-tumoral TKI drug levels with efficacy. A modest correlation was found between tumor concentration and plasma concentration ( $\rho=0.41$ ,  $p=0.049$ ). No statistically significant correlation between tumor concentration and percentage viable tumor cells was found, both when tested numerically assuming a linear relationship and categorically assuming a threshold for efficacy (numerically tested:  $\rho=-0.10$ ,  $p=0.63$ ; categorically tested:  $p=0.49$ ).

Only a modest correlation was found between tumor and plasma concentrations. Therefore, tumor concentrations can provide additional information about distribution and efficacy of pazopanib. Besides, a reason for the modest correlation could also be that in all, except four, patients a  $C_{\min} >20$  mg/L was measured. The previously reported relationship between  $C_{\min}$  and clinical outcomes, suggests the presence of a minimal effective concentration pazopanib in the tumor above this value (6–9).

No statistically significant correlation between tumor concentrations and efficacy was found, but categorical analysis of the data indicates a trend towards less viable tumor cells in patients with high pazopanib concentrations in tumor tissue. We cannot draw strong conclusions based on our research, however the following factors could have contributed to our findings.

First of all, the timing of the tumor biopsy procedure, which was performed on day 22 in our study (4 weeks after start of pazopanib, and 3 weeks after start of radiotherapy), could have affected the results. In order to have an anti-tumor effect pazopanib should be taken up by tumor tissue. This uptake is expected to be dependent on more factors than only pazopanib plasma levels. One of these factors could be the effect of pazopanib itself. Historically, anti-angiogenics like pazopanib were expected to cause tumor vessel death and regression, thereby depriving the tumor of oxygen and nutrients needed for rapid cell proliferation and tumor growth. However, multiple studies have suggested that anti-angiogenic treatment might actually initially lead to enhanced tumor perfusion and oxygenation (17–19). In many tumor micro-environments, there is an overexpression of pro-angiogenic factors like VEGF. This leads to new vessel recruitment to the tumor, but also causes a chaotic vascular network with often leaky vessels (20,21). Anti-angiogenics

normalize the balance of pro- and anti-angiogenic factors, and thereby lead to a better organized vascular network and more adequate vascular pericyte coverage (22,23). This explains the possible synergism when combining anti-angiogenic treatment with radiotherapy or chemotherapy (24,25), as the latter treatment modalities are known to be more effective in well-perfused, oxygenated tumors. The vessel normalization effect is thought to be temporary, and can be described by a 'normalization window' (26–28). With sustained anti-angiogenic treatment, subsequently the balance shifts towards more anti-angiogenic factors, which will lead to regression of blood vessels (22). So, the measured tumor concentrations of pazopanib could be affected by both the normalization of the tumor vasculature, leading to improved distribution of pazopanib to tumor tissue, or by vessel regression, through which pazopanib could limit its own distribution to the tumor.

Additionally, the moment of evaluating tumor response might also influence the results. Four weeks (day -7 until day 22) could be too short for pazopanib to already have a significant effect on the viability of tumor cells. No statistically significant correlation was found between the percentage of viable tumor cells in tumor tissue on day 22 and in the resection specimen (neo-adjuvant treatment until day 33, 4-8 weeks later surgery was performed). In **Supplementary Figure S2** it can be seen that 10 out of 18 patients had 100% viable tumor cells in the tumor at day 22, while only one patient had 100% viable tumor cells in the resection specimen, which suggests that day 22 may be too early to estimate response. Therefore, it might be better to evaluate treatment efficacy at a later time point. In the study in which a correlation between pazopanib plasma concentrations of  $\geq 20.5$  mg/L and efficacy was found, pazopanib plasma concentrations were also measured after 4 weeks and tumor response was evaluated 8 weeks thereafter (6). This supports the choice to evaluate response in the resection specimen for the tumor concentration-response analysis.

A second factor that could play a role in explaining the observed results is heterogeneity, both between tumor types and within the tumor. In our study a wide variety of STS tumor subtypes was included. A difference between tumor types is for example the vasculature of the tumor (29,30). As described before, tumor vasculature could influence the distribution of pazopanib to the tumor. Next to intra-tumoral uptake of pazopanib, intra-tumoral distribution is crucial for the effect of pazopanib (14). Torok *et al.* described that intra-tumoral distribution of pazopanib was inhomogeneous with most pazopanib distributed to necrotic areas (14). We took one image-guided biopsy (16G) per patient. Although the use of imaging ensures that the biopsy is not taken in a necrotic tumor area, the biopsy might not be representative for the whole tumor because of the mentioned inhomogeneity.

Other factors affecting our results could firstly be the concurrent radiotherapy. The effects of the neo-adjuvant therapy we observed in the resection specimen of the patients could also predominantly be due to the effect of radiotherapy. Therefore, the pazopanib tumor tissue concentrations could have been of secondary importance. Furthermore, radiotherapy also affects the tumor vasculature (31). Secondly, the small number of patients, and few responses in the patient population (five patients achieving a pathological complete response), could also be a reason for the lack of a correlation between pazopanib plasma levels and efficacy. This absence of correlation for systemic pazopanib concentrations could, in turn, explain the lack of a correlation between pazopanib tumor concentrations and efficacy.

Lastly, the homogenization procedure and bioanalytical method to measure pazopanib in tumor tissue were not validated. Theoretically it could be possible that not all tumor cells were broken down by the homogenization procedure, and that thereby, not all pazopanib was released from the tumor tissue. This could have influenced the studied correlation between tumor and plasma concentrations, and tumor concentrations and efficacy. However, we conducted a recovery experiment, in which tumor concentrations of pazopanib in the residues were only 5% and <2% compared to the concentration in the tumor homogenate before extra homogenization steps. These findings support the reliability of the used methods.

To avoid some of the limitations we encountered in the current study design in future studies, the following suggestions are proposed in case tumor concentrations of anti-angiogenic drugs are measured: 1) measure drug tumor concentrations at different time points, to be able to study the changes over time, or perform a preclinical study to determine the optimal time for the biopsy procedure; 2) account for tumor heterogeneity and increase the chance that the biopsy of the tumor is representative (e.g., through combination with imaging based analysis of drug distribution).

## CONCLUSION

Measurement of pazopanib concentrations in human tumor tissue is possible. A modest correlation between tumor and plasma concentrations, and no statistically significant correlation between tumor concentrations and percentage of viable tumor cells was found. In a categorical analysis no statistically significant relationship was found either, however, we found a trend towards less viable tumor cells in the 50% of patients with the highest pazopanib tumor tissue concentrations. The non-significant relationship between tumor concentrations and efficacy could possibly be explained by heterogeneity of the tumors and timing of biopsies. For future studies, in which tumor concentrations of anti-angiogenic drugs are measured, it is suggested to measure drug tumor concentrations at different time points or to base the timing of the biopsy procedure on preclinical research and to account for tumor heterogeneity.

## REFERENCES

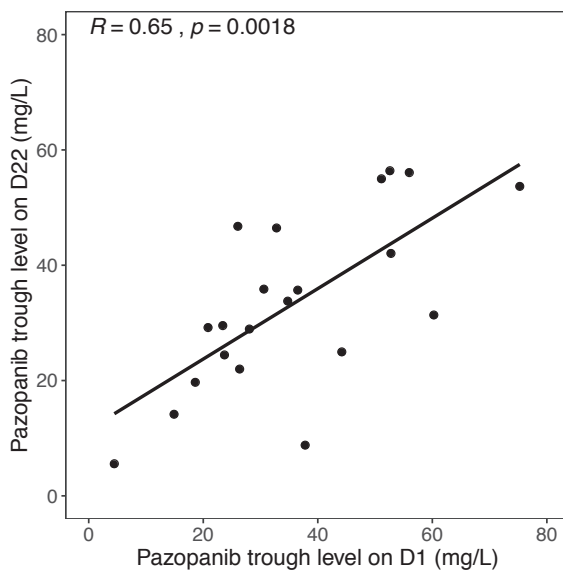
1. European Medicines Agency Committee for Medicinal Products For Human Use (CHMP). Pazopanib European Public Assessment Report [Internet]. 2018 [cited 2020 Apr 1]. Available from: [https://www.ema.europa.eu/en/documents/product-information/votrient-epar-product-information\\_en.pdf](https://www.ema.europa.eu/en/documents/product-information/votrient-epar-product-information_en.pdf)
2. Kumar R, Knick VB, Rudolph SK, Johnson JH, Crosby RM, Crouthamel MC, et al. Pharmacokinetic-pharmacodynamic correlation from mouse to human with pazopanib, a multikinase angiogenesis inhibitor with potent antitumor and antiangiogenic activity. *Mol Cancer Ther*. 2007;6(7):2012–21.
3. Hamberg P, Verweij J, Sleijfer S. (Pre-)Clinical Pharmacology and Activity of Pazopanib, a Novel Multikinase Angiogenesis Inhibitor. *Oncologist*. 2010;15(6):539–47.
4. Haas RLM, Gelderblom H, Sleijfer S, Van Boven HH, Scholten A, Dewit L, et al. A phase I study on the combination of neoadjuvant radiotherapy plus pazopanib in patients with locally advanced soft tissue sarcoma of the extremities. *Acta Oncol (Madr)*. 2015;54(8):1195–201.
5. van Meekeren M, Bovee JVMG, van Coevorden F, van Houdt W, Schrage Y, Koenen AM, et al. A phase II study on the neo-adjuvant combination of pazopanib and radiotherapy in patients with high-risk, localized soft tissue sarcoma. *Acta Oncol (Madr)*. 2021:1–8.
6. Suttle AB, Ball HA, Molimard M, Hutson TE, Carpenter C, Rajagopalan D, et al. Relationships between pazopanib exposure and clinical safety and efficacy in patients with advanced renal cell carcinoma. *Br J Cancer*. 2014;111(10):1909–16.
7. Verheijen RB, Beijnen JH, Schellens JHM, Huitema ADR, Steeghs N. Clinical Pharmacokinetics and Pharmacodynamics of Pazopanib: Towards Optimized Dosing. *Clin Pharmacokinet*. 2017;56(9):987–97.
8. Westerdijk K, Desar IME, Steeghs N, van der Graaf WTA, van Erp NP. Imatinib, sunitinib and pazopanib: From flat-fixed dosing towards a pharmacokinetically guided personalized dose. *Br J Clin Pharmacol*. 2020;86(2):258–73.
9. Verheijen RB, Swart LE, Beijnen JH, Schellens JHM, Huitema ADR, Steeghs N. Exposure-survival analyses of pazopanib in renal cell carcinoma and soft tissue sarcoma patients: opportunities for dose optimization. *Cancer Chemother Pharmacol*. 2017;80(6):1171–8.
10. Bartelink IH, Jones EF, Shahidi-Latham SK, Lee PRE, Zheng Y, Vicini P, et al. Tumor Drug Penetration Measurements Could Be the Neglected Piece of the Personalized Cancer Treatment Puzzle. *Clin Pharmacol Ther*. 2019;106(1):148–63.
11. Haura EB, Sommers E, Song L, Chiappori A, Becker A. A pilot study of preoperative gefitinib for early-stage lung cancer to assess intratumor drug concentration and pathways mediating primary resistance. *J Thorac Oncol*. 2010;5(11):1806–14.
12. Lankheet NAG, Schaake EE, Burgers SA, Van Pel R, Beijnen JH, Huitema ADR, et al. Concentrations of erlotinib in tumor tissue and plasma in non-small-cell lung cancer patients after neoadjuvant therapy. *Clin Lung Cancer*. 2015;16(4):320–4.
13. Labots M, Pham T V., Honeywell RJ, Knol JC, Beekhof R, de Goeij-De Haas R, et al. Kinase inhibitor treatment of patients with advanced cancer results in high tumor drug concentrations and in specific alterations of the tumor phosphoproteome. *Cancers (Basel)*. 2020;12(2).
14. Torok S, Rezeli M, Kelemen O, Vegvari A, Watanabe K, Sugihara Y, et al. Limited tumor tissue drug penetration contributes to primary resistance against angiogenesis inhibitors. *Theranostics*. 2017;7(2):400–12.

15. Fletcher C, Hogendoorn P, Mertens F, Bridge J. WHO Classification of Tumours of Soft Tissue and Bone. IARC Press. 2013;4th ed.
16. Verheijen RB, Yu H, Schellens JHM, Beijnen JH, Steeghs N, Huitema ADR. Practical Recommendations for Therapeutic Drug Monitoring of Kinase Inhibitors in Oncology. *Clin Pharmacol Ther.* 2017;102(5):765–76.
17. Lee CG, Heijn M, Di Tomaso E, Griffon-Etienne G, Ancukiewicz M, Koike C, et al. Anti-vascular endothelial growth factor treatment augments tumor radiation response under normoxic or hypoxic conditions. *Cancer Res.* 2000;60(19):5565–70.
18. Wildiers H, Guetens G, De Boeck G, Verbeken E, Landuyt B, Landuyt W, et al. Effect of anti-vascular endothelial growth factor treatment on the intratumoral uptake of CPT-11. *Br J Cancer.* 2003;88(12):1979–86.
19. Batchelor TT, Gerstner ER, Emblem KE, Duda DG, Kalpathy-Cramer J, Snuderl M, et al. Improved tumor oxygenation and survival in glioblastoma patients who show increased blood perfusion after cediranib and chemoradiation. *Proc Natl Acad Sci U S A.* 2013;110(47):19059–64.
20. Jain RK. Normalizing tumor vasculature with anti-angiogenic therapy: a new paradigm for combination therapy. *Nat Med.* 2001;7(9):987–9.
21. Goel S, Duda DG, Xu L, Munn LL, Boucher Y, Fukumura D, et al. Normalization of the Vasculature for Treatment of Cancer and Other Diseases. *Physiol Rev.* 2012;91(3):1071–121.
22. Goedegebuure RSA, De Klerk LK, Bass AJ, Derks S, Thijssen VLJL. Combining radiotherapy with anti-angiogenic therapy and immunotherapy; A therapeutic triad for cancer? *Front Immunol.* 2019;9(3107):1–15.
23. Jain RK. Normalization of Tumor Vasculature: An Emerging Concept in Antiangiogenic Therapy. *Science.* 2005;307(5706):58–62.
24. Kleibeuker EA, Griffioen AW, Verheul HM, Slotman BJ, Thijssen VL. Combining angiogenesis inhibition and radiotherapy: A double-edged sword. *Drug Resist Updat.* 2012;15(3):173–82.
25. Viallard C, Larrivée B. Tumor angiogenesis and vascular normalization: alternative therapeutic targets. *Angiogenesis.* 2017;20(4):409–26.
26. Winkler F, Kozin S V., Tong RT, Chae S-S, Booth MF, Garkavtsev I, et al. Kinetics of vascular normalization by VEGFR2 blockade governs brain tumor response to radiation. *Cancer Cell.* 2004;6(6):553–63.
27. Dings RPM, Loren M, Heun H, McNiel E, Griffioen AW, Mayo KH, et al. Scheduling of Radiation with Angiogenesis Inhibitors Anginex and Avastin Improves Therapeutic Outcome via Vessel Normalization. *Clin Cancer Res.* 2007;13(11):3395–402.
28. Matsumoto S, Batra S, Saito K, Yasui H, Choudhuri R, Gadiseti C, et al. Antiangiogenic agent sunitinib transiently increases tumor oxygenation and suppresses cycling hypoxia. *Cancer Res.* 2011;71(20):6350–9.
29. Ledoux P, Kind M, Le Loarer F, Stoeckle E, Italiano A, Tirode F, et al. Abnormal vascularization of soft-tissue sarcomas on conventional MRI: Diagnostic and prognostic values. *Eur J Radiol.* 2019;117(June):112–9.
30. Mentzel T, Brown LF, Dvorak HF, Kuhn C, Stiller KJ, Katenkamp D, et al. The association between tumour progression and vascularity in myxofibrosarcoma and myxoid/round cell liposarcoma. *Virchows Arch.* 2001;438(1):13–22.
31. Jarosz-Biej M, Smolarczyk R, Cichoń T, Kutach N. Tumor microenvironment as a "game changer" in cancer radiotherapy. *Int J Mol Sci.* 2019;20(13):18–20.

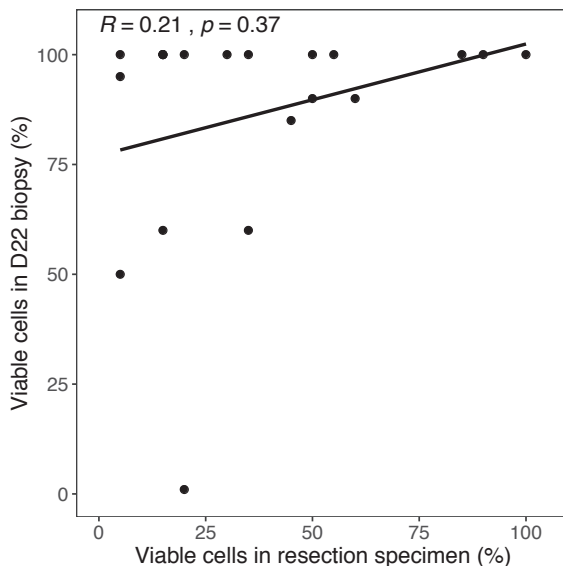


32. Herbrink M, De Vries N, Rosing H, Huitema ADR, Nuijen B, Schellens JHM, et al. Quantification of 11 therapeutic kinase inhibitors in human plasma for therapeutic drug monitoring using liquid chromatography coupled with tandem mass spectrometry. *Ther Drug Monit.* 2016;38(6):649–56.
33. Verheijen RB, Thijssen B, Rosing H, Schellens JHM, Nan L, Venekamp N, et al. Fast and Straightforward Method for the Quantification of Pazopanib in Human Plasma Using LC-MS/MS. *Ther Drug Monit.* 2018;40(2):230–6.
34. Wang Y, Chia YL, Nedelman J, Schran H, Mahon FX, Molimard M. A therapeutic drug monitoring algorithm for refining the imatinib trough level obtained at different sampling times. *Ther Drug Monit.* 2009;31(5):579–84.

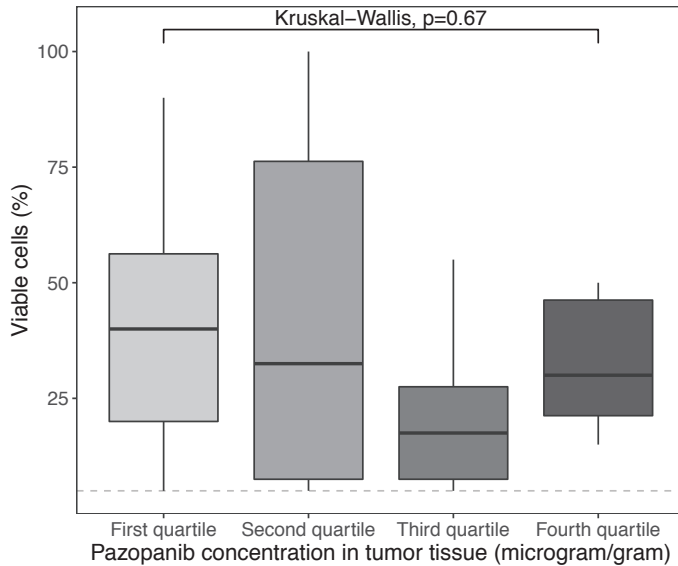
## SUPPLEMENTARY MATERIAL



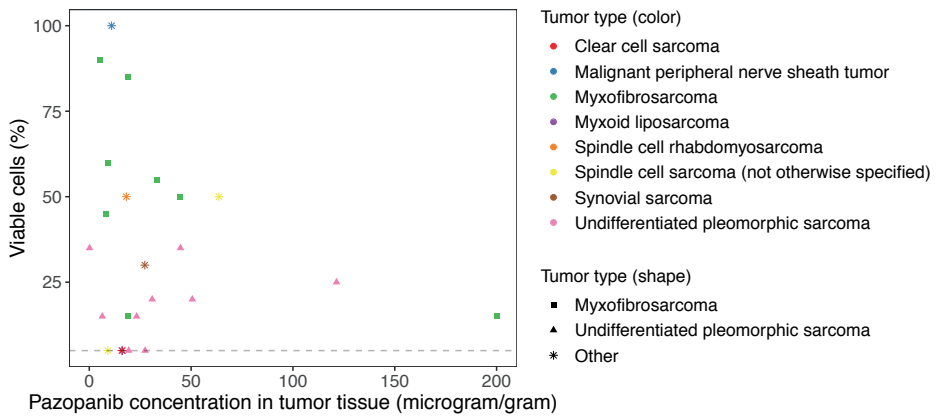
Supplementary Figure S1. Pazopanib trough levels in plasma on day 1 versus day 22. The black line represents the linear trend in the observations. D1, day 1; D22, day 22.



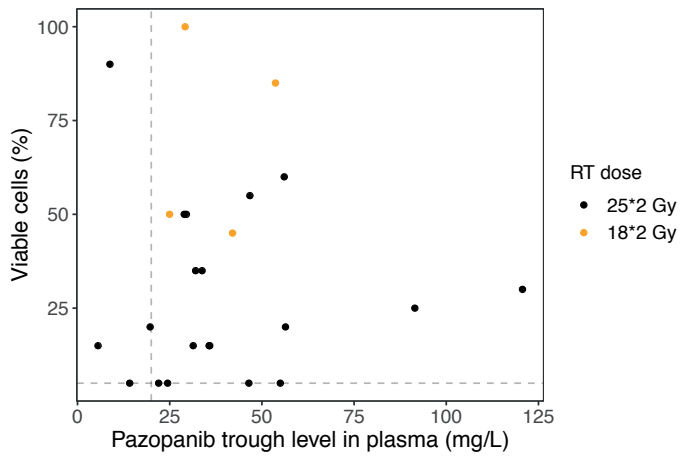
Supplementary Figure S2. Percentage of viable tumor cells in tumor tissue on day 22 versus in resection specimen. The black line represents the linear trend in the observations. D22, day 22.



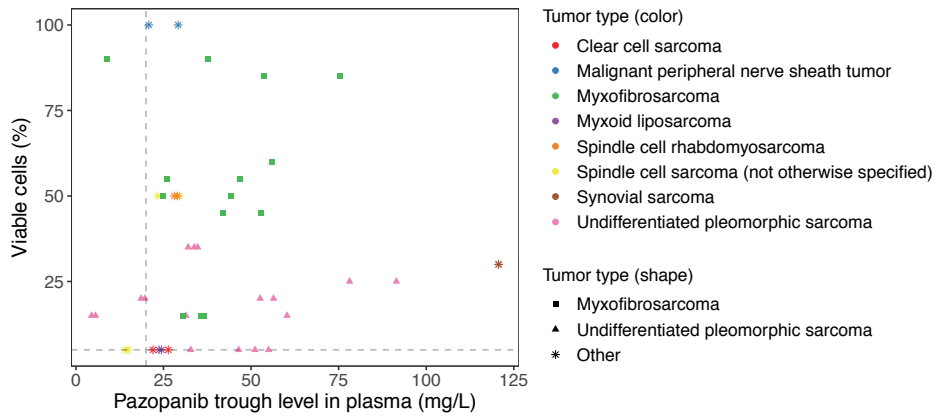
Supplementary Figure S3. Pazopanib concentrations in tumor tissue, divided in quartiles, versus percentage viable tumor cells in resection specimen. The dashed line represents the cut-off value for a good response, which is  $\leq 5\%$  viable tumor cells.



Supplementary Figure S4. Pazopanib concentrations in tumor tissue versus percentage viable tumor cells in resection specimen ( $\rho=-0.10$ ,  $p=0.63$ ). The dashed line represents the cut-off value for a good response, which is  $\leq 5\%$  viable tumor cells. The color and shape of the symbols corresponds with tumor type.

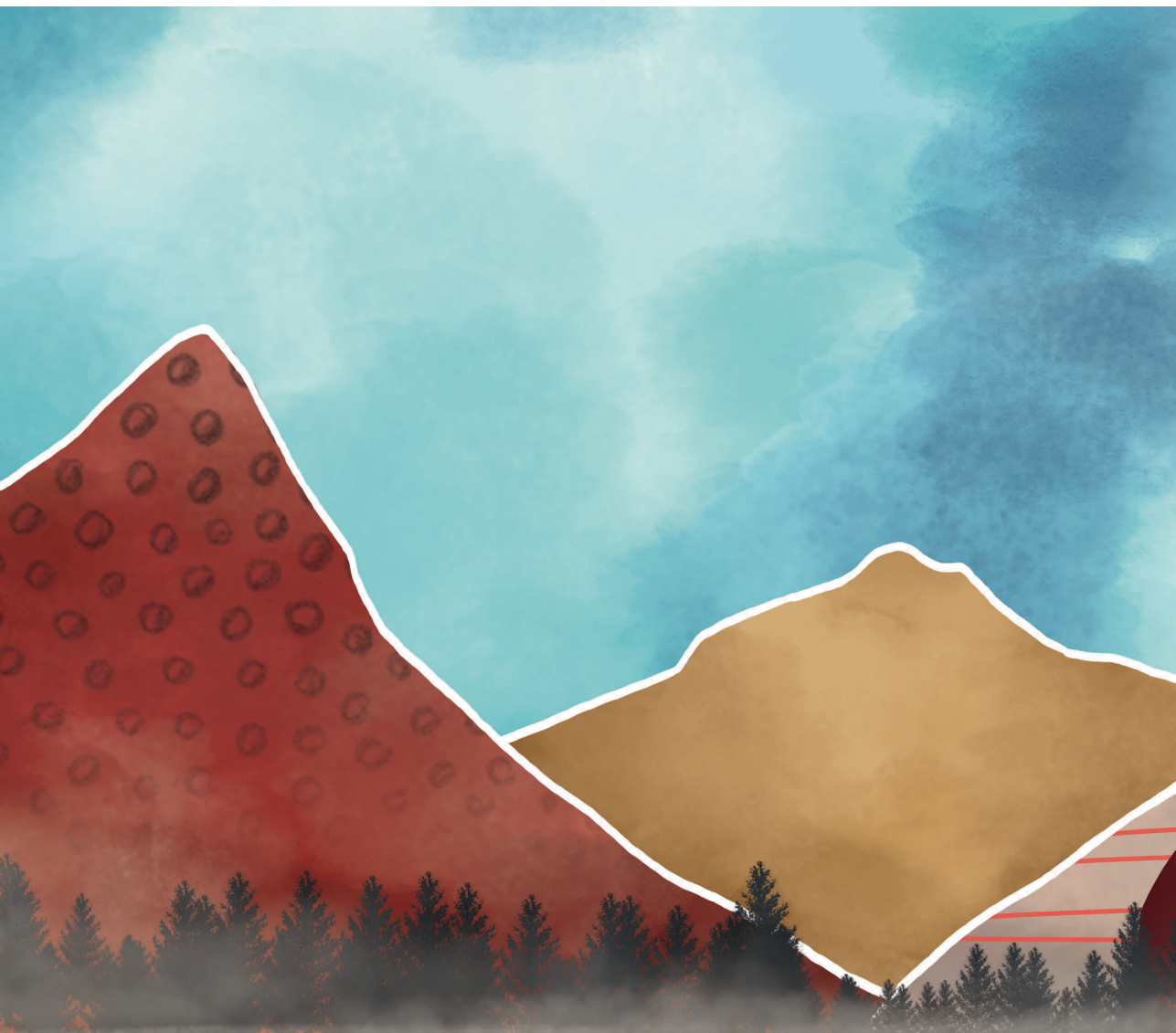


Supplementary Figure S5. Pazopanib trough levels in plasma versus percentage viable tumor cells in resection specimen ( $p=0.11$ ,  $p=0.62$ ). The horizontal dashed line represents the cut-off value for a good response, which is  $\leq 5\%$  viable tumor cells. The vertical dashed line represents a pazopanib trough level of 20 mg/L, which is advised as the target for adequate drug exposure. Patients which are shown as black dots were treated with a radiotherapy dose of 50 Gy, patients which are shown as orange dots were treated with a radiotherapy dose of 36 Gy.



Supplementary Figure S6. Pazopanib trough levels in plasma versus percentage viable tumor cells in resection specimen ( $p=0.11$ ,  $p=0.62$ ). The horizontal dashed line represents the cut-off value for a good response, which is  $\leq 5\%$  viable tumor cells. The vertical dashed line represents a pazopanib trough level of 20 mg/L, which is advised as the target for adequate drug exposure. The color and shape of the symbols corresponds with tumor type.

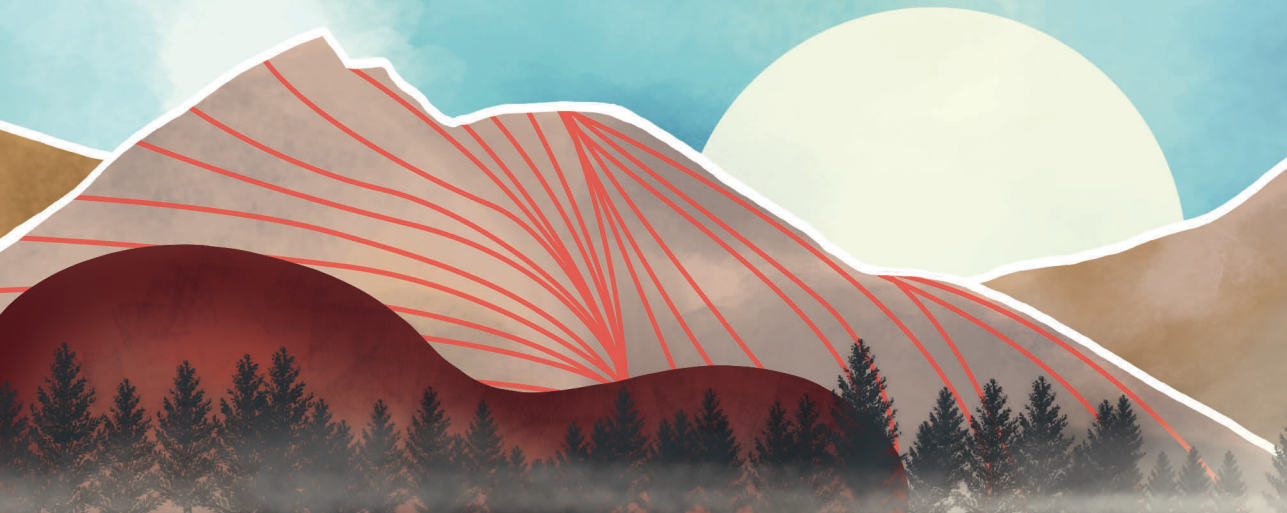




# CHAPTER 4

## Conclusions and perspectives

Author's contribution: LMK conceived and wrote the conclusions and perspectives, and implemented the input and feedback from her PhD supervisors.







## CONCLUSIONS AND PERSPECTIVES

This thesis is focused on dose optimization of anticancer treatment based on: 1) co-medication and drug-drug interactions (DDIs); 2) skeletal muscle mass; 3) drug levels in alternative matrices to predict efficacy or toxicity. Key points extracted from this thesis are summarized in the table on the following page and discussed in more detail in the following paragraphs.

## KEY POINTS

---

How to handle CYP3A based drug-drug interactions early after drug approval	Cancer patients are at high risk of experiencing drug-drug interactions (DDIs). Early after drug approval mostly only results from clinical DDI studies with strong CYP3A inhibitors and inducers are available. The lack of clinical data on the effect of moderate CYP3A inhibitors and inducers can be partly overcome by the use of physiologically based pharmacokinetic (PBPK) simulations, in which data from the conducted clinical DDI studies are combined with patient characteristics and data on other possible perpetrator drugs, to simulate DDIs. In addition, if also no results from PBPK simulations are available, the results from DDI studies with strong inhibitors and inducers can be extrapolated to predict the effect of moderate inhibitors and inducers. In selected cases, clinical DDI studies with moderate inhibitors and inducers should still be performed after drug approval.
Effect of body composition on pharmacokinetics of hydrophilic drugs	Body composition is an important predictor of toxicity and survival of different chemotherapeutic drugs. The pharmacokinetics of hydrophilic drugs are influenced by body composition, but this does not always provide an explanation for the increased toxicity. In registration studies, the effect of body composition on PK should be investigated, to find out for which drugs dose optimization based on body composition is beneficial.
Prediction of treatment outcome by local exposure	Drug concentrations in plasma or whole blood are essentially surrogate markers for drug exposure at site of action, which can be used to evaluate pharmacokinetics and pharmacodynamics. However, drug concentrations can also be measured at the site of action itself, e.g., in tumor tissue and saliva. Measurement of drug concentrations in tumor tissue requires an invasive procedure and it is not easy to homogenize tumor tissue. Therefore, it is difficult to use tumor concentrations in clinical practice. In contrast, saliva sampling is a non-invasive sampling method and can even be done at home. This creates the opportunity to use it for therapeutic drug monitoring, to optimize the dose early after start of treatment. Before this can be applied in clinical practice, the correlation between saliva concentrations and toxicity should be confirmed in a sufficiently powered study.
Value of pivotal studies in real-life patients	The data available from pivotal studies is often not sufficient to accurately predict drug effects in real-life patients. Results from these studies are not always representative, or only limitedly representative, for clinical practice. Therefore, pivotal studies should be extended regarding body composition. After drug approval a structured follow-up should be performed, and if necessary, additional clinical trials should be performed in real-life patients.

---

## HOW TO HANDLE CYP3A BASED DRUG-DRUG INTERACTIONS EARLY AFTER DRUG APPROVAL

Cancer patients are at increasing risk of DDIs. In the past, cancer was merely treated with chemotherapy, but nowadays an increasing number of patients is treated with targeted therapy. Targeted therapy is often administered orally and on a daily basis. Additionally, most oral anticancer drugs are metabolized by the Cytochrome P450 3A (CYP3A) enzyme, which is inhibited or induced by many different drugs. Lastly, cancer patients are often treated with multiple drugs, both for cancer treatment, to treat side effects and for co-morbidities for which medical treatment is required (1,2). Taken together, the risk of DDIs in cancer patients is high. These DDIs are seriously problematic because for many of the oral anticancer drugs exposure-efficacy and exposure-toxicity relationships exist (3). Therefore, a pharmacokinetic DDI could result in a decreased exposure, which could lead to treatment failure, or an increased exposure, which could lead to the occurrence of adverse events, which in turn will hamper quality of life and could cause suboptimal treatment.

The European Medicines Agency (EMA) and U.S. Food and Drug Administration (FDA) oblige manufacturers to conduct DDI studies before approval of a drug, based on the metabolism (4–6). Following the EMA and FDA guidelines, a worst-case approach is used, which means that, in case of metabolism via CYP3A, clinical DDI studies are performed with strong CYP3A inhibitors and mostly also with strong CYP3A inducers. In addition, exposure-response analyses are performed in the pivotal studies, which give an indication of the therapeutic window and thus the relevance of possible DDIs.

In clinical practice, moderate CYP3A inhibitors and inducers are much more frequently used than strong inhibitors and inducers. However, clinical data on the effects of these moderate inhibitors and inducers is mostly not available early after drug approval. The lack of this clinical data is partly overcome by the use of PBPK simulations. In PBPK simulation studies the data from the conducted clinical DDI studies with strong inhibitors and inducers can be combined with patient characteristics (e.g., the difference between healthy volunteers and cancer patients) and data on other possible perpetrator drugs, to simulate DDIs. Also, different situations can be simulated easily, e.g., different duration of co-mediation or a different formulation of the drug.

If also no results from PBPK simulations are available, the results from DDI studies with strong inhibitors and inducers can be extrapolated to predict the effect of moderate inhibitors and inducers, as described in **Chapter 1.1**. The extrapolation of

results from DDI studies with strong inhibitors and inducers, gives the opportunity to optimize the dose of anticancer drugs in case of DDIs with moderate inhibitors and inducers, even if no data is available. In **Chapter 1.1** recommendations on how to do that are given.

In selected cases, clinical DDI studies with moderate inhibitors and inducers should still be performed after drug approval, because of certain disadvantages of DDI studies performed before drug approval. Namely, clinical DDI studies with strong inhibitors or inducers are often performed in healthy volunteers and usually only a single dose of the victim drug is administered. Furthermore, auto-inhibition or -induction, DDI studies not performed at steady-state, and nonlinear dose-exposure relationships can make extrapolation of results from DDI studies challenging. Therefore, it is important to perform a clinical DDI study after drug approval, in case of a large effect of DDIs or a small therapeutic window, when any of the described disadvantages applies. An example of such a selected case is the DDI of palbociclib with moderate CYP3A inhibitors. Palbociclib is a drug with a small therapeutic window, and the clinical DDI study with a strong CYP3A inhibitor was performed in male healthy volunteers with only a single dose palbociclib administered. We studied the effect of the moderate CYP3A inhibitor erythromycin on pharmacokinetics of palbociclib in female breast cancer patients after steady-state concentrations of palbociclib were reached, as described in **Chapter 1.2**.

In short, at the time of drug approval the results from clinical DDI studies with strong CYP3A inhibitors and inducers, and from exposure-response analyses are mostly available. This data can be used to simulate or can be extrapolated to predict the effect of moderate CYP3A inhibitors and inducers, and is therefore sufficient at the time of drug approval. However, in selected cases clinical DDI studies with moderate inhibitors and inducers should still be performed.

## EFFECT OF BODY COMPOSITION ON PHARMACOKINETICS OF HYDROPHILIC DRUGS

Body composition, especially a low skeletal muscle mass or loss of skeletal muscle mass, has been correlated with an increased toxicity and, subsequently, shorter survival in patients treated with chemotherapy (7–9). However, it is unknown how body composition affects toxicity and survival, which is crucial information to optimize treatment. We hypothesized that pharmacokinetics of hydrophilic drugs are altered in patients with a low skeletal muscle mass, which was the basis of the studies described in **Chapter 2**.

Indeed, we did find an effect of skeletal muscle mass on PK of  $\alpha$ -fluoro- $\beta$ -alanine (FBAL), the most hydrophilic metabolite of capecitabine (**Chapter 2.1**), and on cisplatin bound to plasma proteins (**Chapter 2.2**). Therefore, it can be concluded that skeletal muscle mass affects the pharmacokinetics of hydrophilic drugs. For cisplatin, the higher concentration of bound cisplatin in case of a low skeletal muscle mass could theoretically be a reflection of the smaller volume of distribution in this patient group. Consequently, this could explain toxicity because less tissue is available where cisplatin can bind to without doing any harm. In contrast, in case of capecitabine only an effect on PK of FBAL was found, which is inactive and its PK is not related to toxicity. Thus, the effect of body composition on pharmacokinetics does not always explain the increased toxicity and shorter survival.

For drugs where the effect of skeletal muscle mass on PK does explain toxicity, dosing based on skeletal muscle mass might be a good alternative compared to the standard body surface area (BSA) based dosing. One of the aims of the study with cisplatin (**Chapter 2.2**) was to develop a dosing algorithm based on skeletal muscle mass. However, only a relationship between skeletal muscle mass and bound, and thus inactive cisplatin was found, and no relationship with free, and thus active cisplatin. Therefore, development of a dosing algorithm was not endorsed by the study results.

Contrary, in **Chapter 2.3** we suggested to use the CT-enhanced estimate of RenAl FuncTion (CRAFT) to predict creatinine clearance, and subsequently carboplatin clearance. With the CRAFT formula the creatinine production rate is calculated, amongst others, based on body composition, including muscle and fat mass. Indirectly, carboplatin is thus partly dosed based on body composition. In comparison with the in clinical practice often used modified Calvert formula, in which creatinine clearance is calculated by the Cockcroft-Gault formula, this might probably increase dosing accuracy, especially in patients with a low serum creatinine or obesity. This should be confirmed in a prospective clinical trial comparing the two dosing methods.

To summarize, the impact of body composition differs between hydrophilic anticancer drugs. In the era of precision medicine, the effect of body composition should be part of registration studies investigating PK, because this information might be used to optimize the dose of anticancer drugs based on body composition.

## PREDICTION OF TREATMENT OUTCOME BY LOCAL EXPOSURE

For many oral anticancer drugs a relationship between plasma exposure-efficacy and exposure-toxicity has been described (3). In addition to measuring plasma drug concentrations as a surrogate marker for drug exposure at the site of action, it might be attractive to measure drug concentrations locally. Drug concentrations at the site of action can be a stronger biomarker for efficacy, because targeted anticancer drugs exert their effects in tumor cells or in the vicinity of the tumor. In addition, in case of local adverse events, e.g., stomatitis, local drug concentrations reflect the drug concentrations at the site where toxicity actually occurs.

In this thesis we described the feasibility of measuring everolimus concentrations in saliva as predictor of stomatitis in **Chapter 3.1**, and of measuring pazopanib concentrations in tumor tissue as predictor of efficacy in **Chapter 3.2**. In both studies local measurement of drug concentrations was possible and trends were seen between higher local drug concentrations and toxicity (numerically tested) and efficacy (categorical tested), respectively. The relationship between local drug concentrations and toxicity or efficacy needs to be confirmed in sufficiently powered studies.

The measurement of local drug concentrations can be divided according to the use of invasive or non-invasive sampling methods. Measurement of drug concentrations in tumor tissue requires an invasive biopsy procedure. In addition, it is not easy to homogenize tumor tissue. Taken together, use of tumor concentrations for therapeutic drug monitoring does not seem feasible in clinical practice.

In contrast, measurement of drug concentrations in saliva is non-invasive and can possibly be even done at home. Home sampling creates the possibility to measure drug concentrations early after start of treatment, which might be used as early predictor of toxicity, without additional burden of patients because of hospital visits. In the medical community, there is a trend to increasingly involve patients in their treatment plan, also known as shared decision-making. It is also common nowadays, that patients have (partial) insight into their own medical records. In society, also more and more information about health, for example about physical activity by activity trackers, is collected. This collected information can be studied via apps on mobile devices. Taken together these developments, the future might be that patients take a sample at home, e.g., a saliva sample, and send this to the clinic. After analysis of the sample, the result is reviewed by a pharmacist and physician. Subsequently, the

patient can see the result together with an advice of the pharmacist and physician in an online app. In this future image, patients could be even more involved in their own treatment, which might possibly have beneficial effects like an improved treatment adherence. In addition, the major advantage of this approach is that, if necessary, the dose can be adapted early during treatment.



## VALUE OF PIVOTAL STUDIES IN REAL-LIFE PATIENTS

In this thesis, dose optimization of anticancer drugs based on co-medication and drug-drug interactions (**Chapter 1**), skeletal muscle mass (**Chapter 2**), and drug levels in alternative matrices (**Chapter 3**) was described. Overall, it could be concluded that a good prediction of the drug effect is essential to optimize the dose of anticancer drugs. Hereby, the drug effect should be interpreted broadly, e.g., the effect of interacting drugs on pharmacokinetics of victim drugs, or the efficacy and toxicity of anticancer drugs under certain conditions. The data available from pivotal studies is often not sufficient to accurately predict drug effect in real-life patients.

Firstly, as already described previously in this chapter, pivotal DDI studies have disadvantages. For example, these studies are often performed in healthy volunteers after administration of a single dose of the victim drug. As referred to in **Chapter 1.2**, the clinical DDI study with palbociclib and itraconazole was conducted solely in healthy male volunteers, which may not be a representative group for a drug approved for the treatment of breast cancer (10). In such selected cases, when results of pivotal DDI studies are not representative, and the interacting effect is large or the therapeutic window is small clinical studies should be performed after drug approval.

Secondly, it may be asked why chemotherapy is still routinely dosed based on BSA or weight, while these metrics do not give information about the amount of muscle and fat tissue in the body. In **Chapter 2**, we showed that skeletal muscle mass is related to the pharmacokinetics of part of the hydrophilic drugs and their metabolites. Therefore, BSA and weight might not always be the most relevant parameters to describe body composition, and it might be time to let go of standard BSA or weight-based dosing. During drug development the effect of body composition on PK should be investigated, because it could provide a better predictive alternative for BSA or weight-based dosing.

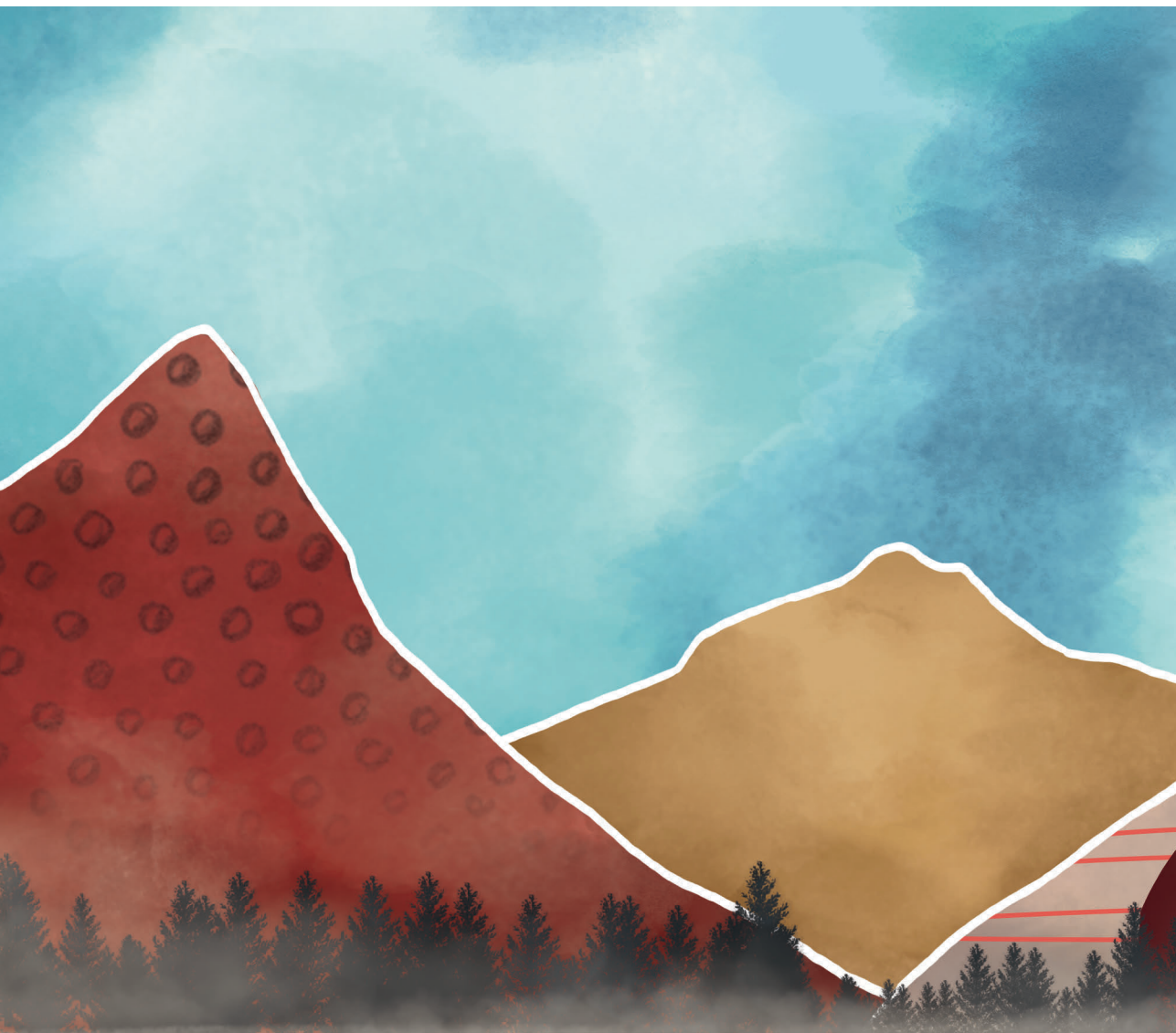
Lastly, during drug development exposure-response analyses are performed, usually with drug concentrations in plasma, which provide crucial information. As mentioned before, this data can for example be used to indicate what the relevance of a pharmacokinetic DDI is. Additional information can be provided by studying the relationship between local drug concentrations and efficacy or toxicity, as described in **Chapter 3**. This information could for example be used for early prediction of the drug effect.

To conclude, an accurate and early prediction of drug effects could contribute to optimization of anticancer drug dosing. Therefore, pivotal studies should be extended regarding body composition, and after drug approval a structured follow-up should be performed, and if necessary, additional clinical trials should be performed in real-life patients.

## REFERENCES

1. Shao J, Markowitz JS, Bei D, An G. Enzyme- and transporter-mediated drug interactions with small molecule tyrosine kinase inhibitors. *J Pharm Sci.* 2014;103(12):3810–33.
2. Blower P, De Wit R, Goodin S, Aapro M. Drug-drug interactions in oncology: Why are they important and can they be minimized? *Crit Rev Oncol Hematol.* 2005;55(2):117–42.
3. Verheijen RB, Yu H, Schellens JHM, Beijnen JH, Steeghs N, Huitema ADR. Practical Recommendations for Therapeutic Drug Monitoring of Kinase Inhibitors in Oncology. *Clin Pharmacol Ther.* 2017;102(5):765–76.
4. Food and Drug Administration. Center for Drug Evaluation and Research. Clinical Drug Interaction Studies - Study Design, Data Analysis, and Clinical Implications Guidance for Industry Draft Guidance [Internet]. 2009 [cited 2020 May 14]. Available from: <http://www.fda.gov/Drugs/GuidanceComplianceRegulatoryInformation/Guidances/default.htm>
5. Food and Drug Administration. Center for Drug Evaluation and Research. Clinical Drug Interaction Studies — Cytochrome P450 Enzyme- and Transporter-Mediated Drug Interactions Guidance for Industry [Internet]. 2020 [cited 2020 Jun 11]. Available from: <https://www.fda.gov/media/134581/download>
6. European Medicines Agency Committee for Medicinal Products For Human Use (CHMP). Guideline on the investigation of drug interactions [Internet]. 2015 [cited 2020 May 14]. Available from: [https://www.ema.europa.eu/en/documents/scientific-guideline/guideline-investigation-drug-interactions-revision-1\\_en.pdf](https://www.ema.europa.eu/en/documents/scientific-guideline/guideline-investigation-drug-interactions-revision-1_en.pdf)
7. Wendrich AW, Swartz JE, Bril SI, Wegner I, de Graeff A, Smid EJ, et al. Low skeletal muscle mass is a predictive factor for chemotherapy dose-limiting toxicity in patients with locally advanced head and neck cancer. *Oral Oncol.* 2017;71:26–33.
8. Kurk S, Peeters P, Stellato R, Dorresteijn B, Jong P De, Jourdan M, et al. Skeletal muscle mass loss and dose-limiting toxicities in metastatic colorectal cancer patients. *J Cachexia Sarcopenia Muscle.* 2019;10(4):803–13.
9. Kurk SA, Peeters PHM, Dorresteijn B, de Jong PA, Jourdan M, Creemers GJM, et al. Loss of skeletal muscle index and survival in patients with metastatic colorectal cancer: Secondary analysis of the phase 3 CAIRO3 trial. *Cancer Med.* 2020;9(3):1033–43.
10. Yu Y, Loi C-M, Hoffman J, Wang D. Physiologically Based Pharmacokinetic Modeling of Palbociclib. *J Clin Pharmacol.* 2017;57(2):173–84.





# APPENDICES



Summary

Nederlandse samenvatting

Author affiliations

List of publications

Dankwoord

Curriculum vitae





# APPENDIX

## Summary





## SUMMARY

The treatment of cancer is rapidly evolving, including a shift to more personalized treatment. Next to choosing the right drug for the right patient, personalized dosing is of importance. This thesis aims to optimize anticancer drug dosing by predicting the drug effect based on co-medication (**Chapter 1**), body composition (**Chapter 2**), and guided by drug levels at the site of action (**Chapter 3**).

In **Chapter 1** pharmacokinetic drug-drug interactions (DDIs) that occur through the metabolism via the Cytochrome P450 3A (CYP3A) enzyme are described. Early after drug approval mostly only clinical data is available on the effects of strong CYP3A inhibitors and inducers. In this chapter it is examined how CYP3A based DDIs can be handled based on this limited data and, additionally, the knowledge gap on the effects of moderate CYP3A inhibitors is reduced by performance of a clinical DDI study.

**Chapter 1.1** reviews the results of DDI studies performed for twelve oral anticancer drugs. The aim of this review was to provide recommendations on how to deal with DDIs where only data from strong CYP3A inhibitors or inducers is available. In clinical practice, frequently patients with polypharmacy are treated and it is important to have guidelines on how to deal with DDIs in these patients. In case data from clinical DDI studies or physiologically based pharmacokinetic (PBPK) simulations with moderate CYP3A inhibitors and inducers is lacking, a change in exposure of 50% compared with strong inhibitors and inducers, respectively, can be used as input for the starting dose. Since the interacting effect of weak inhibitors and inducers was found to be small for the studied drugs, no *a priori* dose adaptations are indicated. For drugs with pharmacologically active metabolites, the metabolic pathway, the ratio of the parent to the metabolites, and the potency of the metabolites should be taken into account.

In **Chapter 1.2** the effect of the moderate CYP3A4 inhibitor erythromycin on the pharmacokinetics of palbociclib, used for the treatment of breast cancer, was assessed in a clinical randomized crossover trial. For palbociclib, only clinical data of a strong CYP3A4 inhibitor was available and based on PBPK simulations, no dose reduction in case of concomitant use with a moderate CYP3A4 inhibitor was recommended. In the clinical trial, increases in the area under the plasma concentration-time curve (AUC), and maximum plasma concentration ( $C_{\max}$ ) of both 43% were found. Therefore, a dose reduction of palbociclib from 125 mg to 75 mg once daily is rational, when used concomitantly with moderate CYP3A4 inhibitors.



**Chapter 2** focusses on the relationship of body composition and the pharmacokinetics of hydrophilic chemotherapeutic drugs. A relationship between body composition and pharmacokinetics could possibly explain the increased toxicity and shorter survival observed in patients with a low skeletal muscle mass whom are treated with chemotherapeutic drugs. The possible relationship is assessed both directly by assessing the covariate effect of body composition on pharmacokinetic parameters, but also indirectly by using body composition to predict renal function.

In **Chapter 2.1** the association between skeletal muscle mass and the pharmacokinetics of the chemotherapeutic drug capecitabine and its metabolites was evaluated. This was done by testing different body composition descriptors, amongst which skeletal muscle mass, as covariates in a previously developed population pharmacokinetic model with solid tumor patients. Only an association between skeletal muscle mass and the pharmacokinetics of the inactive and non-toxic metabolite  $\alpha$ -fluoro- $\beta$ -alanine (FBAL) was found. Since skeletal muscle mass was not associated with the pharmacokinetics of capecitabine and its active metabolite 5-fluorouracil (5-FU), this could not explain the previously identified increased toxicity and decreased survival in patients with a low skeletal muscle mass.

**Chapter 2.2** reports the results of a prospective observational study in which the relationship between skeletal muscle mass and pharmacokinetics of cisplatin in head and neck squamous cell carcinoma patients was studied. A significant relationship was found between skeletal muscle mass and cisplatin pharmacokinetics, however, this was also shown for other body composition descriptors like body surface area. In a simulation, patients with a low skeletal muscle mass reached higher bound cisplatin concentrations. We hypothesized that this higher bound cisplatin concentrations could be seen as a reflection of the smaller volume of distribution, with less tissue available where cisplatin can bind without inducing toxicity. Thus, the altered distribution of cisplatin could explain that patients with a low skeletal muscle mass were more prone to experience cisplatin toxicity in a previously published trial.

In **Chapter 2.3** we evaluated if carboplatin clearance was better predicted using creatinine clearance based on a CT-enhanced estimate of renal function (CRAFT) compared to creatinine clearance based on the Cockcroft-Gault formula by means of a population pharmacokinetic modeling approach. The creatinine clearance calculated by the Cockcroft-Gault formula is generally applied as a proxy for the glomerular filtration rate in a modified Calvert formula, used to dose carboplatin. However, the creatinine clearance based on the Cockcroft-Gault formula was not correlated to carboplatin clearance in a previously published study. This might be due to an inaccurate prediction of the creatinine

production rate by using surrogate markers for muscle mass. The CRAFT formula could be a better alternative because muscle and fat mass as measured on CT-scans are used to predict the creatinine production rate. Indeed, it was shown that the CRAFT formula performed better. The better prediction of the creatinine production rate by the CRAFT formula especially impacts patients with a low serum creatinine. Therefore, the more accurate prediction of carboplatin clearance, used to dose carboplatin, might possibly be an alternative for dose capping which is usually applied in this patient group.

**Chapter 3** addresses the use of drug concentrations at the site of action. Local drug concentrations might provide additional information beyond plasma or whole blood concentrations because it is not clear whether local and systemic drug concentrations are correlated and whether systemic exposure is the best surrogate for pharmacokinetic and pharmacodynamic evaluation. In addition, non-invasive sampling methods to measure local drug concentrations might be used as early predictors of efficacy or toxicity.

**Chapter 3.1** shows the results of a clinical study in which the feasibility of quantifying everolimus saliva concentrations and subsequently use these as a predictor of stomatitis was examined. Stomatitis is the most common adverse event of everolimus and has a serious negative impact on quality of life. It was shown that collection of saliva samples is feasible, everolimus concentrations can be quantified in saliva samples, pharmacokinetics of everolimus in saliva are highly variable, saliva concentrations are poorly correlated with whole blood concentrations, and there is a trend between everolimus saliva concentrations and the occurrence of stomatitis. Therefore, saliva sampling might be used as an early predictor of stomatitis, but cannot replace the use of whole blood concentrations.

**Chapter 3.2** describes a prospective clinical trial in which intra-tumoral drug levels of pazopanib were quantified in non-metastatic sarcoma patients, treated with neo-adjuvant concurrent radiotherapy and pazopanib. A modest correlation was found between tumor and plasma concentrations of pazopanib. No significant relationship was found between tumor concentrations and percentage of viable tumor cells, however, a trend towards less viable tumor cells in patients with high pazopanib tumor concentrations was observed.

To conclude, a good prediction of the drug effect is essential to optimize the dose of anticancer drugs. Information about co-medication, body composition, and drug levels at the site of action can be used for dose optimization. The data available from pivotal studies is not always sufficient to accurately predict drug effect, therefore, clinical trials in real-life patients remain essential.







# APPENDIX

Nederlandse samenvatting



## NEDERLANDSE SAMENVATTING

De behandeling van kanker ontwikkelt zich snel, onder meer door een verschuiving naar een meer gepersonaliseerde behandeling. Naast het kiezen van de juiste behandeling voor de juiste patiënt, is een gepersonaliseerde dosering van belang. Het doel van dit proefschrift is het optimaliseren van de dosering van antikankergeneesmiddelen door het geneesmiddeffect te voorspellen op basis van comedatie (**Hoofdstuk 1**), lichaamssamenstelling (**Hoofdstuk 2**), en geneesmiddelspiegels op de plaats van werking (**Hoofdstuk 3**).

In **Hoofdstuk 1** worden geneesmiddel-geneesmiddelinteracties beschreven die optreden door het metabolisme via het Cytochroom P450 3A (CYP3A) enzym. Kort nadat een geneesmiddel is toegelaten tot de markt, is meestal alleen klinische data beschikbaar met betrekking tot het effect van sterke remmers en inductoren van CYP3A. In dit hoofdstuk wordt onderzocht hoe omgegaan moet worden met geneesmiddelinteracties op basis van CYP3A op basis van deze gelimiteerde gegevens. In aanvulling daarop, wordt het kennishiaat met betrekking tot matige CYP3A remmers verkleind door het uitvoeren van een klinische geneesmiddelinteractiestudie.

**Hoofdstuk 1.1** beoordeelt de resultaten van geneesmiddelinteractiestudies uitgevoerd voor twaalf orale antikankergeneesmiddelen. Het doel van dit onderzoek was om aanbevelingen te geven hoe om te gaan met geneesmiddelinteracties, als alleen informatie over de interactie met sterke remmers of inductoren van CYP3A beschikbaar is. In de klinische praktijk worden vaak patiënten met polyfarmacie behandeld en daarom is het belangrijk om richtlijnen te hebben die beschrijven hoe om te gaan met geneesmiddelinteracties in deze patiënten. Als geen informatie beschikbaar is, vanuit klinische studies of farmacokinetische simulaties gebaseerd op de fysiologie (PBPK-simulaties), over het effect van matige remmers van CYP3A, kan een verandering in blootstelling van 50% in vergelijking met sterke remmers en inductoren, respectievelijk, worden verondersteld en gebruikt als basis voor de startdosering. Aangezien slechts een klein effect van zwakke remmers en inductoren gevonden werd, zijn er bij interactie met geneesmiddelen uit deze groepen geen *a priori* dosisaanpassingen nodig. In het geval van geneesmiddelen met werkzame metabolieten moet rekening worden gehouden met het metabolisme, de ratio van het hoofdgeneesmiddel ten opzichte van metabolieten, en de potentie van de metabolieten.

In **Hoofdstuk 1.2** wordt het effect van de matige CYP3A4 remmer erytromycine op de farmacokinetiek van palbociclib, gebruikt voor de behandeling van borstkanker, bestudeerd in een klinisch gerandomiseerde *cross-over* studie. Voor palbociclib is alleen klinische data beschikbaar over het effect van een sterke CYP3A4 remmer en op



basis van PBPK-simulaties wordt geen dosisreductie aanbevolen bij gelijktijdig gebruik met een matige CYP3A4 remmer. In de klinische studie, toenames in de oppervlakte onder de plasmaconcentratietijdcurve (AUC), en maximale plasmaconcentratie ( $C_{max}$ ) van beide 43% werden gevonden. Daarom is een dosisreductie van palbociclib 125 mg naar 75 mg eenmaal daags rationeel als palbociclib gebruikt wordt in combinatie met matige CYP3A4 remmers.

**Hoofdstuk 2** richt zich op de relatie tussen lichaamssamenstelling en farmacokinetiek van hydrofiële chemotherapieën. Een relatie tussen lichaamssamenstelling en farmacokinetiek zou mogelijk de verhoogde toxiciteit en kortere overleving kunnen verklaren die werd gezien in patiënten met een lage skeletspiermassa die werden behandeld met chemotherapie. De mogelijke relatie werd zowel direct bestudeerd, door het bestuderen van het covariaateffect van lichaamssamenstelling op farmacokinetische parameters, als indirect door lichaamssamenstelling te gebruiken om nierfunctie te voorspellen.

In **Hoofdstuk 2.1** werd de relatie tussen skeletspiermassa en farmacokinetiek van het chemotherapeuticum capecitabine en de metabolieten geëvalueerd. Dit werd gedaan door verschillende manieren om lichaamssamenstelling te beschrijven, waaronder skeletspiermassa, te testen als covariaten in een eerder ontwikkeld farmacokinetisch populatiemodel op basis van patiënten met solide tumoren. Er werd alleen een relatie gevonden tussen skeletspiermassa en de farmacokinetiek van de inactieve en niet-toxische metaboliet  $\alpha$ -fluoro- $\beta$ -alanine (FBAL). Aangezien skeletspiermassa niet gerelateerd was aan de farmacokinetiek van capecitabine en de werkzame metaboliet 5-fluorouracil (5-FU), kon dit de eerder gevonden toegenomen toxiciteit en verkorte overleving in patiënten met een lage skeletspiermassa niet verklaren.

**Hoofdstuk 2.2** rapporteert de resultaten van een prospectieve observationele studie waarin de relatie tussen skeletspiermassa en farmacokinetiek van cisplatine in patiënten met hoofd-halstumoren werd bestudeerd. Een significante relatie tussen skeletspiermassa en farmacokinetiek van cisplatine werd gevonden, echter, dit werd ook gezien voor andere manieren om lichaamssamenstelling te beschrijven, zoals lichaamsoppervlakte. In een simulatie bereikten patiënten met een lage skeletspiermassa hogere gebonden cisplatineconcentraties. Onze hypothese was dat deze hogere gebonden cisplatineconcentraties een reflectie zijn van het kleinere verdelingsvolume, waarbij minder weefsel aanwezig is waar cisplatine kan binden zonder toxiciteit te veroorzaken. Op deze manier zou de veranderde verdeling van cisplatine kunnen verklaren waarom patiënten met een lage skeletspiermassa meer risico liepen op bijwerkingen van cisplatine in een eerder gepubliceerde studie.



In **Hoofdstuk 2.3** hebben we onderzocht of de klaring van carboplatine beter wordt voorspeld als de creatinineklaring op basis van een CT-ondersteunde schatting van de nierfunctie (CRAFT) werd gebruikt in vergelijking met de creatinineklaring op basis van de Cockcroft-Gault-formule. Dit werd bestudeerd aan de hand van farmacokinetische populatiemodellen. De creatinineklaring berekend met de Cockcroft-Gault-formule wordt normaal gesproken gebruikt als benadering van de glomerulaire filtratiesnelheid in een aangepaste versie van de Calvert-formule, die wordt gebruikt om carboplatine te doseren. Echter, was de creatinineklaring op basis van de Cockcroft-Gault-formule niet gecorreleerd aan de carboplatineklaring in eerder gepubliceerde studie. Dit zou kunnen worden verklaard door een inaccuraat voorspelling van de creatinineproductiesnelheid door surrogaatmarkers voor spiermassa te gebruiken. De CRAFT-formule zou een beter alternatief kunnen zijn omdat spier- en vetmassa gemeten op CT-scans worden gebruikt om de creatinineproductiesnelheid te voorspellen. Inderdaad bleek het zo te zijn dat de CRAFT-formule beter presteerde. De betere voorspelling van de creatinineproductiesnelheid bij gebruik van de CRAFT-formule heeft vooral invloed in patiënten met een laag serumcreatinine. Daarom zou de meer accurate voorspelling van de carboplatineklaring, gebruikt om carboplatine te doseren, mogelijk gebruikt kunnen worden als alternatief voor het gebruik van een maximale dosering op basis van nierfunctie, wat gewoonlijk wordt toegepast in deze patiëntengroep.

In **Hoofdstuk 3** komt het gebruik van geneesmiddelspiegels op de plaats van werking aan bod. Lokale geneesmiddelspiegels kunnen aanvullende informatie verschaffen naast concentraties gemeten in plasma of volbloed omdat het niet duidelijk is of lokale en systemische geneesmiddelspiegels aan elkaar gecorreleerd zijn en of systemische geneesmiddelspiegels de beste optie zijn voor farmacokinetische en farmacodynamische evaluatie. Daarnaast, zouden niet-invasieve methodes van monsternamen om lokale geneesmiddelspiegels te meten kunnen worden gebruikt als vroege voorspellers van effectiviteit of toxiciteit.

**Hoofdstuk 3.1** laat de resultaten zien van een klinische studie waarin de haalbaarheid van het bepalen van everolimusconcentraties in speeksel en vervolgens gebruiken als voorspeller van stomatitis werd onderzocht. Stomatitis is de meest voorkomende bijwerking van everolimus en heeft een ernstig negatieve invloed op de kwaliteit van leven. Er werd aangetoond dat het verzamelen van speekselmonsters haalbaar is, dat everolimusconcentraties bepaald kunnen worden in speekselmonsters, dat de farmacokinetiek van everolimus in speeksel erg variabel is, dat speekselconcentraties slecht gecorreleerd zijn met volbloedconcentraties, en dat er een trend te zien was tussen everolimusconcentraties in speeksel en het optreden van stomatitis.



Hieruit volgt dat speekselmonsters zouden kunnen worden gebruikt om stomatitis al vroeg te kunnen voorspellen, maar niet als vervanging van het gebruik van volbloedconcentraties.

**Hoofdstuk 3.2** beschrijft een prospectieve klinische studie waarin tumorspiegels van pazopanib werden bepaald in patiënten met een niet-gemetastaseerd sarcoom die werden behandeld met neoadjuvante radiotherapie in combinatie met pazopanib. Een matige correlatie tussen tumor- en plasmaspiegels van pazopanib werd gevonden. Er was geen significante relatie tussen tumorspiegels en het percentage levensvatbare tumorcellen, maar er werd wel een trend gezien naar een lager aantal levensvatbare tumorcellen in patiënten met hoge pazopanibconcentraties in de tumor.

Concluderend is een goede voorspelling van het effect essentieel om de dosering van antikankergeneesmiddelen te optimaliseren. Informatie over comedicaatie, lichaamssamenstelling, en geneesmiddelspiegels op de plaats van werking kunnen worden gebruikt voor optimalisatie van de dosering. De gegevens die beschikbaar zijn vanuit registratiestudies zijn niet altijd toereikend om het effect van een geneesmiddel goed te voorspellen, daarom blijven klinische studies in patiënten behandeld in de klinische praktijk onmisbaar.







# APPENDIX

## Author affiliations



---

## AUTHOR AFFILIATIONS

Dorieke E.M. van Balen	Department of Pharmacy & Pharmacology, The Netherlands Cancer Institute - Antoni van Leeuwenhoek, Amsterdam, The Netherlands
Jos H. Beijnen	Department of Pharmacy & Pharmacology, The Netherlands Cancer Institute - Antoni van Leeuwenhoek, Amsterdam, The Netherlands Department of Pharmaceutical Sciences, Utrecht University, Utrecht, The Netherlands
Judith V.M.G Bovée	Department of Pathology, Leiden University Medical Center, Leiden, The Netherlands
C. Louwrens Braal	Department of Medical Oncology, Erasmus MC Cancer Institute, Rotterdam, The Netherlands
Remco de Bree	Department of Head and Neck Surgical Oncology, University Medical Center Utrecht, Utrecht University, Utrecht, The Netherlands
Najiba Chargi	Department of Head and Neck Surgical Oncology, University Medical Center Utrecht, Utrecht University, Utrecht, The Netherlands
Lot A. Devriese	Department of Medical Oncology, University Medical Center Utrecht, Utrecht University, Utrecht, The Netherlands
Marloes G.J. van Dongen	Department of Medical Oncology and Clinical Pharmacology, The Netherlands Cancer Institute - Antoni van Leeuwenhoek, Amsterdam, The Netherlands
Thomas P.C. Dorlo	Department of Pharmacy & Pharmacology, The Netherlands Cancer Institute - Antoni van Leeuwenhoek, Amsterdam, The Netherlands



Marta Fiocco	Mathematical Institute, Leiden University, Leiden, The Netherlands Department of Biomedical Data Science, Section Medical Statistics, Leiden University Medical Center, Leiden, The Netherlands
Hans Gelderblom	Department of Medical Oncology, Leiden University Medical Center, Leiden, The Netherlands
Stefanie L. Groenland	Department of Medical Oncology and Clinical Pharmacology, The Netherlands Cancer Institute - Antoni van Leeuwenhoek, Amsterdam, The Netherlands
Rick L.M. Haas	Department of Radiotherapy, The Netherlands Cancer Institute - Antoni van Leeuwenhoek, Amsterdam, The Netherlands Department of Radiotherapy, Leiden University Medical Centre, Leiden, The Netherlands
Laura F.J. Huiskamp	Department of Head and Neck Surgical Oncology, University Medical Center Utrecht, Utrecht University, Utrecht, The Netherlands
Alwin D.R. Huitema	Department of Pharmacy & Pharmacology, The Netherlands Cancer Institute - Antoni van Leeuwenhoek, Amsterdam, The Netherlands Department of Clinical Pharmacy, University Medical Center Utrecht, Utrecht University, Utrecht, The Netherlands Department of Pharmacology, Princess Máxima Center for Pediatric Oncology, Utrecht, The Netherlands
Bart A.W. Jacobs	Department of Pharmacy & Pharmacology, The Netherlands Cancer Institute - Antoni van Leeuwenhoek, Amsterdam, The Netherlands Department of Hospital Pharmacy, Amsterdam University Medical Center, Amsterdam, The Netherlands



---

Stijn L.W. Koolen	Department of Medical Oncology, Erasmus MC Cancer Institute, Rotterdam, The Netherlands Department of Hospital Pharmacy, Erasmus Medical Center, Rotterdam, The Netherlands
Sophie A. Kurk	Department of Radiation Oncology, University Medical Center Utrecht, Utrecht University, Utrecht, The Netherlands Julius Center for Health Sciences and Primary Care, University Medical Center Utrecht, Utrecht University, Utrecht, The Netherlands
Ron H.J. Mathijssen	Department of Medical Oncology, Erasmus MC Cancer Institute, Rotterdam, The Netherlands
Anne M. May	Julius Center for Health Sciences and Primary Care, University Medical Center Utrecht, Utrecht University, Utrecht, The Netherlands
Milan van Meekeren	Department of Medical Oncology, Leiden University Medical Center, Leiden, The Netherlands
Aisha B. Miah	Department of Clinical Oncology, The Royal Marsden Hospital and The Institute of Cancer Research, London, United Kingdom
Pim Moeskops	Quantib, Rotterdam, The Netherlands
Tobias T. Pieters	Department of Nephrology and Hypertension, University Medical Center Utrecht, Utrecht University, Utrecht, The Netherlands
Erik-Jan Rijkhorst	Department of Medical Physics and Technology, The Netherlands Cancer Institute - Antoni van Leeuwenhoek, Amsterdam, The Netherlands
Maarten B. Rookmaaker	Department of Nephrology and Hypertension, University Medical Center Utrecht, Utrecht University, Utrecht, The Netherlands



Hilde Rosing	Department of Pharmacy & Pharmacology, The Netherlands Cancer Institute – Antoni van Leeuwenhoek, Amsterdam, The Netherlands
Neeltje Steeghs	Department of Medical Oncology and Clinical Pharmacology, The Netherlands Cancer Institute - Antoni van Leeuwenhoek, Amsterdam, The Netherlands
Bas Thijssen	Department of Pharmacy & Pharmacology, The Netherlands Cancer Institute - Antoni van Leeuwenhoek, Amsterdam, The Netherlands
Wouter B. Veldhuis	Department of Radiology, University Medical Center Utrecht, Utrecht University, Utrecht, The Netherlands
Remy B. Verheijen	Department of Pharmacy & Pharmacology, The Netherlands Cancer Institute – Antoni van Leeuwenhoek, Amsterdam, The Netherlands
Niels de Vries	Department of Pharmacy & Pharmacology, The Netherlands Cancer Institute – Antoni van Leeuwenhoek, Amsterdam, The Netherlands
Annelie J.E. Vulink	Department of Medical Oncology, Reinier de Graaf Gasthuis, Delft, The Netherlands







# APPENDIX

## List of publications



## LIST OF PUBLICATIONS

### Peer-reviewed articles

1. Chargi N\*, **Molenaar-Kuijsten L\***, Huiskamp LFJ, Devriese LA, De Bree R, Huitema ADR. The association of cisplatin pharmacokinetics and skeletal muscle mass in head and neck cancer patients: the prospective PLATISMA study. Accepted for publication in European Journal of Cancer.
2. **Molenaar-Kuijsten L\***, Braal CL\*, Groenland SL\*, De Vries N, Rosing H, Beijnen JH, Koolen SLW, Vulink AJE, Van Dongen MGJ, Mathijssen RHJ, Huitema ADR, Steeghs N. Effects of the moderate CYP3A4 inhibitor erythromycin on the pharmacokinetics of palbociclib: a randomized crossover trial in patients with breast cancer. Clin Pharmacol Ther. 2021. [Epub ahead of print].
3. **Molenaar-Kuijsten L**, Van Balen DEM, Beijnen JH, Steeghs N, Huitema ADR. A review of CYP3A drug-drug interaction studies: practical guidelines for patients using targeted oral anticancer drugs. Front Pharmacol. 2021;12: 670862.
4. **Molenaar-Kuijsten L**, Jacobs BAW, Kurk SA, May AM, Dorlo TPC, Beijnen JH, Steeghs N, Huitema ADR. Worse capecitabine treatment outcome in patients with a low skeletal muscle mass is not explained by altered pharmacokinetics. Cancer Med. 2021;10(14):4781–9.
5. Achterbergh R, Lammers LA, **Kuijsten L**, Klümpen HJ, Mathôt RAA, Romijn JA. Effects of nutritional status on acetaminophen measurement and exposure. Clin Toxicol. 2019;57(1):42–9.

\* These authors contributed equally



**Conference abstracts**

1. **Molenaar-Kuijsten L**, Chargi N, Devriese LA, De Bree R, Huitema ADR. The association of skeletal muscle mass and cisplatin pharmacokinetics in head and neck cancer patients: the prospective PLATISMA study. ASCO 2021 Virtual Scientific Programme.
2. **Molenaar-Kuijsten L**, Braal CL, Groenland SL, De Vries N, Rosing H, Beijnen JH, Koolen SLW, Vulink AJE, Van Dongen MGJ, Mathijssen RHJ, Huitema ADR, Steeghs N. Effects of the moderate CYP3A4 inhibitor erythromycin on the pharmacokinetics of palbociclib: a randomized cross-over trial in patients with breast cancer. NVKF&B Scientific Meeting 2021, The Netherlands.
3. **Molenaar-Kuijsten L**, Jacobs BAW, Kurk SA, May AM, Beijnen JH, Steeghs N, Huitema ADR. Worse capecitabine treatment outcome in patients with a low skeletal muscle mass is not explained by altered pharmacokinetics. NVKF&B Scientific Meeting 2019, The Netherlands.
4. Lopez JS, Camidge R, lafolla M, Rottey S, Schuler M, Hellmann M, Balmanoukian A, Dirix L, Gordon M, Sullivan R, Henick BS, Drake C, Wong K, LoRusso P, Ott P, Fong L, Schiza A, Yachnin J, Ottensmeier C, Braiteh F, Bendell J, Leidner R, Fisher G, Jerusalem G, **Molenaar-Kuijsten L**, Schmidt M, Laurie SA, Aljumaily R, Rittmeyer A, Gort E, Melero I, Mueller L, Sabado R, Twomey P, Huang J, Yadav M, Zhang J, Mueller F, Derhovanessian E, Sahin U, Türeci Ö, Powles T. Abstract CT301: A phase Ib study to evaluate RO7198457, an individualized Neoantigen Specific immunoTherapy (iNeST), in combination with atezolizumab in patients with locally advanced or metastatic solid tumors. AACR Annual Meeting 2020, Philadelphia.









# APPENDIX

Dankwoord



## DANKWOORD

Onderzoek doe je niet alleen. Dit heb ik de afgelopen jaren mogen ervaren. Ik wil iedereen die heeft bijgedragen aan het tot stand komen van dit proefschrift hier hartelijk voor bedanken! Bij deze wil ik ook een aantal personen specifiek benoemen.

Veel dank aan de **patiënten** die deel hebben genomen aan de klinische studies die onderdeel waren van mijn proefschrift. Ik vind het bijzonder grootmoedig dat zij tijdens een moeilijke periode in hun leven bereid waren om een bijdrage te leveren aan de wetenschap. Met als doel om de behandeling van kanker beter te maken, niet direct voor henzelf, maar voor patiënten in de toekomst.

**Alwin**, je mocht zelf nog wel eens zeggen dat je geen orakel bent, maar ik heb veel bewondering voor jouw scherpe analytische blik en het gemak waarmee jij de link legt tussen onderzoeksresultaten en de klinische praktijk. Daarnaast zorgde jouw aanstekelijke enthousiasme ervoor dat ik menig keer met frisse moed jouw kantoor weer uit ben gelopen.

**Neeltje**, jij stimuleerde me om concrete doelen te stellen en dacht vervolgens mee hoe ik die doelen ook daadwerkelijk kon behalen. Dit heeft er absoluut aan bijgedragen dat ik mijn proefschrift in vier jaar kon afronden. Dat time management een van jouw sterke kanten is bleek ook uit het feit dat je, ondanks je bizar volle agenda, toch regelmatig tijd voor me wist vrij te maken. Daarnaast veel dank voor je klinische input op mijn projecten.

**Jos**, ondanks dat mijn directe begeleiding bij Alwin en Neeltje lag, was ook jij betrokken bij mijn promotieonderzoek. Hierin waardeer ik jouw belangstelling en positiviteit. Zo kon ik na een presentatie op de H3 meeting steevast rekenen op vriendelijke woorden van jouw kant. Dank ook voor de nuttige (handgeschreven) commentaren op mijn manuscripten.

**Frans**, dank voor de begeleiding tijdens mijn opleiding tot klinisch farmacoloog. Door jouw enthousiasme en inzet wordt de opleiding steeds iets mooier.

**Bart**, mijn eerste stapjes op het gebied van modelleren werden door jou begeleid. Jij was hiervoor dan ook de aangewezen persoon, omdat mijn eerste project voortborduurde op het model dat jij had ontwikkeld. Fijn dat jij altijd meer geduld had dan ikzelf, toen ik in het begin regelmatig vastliep. Daarnaast waardeer ik jouw betrokkenheid, ook toen je zelf al niet meer in het AVL werkte.



**Thomas**, bedankt dat je altijd bereid was mee te denken over de farmacokinetische populatiemodellen waar ik mee bezig was, zowel tijdens de NONMEM meeting als daarbuiten. Uiteraard ook dank aan de andere **NKI NONMEM humans** voor hun input.

De ondersteuning vanuit verschillende afdelingen in het AVL was onmisbaar. Alle collega's van de **Clinical Research Unit**, het **Trialbureau**, het **Triallab** en de **Pathologie** wil ik bedanken voor de ondersteuning bij het uitvoeren van klinische studies. Van het **Laboratorium van de Apotheek** wil ik specifiek **Hilde**, **Bas** en **Niels** bedanken voor het meten van alle geneesmiddelspiegels, het valideren van de assay om everolimus in speeksel te kunnen meten en de hulp bij het homogeniseren van de tumorbiopten. **Hans**, **Thea** en **Lara** bedankt voor de algemene ondersteuning op H3.

**Remy**, jij hebt de basis gelegd voor het derde hoofdstuk uit mijn proefschrift. Het was me een waar genoegen deze twee projecten van je over te mogen nemen. Verder kan ik de snelheid waarmee jij manuscripten van feedback voorzag niet ongenoemd laten, meestal had ik ze dezelfde dag weer terug! De kwaliteit van je feedback had hier zeker niet onder te lijden, dankjewel, ik heb er veel aan gehad.

**Steffie**, de Palbo CYP studie heb ik van jou overgenomen toen je jouw promotieonderzoek aan het afronden was. Jij was de ideale persoon om op te volgen, zoals altijd had je je zaken goed op orde en zorgde je voor een soepele overdracht. Als ik toch nog vragen had, stond jij altijd klaar om die te beantwoorden. Dankjewel hiervoor. **Louwrens**, jij was Steffie en mijn alter ego in het EMC. Dank voor je inzet om voldoende patiënten te kunnen includeren en je bereidwilligheid om op wat voor manier dan ook hulp te bieden.

**Sophie**, jij leerde mij als apotheker die vrij weinig CT-scans had gezien, hoe ik de L3 slice van een patiënt kon selecteren en vervolgens de skeletspiermassa in kon kleuren. Onmisbare kennis voor mijn eerste project met skeletspiermassa! Daarnaast zorgde jij dat ik beschikking had over de benodigde software en was je nooit te beroerd om een scan te beoordelen waarvan ik twijfelde of ik die juist ingekleurd had. Bedankt voor je vrolijkheid en behulpzaamheid.

**Najiba**, bedankt voor de samenwerking in de PLATISMA studie. Verschillende tegenslagen zorgden dat de deadline van het KWF moeilijk te halen was, maar uiteindelijk hebben we de studie in vliegende vaart afgerond. Hieraan heeft jouw enorme gedrevenheid zeker bijgedragen.

**Milan**, heel veel dank voor onze samenwerking, die ik als bijzonder prettig heb ervaren. Het was fijn om iemand te hebben waar ik altijd mee kon sparren over ons project en ik denk dat we elkaar goed konden aanvullen vanuit onze verschillende vakgebieden.

**Tobias**, het was leuk aan de slag te gaan met de formule die jij zelf hebt ontwikkeld. Bedankt voor je hulp om deze formule op de juiste manier toe te passen.

**Overige co-auteurs**, als ik iedereen bij naam zou noemen zou mijn dankwoord erg lang worden, desalniettemin bedankt voor alle hulp en opbouwende feedback op mijn manuscripten.

**H3 BeSchHuit OIO's**, zonder jullie was mijn promotieonderzoek lang niet zo leuk geweest. Bedankt voor de gezelligheid op H3, chocolademelk van Vermaat, de ooit nog wekelijkse tripjes naar de markt, leuke etentjes en weekendjes weg, ondersteuning tijdens mijn eerste poging om me voort te bewegen op ski's en vast nog meer.

Lieve **vrienden**, bedankt voor jullie belangstelling naar mijn onderzoek, maar ook voor de momenten dat het even niet over werk ging!

Lieve **Willeke** en **René**, heel erg leuk dat jullie mijn paranimfen willen zijn!

Lieve **papa en mama en de rest van onze alsmaar groeiende familie**, dank voor jullie interesse in mijn werk en de pogingen om te doorgronden waar mijn onderzoek over ging ("Er staan wel erg veel moeilijke woorden in je artikel." "Ik ben maar gestopt na de abstract."). Nog veel meer wil ik jullie bedanken voor een luisterend oor, de steun en het vertrouwen dat jullie in me hadden.

Lieve **Tim**, UPS het is klaar! Fijn dat ik in de afgelopen jaren mijn verhaal altijd bij je kwijt kon. Ik denk dat jouw kennis van farmacokinetiek inmiddels ruim boven het Nederlandse gemiddelde ligt en dat je een heleboel weet over het reilen en zeilen in het AVL zonder er ooit geweest te zijn. Dankjewel dat jij er altijd voor me bent en achter me staat!









# APPENDIX

Curriculum vitae



## CURRICULUM VITAE



Laura is the youngest girl of six siblings, born on January 31<sup>st</sup> 1991 in Bunnik, although she isn't the youngest child. Despite this, a lot of people assumed so since her two-year-younger brother was as tall as she was.

She was a very sweet child, one might think she was easily overlooked. However, she turned out to be a very disciplined girl and that's how she became a dancer/gymnast you couldn't overlook. There were few people shining as she did whenever she was performing her rhythmic gym routine on the floor. And I'm certain no one else combined this with all the activities she did in the way she did. You can imagine the envy of her brothers and sisters.

Laura is also resolute. When it became impossible to train as often as required to stay in the selection squad of rhythmic gym, her parents couldn't find common ground with the trainers to resolve it. Although she was very young, she was so keen to keep joining the group exercises and to stay in competition that she managed to arrange an agreement with the trainers on her own.

Because of her discipline and perseverance, it seemed almost mundane that Laura graduated from high school/secondary school GSG Guido de Brès in Amersfoort in 2009.

Laura surprised her parents with her choice to study pharmacy. She didn't mention it until her choice was as good as finalized. She is and always has been confident in her choices and ability to achieve her ambitions. She studied pharmacy at the University of Utrecht and graduated in 2016.

Her initial post-graduation jobs were at the IJsselland Hospital from May 2016 till May 2017, and at the Erasmus Medical Centre from June 2017 till October 2017. During her time working in these clinical settings she developed a crystalline ambition. She set out to join the research field of clinical pharmacology. To achieve said goal she approached researchers in this field to apply for a PhD candidacy. In October 2017 she embarked on this PhD journey under supervision of prof. dr. Alwin Huitema, prof. dr. Jos Beijnen, and dr. Neeltje Steeghs.



In February 2018 Laura started her training to become a clinical pharmacologist. In August 2021 she finished this study program.

Whatever Laura does, she wants to excel at. In her professional life as well as in sports. I lost count of all the sports that followed one after another, succeeding in all of them with the same familiar smile on her face she displayed during childhood, still hard to overlook. A few years ago, she received a brown belt in karate, and most recently she crossed the finish line in first place during a run in Belgium. At her bachelor party she even showed an aptitude for pole dancing.

And last but not least, she is a Kujsten. In her hands every cutting becomes a flourishing plant. She is without fail eager and stubborn enough to make the very best of any given situation. And so, she will for her patients. Only the best is good enough! To be a successful pharmacist you must work steadfast with your head and hands. I have faith she has it all.

*Her sister, Willeke de Beer-Kujsten*



